Investigating the contribution of AMPK regulation to physiology and lifespan in *C. elegans*.

Daniel Michael Scanlon

Submitted to the University of Kent for the degree of PhD in Genetics.

Submitted by Daniel Michael Scanlon, PhD in the School of Biosciences, lab of Jennifer Tullet, July 2020. All work shown here is my own, unless duly noted otherwise.

Signed: 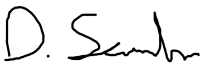

No part of this thesis has been submitted in support of an application for any degree or other qualification of the University of Kent, or any other University or Institution of learning.

Acknowledgements.

My PhD journey has without a doubt been the most formative experience of my life so far. Filled with ups and downs, aspirations, and more than a few obstacles along the way, but I have never regretted my decision to pursue a PhD.

First of all, I would like to thank my supervisor Jennifer Tullet for accepting me into her lab as a newly qualified graduate, and for her supervision. I am still yet met someone who matches her knowledge of the ageing field, and her feedback has been invaluable throughout this project. I would also like to thank all the members of my lab, past and present, who have made my experience of academia thoroughly enjoyable. Special thanks go to Nikolaos Tataridas Pallas, Max Thompson, and Alex Howard, who have each kept me company in the lab during some of those longer evenings, and collectively many of the days. I would also like to thank Isabel Gonçalves Silva and Yasir Malik for their wealth of experience and engaging conversation both in and outside of the lab. A big thanks to Jack Doolan, who together with Nikolaos, has encouraged me to take care of myself physically as well as mentally. Thank you to Alex Bones, for reminding me why we are researchers. I additionally want to thank Abigail King for her endlessly reassuring optimism during the earlier years of my degree, and Sarah Bischoff, for encouraging me to explore outside my comfort zone, and for being a valued friend since the day we met.

A massive thank you to the entire Kent Fungal Group, who have been welcoming and friendly, and provided plenty of opportunities to discuss research and socialise. As well as all of the people mentioned here, there are countless others within the School of Biosciences, and the university, who have been friendly and supportive, making my PhD experience infinitely more enjoyable.

I would also like to acknowledge my examiners, Professor David Carling and Dr. Marina Ezcurra. It is an honour to have you judge the quality and relevance of my work.

Finally, I would like to thank my sister and especially my parents. You have always supported me in whatever I want to do, no matter what, and for that I am forever grateful.

Table of Contents

List of abbreviations.

4E-BP1 – Eukaryotic translation initiation factor 4E (eIF4E)-binding protein 1.

AICAR – 5-Aminoimidazole-4-carboxamide ribonucleotide.

AKT – Protein Kinase B.

AMP – Adenosine monophosphate.

AMPK – AMP-activated protein kinase.

CAMKKβ – Ca^{2+}/Calmodulin-dependent kinase kinase β.

CBD – Carbohydrate-binding domain.

CBS – Cystathionine-β-synthase.

CGC – *Caenorhabditis* Genetics Center.

CRTC-1 – cAMP-responsive element binding protein-regulated transcription coactivator 1.

DR – Dietary restriction.

FOXO – Forkhead box protein (Class O) (DAF-16 in *C. elegans*).

GTP – Guanosine triphosphate.

H_2O_2 – Hydrogen peroxide.

HMGR – 3-Hydroxy-3-methylglutaryl CoA reductase.

HTP – High-temperature pulse/pulsing.

IGF – Insulin-like growth factor.

IGF1R – Insulin-like growth factor-1 receptor (DAF-2 in *C. elegans*).

IIS – Insulin/insulin-like growth factor signalling.

ILP – Insulin-like peptide.

INSR – Insulin receptor.

IRR – Insulin receptor-related receptor.

IRS-1 – Insulin receptor substrate 1.

LKB1 – Liver kinase B1.

MAPK – Mitogen-activated protein kinase.

mTORC1 – Mammalian target of rapamycin complex 1.

NGM – Nematode Growth medium.

PCR – Polymerase Chain Reaction (shorthand for common protocol).

PDB – Protein data bank (online resource).

PDK1 – 3-Phosphoinositide-dependent protein kinase-1.

PFKFB2 – 6-Phosphofructo-2-kinase/fructose-2,6-biphosphatase 2.

PGC-1α – Peroxisome proliferator-activated receptor gamma coactivator-1α.

PI3K – Phosphoinositide 3-kinase (AGE-1 in *C. elegans*).

PIP_3 – Phosphatidylinositol 3,4,5-triphosphate.

PRAS40 – Proline-rich Akt substrate of 40 kDa.

PTEN– Phosphatase and tensin homolog.

qRT-PCR – Quantitative reverse transcription PCR.

Raptor – Regulatory-associated protein of mTOR.

Rictor – Rapamycin-insensitive companion of mammalian target of rapamycin.

ROS – Reactive oxygen species.

RT – Room temperature.

S6K – (p70) Ribosomal S6 kinase β1.

SDS – Sodium dodecyl sulphate.

SEM – Standard error of the mean.

SGK – Serine/threonine kinase subfamily.

SKN-1 – Skinhead-1.

SOD – Superoxide dismutase.

TAK1 – Transforming growth factor-β-activated kinase 1.

TBC1D1 – TBC1 domain family member 1.

TBS-T – Tris-buffered saline (0.1% Tween).

TGF-β – Transforming growth factor β.

TOR – Target of rapamycin.

TSC – Tuberous sclerosis complex.

ULK – UNC-51-like kinase.

WT – Wild-type.

ZMP – AICAR monophosphate.

List of figures.

List of tables.

Abstract.

Life expectancy increased dramatically during the 20th century and gave rise to a variety of age-related diseases which affect modern society. Recent studies investigating the relationship between energy homeostasis and longevity imply that nutrient-sensing pathways are important for determining lifespan. AMP-activated protein kinase (AMPK) is a key metabolic regulator which responds to changes in the AMP:ATP ratio within cells, promoting a metabolic shift towards increased catabolism and autophagy during a low-energy state to promote restoration of cellular energy supply. AMPK is a heterotrimeric protein consisting of α catalytic, β linker and γ regulatory subunits. AMP binds to specific, evolutionary conserved residues in the γ subunit, initiating a conformational change across the kinase and allosterically regulating its activity.

Previous work in the nematode worm *Caenorhabditis elegans* has demonstrated that AMP-sensitivity is important for AMPK-mediated contributions to longevity. Here, I use this genetic model to further explore the functional roles of AMPKγ and investigate the relationship between AMP binding, physiology, and lifespan more closely. *C. elegans* are unusual because they have five different AMPKγ subunits which are believed have different abilities to bind AMP. Using *C. elegans*, I create two alternative models of AMPK function, believed to be AMP-sensitive and AMP-insensitive. Through investigations into AMPK activation, I show that an *aakg-1; aakg-2; aakg-3* knockout is unable to respond normally to AMP, which may contribute to substantial shortening of lifespan. Additionally, I have also found that the sensitivity of AMPKγ to AMP is important for stress resistance, fecundity, and dauer.

Taken together, my analysis shows that alternative modes of AMPK activation affect several aspects of worm physiology, suggesting that AMPKγ holds potential pharmacological relevance, which in some cases can be separated from AMPKα.

Chapter 1 – Introduction.

1.1 Ageing.

Over the course of the last century, relatively huge increases to lifespan have dramatically changed the demographic of the human population worldwide. In the second half of the twentieth century the global population increased more than two-fold – the human population increasing in number quicker than at any other time in recorded history. While the total world population stood at 2.5 billion in 1950, it jumped to 6.5 billion by 2005 (Cohen, 2005; Bongaarts, 2009). This has already substantially affected the way that countries manage their economies, and now more developed countries like the United Kingdom, United States, and Japan are beginning to see the scale of societal challenges that arise with an ageing population. Despite falling birth rates in most developed countries, rapid population expansion is predicted globally as developing countries continue to grow. This will continue to have massive effects on the environment, society and economy in the coming decades (Lutz and Qiang, 2002).

Modern advancements in quality of life have lowered death rates, and this has been largely attributed to advances in medicine and medical technology which have extended the lifespan that most people can now expect to live (Bongaarts, 2009). Over 65s are now the fastest-growing age group worldwide and this is expected to continue, from around 9% in 2019, to 16% over the next 30 years (United Nations: Department of Economic and Social Affairs - Population Division, 2019). In combination with falling birth rates in developed countries, several governments are now being faced with some concerning statistics regarding the future of social care and healthcare. The potential support ratio, which equates the number of working 25-64-year-olds to people over 65 in a country, has been falling. Japan is currently showing the lowest ratio at just 1.8, but ratios are under 3.0 for another 29 countries around the world (Lutz and Qiang, 2002; United Nations: Department of Economic and Social Affairs - Population Division, 2019). One of the biggest issues facing developed countries is the treatment of age-related diseases, many of which require ongoing care. Between April

2017 and March 2018, local authorities spent £17.9 billion supporting adult social care (NHS Digital, 2018). This number is expected to rise consistently in the future, increasing the burden on an already struggling system of healthcare. Current costs are unsustainable, leading many patients to consider private healthcare as an alternative.

Age represents a significant risk factor in the development of chronic conditions (cardiovascular disease, neurological conditions, and cancers), and people often begin to suffer with multiple chronic conditions as they enter the later stages of their life, exacerbating healthcare costs and decreasing quality of life (Barnett *et al.*, 2012; Yarnall *et al.*, 2017). Current treatments often target chronic conditions individually, which not only leaves other existing conditions unaddressed, but treatments themselves can also carry side effects which increase the patient's risk of developing other conditions either during or after treatment.

By choosing to investigate ageing as a common risk factor, it is possible to address the issue of population healthspan; preventing the occurrence of these age-related pathologies could reduce the amount of time that people spend undergoing treatment, and some research suggests that individuals who avoid development of chronic conditions display longer lifespans (Doblhammer and Kytir, 2001; Christensen *et al.*, 2009). Despite the relative youth of ageing as a field of study, some potential interventions are already being investigated, using what we know about the genetic, metabolic, and environmental factors that affect ageing.

Ageing is a process that affects most organisms, although a few exceptions exist in nature (hydras, some jellyfish and the rougheye rockfish to name a few (Guerin, 2004; Boehm *et al.*, 2012)). However, organisms which demonstrate extreme longevity often prove to be "exceptions to the rule", and therefore the transferability of information gained from studying these organisms is questionable. Therefore, ageing research often refers to a small selection of organisms used for investigation in a laboratory setting, collectively known as model organisms. These organisms include the yeast *Saccharomyces cerevisiae*, the nematode *Caenorhabditis elegans*, the fruit fly *Drosophila*

melanogaster, as well as rodent species like mice and rats (Guarente and Kenyon, 2000). The species have been chosen because they demonstrate a significant degree of conservation (in terms of genetic or metabolic processes) to aspects of human biology.

There is considerable variation in lifespan across nature, and the environmental factors which contribute to the lifespan of an organism are still not completely understood. The ability to generate lifespan extensions in laboratory animals provides the basis for modern ageing research and has already provided several potential avenues for investigation. The existence of genetic knockout strains which can display substantial lifespan extensions suggests that animal biology may contain the latent potential to extend natural lifespan. In particular, mutation of single genes involved in endocrine signalling have most consistently been linked with effects related to lifespan and healthspan in model organisms. Disruption of gene expression is thought to yield lifespan extensions by altering metabolism, or more specifically the metabolic rate, slowing the accumulation of toxic intermediates or damage (Guarente and Kenyon, 2000). In *C. elegans* the first example of this was a mutation in the *daf-2* gene, which encodes a receptor that regulates insulin signalling in worms. *daf-2* mutations can yield lifespans 2-3-fold longer than that of wild-type (WT) controls (Kenyon *et al.*, 1993; C. J. Kenyon, 2010).

Furthermore, similar mechanisms of lifespan extension may exist in humans – a study following a group of Ashkenazi Jewish centenarians discovered an increased occurrence of insulin-like growth factor-1 receptor (IGF1R) mutations compared to a control population (Suh *et al.*, 2008). Similarly, several studies have identified populations across the globe which link longevity to variants of a transcription factor called class O forkhead box protein (FOXO3A) (Willcox *et al.*, 2008; Flachsbart *et al.*, 2009; Li *et al.*, 2009; Pawlikowska *et al.*, 2009). These populations of long-lived individuals imply that genetics influences lifespan in humans and lend credit to the idea that longevity genes could be evolutionary advantageous. This is important because it indicates that genetic potential for lifespan extension exists within our own genome and is not limited to the genomes of laboratory models.

Understanding the mechanisms which dictate the activity of key metabolic pathways relating to longevity could offer us greater control over how we age.

Senescence is the term used to describe the process of deterioration with age, and is defined by loss of cellular power, hindering somatic processes such as division and growth. This loss of cellular capacity occurs naturally over time: the result of damage accumulated throughout an organism's lifespan, producing inefficiencies in key cellular processes. One characteristic associated with increasing age is the declining quality of protein maintenance, allowing damage to key cellular machinery to accumulate over time (Knoefler *et al.*, 2012).

Cellular stress can be caused through several means, including reactive oxygen species (ROS), heat shock, and extended periods of metabolic stress (Lithgow *et al.*, 1995; Haigis and Yankner, 2010). During prolonged periods of cellular stress, proteins become damaged, and this is a hallmark of cellular ageing. The way an organism responds to these stressors by adapting its metabolism is a major factor in the process of ageing. Supporting this, nutrient and stress sensors contribute to lifespan extension mechanisms in many organisms, in response to a wide variety of environmental and physiological signals (Greer and Brunet, 2008; Kumsta *et al.*, 2014; Luo *et al.*, 2017). During stressful conditions, these sensors can induce a metabolic shift towards cell protection and maintenance; protecting the animal from environmental stress and extending lifespan (C. J. Kenyon, 2010; Haigis and Yankner, 2010; Gladyshev, 2014; Riera *et al.*, 2016). An increased ability to effectively respond to stress, and combat its negative effects, is implicated as a potential mechanism for longevity. This is part of the oxidative damage theory of ageing (Brys, Vanfleteren and Braeckman, 2007). By extension, increased stress resistance can arise from repeated exposure to low amounts of toxins, this is known as hormesis (Gems and Partridge, 2008; Hartwig *et al.*, 2009; Hwang *et al.*, 2014).

In recent years, there has been extensive investigation into ROS, to ascertain how this volatile chemical species contributes to the accumulation of protein damage. Generally, organisms encounter ROS most often during respiration, when superoxide radicals are released from complexes 1 and 3 of

the electron transport chain in mitochondria (Chen *et al.*, 2003). Normally, the adverse effects of superoxide exposure are combatted by the catalysis of these radicals into hydrogen peroxide (H_2O_2) by superoxide dismutase (SOD), and subsequent reduction of H_2O_2 to water by glutathione peroxidase and catalase (Chance, Sies and Boveris, 1979; Okado-Matsumoto and Fridovich, 2001; Madamanchi and Runge, 2007). However, incremental damage over time can introduce inefficiencies in the dismutase response, allowing protein-damaging radicals to escape the mitochondria and wreak havoc on cellular machinery (Landis and Tower, 2005). Thus, effective resistance to oxidative stress may contribute to lifespan. Use of longevity mutants in laboratory models supports this theory: in *C. elegans*, animals showing deficient insulin signalling (*daf-2* mutants) live longer and are often more resistant to oxidative damage, and cell culture of mammalian species which naturally display relatively high lifespans show increased stress resistance as well (McElwee *et al.*, 2004; Kenyon, 2005). While it is understood that ROS can damage the protein machinery of cells, and that older cells show higher levels of protein disrepair, researchers continue to debate the role of ROS in ageing. This is in part because differences in exposure time produce substantial variation between ROS studies, and because of the degree of variation in responses to ROS between model organisms (Keaney *et al.*, 2004; Lapointe and Hekimi, 2010; Gladyshev, 2014; Tullet *et al.*, 2017; Santos, Sinha and Lindner, 2018).

There is also an ongoing effort to determine whether a relationship exists between longevity and reproductive health. Using *D. Melanogaster*, a study which profiled longevity in a fly population reported that long-lived flies displayed reduced progeny production, while another study found that flies which produced progeny later in life displayed extended lifespan (Luckinbill *et al.*, 1984; Zwaan, Bijlsma and Hoekstra, 1996). The latter phenomenon may also be present in human biology, since later onset of the menopause in women has been associated with increased life expectancy, suggesting that reproductive timeline may be relevant to longevity (Gagnon, 2015). Declining reproductive capacity is one of the earliest hallmarks of age in women (te Velde and Pearson, 2002; Cohen, 2004) and reproductive decline begins prior to the menopause; chances of unsuccessful pregnancies, infertility, and birth defects increase over a decade before exhaustion of oocyte supply

or significant neuroendocrine changes (te Velde and Pearson, 2002). These early indicators of reproductive decline have been associated with a reduction in oocyte quality, which increases the frequency of chromosomal abnormalities like aneuploidy (te Velde and Pearson, 2002). Despite this, human biology presents relatively long post-reproductive lifespan in women, and this phenomenon has been documented in females from other mammalian species as well; including non-human primates, dogs, and laboratory rats (Cohen, 2004).

Meanwhile, one prevalent theory in recent literature, the disposable soma theory, suggests that organisms prioritise use of energy stores through control of metabolism, balancing energy usage between two physiological states – maintenance of soma (body cells) through cellular maintenance, or maintenance of germ cells for reproductive health (Kirkwood and Austad, 2000). This theory is supported by the existence of species which die quickly (or experience shortened lifespan) after mating, (C. J. Kenyon, 2010). However, this theory remains controversial since it does not represent the norm in mammals. Additionally, there are flaws in the aforementioned reasoning for the disposable soma theory, namely the largely unexplored influence of environmental factors and predator interactions in wild populations (Humphries and Stevens, 2001; Oakwood, Bradley and Cockburn, 2001).

1.2 *Caenorhabditis elegans* (*C. elegans)* as a model organism.

C. elegans is a free-living, non-parasitic soil roundworm, part of the phylum 'Nematoda'. It is around 1mm in length, and its transparency makes observation of internal reporters much easier than other model organisms. In the lab, *C. elegans* are fed with bacteria such as OP50 (a non-pathogenic B strain of *Escherichia coli*) and in combination with ease of maintenance, the small size of *C. elegans* means that populations are relatively cheap to house and cultivate (Riddle *et al.*, 1997).

C. elegans displays sexual dimorphism, occurring naturally as males or hermaphrodites. Hermaphrodites predominate in populations, while males are produced very occasionally (representing 0.1-0.2% of the population (Hodgkin and Doniach, 1997)). Hermaphrodites are capable

of self-fertilisation, further contributing to ease of strain maintenance, and this allows for straightforward genotypic control of populations, by maintaining strains on separate agar plates. The male: hermaphrodite ratio displayed in offspring can be increased in a population primarily through two methods: heat shock at 30°C for a 3-5 hours, or alternatively, the ratio is increased to an approximate 50-50 split when males mate with a hermaphrodite. Since sperm produced from males preferentially fertilises eggs over hermaphrodite sperm, crossing using males facilitates mixing of genetic backgrounds, which is extremely useful during genetic knockout studies (Ward and Carrel, 1979; Wood, 1988). Sex determination in *C. elegans* relies on the ratio of autosomal chromosomes to sex chromosomes, incorporating a system of dosage compensation. After fertilisation, X chromosome transcript expression is repressed by half. Hermaphrodites start with two X chromosomes (XX), while males possess only one (XO), thus determining the sex of the worm (Zarkower, 2006). Some groups have explored the reasons for retention of male worms in both natural and laboratory populations, and it is widely believed that fertilisation of hermaphrodites by males (outcrossing) can be beneficial from a genetic perspective, increasing potential genetic recombination after fertilisation. This is thought to become relevant during adaptation to a new environments (Morran, Parmenter and Phillips, 2009; Chasnov, 2013).

Another interesting aspect of *C. elegans* biology is that WT adults always contain exactly 959 somatic cells. This is advantageous in a model organism because the position of these cells remains constant once worms reach maturity. *C. elegans* biology does have some obvious differences from mammalian organisation (e.g. the lack of circulatory system) as it contains several specialised tissues: the cuticle; and intestinal, muscle, and neuronal tissues. The transparency of the worm membrane presents another advantage over other models; allowing most cells to be easily identified, and phenotypic effects arising from genetic manipulation can be observed in a living multicellular eukaryote (Wood, 1988). A transparent membrane allows for easy visualisation of gene/protein expression: with the use of fluorescent reporter strains, this can be monitored in *C. elegans* far more easily than in higher models.

The sharing of libraries of mutants is a further benefit of using *C. elegans*, and availability of both WT and mutant strains increased dramatically when John Sulston developed a technique for freezing strains, allowing mutant strains to be archived safely and thawed out at a later date (Riddle *et al.*, 1997). In recent years, the CRISPR-Cas9 system has also been utilised to great effect in *C. elegans*, facilitating the generation of new mutant strains quicker than ever (Paix *et al.*, 2015). Additionally, *C. elegans* was one of the first organisms to have its genome completely sequenced; many mutations are now catalogued online, and entries are available to access freely on resources like Wormbase (https://wormbase.org), increasing the accessibility of knowledge relating to *C. elegans.* Overall, the pooling of resources by researchers adds further incentive for the use of *C. elegans* in research.

1.2.1 *C. elegans* as a model for studying lifespan and stress-sensitivity.

C. elegans is one of the most commonly used and well-studied model organisms used for research into ageing. When investigating lifespan, *C. elegans* is an extremely appropriate choice given its short life cycle; allowing lifespan investigations to be completed considerably quicker than in mice or humans. *C. elegans* pass through four larval stages before adulthood (Figure 1.1), and a fertilised egg takes approximately three days to mature into a gravid adult (capable of producing its own eggs). The lifespan of WT *C. elegans* is between 2-3 weeks under optimal conditions (Riddle *et al.*, 1997). This lifespan enables the generation of population survival curve data over a series of months, rather than the years required to find similarly impactful findings in a human study. The fact that *C. elegans* can effectively model several age-related disease states (and can be used effectively in small-molecule screening) means that worms continue to be an attractive model for consideration when testing new drugs.

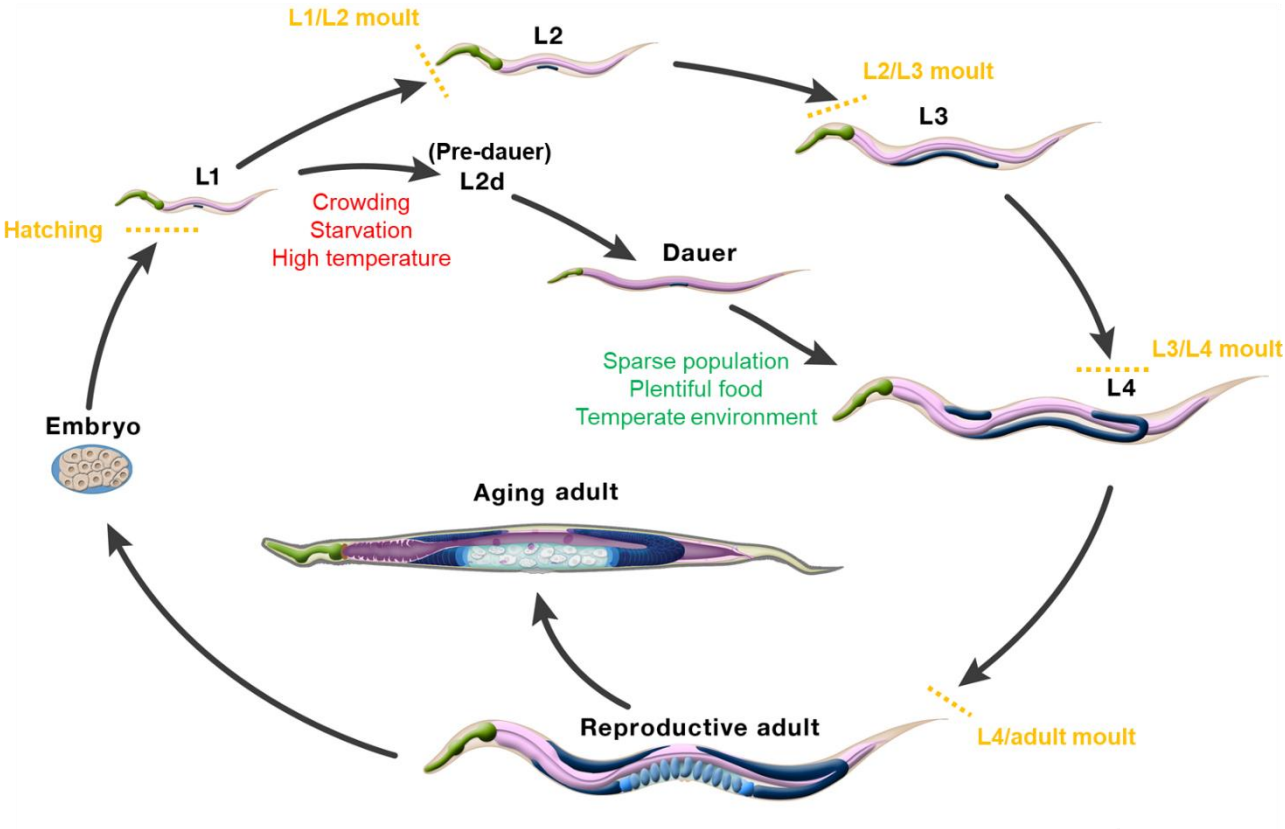

Figure 1.1| The *C. elegans* life cycle. *C. elegans* larval development includes four larval stages (named L1 through L4). Once L4 larvae moult into adults, they survive for approximately three weeks under normal laboratory conditions, and various ageing phenotypes develop through adult life. Under harsh environmental conditions, L1 larvae enter an alternative developmental stage called dauer. The dauer stage is adapted for long-term survival (up to four months) and increases chances of dispersal to new, more accommodating environments. Once in a more favourable environment, dauer larvae return to reproductive development by moulting into the L4 larval stage and progressing through the rest of the life cycle normally. Figure adapted from wormatlas.org.

Oxidative stress can be stimulated in *C. elegans* using a variety of compounds (Arsenite, H_2O_2, juglone, etc.), enabling the effects of a wide range of environmental stressors and compounds to be effectively assayed in *C. elegans*, and promoting its use when investigating pathways which mediate the phenotypic effects of stress signalling. Numerous studies have linked the activities of stress response pathways to longevity, which validates investigations into stress response when considering lifespan (Larsen, 1993; Heidler *et al.*, 2010; Schmeisser *et al.*, 2013; Schaar *et al.*, 2015). In later sections of this thesis, I explore this relationship through arsenite survival and lifespan assays, and report that oxidative stress resistance and longevity are linked in *C. elegans* mutants which demonstrate altered sensitivity to cellular energy status (Chapters 3 and 4).

1.2.2 *C. elegans* as a model for testing lifespan and reproductive capacity.

C. elegans may initially seem an unlikely choice when choosing a model for human reproduction, but several similarities exist between management of reproductive health in *C. elegans* and mammals. *C. elegans* shows declining oocyte quality with age, and there is a notable degree of evolutionary conservation in the regulatory mechanisms which maintain oocyte quality and determine reproductive health in *C. elegans*, mice and humans (Hamatani *et al.*, 2004; Steuerwald *et al.*, 2007; Luo *et al.*, 2010). Interestingly, the reproductive window in hermaphrodite worms spans somewhere between a third and half of lifespan when well-fed (Hughes *et al.*, 2007; Luo *et al.*, 2010). This regularity in reproductive timeline and oocyte quality means that progeny production is often used as a general measure of overall health for *C. elegans* strains.

Removal of the *C. elegans* reproductive system in its entirety does not result in lifespan extension, suggesting that a direct trade-off mechanism does not exist. On the other hand, a lifespan extension of 60% occurs when germs cells are removed but other reproductive tissues are left intact (Arantes-Oliveira *et al.*, 2002; C. J. Kenyon, 2010). Overall, there is support for link between lifespan to reproductive health, but tissue-specific and time-dependent reproductive signalling are implicated in determining the rate at which an organism will age (Arantes-Oliveira *et al.*, 2002; C. Kenyon, 2010).

1.2.3 Dauer.

In nature, young (L1 and L2 stage) worms enter a state of diapause in response to harsh environmental stresses, namely reduced nutritional availability or high temperature (Figure 1.1) (Ailion and Thomas, 2003). These worms display arrested growth, and development only resumes after conditions improve, yet developing worms can persist in a long-lasting stage known as dauer. One interesting by-product of the dauer state is that it allows worms with adaptations which provide improved survival mechanisms to persist through stressful environmental conditions; allowing them to survive long enough to pass on their alleles, while other species may lose some adaptations through natural selection (Kenyon, 2005).

Dauer larvae show significant morphological differences compared to larvae that develop in nutritionally replete conditions, allowing them to be identified in multiple-stage populations of *C. elegans*. Dauer larvae are radially constricted, causing them to maintain a thinner diameter in comparison to L3-stage larvae and subsequent developmental stages. They also possess a specialised cuticle, visible when identifying dauers under a microscope (Cassada and Russell, 1975). The buccal cavity of dauer larvae is closed through secretion of an internal plug, while the pharynxes are constricted and effectively do not pump, restricting food intake for the duration of dauer (Cassada and Russell, 1975; Riddle, Swanson and Albert, 1981; Vowels and Thomas, 1992). These changes are understood to provide resistance to number of chemical stressors, including 1% sodium dodecyl sulphate (SDS) solution, and this has been reported as a selection pressure for identifying dauers within *C. elegans* populations (Cassada and Russell, 1975).

Dauers also demonstrate significantly altered metabolism compared to other larval stages. Between L1 and L2 stages, L1 worms undergo significant metabolic change: shifting from focusing on glyoxylate cycle activity and producing carbohydrates from fat stores, to relying on oxidative metabolism and the TCA cycle. Dauer larvae do not undergo this metabolic shift, instead continuing to rely on lipid stores built up before entrance into dauer (Wadsworth and Riddle, 1989; Burnell *et al.*,

2005). Additionally, dauer larvae have reliably shown increased SOD activity, implying that dauer larvae are more resistant to metabolic stress during this unusual metabolic state (Larsen, 1993; Vanfleteren and De Vreese, 1995).

The dauer state is quite specific to *C. elegans*, and while a few other organisms have similar strategies (collectively termed cryptobiosis), human biology lacks anything similar physiologically. However, investigating dauer can still reveal the molecular mechanisms which govern the ability of *C. elegans* to drastically manipulate its metabolism, and persist in this state for an extended period. Moreover, researching dauer might provide transferrable insights into processes which determine the limits of human metabolism, since key energy metabolism pathways have been well-conserved between *C. elegans* and humans (Jones and Ashrafi, 2009). In addition, dauer can act as an indicator of substantial metabolic change during development, since dauer entry has been associated with disruption of key signalling networks like the insulin/insulin-like growth factor signalling (IIS) and transforming growth factor β (TGF-β) pathways (Ren *et al.*, 1996; Kimura *et al.*, 1997; Wolkow *et al.*, 2000). Furthermore, conventional agonists associated with induction of dauer recovery do not induce recovery in *daf-2* mutants, suggesting that IIS is important for recovery from dauer as well as entry (Tissenbaum *et al.*, 2000). Therefore, IIS was considered during generation of new mutant strains during this project (Chapter 3.2), facilitating investigations into dauer entry and recovery in response to altered energy regulation, described in further detail later (Chapter 4.4).

1.3 Pathways and processes that control ageing (in *C. elegans*).

The process of ageing is regulated by an extensive network of interactions between key signalling pathways, predominantly involving nutrient-sensing pathways, including the IIS and target of rapamycin (TOR) pathways (Kenyon *et al.*, 1993; Vellai *et al.*, 2003). Other central metabolic regulators like AMPK also play a key role, transmitting metabolic changes which alter the balance between cellular anabolism and catabolism (Apfeld *et al.*, 2004). Additionally, recent literature has revealed how AMPK, IIS, and TOR can each be manipulated through approaches like dietary restriction

(DR), whereby control of diet modulates the activity of key metabolic controllers found in nutrient-sensing pathways (Greer, Dowlatshahi, *et al.*, 2007; Panowski *et al.*, 2007; Greer and Brunet, 2009; Honjoh *et al.*, 2009). These processes will be explored in detail in the following sections.

1.3.1 Insulin/insulin-like growth factor signalling (IIS).

Many key signalling pathways in *C. elegans* show a high degree of conservation with mammalian orthologues, establishing it as an invaluable model to explore the genetic basis of a wide variety of pathways, including those involved in energy metabolism (Hardie and Hawley, 2001; Jia, Chen and Riddle, 2004; Jones and Ashrafi, 2009). As an important signalling cascade, many elements of IIS have been conserved between *C. elegans* and humans (Wolkow *et al.*, 2002; Kenyon, 2005). One key difference is the number of receptors between these two species. Three IIS receptors are present in mammals: the insulin receptor (INSR), IGF1R, and insulin receptor-related receptor (IRR) (Mathi, Chan and Watt, 1995; Hirayama *et al.*, 1999; Boucher, Tseng and Kahn, 2010; Deyev *et al.*, 2011). In contrast, there is only one insulin receptor in *C. elegans*. Encoded by the *daf-2* gene, the DAF-2 receptor is similar in identity to IGF1R and INSR in mammals. The presence of only one IIS receptor makes *C. elegans* an excellent model to investigate the effects of reduced IIS.

In *C. elegans*, the IIS pathway is activated through insulin-like peptide (ILP) ligands and circulating levels of ILPs vary in response to sensory information and nutrient availability. Approximately 40 genes encode putative ILPs, and this includes both agonists and antagonists of the DAF-2 receptor; DAF-2 regulates IIS in response to ILP binding, which catalyses an extensive signalling cascade through downstream effectors which influence a wide variety of physiological processes (Pierce *et al.*, 2001; Li, Kennedy and Ruvkun, 2003; Fernandes de Abreu *et al.*, 2014). In contrast, the mammalian insulin-like superfamily contains 10 ILPs, but only insulin and insulin-like growth factors (IGF-1 and IGF-2) show IIS-related tyrosine kinase binding (i.e. involving IGF1R and INSR). Additionally, circulating levels of IGF-1 and IGF-2 are regulated by growth hormone signalling and IGF-binding proteins (Werner, Weinstein and Bentov, 2008). The *C. elegans* DAF-2 receptor shares ~30% sequence

homology with the human INSR receptor, though the basic composition of IIS receptors (two heterodimers with an extracellular α domain) is largely conserved across species (Kimura *et al.*, 1997). Deletion mutants of *daf-2* are not viable, so point mutations of *daf-2* are used to partially reduce function. The location of mutation on the DAF-2 receptor impacts upon the severity of phenotypes, and point mutations are typically clustered around key domains of the receptor (Patel *et al.*, 2008). Additionally, *daf-2* mutant alleles are classified as either class 1 or class 2 mutations based on the severity of resulting phenotypes (Gems *et al.*, 1998).

Reduced IIS causes *C. elegans daf-2* mutants to exhibit arrested growth during development and enter dauer, a prolonged state of diapause, normally induced in response to harsh environmental conditions (Figure 1.1)(Gottlieb and Ruvkun, 1994). Admittedly, most *daf-2* alleles produce temperature-sensitive dauer entry (entry at lower temperatures than WT worms), but the *daf-2(m65)* allele results in unconditional dauer entry, requiring genetic balancers to enable maintenance of the strain (Gems *et al.*, 1998). Importantly, mutations which reduce DAF-2 activity consistently produce longevity phenotypes in non-dauer worms, approximately doubling lifespan (Kenyon *et al.*, 1993; Lin *et al.*, 1997). This has contributed to the status of *C. elegans* as a model organism of choice when exploring the biological processes which link energy metabolism to longevity.

Mammalian symptoms of reduced IIS can be more severe – knocking out the insulin receptor gene in adult mice causes animals to suffer with diabetes (C. J. Kenyon, 2010; Wang *et al.*, 2019). However, similarly to worm and fly models, partial inactivation of IGF1R in mice has been associated with lifespan extension. Brain-specific reduction of IGF1R has been connected to both metabolic change and lifespan extension, suggesting that neuroendocrine signalling during development might contribute to determination of mammalian lifespan (Holzenberger *et al.*, 2003; Kappeler *et al.*, 2008). In addition, murine studies report that both direct and indirect reduction of circulating levels of active IGF-1 extend lifespan, while reducing insulin levels can extend lifespan independently of circulating levels of IGF-1 or *Igf1* expression (Svensson *et al.*, 2011; Lorenzini *et al.*, 2014; Templeman *et al.*, 2017).

In human studies, longevity has been linked to mutation of both *IGF1R* and *INSR* (Kojima *et al.*, 2004; Suh *et al.*, 2008). Variations in *IGF1R* result in lower circulating levels of IGF-1 and are more common in long-lived individuals (Bonafè *et al.*, 2003).

Binding of insulin-like agonists to DAF-2/IGF1R catalyses a phosphorylation-induced signalling cascade which is mediated through two key transduction pathways: phosphoinositide 3-kinase (PI3K)/protein kinase B (AKT) and Ras/mitogen-activated protein kinase (MAPK)(Figure 1.2). Although the Ras/MAPK pathway shows a substantial degree of conservation between *C. elegans* and humans, and influences germline proliferation and dauer larval development, here I choose to focus on the more canonical PI3K/AKT pathway. I focus on PI3K/AKT because it is more directly involved in the regulation of the transcription factor DAF-16/FOXO (known as DAF-16 in *C. elegans*), which has been more extensively linked to AMPK – the subject of this thesis (Nanji, Hopper and Gems, 2005; Chi *et al.*, 2016; Templeman and Murphy, 2018). Furthermore, inhibition of Ras/MAPK signalling in flies only extends lifespan by as much as 8%, so currently the PI3K/AKT pathway appears to hold greater potential for new ageing intervention therapies (Slack *et al.*, 2015).

In the PI3K/AKT pathway, DAF-2/IGF1R activates AGE-1/PI3K (known as AGE-1 in *C. elegans*), which is mediated by insulin receptor substrate 1 (IRS-1) in mammals (Figure 1.2), whereas *C. elegans* IIS uses an adaptor subunit (AAP-1) and putative IRS homolog (IST-1) to communicate this event (Wolkow *et al.*, 2002). Activation of AGE-1/PI3K catalyses the generation of the second messenger molecule phosphatidylinositol 3,4,5-triphosphate (PIP_3). PIP_3 levels are negatively regulated at this stage via phospholipid phosphatases including DAF-18/phosphatase and tensin homolog (PTEN; known as DAF-18 in *C. elegans*)(Maehama and Dixon, 1998). PIP_3 then stimulates the recruitment and activation of 3-phosphoinositide-dependent protein kinase-1 (PDK1); in turn activating AKT (Templeman and Murphy, 2018). Curiously, *C. elegans* contains two AKT proteins, AKT-1 and AKT-2, and combined knockdown is required to ablate the physiological effects of AKT signalling (Paradis *et al.*, 1999). In both organisms, AKT has many targets, though one of principal importance to longevity,

stress and reproduction is the transcription factor DAF-16/FOXO (Brunet *et al.*, 1999; Kops *et al.*, 1999; Salih and Brunet, 2008). Phosphorylated FOXO is unable to enter the nucleus where it modulates target gene expression, and its exclusion leads to reduced expression of genes involved in cell maintenance, stress responses, protein homeostasis, and metabolic regulation (Murphy *et al.*, 2003; Webb, Kundaje and Brunet, 2016).

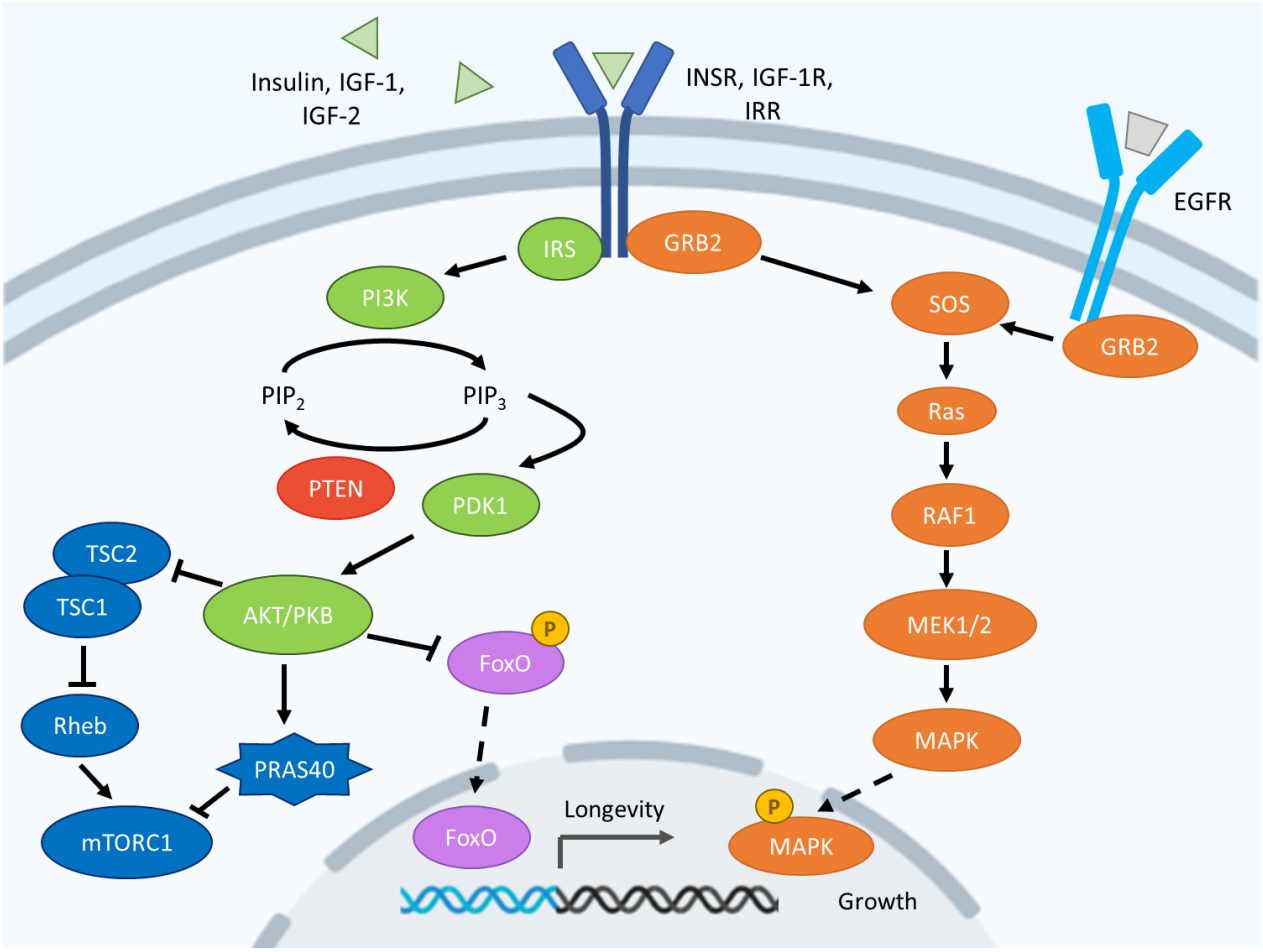

Figure 1.2| Insulin Receptor Signalling. In mammalian cells, IIS is initiated through binding of insulin or IGF-1/2 to INSR and IGF1R. Insulin is the primary ligand for the INSR receptor, though IGF-1 and IGF-2 can bind with reduced affinity (Boucher, Tseng and Kahn, 2010). Another receptor, IRR, responds to increased (alkaline) pH and is found in the stomach, kidneys, and pancreas (Mathi *et al.*, 1995; Hirayama *et al.*, 1999; Deyev *et al.*, 2011). Receptor activation promotes the activation of PI3K by IRS, which catalyses an intracellular signalling cascade known as the PI3K/AKT pathway. This culminates in up-regulation of AKT activity, which acts to inhibit function of the FOXO transcription factor family (FOXO1,3 and 4 (Brunet *et al*., 1999; Kops *et al*., 1999; Salih and Brunet, 2008)). When IIS is reduced, the FOXO transcription factor remains unphosphorylated. Nuclear FOXO is typically found unphosphorylated at the AKT site and acts on promoter sequences of genes associated with longevity and stress resistance, up-regulating their expression. When active, AKT additionally modulates mammalian target of rapamycin complex 1 (mTORC1) activity. AKT removes inhibition of mTORC1 via tuberous sclerosis complexes 1 and 2 (TSC1/2) and phosphorylates the inhibitory mTORC1 component proline-rich AKT substrate of 40 kDa (PRAS40). Activation of the insulin receptors also triggers another signalling cascade through the Ras/MAPK pathway. The Ras/MAPK cascade can also be activated by other key signalling receptors, such as epidermal growth factor receptors (EGFR), and culminates in the promotion of growth response, via the activity of phosphorylated MAPK in the nucleus.

The relevance of IIS to longevity is apparent from investigations into its downstream components. Complete knockouts of AGE-1/PI3K in *C. elegans* enter dauer, then eventually recover and display lifespans up to ten times longer than WT worms (Ayyadevara *et al.*, 2009). Lifespan extensions of this scale are not as commonly reported in mammalian studies, and impressive lifespan increases like this provide further incentive to continue investigating ageing in *C. elegans*. Decreased expression levels of the AGE-1 catalytic subunit also extend lifespan in *C. elegans*, alleviating DAF-16 inhibition via AKT (Friedman and Johnson, 1988). Reduction-of-function mutations which influence PI3K/AKT signalling can additionally affect *C. elegans* lifespan through similar components and mechanisms that contribute to improved dauer survival (Wang and Kim, 2003; Ewald *et al.*, 2015). Moreover, a branch of TGF-β signalling associated with dauer entry also contributes to longevity through interactions with the IIS pathway and resulting effects on DAF-16 localisation (Shaw *et al.*, 2007). Importantly, modulation of IIS pathway can produce longevity phenotypes in animals which have never entered the dauer stage, and show normal reproductive competency; indicating that lifespan can be extended independently of the metabolic reprogramming associated with dauer (Kenyon *et al.*, 1993; Dillin, Crawford and Kenyon, 2002).

There are a few factors which reportedly distinguish between aberrations to IIS which result in longevity, and those which produce shorter lifespans. In both *C. elegans* and *D. melanogaster*, longevity phenotypes are linked to a reduction of insulin production, or decreased insulin receptor signalling. This reduces IIS flux, promoting DAF-16/FOXO activity (Figure 1.2), which is consistently linked with longevity and a metabolic shift towards cell maintenance (Kenyon, 2005). This suggests there is a conserved role in longevity for the IIS receptor and DAF-16/FOXO in both *C. elegans* and *D. melanogaster*, because reduction-of-function mutations can produce lifespan-extending phenotypes (Kenyon *et al.*, 1993; Tatar *et al.*, 2001). In both worms and flies, respective FOXO homologues have been extensively linked to longevity, establishing FOXO as key effector of IIS signalling (Lin *et al.*, 1997; Ogg *et al.*, 1997; Slack *et al.*, 2011). Importantly, *daf-2* longevity is dependent on the DAF-16 transcription factor. This was demonstrated through suppression of *daf-16* expression in *daf-2(e1370)*

mutants, where *daf-2; daf-16(m26)* combination mutants do not display increased lifespan (Kenyon *et al.*, 1993). Reduction-of-function *daf-2* mutants also exhibit an extended reproductive period, which is dependent on DAF-16 activity in somatic tissue (some *daf-2* alleles additionally report lower numbers of progeny) (Kenyon *et al.*, 1993; Hughes *et al.*, 2007; Luo *et al.*, 2010). Consequently, DAF-16 has been investigated extensively in recent literature, to ascertain the mechanisms involved in its contribution to *daf-2*-mediated longevity. DAF-16 is a key regulator of many genes (including regulatory subunits of AMPK in *C. elegans*), which makes it difficult to ascertain a core mechanism for its contribution to *daf-2* mutant longevity. Target proteins of DAF-16 are typically regulators of signalling pathways; often kinases, phosphatases, and other transcription factors, which might explain the range of effect arising from DAF-16 activity.

Several other transcription factors (e.g. Heat shock factor 1, skinhead-1 (SKN-1) and PQM-1) have been linked to IIS- and DAF-16-mediated effects on stress resistance, metabolism and innate immunity that contribute to longevity (Tullet *et al.*, 2008; Chiang *et al.*, 2012; Ewald *et al.*, 2015). In many cases these transcription factors act in combination with DAF-16, and affect other pathways as well – the level of cross talk which occurs between major signalling pathways is extensive, and this level of complexity must be carefully considered when examining processes like ageing, stress resistance and reproduction (Seo *et al.*, 2013; Tepper *et al.*, 2013).

Interestingly, lifespan extension achieved through removal of germ cells is associated with increased activity of DAF-16 (Arantes-Oliveira *et al.*, 2002; C. Kenyon, 2010). Somatic changes in IIS have already been extensively linked to both lifespan and reproductive status, and reproductive tissues are also reported to have non-cell-autonomous effects towards lifespan, suggesting that additive extensions of lifespan are possible. For example, the lifespan of long-lived *daf-2* mutants can be further extended when the germ line is absent. Loss of the germ line produces disruptions to steroid signalling which culminate in the activation of *tcer-1* gene expression (Amrit *et al.*, 2016). Nuclear accumulation of the transcription factor DAF-16 in intestinal cells (initiated by loss of the germline) is

thought to act together with transcription elongation regulator homolog-1 to increase transcription of lipase mRNA. It is implied that increased DAF-16-regulated lipase activity may facilitate further extension of lifespan, independent from conventional reduced IIS/DAF-16 mechanisms (C. J. Kenyon, 2010).

Investigations into some key mechanisms affecting reproductive processes appear to imply interdependence between reproductive health and longevity in *C. elegans*. In *C. elegans*, complete ablation of germline stem cells confers a substantial lifespan extension, though this does not represent complete infertility; additional ablation of the supporting somatic gonad tissue removes this longevity phenotype (Arantes-Oliveira *et al.*, 2002). Additionally, mutations which result in infertility through effects on oocyte or sperm formation do not produce lifespan extensions (Arantes-Oliveira *et al.*, 2002). In reported cases where germline loss results in lifespan extension, signalling changes in the associated somatic tissues are required to modulate the nuclear localisation of DAF-16, a conserved target of the IIS pathway in worms and humans (Berman and Kenyon, 2006; Ghazi, Henis-Korenblit and Kenyon, 2009). Alteration of DAF-16 activity affects processes like fatty acid synthesis and autophagy, and DAF-16 is capable of communicating non-cell-autonomously, which increases its range of effect to several tissues throughout worms, including reproductive tissues. Still, DAF-16/FOXO and other downstream components of IIS are the not the only effectors which demonstrate a link between reproduction and lifespan. Similar signalling strategies have been found with TGF-β signalling via the Sma/Mab pathway, where non-cell-autonomous effects generated in somatic tissues have been linked to the rate of reproductive ageing and maintenance of oocyte quality (Luo *et al.*, 2010).

A high degree of complexity becomes apparent when dissecting approaches which affect lifespan and reproductive health in *C. elegans*. While *daf-2* RNAi treatment during adulthood results in extended lifespan, down-regulation of IIS during late larval stages or early adulthood has additional effects on reproduction; highlighting the importance of developmental signalling in proper control of somatic and reproductive maintenance (Dillin, Crawford and Kenyon, 2002; Luo *et al.*, 2010).

Additional complexity becomes apparent when considering the influence of tissue-specific regulation on longevity and reproductive health. DAF-16 activity in hypodermis and intestine, but not muscle tissue, contributes to the longevity phenotype displayed by *daf-2* mutants (Libina, Berman and Kenyon, 2003; Zhang *et al.*, 2013). At the same time, DAF-16 extends the reproductive window of *daf-2* mutants through its effects on intestinal and muscle tissues, and additionally acts in the somatic gonad tissues to support maintenance of progenitor cells in the germline (Luo *et al.*, 2010; Qin and Hubbard, 2015). The tissue-specific and time-dependent roles of DAF-16 in regulation of lifespan and reproductive health explain why common mechanisms which benefit both lifespan and reproduction have been so difficult to determine. Despite this, the *C. elegans* intestine is one tissue that has been associated with control of both lifespan and reproduction and is now proving to be an important regulatory tissue in *C. elegans*, further implicating the relevance of energy metabolism to longevity and reproductive health (D. Chen *et al.*, 2013).

Across species, down-regulation of IIS is consistently associated with longevity, suggesting that the role of IIS in longevity is conserved to some extent between *C. elegans* and humans (Tatar *et al.*, 2001; Murphy *et al.*, 2003; Murphy, Lee and Kenyon, 2007; Taguchi, Wartschow and White, 2007; Templeman *et al.*, 2017). In mice, inactivation of PI3K extends lifespan, while haploinsufficiency of the gene *Akt1* also extends lifespan (Foukas *et al.*, 2013; Nojima *et al.*, 2013). In humans, a centenarian population displayed lower fasting insulin levels than a >75 year group, and increased incidence of gene variants predicted to reduce IIS flux was linked to reduced mortality in women (Paolisso *et al.*, 1996; Van Heemst *et al.*, 2005). Similarly to worms and flies, human longevity has also been linked with genetic variants of FOXO1 and FOXO3A (Lunetta *et al.*, 2007; Willcox *et al.*, 2008; Flachsbart *et al.*, 2009; Li *et al.*, 2009). Furthermore, overexpression of FOXO transcription factor variants has been connected to increased longevity in humans, implying a conserved role for FOXO in regulation of lifespan (Li *et al.*, 2009).

1.3.2 Target of Rapamycin (TOR).

Longevity-inducing drugs may have already been discovered. One promising candidate, rapamycin, inhibits the TOR signalling pathway and produces lifespan extensions in mice, even when administered during late life (Harrison *et al.*, 2009). The TOR pathway represents an important nexus of metabolic signalling, driving anabolism and growth, and acting in contrast to AMPK signalling which promotes catabolism and autophagy. TOR consists of two protein complexes: TORC1 and TORC2. In *C. elegans*, treatment with rapamycin, which inhibits both TOR complexes, results in lifespan extension (Robida-Stubbs *et al.*, 2012). Alternatively, genes influencing TORC activity have also been identified in *C. elegans*: *daf-15* encodes the TORC1 component regulatory-associated protein of mammalian TOR (Raptor), while *rict-1* encodes the TORC2 component rapamycin-insensitive companion of mammalian TOR (Rictor). In *C. elegans*, inhibition of TOR can extend lifespan, as demonstrated through the use of *daf-15/*Raptor or *let-363*/TOR mutants (Vellai *et al.*, 2003; Jia, Chen and Riddle, 2004). Interestingly, longevity in *rict-1/*Rictor mutants is sensitive to diet, and extension of adult lifespan via *rict-1* RNAi requires the transcription factor *skn-1* (Soukas *et al.*, 2009; Robida-Stubbs *et al.*, 2012). Existing literature uses the wide variety of effects displayed by different TOR pathway components to suggest that an extensive level of interaction exists between TOR and other key signalling pathways related to longevity (AMPK, IIS, and DAF-16/FOXO).

In mammals, IIS up-regulates mammalian target of rapamycin complex 1 (mTORC1) activity (Figure 1.2). AKT phosphorylates an inhibitory component of mTORC1, proline-rich AKT substrate of 40 kDa (PRAS40), preventing the association of PRAS40 with the complex and permitting increased mTORC1 activity (Sancak *et al.*, 2007). Additionally, tuberous sclerosis complex (TSC1/2)-mediated inhibition of mTORC1 is alleviated via the action of downstream kinases in the PI3K/AKT and Ras/MAPK branches of IIS including AKT, MAPK and ribosomal S6 kinase (Manning *et al.*, 2002; Roux *et al.*, 2004; Ma *et al.*, 2005). Interestingly, mTORC1 negatively regulates IIS through inhibitory phosphorylation of IRS-1 via ribosomal S6 kinase β1 (S6K), implying that a negative feedback pathway could exist here between mTORC1 and the PI3K/AKT branch of IIS (Takano *et al.*, 2001).

Mammalian FOXO3A also plays a role in regulation of mTORC1 by transcriptionally up-regulating TSC1 expression (Khatri *et al.*, 2010). Investigations in *C. elegans* suggest a similar level of interaction, since DAF-16 activity is reported to repress Raptor expression, while Raptor-mediated lifespan extension requires DAF-16 (Jia, Chen and Riddle, 2004). Interestingly, lifespan extensions achieved through mutation of TOR or treatment with rapamycin do not require *daf-16* (Vellai *et al.*, 2003; Robida-Stubbs *et al.*, 2012). Additionally, *daf-16* is not required for lifespan extensions achieved using genetic knockouts or RNAi-induced knockdown of downstream effectors of the mTOR pathway, like S6K and eukaryotic translation initiation factors eIF4E and eIF4G (Hansen *et al.*, 2007; Pan *et al.*, 2007). In *D. Melanogaster*, the mTORC1 target protein d4E-BP/eIF4E-binding protein 1 (4E-BP1) is a transcriptional target of FOXO, suggesting that the evolutionary relationship between FOXO and mTOR might extend to invertebrate species (Tettweiler *et al.*, 2005).

Mammalian cell studies have revealed additional interactions exist between IIS and mTOR signalling through mTORC2, which up-regulates AKT activity, suppressing FOXO1 and FOXO3 activity (Guertin *et al.*, 2006). Taken together, these investigations suggest that mTOR influences ageing through mechanisms that show extensive complexity and a high degree of crosstalk with neighbouring pathways, including IIS. This complexity is also apparent through the interactions of TOR with AMPK, and both TOR and AMPK continue to yield potential therapeutic targets that are functionally distinct from IIS.

1.3.3 Dietary restriction (DR).

While there is now greater understanding of pathways which contribute to ageing, we are still a long way from accessible treatments to counteract its effects, and the sheer degree of crosstalk that exists between key signalling pathways generates additional complexity when testing new treatments. A promising alternative strategy for slowing the rate of ageing is DR. Some DR protocols report impressive extensions to both lifespan and healthspan, although whether these DR protocols extend lifespan through overlapping or distinct pathways is still unclear. *C. elegans* provides a good model

system to investigate the genetic determinants of lifespan extension achieved through different DR regimens, and there are now several different approaches that have been developed to investigate DR (Greer and Brunet, 2009). Although there is significant variation between these DR protocols, the effects are often mediated through modulation of common regulators of metabolism: IIS, TOR, AMPK and sirtuins (Hansen *et al.*, 2007; Mair and Dillin, 2008; Honjoh *et al.*, 2009).

Interestingly, there is growing evidence suggesting that AMPK is essential for some DR protocols to generate lifespan extensions (Greer, Dowlatshahi, *et al.*, 2007; Schulz *et al.*, 2007; Greer and Brunet, 2009; Weir *et al.*, 2017). Moreover, while overexpression of AMPK is known to increase lifespan in *C. elegans*, activation of AMPK achieved through DR (or treatment with putative DR mimetic metformin) has also been associated with lifespan extension (Apfeld *et al.*, 2004; Curtis, O'Connor and DiStefano, 2006; Onken and Driscoll, 2010). Together these studies suggest that AMPK is an important mediator of DR-mediated longevity.

1.4 AMP-activated Protein Kinase (AMPK).

Maintenance of energy homeostasis in cells relies on several complex pathways which respond to both metabolic demand and energy store availability (Moreno-Arriola *et al.*, 2016). A common regulator of these pathways is AMPK, which can respond to increased intracellular concentrations of adenosine monophosphate (AMP). Increased concentrations of AMP indicate the depletion of ATP, which is the main energy carrier found in cells. Thus, AMPK is particularly important for maintaining cellular homeostasis during periods of low energy availability (prolonged fasting or starvation). AMP-binding catalyses the activation of AMPK, triggering phosphorylation of target proteins to restore normal energy homeostasis. Furthermore, the influence of AMPK on key signalling pathways (IIS, TOR, and DR) is associated with lifespan extension, providing even stronger incentive to investigate the mechanism of this central metabolic regulator (Apfeld *et al.*, 2004; Greer, Dowlatshahi, *et al.*, 2007). Here I begin by discussing mammalian AMPK (which is more completely understood) before discussing *C. elegans* AMPK later (Chapter 1.5).

1.4.1 Structure and Regulation.

AMPK is formed of three subunits: α, β and γ. The α subunit is the kinase domain, which phosphorylates target proteins using a serine/threonine mechanism; the γ subunit plays a significant regulatory role; and the β subunit links these domains (Woods *et al.*, 1996; Xiao *et al.*, 2011). The mammalian structure is shown below (Figure 1.3). AMPKα contains a N-terminal kinase domain and a C-terminal scaffolding domain (Xiao *et al.*, 2013). The β subunit holds an important role as a linker domain between AMPKα and AMPKγ, but it also contains a carbohydrate-binding domain (CBD) which provides additional regulation of AMPK activity in response to glycogen (Woods *et al.*, 1996; McBride *et al.*, 2009; Li *et al.*, 2015). Both the centrally-located CBD domain (AMPKβ) and C-terminal scaffolding domain are (AMPKα) well conserved in eukaryotes, implying that these regions contribute significantly to the functional regulation of AMPK (Hudson *et al.*, 2003; Hardie, 2008). The γ subunit contains four cystathionine-β-synthase (CBS) domains, which provide a structural basis for AMP-binding (Bateman, 1997; Scott *et al.*, 2004; Xiao *et al.*, 2007). AMPKγ is essential for sensing AMP levels within the cell and demonstrates allosteric regulation in response to AMP-binding (Adams *et al.*, 2004; Sanders *et al.*, 2007).

Multiple isoforms of each AMPK subunit exist in both mammals and worms (Table 1.1). There two isoforms of α and β subunits in humans, and three isoforms of AMPKγ. Expression studies in mammalian cells have revealed that the presence of all three subunits (α, β, and γ) is effectively required to provide functionally significant kinase activity (Dyck *et al.*, 1996). Interestingly, AMPK subunit isoforms show different expression between tissues, and under different conditions (Turnley *et al.*, 2001; Niesler, Myburgh and Moore, 2007; Wu *et al.*, 2013). Specifically, AMPK complexes containing the α2 isoform show increased nuclear localisation compared to AMPK containing the α1 isoform (Salt *et al.*, 1998). β1 and β2 isoforms exhibit opposite patterns of expression in rat liver and skeletal muscle tissues, and while γ1 accounts for the majority of AMPK activity in most rat tissues, all three γ isoforms contribute similarly to activity in the rat brain. (Thornton, Snowden and Carling, 1998; Cheung *et al.*, 2000). Expression levels of α and γ subunits also reportedly change with age, as

demonstrated in rat skeletal muscle (Hardman *et al.*, 2014). Together these studies suggest that tissue-specific expression and age significantly influence AMPK activity *in vivo*.

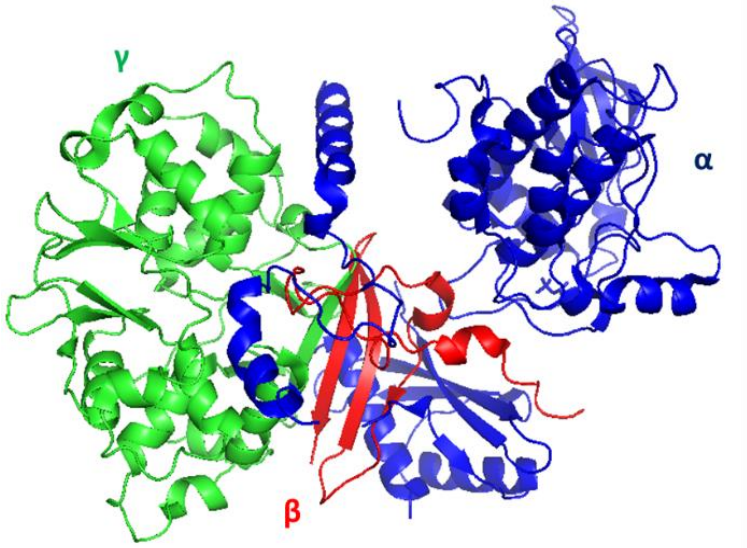

Figure 1.3| The structure of AMPK. AMPK has three subunits: α (catalytic), β (linker), and γ (AMP-sensitive). The mammalian structure is shown (PDB ID: **4CFH**). During this project, I was mainly interested in regulatory function of the γ subunit, which can bind AMP, ADP or ATP to regulate the kinase function of the α subunit.

Subunit	*H. Sapiens*	*C. elegans*
AMPKα	*PRKAA1*	*aak-1*
	PRKAA2	*aak-2*
AMPKβ	*PRKAB1*	*aakb-1*
	PRKAB2	*aakb-2*
AMPKγ	*PRKAG1*	*aakg-1*
	PRKAG2	*aakg-2*
	PRKAG3	*aakg-3*
		aakg-4
		aakg-5

Table 1.1| Genes encoding AMPK subunits in humans and *C. elegans*. There are two isoforms of AMPKα and AMPKβ in humans and *C. elegans*. However, *C. elegans* contains two more isoforms of AMPKγ in comparison to humans: *aakg-4* and *aakg-5*.

1.4.2 Activation.

AMPK detects cellular energy status through the identity of bound adenine nucleotides (AMP, ADP, or ATP). Periods of extended fasting generate increases in the cellular AMP:ATP ratio, increasing displacement of bound ATP with AMP on AMPKγ. The sensing functionality of AMPKγ is provided by four CBS domains, which are essential for proper regulation; facilitating the binding of adenine nucleotides to the protein and enabling it to respond to the metabolic status of the cell (Xiao *et al.*, 2011, 2013). AMPK has three sites which bind three adenine nucleotides: AMP, ADP, or ATP. The identity of the adenine nucleotides bound at these sites reflects the metabolic status of the cell (Xiao *et al.*, 2011, 2013). The presence of bound ATP on inactive AMPK is reflective of cellular environment – intracellular levels of ATP are often higher than AMP to maintain electrochemical gradients required for essential catabolic processes (Li *et al.*, 2015). As the AMP:ATP ratio increases, AMP eventually binds to these sites with higher affinity than ATP, replacing bound ATP (Xiao *et al.*, 2007). In this way, AMPK reliably senses metabolic status. Several key AMP-binding residues that hold particular relevance to this project are highlighted below (Figure 1.4).

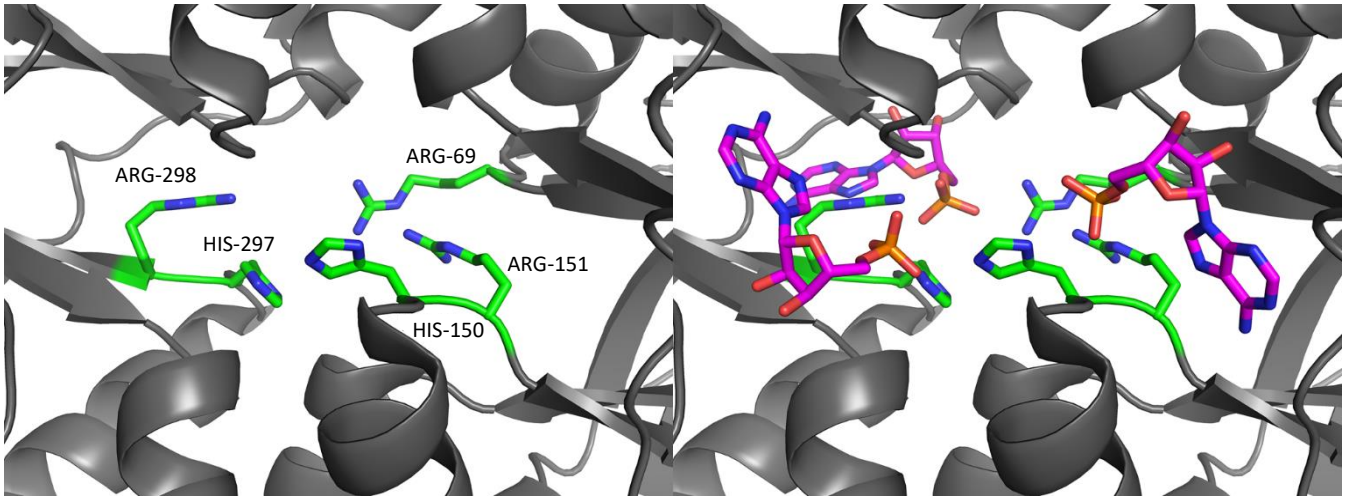

Figure 1.4| AMP-binding residues in the AMPKγ subunit. Predicted binding residues (Arg69, His150, Arg151, His297 and Arg298; PRKAG1 numbering) are shown in green. AMP molecules are coloured magenta. Additionally, important elements relevant for charge interactions are highlighted in blue (nitrogen), orange (phosphorus), and red (oxygen). An existing structural file was used to model the mammalian structure here, and provide coordinates for AMP molecules in PyMOL (PDB ID: **2V8Q**). These AMP-binding residues are conserved between a mammalian AMPKγ and *C. elegans* isoforms AAKG-1, AAKG-2, and AAKG-3; while AAKG-4 shows no conservation, and AAKG-5 only retains one pair of binding residues (equivalent to His150 and Arg151, PRKAG1 numbering)(Figure 3.1)(Tullet *et al.,* 2014).

In mammals, the sensing mechanism is based on the binding of adenine nucleotides to three binding sites on AMPKγ (Xiao *et al.*, 2007). ADP binding has been reported in mammals, but AMP binds with higher affinity (due to the stereochemistry of the binding pocket)(Hardie and Carling, 1997; Xiao *et al.*, 2011; Tullet *et al.*, 2014). Two sites on AMPKγ (site 1 and site 3) competitively bind AMP, ADP, and ATP, and are primarily responsible for the sensing properties of AMPK. Another site (site 4) does not undergo exchange and AMP remains bound (Xiao *et al.*, 2011). As previously mentioned, the AMP:ATP ratio determines binding of adenine nucleotide species to the binding sites, but AMPK also displays allosteric regulation (Sanders *et al.*, 2007; Xiao *et al.*, 2007). In fact, a 2-3-fold increase in AMP concentration is enough to catalyse replacement of bound ATP with AMP in AMPKγ binding pockets, assisted through the aforementioned allosteric activation mechanism (Xiao *et al.*, 2007). Ultimately though, the AMP: ATP ratio directly controls the kinase function of AMPK since optimal catalytic activity is only achieved once AMP replaces ATP, resulting in conformational change across the kinase which exposes a key residue on AMPKα, threonine-172. Phosphorylation of Thr172 on AMPKα represents a second level of activity regulation, and its exposure increases kinase activity more than 100-fold (Hawley *et al.*, 1996). Exposure of Thr172 is a tightly regulated event, additionally requiring myristoylation of a glycine residue (Gly2) in the N-terminal region of mammalian AMPKβ (Oakhill *et al.*, 2010).

Phosphorylation of Thr172 is known to be mediated through three upstream kinases (Figure 1.5): liver kinase B1 (LKB1), Ca^{2+}/calmodulin-dependent kinase kinase β (CAMKKβ), and transforming growth factor-β-activated kinase 1 (TAK1)(Shaw *et al.*, 2004; Hawley *et al.*, 2005; Momcilovic, Hong and Carlson, 2006). Of these, LKB1 is most consistently associated with energy stress and AMP-binding. In opposition to this, phosphorylated Thr172 can be de-phosphorylated by three phosphatases: Protein Phosphatase 1, Protein Phosphatase 2A, and Protein Phosphatase 2C (Garcia-Haro *et al.*, 2010).

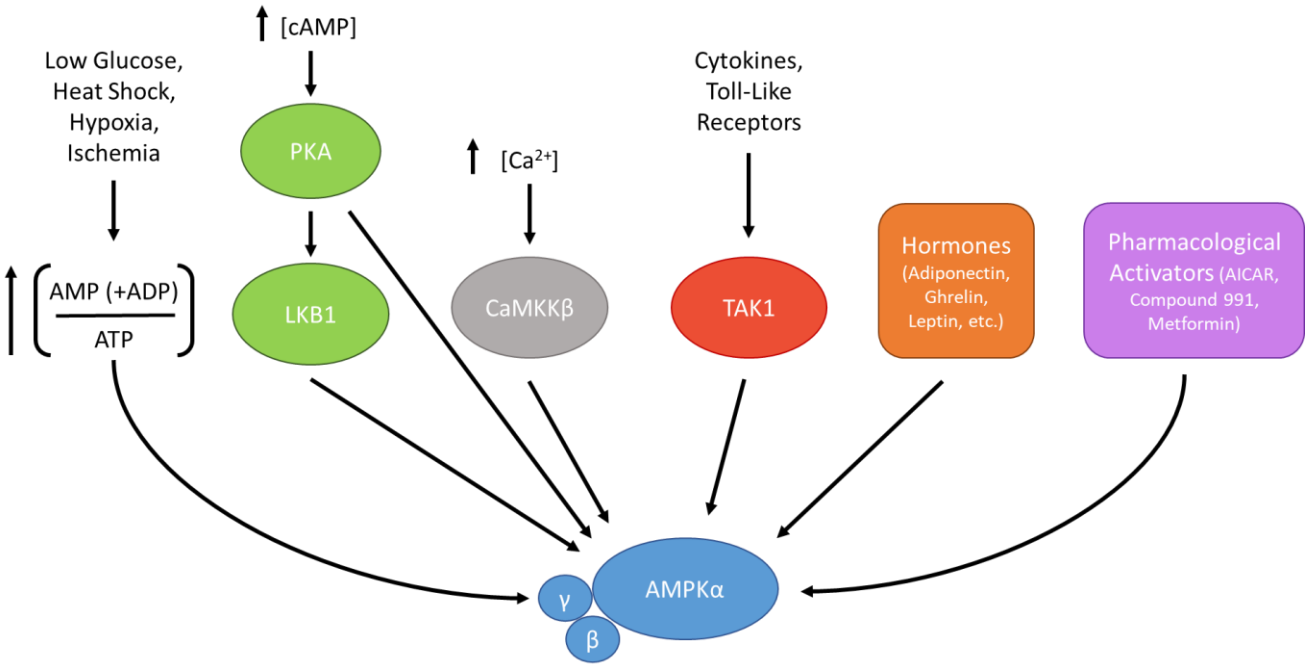

Figure 1.5| Mechanisms of AMPK activation. AMPK can be activated by a variety of mechanisms. Primarily, the AMP:ATP ratio contributes to a conformational change which improves phosphorylation via LKB1. LKB1 phosphorylation can also be up-regulated via the cAMP/Protein Kinase A (PKA) pathway, while PKA is reportedly also capable of activating AMPK itself. Tissue specificity also influences primary methods of AMPK activation; for example, the CaMKKβ pathway is believed to be more important in neuronal tissue (Hawley *et al.* 2005). Additionally, immune responses can influence AMPK activation via cytokine signalling and TAK1. Hormonal signalling also affects AMPK regulation, though hormonal effects can vary between mammalian tissue types. For example, leptin is activator of AMPK in skeletal muscle, while it acts as an AMPK inhibitor in the hypothalamus (Kola 2008). In addition, a number of pharmacological activators of AMPK have been identified, which vary in both mechanism and efficacy: 5-aminoimidazole-4-carboxamide ribonucleotide (AICAR) is an AMP-mimetic, other compounds target the CBD. There are also biguanide drugs (metformin and phenformin), though mechanism of these drugs is not fully understood (though it has been linked to LKB1 activity).

Interestingly, between the N-terminal kinase and C-terminal scaffolding region, part of the α subunit interacts with the γ subunit. This segment, referred to as the α2-hook (or α-RIM), provides an additional level of regulation to AMPK activation; communicating the presence of AMP/ADP or ATP at site 3 through interaction with Arg69 (PRKAG1 numbering), a residue which is directly involved in binding AMP (Figure 1.4)(L. Chen *et al.*, 2013; Xiao *et al.*, 2013). Crucially, the α2-hook is important for both allosteric regulation and protection of Thr172 from dephosphorylation. In summary, three outcomes arise from the binding of AMP to the γ subunit: AMPK is allosterically activated (2-3-fold), phosphorylation of the Thr172 residue is promoted, and dephosphorylation of Thr172 is inhibited by conformational change in the α subunit (Oakhill *et al.*, 2011; Xiao *et al.*, 2011; Gowans *et al.*, 2013). Overall, AMPK presents itself as a kinase with finely tuned regulation; relying on sensitive control mechanisms which regulate its activity. Importantly, structural investigations suggest that since different activation pathways exist, subtle differences in AMPK function may be possible (Xiao *et al.*, 2007; Hawley *et al.*, 2010; Slack, Foley and Partridge, 2012).

1.4.3 Pharmacological activation of AMPK.

AMPK can be naturally activated through moderate exercise, when muscle contraction increases the AMP: ATP ratio in cells, but AMPK can also be activated by certain drugs (Figure 1.4)(Lee-Young *et al.*, 2009; Coughlan *et al.*, 2014). Several pharmacological activators of AMPK have now been identified, including biguanide drugs like metformin and phenformin. Metformin is already used as an anti-diabetic in medicine, but it is also reported to extend lifespan in mice (Fryer, Parbu-Patel and Carling, 2002; Anisimov *et al.*, 2008). Metformin holds particular interest for the pharmaceutical industry since it is being explored as a potential therapy for neurodegenerative conditions such as vascular dementia, Alzheimer's disease and stroke; recent research suggests that there may be significant links between dysfunctional metabolism and development of these conditions (Risner *et al.*, 2006). Even though the mechanism of metformin is not fully understood, existing literature reports that treatment with metformin can alleviate symptoms of hyperglycaemia through inhibition of glucose production in liver tissue, and by enhancing glucose uptake in muscle (DeFronzo, Barzilai and

Simonson, 1991; Musi *et al.*, 2002; Kristensen *et al.*, 2014). Forced activation of AMPK via metformin treatment increases the activity of glycolytic and oxidative metabolism, resulting in increased lactate production, mitochondrial oxygen consumption, and decreased fatty acid/lipid stores (Moreno-Arriola *et al.*, 2016). Despite extensive evidence supporting the activation of AMPK through metformin and phenformin, the biguanide mechanism remains poorly understood, leaving the market open for alternative activators of AMPK.

Naturally occurring activators of AMPK have also been discovered in the polyphenol class of organic compounds. The polyphenol resveratrol activates AMPK, but also catalyses a number of other metabolic changes associated with lifespan extension, including increased insulin-sensitivity and reduced circulating IGF-1 levels (Baur *et al.*, 2006). Researchers have also investigated development of synthetic compounds which show more efficient activation of AMPK. The adenosine analogue, 5-aminoimidazole-4-carboxamide ribonucleotide (AICAR), catalyses phosphorylation of AMPK, acting as an AMP-mimetic. AICAR is taken into cells and phosphorylated by adenosine kinase, generating AICAR monophosphate (ZMP). ZMP then mimics AMP-induced AMPK activation, inducing allosteric activation and preventing Thr172 dephosphorylation, but ZMP can bind to AMPK irrespective of the AMP:ATP ratio (Corton *et al.*, 1995).

While both AICAR and metformin have consistently shown the ability to activate AMPK, AMPK-independent effects on glucose metabolism have been reported (Guigas *et al.*, 2006; Madiraju *et al.*, 2014). Subsequently, other activators of AMPK were discovered which appear to be more specifically targeted to AMPK. A thienopyridone compound, A-769662, directly activates AMPK as a AMP mimetic, again stimulating allosteric AMP-binding and protecting Thr172 from dephosphorylation (Göransson *et al.*, 2007). However, AMPK activation via A-769662 treatment is dependent on the integrity of the CBD on AMPKβ1 which responds to glycogen (Sanders *et al.*, 2007; Scott *et al.*, 2008). More recently, compound 991, a benzimidazole derivative, was identified and demonstrates a similar mechanism to A-769662 but shows greater potency (Xiao *et al.*, 2013). 991

also exhibits effects on glucose metabolism, but it can activate AMPK containing either AMPKβ isoform, though *in vitro* studies report a more efficient response with β1-containing complexes (Xiao *et al.*, 2013; Lai *et al.*, 2014; Bultot *et al.*, 2016). Different efficacies displayed by 991-induced AMPK activation suggests that there are still additional factors affecting regulation of AMPK activation that remain undiscovered (Xiao *et al.*, 2013; Willows *et al.*, 2017).

1.4.4 Targets of AMPK signalling.

Responding to both hormonal and nutrient signals, AMPK is involved in a wide array of processes including glucose homeostasis, lipid metabolism and body weight (Viollet *et al.*, 2003; Minokoshi *et al.*, 2004; Kola, 2008). Generally, AMPK is responsible for promoting a metabolic shift towards catabolism, and simultaneously reducing the activity of ATP-consuming (anabolic) pathways, so that cellular energy stores (in the form of ATP) can be restored. AMPK phosphorylates numerous proteins involved in processes like glycogenolysis and lipolysis, to increase the availability of ATP in cells and restore energy homeostasis (Figure 1.6). Additionally, in the mammalian brain, AMPK has been shown to promote hunger responses through regulation of a hypothalamic circuit which responds to peripheral hormones like ghrelin and leptin (Andersson *et al.*, 2004).

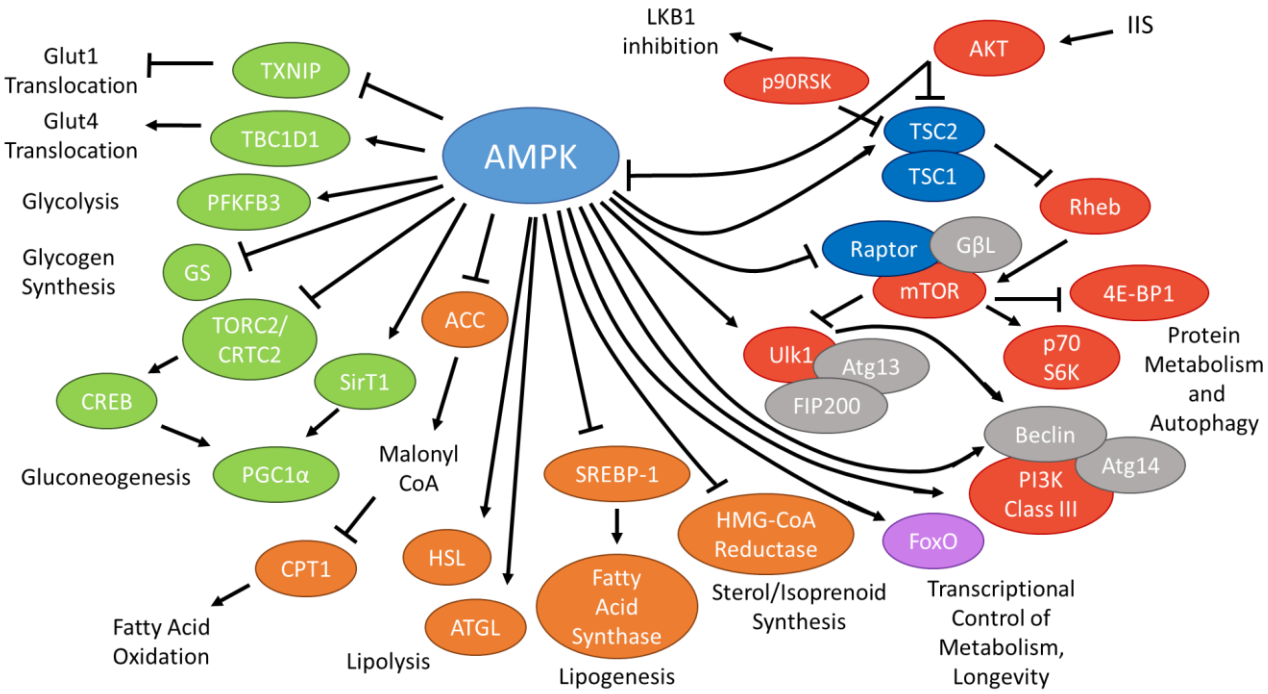

Figure 1.6| Functions of AMPK. AMPK has an extensive range of effects, regulating the action of several key metabolic pathways within glucose, lipid, and protein metabolism. A selection of functions are highlighted above. In combination with effects related to transcriptional control of longevity, AMPK contributes to a whole-organism metabolic shift towards catabolism and autophagy.

The wide array of processes regulated by AMPK has prompted substantial investigation into its mechanism. In terms of kinase activity, targets of AMPK phosphorylation have a conserved sequence motif surrounding the residue which undergoes serine/threonine phosphorylation (Hardie, Schaffer and Brunet, 2016). The presence of basic residues at -4 or -3 positions and hydrophobic residues at -5 and +4 positions (relative to the phospho-acceptor site) has been described as a recognisable motif for AMPK target proteins (Dale *et al.*, 1995; Hardie, Schaffer and Brunet, 2016).

AMPK modulates the activity of several regulatory proteins and kinases across multiple pathways to re-establish energy homeostasis. To restore levels of ATP, AMPK induces the translocation of the GLUT4 glucose transporter to the plasma membrane, enhancing glucose uptake in muscle cells (Hardie, Ross and Hawley, 2012). Within muscle cells, storage vesicles which contain GLUT4 rely on RAB-family proteins to enter an active guanosine triphosphate (GTP)-bound state. When muscle contraction occurs, AMPK phosphorylates a RAB-GAP protein, TBC1 domain family member 1 (TBC1D1), which maintains RAB proteins in the inactive GDP-bound state. The phosphorylation of TBC1D1 induces association with 14-3-3 protein, and TBC1D1 subsequently dissociates from storage vesicles. Dissociation of TBC1D1 allows the RAB protein to be converted to its active GTP-bound state, and GLUT4 storage vesicles then fuse with the plasma membrane (Geraghty *et al.*, 2007; Sakamoto and Holman, 2008; Treebak *et al.*, 2009; Chen *et al.*, 2011). In addition to the release of GLUT4 from vesicles, AMPK also stimulates increased glucose uptake through activation of the GLUT1 transporter, which is expressed in many cell types (though GLUT1 activation is not stimulated in liver, muscle, or adipose tissue) (Barnes *et al.*, 2002).

AMPK further acts on glucose metabolism through up-regulation of glycolysis – AMPK phosphorylates 6-phosphofructo-2-kinase/fructose-2,6-biphosphatase 2 (PFKFB2). Once activated through phosphorylation, PFKFB2 catalyses the production of fructose-2,6-biphosphate; an allosteric activator of the glycolytic enzyme phosphofructokinase-1 (Marsin *et al.*, 2000, 2002). While acting to increase glucose metabolism, AMPK also supports a metabolic shift away from anabolism by inhibiting

glycogen synthesis. This is primarily achieved by targeting glycogen synthase, as well as gluconeogenic enzymes such as phosphoenolpyruvate carboxykinase and glucose 6-phosphatase (Jørgensen *et al.*, 2004; Koo *et al.*, 2005; Mihaylova *et al.*, 2011).

AMPK is also understood to mediate changes in lipid metabolism, preventing storage of energy as fats. These effects are coordinated through up-regulation and down-regulation of reciprocal pathways: fatty acid uptake and β-oxidation are up-regulated, while lipogenesis, fatty acid synthesis, and triglyceride synthesis are down-regulated. Fatty acid uptake into cells is promoted via CD36-containing vesicle translocation, and in combination with this, mitochondrial uptake of fatty acids is also promoted (Habets *et al.*, 2009). Malonyl-CoA acts as inhibitor of fatty acid entry into the mitochondria, inhibiting carnitine palmitoyl transferase 1, which controls the rate-limiting step in fatty acid uptake and oxidation for mitochondria. When AMPK catalyses the phosphorylation and subsequent inactivation of acetyl-CoA carboxylase β, the inhibitory effect of Malonyl-CoA on fatty acid oxidation/uptake is diminished (Merrill *et al.*, 1997). AMPK also acts to down-regulate lipogenesis by inhibiting activity of the transcription factor sterol regulatory element binding protein 1c (Li *et al.*, 2011). In addition, AMPK inhibits triglyceride, fatty acid, and cholesterol synthesis by targeting glycerol phosphate acyl-transferase, acetyl-CoA carboxylase 1, or 3-hydroxy-3-methylglutaryl CoA reductase (HMGR), respectively (Clarke and Hardie, 1990; Davies *et al.*, 1992; Muoio *et al.*, 1999).

As an important regulator of energy metabolism, AMPK has clear effects on control of energy production and storage, but it also affects other processes related to catabolism and autophagy. AMPK employs two major strategies affecting protein metabolism: protein synthesis pathways are inhibited; and autophagy is promoted generally, but AMPK particularly encourages increased protein degradation. AMPK phosphorylates and inactivates eukaryotic elongation factor 2, directly inhibiting protein synthesis, as well as phosphorylating TSC2 and Raptor to inhibit the mTOR pathway (Horman *et al.*, 2002; Gwinn *et al.*, 2008). Inhibition of mTOR decreases phosphorylation of S6K and 4E-BP, further reducing protein synthesis (Dowling *et al.*, 2007). Additionally, AMPK affects protein synthesis

at the transcriptional level through inhibition of transcription initiation factor-1A, which regulates the expression of RNA polymerase 1 (Hoppe *et al.*, 2009).

Autophagy is the term used to described the recycling of organelles and cytosolic content, and activation of autophagy has been linked to AMPK activity in both mammals and yeast (Wang *et al.*, 2001). AMPK forms stable complexes with UNC-51-like kinases 1 and 2 (ULK1/2) and phosphorylates them; triggering autophagy through the activation of VPS34 (a class III PI3K), and prompting cellular trafficking events to support autophagy-related processes (Behrends *et al.*, 2010; Egan *et al.*, 2011; Russell *et al.*, 2013). In addition, phosphorylation of the regulatory protein beclin-1 by AMPK also helps to promote more effective use of these VPS34 complexes, encouraging the formation of pro-autophagy complexes (over complexes unrelated to autophagy signalling)(Kim *et al.*, 2013). Autophagy is also promoted via the inhibitory action of AMPK on the formation of mTORC1– AMPK directly phosphorylates Raptor, a key component of the complex, preventing mTORC1 assembly (Gwinn *et al.*, 2008). AMPK further inhibits mTORC1 assembly through activation of TSC1/2, which converts Rheb-GTP to its inactive GDP-bound state (Yang *et al.*, 2006; Hardie, Ross and Hawley, 2012). Rheb is an activator of mTORC1 kinase activity, promoting protein synthesis and growth. Indirect inactivation of Rheb by AMPK (via TSC1/2) hinders growth, while autophagy-related trafficking and signalling are simultaneously up-regulated (Inoki, Zhu and Guan, 2003). However, when nutrient intake is above a fasting response threshold, mTORC1 opposes AMPK function through antagonistic phosphorylation of ULK1 (at serine residue 757), which disrupts the interaction between AMPK and ULK1 (Kim *et al.*, 2011).

Another phenomenon which somewhat intuitively displays strong links to lifespan is the loss of mitochondrial homeostasis as organisms age (Petersen *et al.*, 2003). AMPK has several roles relating to mitochondrial biology, and drives the metabolic switch from carbohydrate to lipid metabolism in fasted skeletal muscle cells (Cantó *et al.*, 2010). AMPK stimulates mitochondrial biogenesis by altering activity of peroxisome proliferator-activated receptor gamma coactivator-1α (PGC-1α). PGC-1α up-

regulates expression of mitochondrial genes within the nucleus, increasing the capacity of the cell to generate ATP (Lin, Handschin and Spiegelman, 2005). A positive feedback loop exists here, whereby AMPK increases its own transcription through phosphorylation of PGC-1α (Jager *et al.*, 2007). An additional indirect pathway also contributes to this effect – AMPK activity increases the concentration of NAD^+ within the cell, up-regulating sirtuin 1 activity. Sirtuin 1 deacetylates PGC-1α, increasing its activity and up-regulating AMPK expression in the process (Cantó *et al.*, 2010).

AMPK also contributes to the turnover rate of damaged or worn-out mitochondria (a.k.a. mitophagy). Earlier, phosphorylation of ULK1 by AMPK was described. Interestingly, inhibition of ULK1 phosphorylation results in a build-up of mitochondria with irregular morphology. Irregular mitochondria exhibit reduced functionality, and display a reduced ability to maintain an effective membrane potential (Egan *et al.*, 2011). Through control of ULK phosphorylation status, AMPK has a key role in the removal of exhausted/misshapen mitochondria from cells. Thus, AMPK ensures that resources are recycled to maintain an efficient network of mitochondria for ATP-production, better supporting fasted cells. Additionally, a well-functioning network of mitochondria is important for maintaining muscle performance with age, and AMPK can help to sustain this network over time by promoting coordination with peroxisomes and the uptake of fatty acids into mitochondria during energy stress (Weir *et al.*, 2017). Pharmacological (AICAR-induced) activation of AMPK increases endurance during exercise in older mice, and also increases mitochondrial gene expression in rat skeletal muscle (Winder *et al.*, 2000; Narkar *et al.*, 2008).

1.4.5 Effects of AMPK on Lifespan and reproduction.

The effects of AMPK signalling on longevity have not yet been directly investigated in mammals (mammalian studies often focus on interactions of AMPK with mTOR and immune pathways), but decreased AMPK activation with age has been reported in several tissues in both rat and mice studies (Salminen and Kaarniranta, 2012). Interestingly, older rat skeletal muscle exhibits stunted activation of AMPKα2 versus younger muscle tissue, when activated via the pharmacological

activator AICAR (Reznick *et al.*, 2007). The authors of that study suggest that this effect may contribute to the development of increased insulin resistance and incidence of type 2 diabetes with age. AMPK has also been associated with mammalian reproductive health. *In vitro* treatment of rat granulosa cells with an AMPK-activating adenosine analogue reduced progesterone secretion and altered levels of cell-cycle regulators, suggesting AMPK holds a role in the regulation of sex hormone production and limiting proliferation of ovarian granulosa cells (Tosca *et al.*, 2005; Kayampilly and Menon, 2009).

In summary, AMPK is a key regulatory kinase which regulates metabolic shifts towards catabolism and autophagy, and simultaneously opposes the mTOR pathway (which promotes use of energy stores for growth and blocks autophagy). Three major interventions are consistently involved in mediating longevity: the reduction of IIS, manipulation of the mTOR pathway, and DR. AMPK has been linked with all three of these. Importantly, interventions involving disruption of nutrient-sensing pathways and DR appear to improve lifespan while also inhibiting tumour development, as opposed to other strategies like telomere elongation (Kenyon, 2005; Pinkston *et al.*, 2006).

1.5 AMPK in *C. elegans*.

1.5.1 Structure and activation.

Comparison of AMPK genes in *C. elegans* and humans suggests that key elements of the structure of AMPK have been largely conserved through evolution. Orthologues of mammalian AMPKα exist in *C. elegans*: encoded by genes *aak-1* and *aak-2*, these isoforms show 40% and 52% identity to human PRKAA1 in terms of overall structure, respectively (Apfeld *et al.*, 2004). While this may not seem substantial, key functional regions within the α subunit kinase domain display substantially higher conservation – 71% and 80% for AAK-1 and AAK-2, respectively. Crucially, increased Thr172 phosphorylation in response to AMP-binding appears to be an conserved event, supporting the idea that the mammalian allosteric activation mechanism (Chapter 1.4.2) is conserved in *C. elegans* AMPK (Apfeld *et al.*, 2004). Additionally, AAK-2 activity has been reported following phosphorylation of threonine-243, further mirroring allosteric activation of mammalian AMPKα.

Thr243 is predominantly phosphorylated by upstream kinase PAR-4 (mammalian homologue LKB1) and improves AMPK activity as much as 100-fold (Lee *et al.*, 2008). Notably, Thr243 and equivalent residues in other models are often referred to as Thr172 in existing literature, to enable quick recognition of the residue when discussing AMPK activation. In line with this, the *C. elegans* AMPKα activation residue will be referred to as Thr172 in later chapters of this thesis.

During my examination of the literature, I found only one source discussing the level of conservation between AMPKβ in humans and *C. elegans*. *C. elegans* homologues of human AMPKβ are encoded by *aakb-1* and *aakb-2*, and β subunit alignments report approximately 30% identity and 84% similarity in AAKB isoform residues compared to human AMPKβ (Ahmadi and Roy, 2016). The authors claim that AAKB subunits also show significant homology with PRKAB1, but I could not find the original articles to support these comparisons.

C. elegans has an expanded system of AMPK regulation, with five *aakg* subunits (Table 1.1), and these remain less understood than human orthologs *PRKAG1-3*. It is thought that any combination of *C. elegans* AMPK subunit isoforms (α, β, and γ) can form a functioning heterotrimer (assuming that isoform expression occurs in the same tissue), since most subunits show high conservation of key domains when compared with mammalian orthologs in genetic analyses. However, this has yet to be proven through structural investigations. The expanded network of regulatory subunits here is significant, and during this project I sought to determine similarities and differences between AMPKγ isoforms where possible. Orthologues of *aakg-4* and *aakg-5* are present across a group of nematode roundworms called Chromadorea which includes *Brugia malayi* and *Pristionchus pacificus,* among others, suggesting that these isoforms may provide some benefit to these organisms (Tullet *et al.*, 2014). Additionally, the presence of five AMPKγ isoforms in *C. elegans* (rather than the three found across mammalian models) could suggest a considerable level of complexity in *C. elegans* AMPK function, or that some AAKG isoforms may demonstrate functional redundancy. While AAKG-1, AAKG-2, and AAKG-3 seemed to be highly conserved, the non-conservation of predicted AMP-binding

residues in AAKG-4 and AAKG-5 has been hypothesised to facilitate alternative regulation of AMPK catalytic activity (Tullet *et al.*, 2014). This concept provided the basis for grouping *aakg* isoforms as AMP-sensitive and AMP-insensitive families which will be discussed in further detail later in this thesis. In humans, some of these predicted AMP-binding residues (Arg69, His150, Arg151, highlighted in figure 1.4) have been implicated in the pathogenesis of Wolff-Parkinson-White syndrome, resulting in abnormal cardiac activation (Gollob *et al.*, 2001; Daniel and Carling, 2002; Adams *et al.*, 2004). In *C. elegans*, AAKG-4 does not show conservation of any of the predicted AMP-binding residues, while Arg69 (PRKAG1 numbering) is not conserved in AAKG-5, suggesting that these isoforms may also exhibit dysfunctional regulation of AMPK activity (Tullet *et al.*, 2014).

1.5.2 AMPK and *C. elegans* lifespan.

Over the last few decades, many assays have been developed in *C. elegans*, and refining of these protocols has enabled *C. elegans* researchers to effectively investigate whole-organism significance of AMPK function. During this project, AMPK functionality was investigated with the aim of understanding several aspects of *C. elegans* biology: including lifespan, dauer and fecundity.

Many *C. elegans* researchers choose to focus on the catalytic (α) subunit of AMPK. *aak-2(ok524)* mutants consistently display reduced lifespan compared to WT animals (approximately 12% shorter)(Apfeld *et al.*, 2004; Curtis, O'Connor and DiStefano, 2006; Schulz *et al.*, 2007; McQuary *et al.*, 2016). Additionally, transgenic animals with elevated expression of *aak-2* display an average 13% extension of lifespan, suggesting that *aak-2* may contribute to regulation of lifespan in a dose-dependent manner (Apfeld *et al.*, 2004). Expression of a N-terminal truncated form of *aak-2*(aa 1-321) in also extends *C. elegans* lifespan (Mair *et al.*, 2011). in *D. melanogaster*, extended lifespan is also observed in response to overexpression of AMPKα in the muscle tissue or fat bodies, while lifespan is reduced when AMPK is knocked down through RNAi in the same tissues (Stenesen *et al.*, 2013). Interestingly, *aak-2* mutants generally exhibit more pronounced phenotypes than *aak-1* mutants; suggesting that *aak-1* may occupy a more niche role.

In *C. elegans*, lifespan extension resulting from truncated *aak-2* has been linked to phosphorylation of cAMP-responsive element binding protein-regulated transcription coactivator 1 (CRTC-1)(Mair *et al.*, 2011). Phosphorylation of CRTC-1 by AMPK results in its exclusion from the nucleus, rendering it inactive. This truncated form of *aak-2* acts by altering the whole-body transcription profile, and is associated with changes to mitochondrial metabolism, which are likely effected through CRTC-1 activity (Burkewitz *et al.*, 2015). Expression of an modified form of CRTC-1 that is resistant to this phosphorylation event removes the lifespan extension phenotype seen with truncated *aak-2* (Mair *et al.*, 2011). In fact, expression of modified CRTC-1 exclusively in *C. elegans* neurons is enough to abolish the longevity effects (Burkewitz *et al.*, 2015). Interestingly, modified CRTC-1 did not seem to affect the influence of AMPK signalling on reproductive health – thus AMPK represents an example of a signalling nexus where longevity and reproductive effects may be uncoupled (Burkewitz *et al.*, 2015). This is important because it increases the appeal for investigation of AMPK, and later in this thesis the contribution of *aakg* isoforms to longevity and reproductive health will be discussed in detail (Chapter 4). Evidence of similar scenarios would promote AMPK as a more tactical choice for drug design when targeting lifespan and reproductive health, since it may be possible to target these processes with greater specificity and less undesirable side effects. Understanding the regulation of AMPK through the AAKG subunit holds the prospect of accessing this nexus, potentially with higher specificity than is offered when targeting the kinase domain. Lifespan extension effects in *C. elegans* are thought to occur primarily through this regulation of CRTC-1, rather than mTORC1 which has been investigated in mammals (Mair *et al.*, 2011; Johnson, Rabinovitch and Kaeberlein, 2013). Notably, there has been no direct evidence in *C. elegans* that AMPK regulates mTORC1.

IIS components also show extensive interaction with AMPK in *C. elegans*, and AMPK regulates IIS as well. *C. elegans* AMPK phosphorylates regulatory sites on both DAF-16 and its mammalian homologue FOXO3, increasing their transcriptional activity (Greer, Dowlatshahi, *et al.*, 2007; Greer, Oskoui, *et al.*, 2007). Also, genetic investigations have revealed the apparent existence of a signalling

circuit required for *daf-2*-mediated longevity. While *daf-2* mutants display longevity phenotypes, a *daf-2(m577); aak-2(ok524)* mutant exhibits similar lifespan to an *aak-2* mutant (shorter than WT), suggesting that *daf-2*-mediated lifespan extension could be *aak-2*-dependent, and placing AAK-2 activity downstream of DAF-2 signalling (Apfeld *et al.*, 2004). Meanwhile, *daf-2; aak-2* knockout strains carrying stronger *daf-2* mutant alleles display shorter lifespans compared to respective *daf-2* background mutants, but not WT, suggesting that *aak-2*-independent mechanisms exist as well. Interestingly, *daf-2* mutants do not exhibit any difference in AMP:ATP ratio compared with WT worms, so *daf-2*-mediated lifespan extension occurs independent of AMP:ATP ratio (Apfeld *et al.*, 2004). Furthermore, considering DAF-16 as a key downstream effector of DAF-2 signalling, a *daf-16(mu86); aak-2(ok524)* double knockout strain demonstrates a 15% additive lifespan reduction compared to respective single mutant strains, indicating that *aak-2* can manipulate lifespan independently from *daf-16* (both single mutants are short-lived compared to WT). Since literature reports that *daf-16* is required for *daf-2*-mediated lifespan extension, additive suppression of lifespan implies that AAK-2 and DAF-16 act in parallel to influence lifespan (Kenyon *et al.*, 1993; Apfeld *et al.*, 2004).

1.5.3 AMPKγ and *C. elegans* lifespan.

The function of *C. elegans* AMPKγ in regulating lifespan has also been investigated. While, *aakg-4* and *aakg-5* do not appear to be conserved in higher organisms, these isoforms can still reveal the relevance of key AMP-binding residues to AMPK regulation. Transgenic expression of a constitutively active form of AMPK, generated through a point mutation (R81Q) in the AMP-binding pocket of *aakg-2* results in lifespan extension, implying that AMP-sensitivity is important for longevity (Greer, Dowlatshahi, *et al.*, 2007). An interesting aspect of AMPK regulation is how AMP:ATP ratio increases with age. In *C. elegans*, an eight-fold increase in the AMP:ATP ratio occurs between day 4 and day 18 animals (Apfeld *et al.*, 2004). This represents a possible hallmark of ageing and adds further incentive for investigation of AMPK. Moreover, since AMPKγ responds directly to the AMP:ATP ratio it holds a favourable position for designing assays to monitor this trend. Furthermore, behavioural phenotypes have been linked to this phenomenon. When spontaneity of movement within

populations was grouped into two classes, animals which moved more readily displayed a lower AMP:ATP ratio, and subsequently displayed longer lifespans. While AMP:ATP ratio has not been assayed during this project, phenotypes discussed here could be linked to behavioural phenotypes in further studies.

IIS and AMPK have been further linked through IIS-mediated regulation of DAF-16 activity. Activation of DAF-2 directly influences AKT and serine/threonine kinase (SGK) activity, which maintains cellular localisation of DAF-16, regulating its activity (Figure 1.7). In the absence of phosphorylation via AKT, DAF-16 localises in the nucleus, where it promotes expression of several genes including several AMPK subunits: *aak-2, aakb-1, aakg-4* and *aakg-5* (Schuster *et al.*, 2010). However, a later study could not confirm DAF-16-mediated up-regulation of *aakg-5* expression (Tullet *et al.*, 2014). Still, DAF-16-mediated transcriptional control could imply that these isoforms could hold some role in mediating at least some of the effects of DAF-16 activity, which is associated with longevity and increased stress resistance (Lin *et al.*, 1997; Henderson and Johnson, 2001; Murphy *et al.*, 2003).

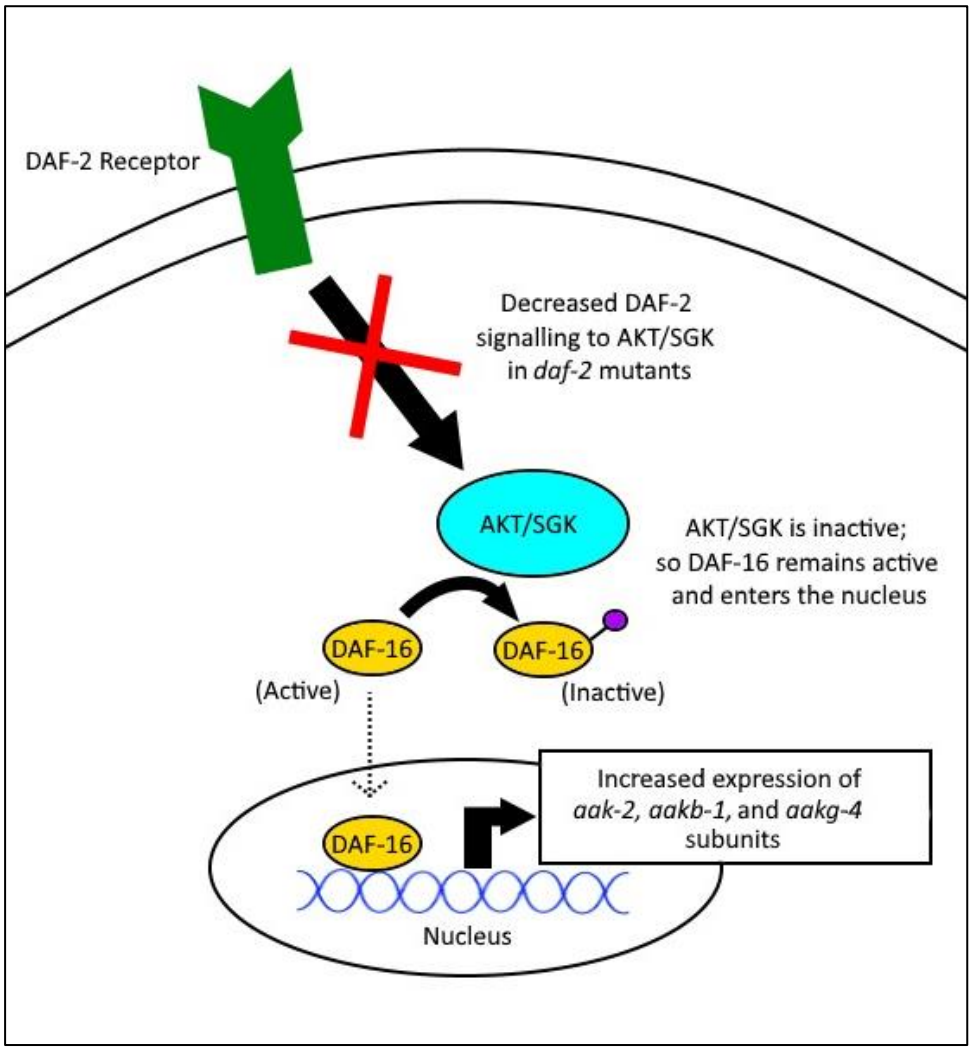

Figure 1.7| DAF-16 is key regulatory element of the insulin pathway in *C. elegans*. This figure highlights DAF-16 inactivation through its phosphorylation by AKT and SGK. The red cross indicates reduced DAF-2 receptor signalling, which allows DAF-16 to remain active, increasing expression of *aakg-4*. The existing hypothesis suggests that this increases translation of *aakg-4* and generates constitutively active AMPK complexes (Tullet *et al.,* 2014).

Increased expression of *aakg-4* through DAF-16 activity is likely to increase the number of AMPK complexes containing AAKG-4, thereby promoting a shift towards AMP-independent AMPK activity and any subsequent metabolic benefits. Not found in higher organisms, *aakg-4* and *aakg-5* are both thought to be insensitive to AMP, due to a lack of AMP-binding residue conservation compared other *C. elegans* isoforms (*aakg-1, aakg-2, and aakg-3*) and mammalian orthologues (Tullet *et al.*, 2014). The existing hypothesis suggests that incorporation of AMP-insensitive *aakg-4* or *aakg-5* isoforms results in constitutively active AMPK complexes, achieved through loss of AMP-sensitivity (Tullet *et al.*, 2014). This was then used to explain a role of *aakg-4* in *daf-2*-mediated longevity. Expression of *aakg*-4 is increased in *daf-2* mutants in a *daf-16* dependent manner, supporting the idea that *aakg-4* may contribute to *daf-2*-mediated lifespan extension. Furthermore, interdependence between AMPK and DAF-16 is evident through the existence of a positive feedback loop: AMPK promotes DAF-16, increasing expression of DAF-16 target genes, which may further increase expression of AMP-insensitive AMPK complexes (Schuster *et al.*, 2010; Tullet *et al.*, 2014). During this project, *aakg* mutants were established in WT and *daf-2* backgrounds (Chapter 3.2), to explore the influence of IIS on AMPK regulation in *C. elegans*. The relationship between both AMPK and IIS is a point of relevance for this project and will be discussed further in later chapters. Notably, a similar extent of interaction between FOXO and AMPK has been reported in higher organisms, and if this relationship is conserved, it could offer novel mechanisms through which the rate of ageing could be manipulated in humans (Lützner, De-Castro Arce and Rösl, 2012).

1.5.4 AMPK and stress resistance in *C. elegans*.

The influence of environmental stress on lifespan extension has also been explored in literature. Pre-fertile adult WT worms that were exposed to 35°C for 2 hours lived on average 30% longer than untreated worms, and interestingly, *aak-2* mutants did not show any lifespan extension under the same conditions; suggesting that *aak-2* is required to extend lifespan through high-temperature pulsing (HTP) treatment (Apfeld *et al.*, 2004). Environmental stresses (like high temperature) are associated with transient increases in the intracellular AMP:ATP ratio, which

increase AAK-2 activity and extend lifespan. Although the transient increase in AMP:ATP ratio fades relatively quickly after HTP treatment, it is hypothesised that increased AAK-2 activity and subsequent phosphorylation of downstream targets produces some level of molecular memory, resulting in the activation of lifespan-extending mechanisms that remain active after removal of the environmental stressor (Apfeld *et al.*, 2004).

AMPK is also a well-known antagonist of the TOR pathway. Sufficient nutritional intake permits TOR pathway signalling, which promotes growth and inhibits autophagy. AMPK opposes the effects of TOR, promoting autophagy and increasing the turnover rate of cellular components (enzymes, transcription factors, etc.). Inhibition of TOR signalling in *C. elegans* has been associated with increased stress resistance via the action of transcription factors DAF-16 and SKN-1 (Robida-Stubbs *et al.*, 2012). Effective inhibition of TOR achieved by targeting AMPK regulation represents one potential avenue for investigation when designing drugs which regulate TOR signalling.

1.5.5 The role of AMPK in *C. elegans* fecundity.

AMPK is reported to contribute some level of control over reproductive health in *C. elegans*. *aak-2(ok524)* mutants show reduced brood size compared to WT worms (Apfeld *et al.*, 2004). Similarly, an *aak-1(tm1944); aak-2(ok524)* double knockout strain displays sterility in adults following emergence from L1-arrest (a state of delayed development in response to starvation)(Fukuyama *et al.*, 2012). The latter finding suggests a substantial role of AMPK signalling during nutrient-poor conditions which determines the future reproductive function of *C. elegans* larvae. Other evidence reports a crucial role for AMPK in the determination of the *C. elegans* reproductive window. Transgenic expression of a constitutively active AAK-2 shifts the reproductive window of *C. elegans*, highlighting the importance of intracellular energy regulation: worms expressing truncated AAK-2 initially lay fewer eggs (compared to WT animals), but recover numbers of offspring later in the reproductive window (Burkewitz *et al.*, 2015).

In *C. elegans* larvae, AMPK is responsible for regulation of whole-body energy store usage and influences the cell cycle of germline stem cells during times of energy stress. In both L1-arrested and dauer stage animals, AMPK is required to pause proliferation of the germline stem cells (though involvement with TOR signalling is also implied) (Narbonne and Roy, 2006; Fukuyama *et al.*, 2012). A relationship between stress responses and reproductive health has also been explored. Animals exposed to HTP early in life suffered with lower energy levels, and this establishes an early-life metabolic shift toward somatic maintenance (Apfeld *et al.*, 2004). These worms also displayed a lower total brood size, and this phenomenon occurred in an *aak-2*-dependent manner; WT animals demonstrate a more severe reduction in brood size than *aak-2* mutants after HTP treatment. Thus, fecundity, stress resistance and the earlier described effects on longevity (Chapter 1.5.4) all appear to be linked to *aak-2* expression (Apfeld *et al.*, 2004).

1.5.6 AMPK and Dauer.

Dauer is a branch of *C. elegans* development where larvae become extremely stress resistant and enter a state of diapause, which is thought to have arisen during evolution because it is advantageous to allow individuals to survive periods of extreme stress, maintaining future genetic variation through subsequent maturation and reproduction. During this state, animals do not feed, and metabolic flux is reduced to allow worms to remain in this stage for several months if necessary. It seems reasonable to suggest that AMPK signalling could influence the metabolic shift that occurs as worms enter dauer, and possibly is also involved in the resumption of normal metabolism when exiting from dauer.

As described earlier, *daf-2* mutations can encourage developing *C. elegans* larvae to dauer (Chapter 1.3.1). Existing literature reports that *daf-2(e1370)* background dauers lacking PAR-4/AMPK signalling quickly use up energy stores and perish prematurely due to failure of excretory and hypodermal regulation (Narbonne and Roy, 2009). The hypodermis provides body form and overall structure in *C. elegans*, similar to human skin, but worm hypodermal cells (along with intestinal cells)

hold an additional role in the accumulation of fat reserves when preparing to enter dauer (Burnell *et al.*, 2005). Loss of function mutations to both catalytic AMPKα isoforms in an *aak-1; aak-2* double knockout strain reduces the viability of L1-arrested larvae (Fukuyama *et al.*, 2012). Interestingly, a *daf-2; aak-1* mutant does not show significant deficits to dauer survival, but *daf-2; aak-2* and *daf-2; aak-1; aak-2* mutants do show decreased survival, suggesting that *aak-2* contributes predominantly to maintenance of metabolism during dauer (Narbonne and Roy, 2009). Additionally, *aak* expression studies have highlighted the relevance of cell type-specific regulation, demonstrated through the substantial impact that *aak-2* expression in *C. elegans* hypodermal cells has on dauer longevity. Premature mortality occurs in *aak-2* mutant dauers primarily through two mechanisms: increased oxygen consumption resulting in the rapid consumption of energy stores, and phosphorylation of adipose triglyceride lipase, a reported inhibitory target of AMPK (Narbonne and Roy, 2009). Interestingly, ablation of *aak-2* expression in dauers carrying more severe (class I) *daf-2* mutant alleles can exacerbate the disruption of energy store regulation: *daf-2(e1368); aak-2(ok524)* double mutants do not enter the dauer state at all, instead continuing development into fertile adults at 25°C (Apfeld *et al.*, 2004). Studies in unicellular systems have demonstrated the potency of AMPK as a homeostatic energy regulator. If this potency is conserved in eukaryotes, cell-autonomous AMPK function could contribute to the long-term survival of multi-cellular animals under conditions of energy stress (Narbonne and Roy, 2009; Hardie and Ashford, 2014). Intriguingly, *aak-2* is required for long-term survival of dauer larvae, but not for normal morphology (Narbonne and Roy, 2006). In contrast, single *aakb* (AMPKβ) isoform mutants display no effect on dauer longevity, but an *aakb-1(tm2658); aakb-2(rr88)* mutant shows substantially reduced dauer lifespan. This implies that *aakb* isoforms are functionally redundant (regarding dauer longevity), but complete absence of this structural linker domain prevents correct assembly of AMPK complexes (Narbonne and Roy, 2009).

At the time of writing, I could not find any literature commenting on the influence of *aakg* expression on dauer: existing literature often focuses on the roles of *aakg* isoforms in adult longevity and stress resistance (Greer, Dowlatshahi, *et al.*, 2007; Sagi and Kim, 2012; Tullet *et al.*, 2014). In this

project I investigate the contributions of *aakg* to several aspects of dauer physiology, including entry, recovery, SDS resistance, and body size.

1.6 This thesis.

Research has revealed several key signalling pathways which influence ageing. Amongst these pathways, AMPK represents an important nexus of energy homeostasis signalling. Multiple levels of AMPK regulation and the proximity of AMPK to TOR (through inhibitory effects) could yield additional therapeutic mechanisms to extend lifespan. In this respect, investigating AMPKγ is appealing, since AMPK exhibits fine-tuned regulation, and further research into how this regulation affects AMPK activity might reveal how the kinase function of AMPK might be modulated with more finesse by targeting AMPKγ rather than AMPKα.

The primary focus of this project involves the use of genetic knockouts of the AMPKγ subunit in *C. elegans* (*aakg* mutants) to characterise the role of AMPK activity on key aspects of physiology and ageing. Given that the contribution of *aakg-4* to longevity was initially established in a *daf-2* background, I examine AMPK regulation in two genetic backgrounds of *C. elegans*: WT and a reduced IIS mutant (*daf-2(m577)*). Using a collection of genetic knockout strains, several aspects of *C. elegans* biology (lifespan, stress resistance, fecundity and dauer) have been assayed, revealing interactions between IIS and AMPK signalling. The third chapter presents data which reveals the inability of *aakg-1; aakg-2; aakg-3* knockout worms to respond normally to AMP-binding. The fourth chapter then describes phenotypic characterisation of *aakg* mutants. Results support previous suggestions of positive correlation between lifespan and stress resistance, but do not support the idea of a reproductive trade-off which sacrifices fecundity to extend lifespan (disposable soma theory). Additionally, I report differences in dauer body size between *aakg* knockout strains, which suggest that *aakg* may hold a role in maintenance of dauer metabolism. Overall, my results suggest that AMP-sensitive isoforms are required for AMPK to effectively respond to energy status in *C. elegans*, and both AMP-sensitive and AMP-insensitive isoform families display subtle

differences in contributions to lifespan, fecundity, and dauer. I then discuss how these effects might be mediated, and comment on potential redundancy between *aakg* isoforms.

To summarise, this project focuses on functional characterisation of the *C. elegans aakg* isoforms and investigates factors influencing both the molecular biology of AMPK, and the phenotypic effects that result from aberrant AMPK regulation. Investigating AMPK regulation in *C. elegans* could provide greater understanding of conserved mechanisms of energy homeostasis and metabolism in humans, providing considerations for future pharmacological application.

Investigations in chapter three were designed to satisfy the following aims:

- **To model key nucleotide binding residues in each AAKG isoform using *in silico* techniques and determine similarities and differences between the five subunits.**
- **Generate genetic tools to explore the role of AMPKγ subunits in *C. elegans,* both in WT and IIS mutant backgrounds.**
- **Determine the role of AMPKγ subunits in regulating *C. elegans* AMPK activity.**

In chapter four, the following aims were met:

- **Determine the role of AMPKγ subunits in a range of *C. elegans* physiological phenotypes (lifespan, stress resistance, reproduction and dauer).**
- **Determine how the IIS pathway impacts physiological effects of *aakg* mutation.**

Chapter 2 – Materials & methods.

2.1 Maintenance techniques:

2.1.1 Nematode growth medium (NGM).

NGM was prepared to the following concentrations: 51mM NaCl [Fisher Bioreagents], 1.7% w/v agar [Melford] and 0.25% w/v Bacto™peptone [Difco]; made up to 1L with double-distilled H_2O. The mix was autoclaved to a maximum of 126°C then allowed to cool in a water bath to 55°C.

The following buffers were added before pouring: 1mM $MgSO_4$, 1mM $CaCl_2$, 5µg/ml cholesterol (in ethanol), and 25mM KH_2PO_4 (pH 6.0). Any required antibiotics (e.g. 0.1 mg/ml Streptomycin for OP50-1 culture plates) or other additions were added to the agar at this point. 15ml of agar solution was poured into 6cm petri dishes and left to solidify for at least 24 hours before use.

2.1.2 *C. elegans* husbandry.

Animals were grown on standard NGM using *E. coli* strain OP50 as a food source. A streptomycin-resistant variant OP50-1 was used in later assays to reduce risk of contamination. Whether OP50 or OP50-1 was used is stated where appropriate for each protocol (Chapters 2.3 – 2.6). OP50 was cultured in Lysogeny Broth [Miller, Fisher Bioreagents], and grown overnight at 37°C. OP50-1 cultures additionally contained 0.1 mg/ml streptomycin. 200µl of liquid culture was pipetted onto 6cm NGM plates, then left for 48 hours at room temperature (RT) before use: enough time for a lawn of bacteria to develop (OP50 growth is limited on standard NGM).

Stocks were cultured at 20°C (unless stated otherwise), apart from *daf-2*(*m577*)-background strains which were cultured at 15°C to improve sensitivity to temperature-sensitive induction of the *daf-2(m577)* mutation at 25°C. All culture temperatures were maintained through storage of strains in FOC215E cooled incubators [Velp Scientifica].

After several days, worms starve due to complete depletion of the bacterial lawn, unless transferred to a fresh seeded plate. Thus, populations of *C. elegans* were maintained avoiding starvation by picking between 5 to 8 L4-stage or young adult worms to a fresh NGM plate. Populations of *C. elegans* were observed using a Leica M80 dissecting microscope in a sterile environment, next to bunsen burners. Burners provided an upward airflow, reducing contamination from floating particles.

Worms were generally manipulated during observation with the Leica dissecting microscope using a technique known as picking. This technique uses a "worm pick", where a length of platinum wire is melted into a glass pipette and OP50-1 bacteria is collected on the flat end of the wire. This end is then used to gather worms and transfer them when required. Platinum wire was selected because it cools rapidly after heating. This allows the platinum pick to be sterilised for several seconds in a bunsen burner before use, reducing the risk of strain contamination or infection.

An alternative method used for transferring worms is called chunking. In this case, a sterilized scalpel is used to move a chunk of the NGM from the old plate to a fresh plate, often transferring greater numbers of worms with ease.

2.1.3 Population synchronisation - Bleach prep.

Bleaching was used to synchronise populations of *C. elegans* for assays, or to cleanse populations of infection. M9 buffer was used for washing worms and made to the following concentrations: 22mM KH_2PO_4, 42mM Na_2HPO_4, 9mM NaCl and 19mM NH_4Cl; made up to 1L with double-distilled H_2O. Gravid adults were washed off 6cm plates using 2ml M9 per plate into 15ml falcon tubes and allowed to settle for 5 minutes. Excess M9 was removed and 1ml of bleach solution (7:8 100% thin bleach: 4M NaOH) was added. The animals were gently agitated (manually) for 5 minutes. The bleach solution was immediately quenched by making the volume up to 15ml with M9, and tubes were centrifuged at 3000rpm for 5 minutes [Heraeus Megafuge 16R, Thermo Scientific]. Two further wash steps with 5ml M9 were performed. Then, the egg solution was diluted up to 800µl with M9 and split evenly across four NGM plates (200µl per plate) to hatch.

2.1.4 Freezing and thawing of *C. elegans* stocks.

During this project, several new *C. elegans* strains were generated and stored at -80°C. *C. elegans* strains can be stored indefinitely at -80°C and thawed out as required. Before freezing, strains were starved which causes progeny to arrest at the L1 stage. Individuals at this stage are more resistant to the freezing process than other stages. Starved L1 larvae from five 6cm NGM plates were washed off using 2ml M9 and diluted 1:1 in a 15ml falcon tube with 2x freezing media (30% glycerol, 5.9mg/ml NaCl, 6.8mg/ml KH_2PO_4, 0.3% 0.1M $MgSO_4$ added after autoclaving). 4ml of worm freezing mix was pipetted equally across four cryotubes [Sigma] and placed in a slow-freezing container [Nalgene® Mr. Frosty, Sigma] in the -80°C freezer. One tube was thawed a day after freezing for a test-thaw, to ensure that the strain had survived the freezing process. Strains were thawed on ice and immediately pipetted onto two seeded NGM plates, 500µl of the thawed stock being placed onto each plate. Animals were recovered at an appropriate temperature for strain maintenance and moved to a new NGM plate as soon as possible.

2.2 Strains.

Some strains were acquired from the *Caenorhabditis* Genetics Center (CGC) at the University of Minnesota. PHX409, PHX410, and PHX411 were generated using CRISPR-Cas9 gene editing, by Sunybiotech. Because Sunybiotech strains were generated in our lab N2 strain (CGCM) using the CRISPR-Cas9 gene editing technique, this eliminated the need for backcrossing after strain generation. Derivative strains (JMT55 – JMT74) were generated through a crossing strategy, described in detail later (Chapter 3.2). All strains used during this project are shown below (Table 2.1).

Strain name	Genotype	Additional Details
DR1567	*daf-2(m577)*	Used as a control strain in all *daf-2* background lifespans, brood sizes, stress assays, and microscopy.
GA1001	*aak-2(ok524)*	Used as positive control in kinase activity analysis.
GA1071	*aakg-4(tm5539)*	Used with JMT48 to evaluate possible redundancy in WT lifespans.
GA1072	*daf-2(m577); aakg-4(tm5539)*	Used with JMT43 to evaluate possible redundancy in *daf-2* lifespans.
JMT9	*aakg-5(tm4052)*	Used with JMT48 to evaluate possible redundancy in WT lifespans.
JMT30	*daf-2(m577); aakg-5(tm4052)*	Used with JMT43 to evaluate possible redundancy in *daf-2* lifespans.
JMT43	*daf-2(m577); aakg-4(tm5539); aakg-5(tm4052)*	
JMT48	*aakg-4(tm5539); aakg-5(tm4052)*	
JMT61	*aakg-1(syb409); aakg-2(syb410); aakg-3(syb411)*	
JMT74	*daf-2(m577); aakg-1(syb409); aakg-2(syb410); aakg-3(syb411)*	
PHX409	*aakg-1(syb409)*	
PHX410	*aakg-2(syb410)*	
PHX411	*aakg-3(syb411)*	

Table 2.1| List of *C. elegans* strains used in this study. Bristol N2 derived from the standard CGC male (CGCM) stock was used as a WT control strain.

2.3 Physiological Assays:

2.3.1 Lifespan assay.

All strains used in lifespans were grown and maintained (unstarved) at 15°C for at least 3 generations prior to use (to avoid potential epigenetic effects of starvation)(Rechavi *et al.*, 2014). L4 worms were selected to synchronise populations without the use of bleach. Day 0 refers to the day that L4s were picked onto assay plates. Each plate contained ~20 worms, with each strain per assay being represented by >80 individuals in 90% of trials. Worms were split between 5 plates. All lifespans were incubated at 25°C and 10µM 5-fluro-deoxyuridine [Sigma] was pipetted onto a 48 hour-old lawn of OP50-1 bacteria, to prevent progeny production in all lifespan assays.

Animals were scored every 2-3 days as alive, dead, or censored. Alive/dead status was determined through the response to a light touch to the body of the worm using a platinum pick. Animals that were not otherwise moving or failed to respond after 3 touches were scored as dead. Animals that either escaped the plate or died from causes other than ageing (e.g. dried out on plate edge, intestinal explosion) were recorded as censored. Statistical analysis was performed by log-rank test, using the open online application OASIS 2 (Han *et al.*, 2016).

2.3.2 Oxidative (arsenite) stress survival assay.

All strains used were grown and maintained (unstarved) at 15°C for at least 3 generations prior to use (to avoid potential epigenetic effects of starvation)(Rechavi *et al.*, 2014). Animals were synchronized to day 1 adult by picking L4 worms the day before the experiment. In a 96-well plate, 100µl of 5mM sodium arsenite (working stock diluted with M9) was pipetted in the required number of wells and diluted 1:1 with 100µl of OP50 overnight culture to produce a final concentration of 2.5mM sodium arsenite. This concentration was chosen to highlight differences between strains effectively when analysing survival curves. Day 1 adult animals were picked directly into the wells; 5 wells each containing 10 animals was standard for each experimental condition. Animals were scored as alive or dead based upon response to light tapping with a platinum pick every morning and

afternoon. An 8-hour interval existed between morning and afternoon observations, and the same hours were used for observation over consecutive days, then survival curves were generated from this data. Animals which died from other causes were recorded as censored. Statistical analysis was performed by log-rank test using OASIS 2 (Han *et al.*, 2016).

2.3.3 Brood size assay.

All strains used were grown and maintained (unstarved) at 15°C for at least 3 generations prior to use (to avoid potential epigenetic effects of starvation)(Rechavi *et al.*, 2014). L4 stage animals were picked individually onto NGM plates seeded with OP50-1 bacteria; one worm per plate. Each strain was represented by 10 animals per assay, which were maintained at 25°C for the duration of the experiment. Each day, parent animals were moved to a new seeded plate, and the old plate (containing progeny from previous 24 hours) was incubated at 20°C for one day before counting. This provided age-specific brood data as well as total brood size. The assay was discontinued once animals began laying unfertilized oocytes - confirmed visually based on morphological differences. Statistical analysis was performed using Student's *t*-test, using the T.TEST function in Microsoft Excel.

2.4 Dauer Assays:

2.4.1 Dauer entry and exit assay.

Strains DR1567, JMT43 and JMT74 were used to investigate whether AMPKγ subunit mutation affected entry and/or recovery from the dauer stage of *C. elegans* development. 100 eggs (per strain) were picked from busy (unstarved) plates, and transferred to a fresh, seeded OP50-1 plate. Eggs were left to develop (and enter dauer) at 25°C for three days, enough time to ensure entry. Dauer animals were counted, then moved to a 15°C incubator to promote exit from dauer. Every 24 hours, over 4 days, animals were recorded as dauer, recovered, or censored. No animals remained in dauer longer than four days at 15°C. Statistical analysis was performed using Student's *t*-test, using the T.TEST function in Microsoft Excel.

2.4.2 Dauer sodium dodecyl sulphate (SDS) resistance assay.

Strains DR1567 and JMT43 were used to investigate whether mutation of AMPKγ subunits would affect resistance to detergent stress in dauer stage animals. The protocol was adapted from a 1% SDS dauer selection protocol, except dauer animals were generated beforehand using a 2-hour timed egg lay (Karp, 2018). After 3 days at 25°C, an 8µl droplet of 1% SDS (diluted in M9) solution was pipetted onto an unseeded NGM plate, and approximately 40 dauer animals were placed in the droplet for either 30 minutes or 2 hours. Animals were then removed from the treatment plate and allowed to recover on a fresh OP50-seeded NGM plate at 25°C. Animals were scored as alive, dead, or censored immediately after exposure, and again at 24 hours after exposure. Statistical analysis was performed using Student's *t*-test, using the T.TEST function in Microsoft Excel.

2.4.3 Dauer morphology.

Dauer stage animals were generated through a 2-hour timed egg lay using 10 gravid adult worms. Adults were removed from OP50-1 plates at the end of the egg-laying period. Offspring were incubated at 25°C for 3 days to ensure dauer entry, and dauers were only selected for microscopy after 7 days. An Olympus IX81 inverted microscope was used to visualise dauers, the light source was produced by a CooLED pE4000 illumination system. Images were captured using a Zyla 4.2 PLUS sCMOS camera [Andor]. Dauers were viewed in bright-field, using a 100x objective lens with a drop of Immoil-F30CC immersion oil [Olympus]. Approximately 40 dauers were mounted on a 2% agarose pad on a microscope slide, and 5µl 0.06% tetramyzole hydrochloride (diluted in M9) was pipetted onto the pad to anaesthetise dauers before imaging. Images were processed using the FIJI distribution package for ImageJ (https://fiji.sc/). For measurement of dauer worms, the measurement pane and line tool in ImageJ software were used. Diameter measurement was recorded across the grinder in each image (Supplementary figure 4). Measurements in pixels were converted to micrometres using a calculation which considered the physical size of the sensor (6.5nm) and 100x magnification used. Statistical analysis was performed using one-way ANOVA, followed by pairwise comparison using Tukey's test.

This required use of the base R functions 'aov' and 'TukeyHSD' respectively, viewed in RStudio (Team, 2013).

2.5 Molecular Biology:

2.5.1 Worm genotyping.

To confirm genotypes, genomic DNA was extracted from whole worms, using a single or multiple worm polymerase chain reaction (PCR) protocol. Using 5µl worm lysis buffer (50mM KCL, 10mM Tris (pH 8.3), 2.5mM $MgCl_2$, 0.45% NP40, 0.45% Tween20, 0.01% Gelatine, 0.1mg/ml proteinase K) animals were placed in 200µl PCR tubes, and lysed in a T100 thermocycler [Bio-Rad] using our lysis protocol (70°C: 60 minutes → 95°C: 15 minutes → 12°C: ∞). If PCR was not run immediately after lysis, the lysate could be stored safely in a fridge at 4°C for a few days.

A pre-made PCR mix, 2x PCRBIO Taq Mix Red (Product manual lists reagents as: PCRBIO Taq DNA Polymerase, 6mM MgCl2, 2mM dNTPs, enhancers, stabilizers, and a red dye) was used. PCR reactions were prepared with 10µl Taq Mix, 3µl of a 10mM primer mix (10mM in Milli-Q H_2O) and 2µl of Milli-Q H_2O. This was added to the 5µl worm lysate, and the reaction mix was placed into a T100 thermocycler and treated according to the required PCR protocol (94°C: 60s → 94°C: 30s → X°C (determined by primer set): 30s → 72°C: 60s → (Repeat previous 3 steps for 30 cycles) →72°C: 7 minutes →12°C: ∞). PCR products were then analysed on 1-2% agarose gels using 1Kb plus DNA ladder [Promega]. Gels were visualised using a Syngene G: Box.

2.5.2 Sample collection – Quantitative reverse transcription PCR (qRT-PCR).

RNA was extracted for synthesis of cDNA, required for qRT-PCR. Strains were maintained on OP50-1-seeded NGM plates prior to use. Strains were bleached to synchronise populations before extraction. Gravid adults were washed off three 6cm plates in 2ml M9 per plate. Worms were settled in a 15ml falcon tube for 5 minutes, then volume was reduced to 2ml, and the worm slurry transferred to an RNase-free eppendorf tube using a glass pipette. Samples were washed twice more using 1ml

M9 and allowed to settle for 3 minutes each time. Excess M9 was removed, and a final volume of 75-100µl of animals was used for most samples.

2.5.3 RNA extraction.

After addition of 500µl TRIzol reagent [Life Technologies], samples underwent 10 freeze-thaw cycles; samples were frozen at -80°C for 15 minutes then thawed for 3 minutes at 37°C [Heating block, Grant Instruments]. Samples were vortexed for 30 seconds each cycle [TopMix FB15024, Fisher Scientific] to ensure animals were effectively lysed and proteins denatured. 125µl of 1-Bromo-3-chloropropane [Sigma] was added, the mixture inverted five times, then incubated for 3 minutes at RT. The sample was centrifuged (12,000 rpm, 4°C, 10 minutes) using a Micro-star 17R benchtop centrifuge [VWR] and the clear RNA-containing phase transferred to a new RNase-free tube.

An equal volume of 70% ethanol (diluted with RNase-free H_2O [Melford]) was added, and the new mixture pipetted onto an RNAeasy® mini kit extraction column [Qiagen]. RNA extraction was conducted according to the 'Quick start, part 1' RNAeasy® protocol [Qiagen] and the final RNA was eluted with 35µl of RNase-free H_2O. RNA concentration and purity were analysed using a Nanodrop™-1000 Spectrophotometer [Thermo Fisher-Scientific], where 260/280 ratios of 1.9 – 2.2 were deemed acceptable. In cases of phenol contamination, residual TRIzol reagent was removed from the RNA sample using the 'RNA clean-up' protocol included with the RNAeasy® kit. RNA samples were stored short-term (<1 week) at -20°C before use in cDNA synthesis (stored long-term at -80°C). For this project, six biological repeats were collected to account for variation seen in previous work. All strain populations in each biological repeat were processed (and bleach prepped) simultaneously.

2.5.4 cDNA synthesis.

Prior to cDNA synthesis, genomic DNA was removed from RNA samples through DNase I treatment. 1µg of (total) RNA was digested with 1µl of DNase I (1 unit/µl) in the presence of 1x DNase I buffer to a final volume of 10µl. RNase-free H_2O was used. DNase I digest was performed at RT for 15 minutes. Then Mg^{2+}-mediated degradation of RNA was inhibited by addition of 1µl 25mM EDTA,

followed immediately sample heating at 65°C for 10 minutes in a T100 thermocycler, deactivating the DNase I enzyme. This digest product was then used in cDNA synthesis.

cDNA synthesis was performed by preparing an initial mix of 1µl oligo(dT) 12-18 (500µg/ml), 1µg total RNA, and 1µl dNTP mix (10mM). The reaction mix was heated in a T100 thermocycler to 65°C for 5 minutes then immediately chilled on ice. 4µl 5x first-strand buffer and 2µl 0.1M DTT were added and incubated for 2 minutes at 42°C. At this point, 1µl of Superscript II Reverse Transcriptase [SSIIRT, Thermo Fisher-Scientific] was added to samples and the mix was incubated at 42°C for 50 minutes, then inactivated by heating to 70°C for 15 minutes. Finally, 1µl of *E. coli* RNase H and 2µl RNase H buffer [New England Biolabs] were added, and the cDNA mix incubated at 37°C for 20 minutes. Finally, mixes were diluted up to 100µl using RNase-free H_2O and stored at -20°C before use in qRT-PCR. For negative controls, SSIIRT was replaced with RNase-free H_2O.

2.5.5 qRT-PCR.

qRT-PCR primers were designed with the aid of the Sigma primer design tool (OligoArchitect™, www.oligoarchitect.com), taking care to ensure that primers crossed exon-exon boundaries. Primer sets were designed to perform optimally at 60°C and were tested before use. Efficiency was determined for *aakg-1*, *aakg-2,* and *aakg-3* primer sets by analysis of a smaller sample set; Ct values needed to be acceptable for the N2(WT) strain (20-30 cycles) and melting curve profiles indicated production of only one product. Primer sets for *aakg-4* and *aakg-5* were custom-designed and optimised previously by the Gems Lab, and synthesized by PrimerDesign Ltd. (Tullet *et al.*, 2014).

qRT-PCR reaction mixes were prepared to a total volume of 10µl as follows: 2µl cDNA, 5µl SYBR green iTaq super-mix [Bio-Rad], 2.6µl RNase-free H_2O and 0.4µl of relevant primer mix. Each sample was plated in triplicate. mRNA levels were normalized to the geometric mean of 3 housekeeping genes – *cdc-42*, *pmp-3* & *Y45F10D.4* (Table 2.2) (Hoogewijs *et al.*, 2008). qRT-PCR assays were set up on a 96-well plate format, and all samples were measured in technical triplicates.

qRT-PCR protocols were optimised, and annealing temperature settings changed if necessary. An example protocol is shown below:

95°C 2 minutes → (95°C 20s → X°C 20s → 70°C 20s → plate read) X 44 cycles → melt curve 55-95°C

Where X denotes the anneal temperature determined by predicted Tm for each primer set.

Before starting the reaction, plates were spun down for 5 minutes at 4000rpm to remove air bubbles in the reaction mix. All plates were run using the CFX96 Connect Real-Time PCR detection system [Bio-Rad], and analysed using the associated Bio-Rad CFX Manager software.

For relative gene expression analysis, RNA was extracted (as described in chapter 2.5.2) from 6x N2, 6x *aakg-1*(*syb409*); *aakg-2*(*syb410*); *aakg-3*(*syb411*) and 6x *aakg-4*(*tm5539*); *aakg-5*(*tm4052*) samples. The *daf-2* background used RNA samples harvested from 6x N2, 6x *daf-2*(*m577*), 6x *daf-2*(*m577*); *aakg-4*(*tm5539*); *aakg-5*(*tm4052*), 6x *daf-2*(*m577*); *aakg-1*(*syb409*); *aakg-2*(*syb410*); *aakg-3*(*syb411*). Primers listed in table 2.2.

Each 94-well plate contained triplicate wells of each population for statistical accuracy, and six biologically independent populations of each strain were used to account for variation. Statistical analysis was performed using Student's *t*-test, using the T.TEST function in Microsoft Excel.

2.6 Kinase activity analysis (Western Blotting):

2.6.1 Sample collection.

Phenformin was used in this assay to induce activation of AMPK in *C. elegans*. A 450mM phenformin stock solution [Sigma] was added to 1L NGM after cooling (dilution 1:100), producing a final concentration of 4.5mM in agar plates.

Animals were synchronised through bleach prep and grown on NGM plates seeded with OP50-1. L4 stage animals were washed off 12 plates in M9, washed twice more in 1ml M9 to reduce cross-contamination, and pipetted onto control or 4.5mM phenformin plates.

After 48 hours treatment animals were washed off using 2ml M9 into a 15ml falcon tube, where the sample settled for 5 minutes. After settling, excess M9 was removed and 2ml M9 was added so that worm slurry could be transferred into an eppendorf using a glass pipette. Animals were washed twice more in 1ml M9 to reduce bacterial contamination. Excess M9 was removed, and the sample was frozen at -80°C. Samples consisted of a dense pellet of animals, between 75-100µl.

2.6.2 Protein extraction (Sonication).

After approximately 10 minutes, samples were removed from the freezer and 100-150µl of Phosphosafe™ extraction agent [Merck-Millipore] and protease inhibitor cocktail [Roche] was added while the sample was thawing, to preserve the protein phosphorylation state as effectively as possible. The volume of protease inhibitor cocktail – Phosphosafe™ mix added was dependent on the original sample volume; an approximate 1.5:1 ratio of Phosphosafe™ mix to sample allowed for effective sonication.

Once the sample was completely thawed, the sample was sonicated for 30 cycles (30 seconds on, 30 seconds off, in 4°C cooled water) in a Diagenode Bioruptor. Complete breakdown of the sample was confirmed visually through a Leica dissecting scope. Samples were spun down in a benchtop centrifuge (13,000 rpm, 4°C, 300 minutes) and the supernatant was pipetted into a fresh 1.5ml Eppendorf tube, and stored at -20°C.

2.6.3 Protein quantification.

The Bradford method was used to quantify protein levels. This assay allows quantification of proteins through a shift in the maximum absorption of the dye between 465nm to 595nm; producing a colour change from red to blue, which occurs when the dye binds to protein (Bradford, 1976). 5µl of cell lysate was mixed with 250µl of 1x Quick start Bradford dye reagent [Bio-Rad] in a 96-well plate [Greiner]. The optical density of each well was read in the plate reader at 595nm. All samples were allowed to mix with dye for 5 minutes before reading.

Protein concentration was calculated through standard curve gradient analysis - The R^2 correlation coefficient was checked to confirm the quality of the standard curve, and the 'y=mx+c' equation was used to determine the 'x' value, which represented concentration (ug/ml). This value could then be used to find out the required volume for 30ug of protein. A new standard curve was generated for each protein extraction.

2.6.4 Western Blotting Polyacrylamide Gel Electrophoresis.

30µg protein samples of consistent volume were prepared by diluting the protein up to 15µl with double-distilled H_2O. 15µl of 2x Laemmli sample buffer [Bio-Rad] was added to the sample and boiled at 95°C for 5 minutes in a heating block. Samples were spun down in a microcentrifuge before loading and 25µl of the 30µl total sample volume was loaded onto a hand-poured SDS-polyacrylamide gel.

Protein samples were run using Tris-Glycine running buffer, initially through a 4% stacking section at a constant 50V, followed by resolution in a 10% separating gel (150V constant). Once the dye front had progressed to approximately 1cm from the bottom of the gel, proteins were transferred to the nitrocellulose membrane using a semi-dry blotter [Trans-Blot SD, Bio-Rad]. Chilled Transfer Buffer (1X Transfer Buffer, 20% methanol) was used, and protein transfer ran at 70mA constant for 1 hour. After transfer, blots were blocked in 5% BSA + Tris-buffered saline, 0.1% Tween (TBS-T), under constant agitation for 2 hours.

2.6.5 Western Blotting

Blots were treated overnight at 4°C with 1:1000 dilution of phospho-AMPKα (Thr172) antibody [Rabbit, Cell Signaling Technology] in 5% BSA+TBS-T. Between antibody treatments, blots were washed 3 times for 5 minutes with 15ml of TBS-T buffer. All antibody treatments and wash steps were performed under constant agitation/rocking.

Blots were subsequently treated with a 1:5000 dilution of anti-rabbit-HRP [Sigma] for 1 hour at RT. After this, blots were washed again, before the addition of Clarity™ Western ECL substrate [Bio-Rad].

Once the chemiluminescent compounds had been mixed, 3ml of substrate solution was poured over the blot. Each blot was exposed to a piece of green/blue-sensitive x-ray film [Superfilm, GE Healthcare Amersham] in a dark room, under red light. Film was placed over the blot in a light-locked box for a specific number of minutes/seconds, then removed and promptly run through an Optimax 2010 X-ray film processor [Protec].

Immediately after capturing phospho-AMPKα chemiluminescence on film, the blot was washed again 3 times in TBS-T to remove residual ECL reagent. Blots were then incubated in 1:1000 dilution of β-actin antibody [Mouse, Santa Cruz] for 1 hour at RT. Following another set of washes in TBS-T, blots were incubated with 1:5000 anti-mouse-HRP [Dako] for 1 hour at RT. After treatment with this second set of (β-actin-specific) antibodies, the blot was washed, then treated with Clarity™ Western substrate and exposed using X-Ray film, as described previously.

X-ray film images were captured using manual mode on a smartphone camera, capture settings were kept consistent throughout each session (No flash, shutter speed=1/750, ISO=100, exposure=0.5). Comparative quantification of P-AMPKα vs β-actin bands was carried out using the ellipse analysis tool in Image Studio Lite (Ver 5.0, LI-COR). P-AMPKα band intensity was normalised to the respective β-actin band for each sample. Five background readings were recorded and used to reduce the influence of background noise in band intensity measurements. Statistical analysis was performed using Student's *t*-test, using the T.TEST function in Microsoft Excel.

2.7 PyMOL Modelling:

Sequence files for each of the *aakg* isoforms were obtained from Wormbase (wormbase.org). FASTA sequences were run through the Phyre2 (www.sbg.bio.ic.ac.uk/phyre2) modelling engine, and protein data bank (PDB) files were viewed in PyMOL (PyMOL Ver.1.7.4.5). Mammalian structural files

were obtained from the protein data bank (www.rcsb.org/) which were uploaded by the Carling/Gamblin labs. Initially, each *aakg* isoform structure was overlaid with the mammalian structure, to determine whether there were any obvious changes to secondary-structure elements (α-helices, β-sheets, and loops).

Locations of key predicted binding residues from Tullet *et al*. (2014) were identified in each structural file and compared; modelling these residues enabled quick visualisation of potential interactions of binding residues with adenine nucleotides (AMP/ADP/ATP) and highlighted how this may be perturbed in *aakg-4* and *aakg-5* isoforms (Chapter 3.1, figure 3.1).

2.8 Primer table:

Target	Forward/Internal/Reverse	Sequence 5'-3'	Annealing Temperature (X°C)
aakg-1 genotyping	F	GGCATGGGACACTCTGACA	66.1
	IN-R	GGCTACTATTGTCGTTGAGC	
aakg-2 genotyping	F	GCGGTCTACATTTCCCTCCT	60.0
	IN-R	TCATGTGACTGATTCGTTGG	
	R	CTCATTGTCCCGAACAGATA	
aakg-3 genotyping	F	CTACTTGCACTCTAAGTTTC	60.0
	IN-R	AAGTTGTGGCCTTATTGCG	
	R	AGGGTCACTAAAATCTTGAC	
aakg-4 genotyping	F	AGTCTCTGACACGCCGAGTT	60.0
	IN-R	GCACAGGCTTTTAGACTTCG	
	R	GGCATACTCGATGTGCTAGA	
aakg-5 genotyping	F	GGTGCAGAGAAATTGGAACAG	59.2
	IN-F	GACAATGGATTCCGAAGACC	
	R	GTACTGATGATAGGGATCCG	
qRT-PCR control *cdc-42*	F	CTGCTGGACAGGAAGATTACG	61.0
	R	CTCGGACATTCTCGAATGAAG	
qRT-PCR control *pmp-3*	F	GTTCCCGTGTTCATCACTCAT	58.0
	R	ACACCGTCGAGAAGCTGTAGA	
qRT-PCR control *Y45F10D.4*	F	GTCGCTTCAAATCAGTTCAGC	61.0
	R	GTTCTTGTCAAGTGATCCGACA	
qRT-PCR *aakg-1*	F	GACATCGTCCAAATTAGTGGTATT	60.0
	R	GTCTCCTTTGTCGTAGTGCTT	
qRT-PCR *aakg-2*	F	TGCTCAATAAAGGAGTCTCTGGA	60.0
	R	AGATACTACACGCTCATCATTCTT	
qRT-PCR *aakg-3*	F	GGAGTTCTTTCGGTTACGGACTTCATTA	65.0
	R	CCTTTCGTTTCAAGACATCCTTTCCATC	
qRT-PCR *aakg-4*	F	AGCGACTTTGGAGATGCAAT	60.0
	R	CGTGGTATTCAAGCCGATCT	
qRT-PCR *aakg-5*	F	CTCGTCCGATCTCGTTCAAT	60.0
	R	CGGGTAGTAGGAGTCGATGC	

Table 2.2| Primer sequences and respective annealing temperatures for genotyping and quantitative real-time PCR. The intended application for each primer set is indicated in the target column to the left of each sequence. Genotyping PCR primers for *aakg-1, aakg-2,* and *aakg-3* isoforms were designed during this project. Additionally, qRT-PCR primers for all aakg isoforms were designed during this project.

Chapter 3 – A functional investigation into AMPKγ regulation in *C. elegans*.

AMPK is a heterotrimeric kinase and key metabolic regulator. Although AMPK regulation has been investigated to a considerable degree in mammalian models, its regulation in *C. elegans* remains poorly understood. Most research groups who have explored the function of AMPK previously have focused on its catalytic α subunit – which is actively involved in phosphorylating target proteins. However, the α subunit is just one component of the heterotrimeric complex. I chose to instead focus on AMPKγ which binds (and is allosterically regulated by) AMP/ADP, determining how AMPK functions as a cellular energy sensor. As a central metabolic regulator closely involved with several pathways (Figure 1.6), including the TOR pathway (another key regulator of metabolism), there are clear incentives to further understand the regulation of AMPK; it can offer mechanistic insights, as well as potentially revealing novel drug targets. Regarding structural biology, studying AMPK in *C. elegans* could produce further understanding of key elements of the AMP-binding sites, and modification of structural elements can reveal how these elements affect the function of AMPK.

Although some *aakg* (*C. elegans* AMPKγ) isoforms have been investigated previously (Apfeld *et al.*, 2004; Sagi and Kim, 2012; Hwang *et al.*, 2014; Tullet *et al.*, 2014), here I aim to increase understanding through investigation of all five *C. elegans* AMPKγ isoforms either independently or in combination with each other. In this chapter I explore regulation in three ways: Firstly by using computational modelling to examine the nucleotide binding sites in each AMPKγ isoform, secondly by using classical genetics techniques to investigate individual and combination AMPKγ mutants in *C. elegans*, and thirdly by examining these mutants in AMPK activity assays.

Investigations were designed to satisfy the following aims:

- To model key nucleotide binding residues in each AAKG isoform using *in silico* techniques and determine similarities and differences between the five subunits.
- Generate genetic tools to explore the role of AMPKγ subunits in *C. elegans,* both in WT and IIS mutant backgrounds.
- Determine the role of AMPKγ subunits in regulating *C. elegans* AMPK activity.

3.1 Structural modelling of AMPKγ subunits.

AMPKγ in *C. elegans* contains five isoforms (Tables 1.1 and 3.1). Isoforms *aakg-1, aakg-2,* and *aakg-3* are effectively conserved between *C. elegans* and humans (Table 3.2 and supplementary figure 1)(Xiao *et al.*, 2007; Tullet *et al.*, 2014). In contrast, *aakg-4* and *aakg-5* are not conserved in mammals or higher organisms. Previous work reports that AAKG-4 and AAKG-5 do not show conservation of predicted key binding residues – AAKG-4 displays no conservation, while AAKG-5 shows conservation of only one pair of residues (Table 3.1) (Tullet *et al.*, 2014). All AAKG isoforms were 3D modelled to investigate whether these residue differences would be significant enough to potentially inhibit normal interactions with AMP/ADP.

A 3D modelling program, PyMOL (pymol.org), was chosen to model the interactions between AMPKγ and AMP (Chapter 2.7). PyMOL is a powerful tool, though it requires that information be provided in a suitable format, allowing for interpretation and display of 3D model structures. Some information already existed, the structural file for mammalian AMPK (PDB ID: 2V8Q) was downloaded from PDB (Xiao *et al.*, 2007). However, for *C. elegans* AAKG isoforms, there was no resource bank available, so I used the Phyre2 modelling server to generate PDB files for each of the AAKG isoforms.

Once PDB files were generated, they were loaded into the PyMOL program alongside the mammalian structural file of AMPK. The PyMOL display interface allows the user to align multiple protein models to each other, and the view around a structure can be manipulated. Different elements of structure can be highlighted and colour-coded to preference, and this allows for a large amount of structural information to be visualised and interpreted on-screen.

Gene:	Residue Locations:					Total residues in FASTA file:
PRKAG1	R69	H150	R151	H297	R298	330
AAKG-1	R248	H332	R333	H479	R480	582
AAKG-2	R81	H177	R178	H327	R328	423
AAKG-3	R136	H232	R233	H383	R384	425
AAKG-4	I187	S261	F262	S415	S416	465
AAKG-5 (Isoform b)	T208	H280	R281	Q426	S427	488

Table 3.1| Predicted key AMP-binding residues are not conserved in *C. elegans* AAKG-4 and AAKG-5. AMPKγ protein sequences were aligned using the NCBI tool Blastp (https://blast.ncbi.nlm.nih.gov). PRKAG1 numbering was obtained from the 'PRKAG1 Isoform 1' FASTA sequence file on Uniprot.org (Uniprot ID: **P54619-1**). Conserved residues in *C. elegans* AAKG isoforms are highlighted in green, whereas non-conserved residues are shown in red, as in figure 3.1 below. For AAKG-5, residues Q426 and S427 did not appear in the Blastp alignment, but residue changes were previously reported by Tullet *et al.* (2014). Since there is only one location where a glutamine (Q) residue is followed by a serine (S) residue in the FASTA sequence file, the location of these residues could be determined and are reported above. It is important to note that residue numbering may change as more complete structural data becomes available for some *C. elegans* AAKG isoforms.

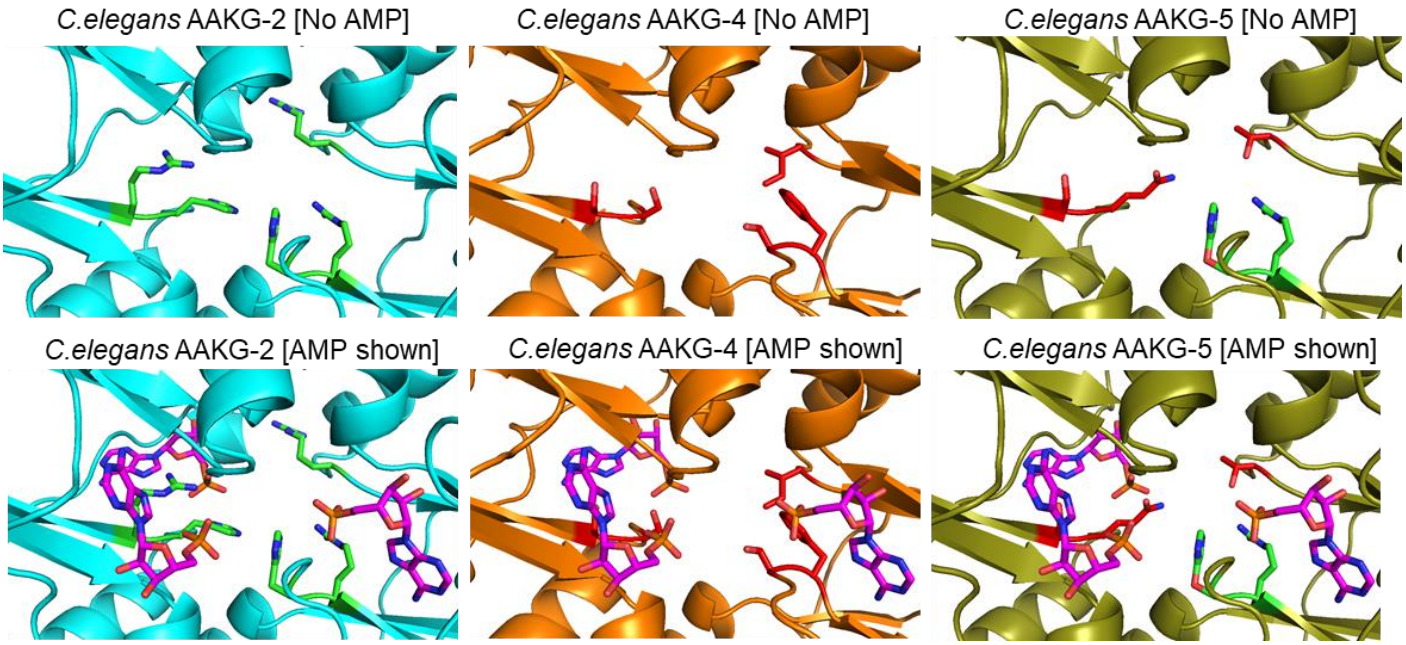

Figure 3.1| The AMP-binding sites of AAKG-2, AAKG-4, and AAKG-5. AMPKγ subunits were modelled using PyMOL. AAKG-2 was chosen as a representative isoform for AAKG-1-3, which all show conservation of predicted key AMP-binding residues with mammalian PRKAG1 (Table 3.1). However, there is no conservation or limited conservation of AMP-binding residues in AAKG-4 and AAKG-5 respectively, so these isoforms are shown in separate panels above. In cases where multiple isoform sequences existed, the longest protein sequence was selected for modelling. For each isoform, the predicted binding residues have been coloured differently from the rest of the cartoon structure and shown as sticks: residues highlighted in green are conserved, while those shown in red are not (as in table 3.1). An existing structure file (PDB ID:**2V8Q**) was used for the generation of AMP molecules in PyMOL. AMP molecules are coloured in magenta. Dark blue shading indicates the presence of nitrogen atoms, a constituent part of charged amine groups on histidine and arginine side chains. Pale red and orange shading represents oxygen and phosphorus atoms, respectively, highlighting phosphate groups on AMP molecules. The predicted binding residues consist of histidine and arginine residues which interact with phosphate groups through positively charged sidechains. In isoforms AAKG-4 and AAKG-5, there is no conservation or less conservation of these key residues, respectively, which is expected to negatively impact on the ability of these isoforms to bind and respond to AMP (as well as other adenosine compounds).

Gene:	Total residues in FASTA file:	Identity % (PRKAG1):	E-value (PRKAG1):
PRKAG1	330	-	-
AAKG-1	582	55	3e-120
AAKG-2	423	36	1e-60
AAKG-3	425	31	5e-57
AAKG-4	465	27	1e-22
AAKG-5 (Isoform b)	488	25	1e-20

Table 3.2| Identity scores of *C. elegans* AAKG isoforms compared to human PRKAG1. AMPKγ protein sequences were aligned using the NCBI tool Blastp (https://blast.ncbi.nlm.nih.gov). PRKAG1 numbering was obtained from the 'PRKAG1 Isoform 1' FASTA sequence file on Uniprot.org (Uniprot ID: **P54619-1**). Gene names have been shaded to reflected conservation of the predicted AMP-binding residues, as described in table 3.1, above. The total number of residues in the FASTA sequence is shown, since the same sequences were used for alignment and modelling (Table 3.1 and figure 3.1). Identity reflects the percentage of residues conserved between protein sequences. The e-value score for each alignment indicates confidence in the alignment result. Alignments were scored using default algorithm parameters, including alignment scoring using the BLOSUM62 matrix and conditional compositional matrix adjustment. Screenshots of these alignments are shown in supplementary figure 1.

The interaction of AMP with key predicted binding residues was modelled for different AMPKγ isoforms (Figure 3.1). AMP-binding on AMPKγ is predicted to involve interactions between three arginine residues and two proximal histidine residues (highlighted in figure 3.1 and table 3.1). Collectively, these residues corresponded to AMP-binding sites 1 and 3 in mammalian AMPKγ, which demonstrate weak affinity and high affinity for AMP, respectively, and provide the basis for AMP-sensitive regulation of AMPK (Gu *et al.*, 2017). Non-conservation of these binding residues in the AAKG-4 and AAKG-5 isoforms is likely to substantial disrupt interaction between these AAKG isoforms and adenine nucleotides (AMP, ADP, and ATP). In a peptide sequence, both histidine and arginine can become positively charged, which encourages binding through interaction with the phosphate groups in AMP, ADP, and ATP (Figure 1.4). The loss of arginine and histidine residues in binding pockets of AAKG-4 and AAKG-5 could result in increased steric hindrance during adenine nucleotide binding, providing a rationale for a potential reduction of AMP-sensitivity in these isoforms (AAKG-5 would display reduced sensitivity to AMP; AMP-sensitivity could be largely ablated in AAKG-4).

All AAKG isoforms were aligned to the structural file for AMPK (PDB ID: 2V8Q), allowing for additional comparisons of AAKG-1-5 with mammalian AMPKγ. Alignments revealed that secondary

structure has been well-conserved in all AAKG isoforms compared to mammalian AMPKγ1 (Supplementary figure 2), but crucially modelling illustrated the complete conservation of key predicted binding residues in AAKG-1, AAKG-2, and AAKG-3 (Table 3.1). Following this, I was confident that changes to AMP-binding residues could be examined between the *C. elegans* AAKG isoforms themselves.

Each isoform was visualised in a pairwise manner, and non-conservation of key binding residues was confirmed visually. Additionally, both AAKG-4 and AAKG-5 were aligned with AAKG-1, AAKG-2, and AAKG-3 which allowed me to evaluate the extent of overall structural conservation between non-conserved and conserved AAKG isoforms, respectively. Displaying isoforms alongside each other in this way allowed for quick comparison of structural elements – but no obvious changes to secondary structure were observed between any of the AAKG isoforms (data not shown). This overall conservation of secondary structure (helices, sheets, and loops) is interesting to note, however the fact that it is similar between the isoforms suggests that secondary structure does not contribute to the proposed changes in AMP-sensitivity for AAKG-4 and AAKG-5 isoforms.

3.2 Developing genetic models to study the biological role(s) of *C. elegans* AMPKγ subunit families.

The importance of *aakg* to *C. elegans* AMPK function had already been established in existing literature, although usually select isoforms have been chosen as focal points of discussion, based on genetic screening/microarray data or roles in lifespan (Greer, Dowlatshahi, *et al.*, 2007; Tullet *et al.*, 2014). While investigating the role of *aakg-4* and *aakg-5* during the early stages of this project, it seemed worth examining the contributions of *aakg-1, aakg-2,* and *aakg-3* to AMPK regulation as well. Visualisation of AMP interactions through modelling showed how *aakg-4* and *aakg-5* could be more insensitive to AMP-binding than *aakg-1, aakg-2, and aakg-3* (Chapter 3.1), and this had previously been discussed in Tullet *et al.* (2014). Therefore, based on findings from PyMOL modelling combined with previously published data, the *aakg* subunits were grouped into two families: *aakg-1-3* (AMP-

sensitive) and *aakg-4* and *aakg-5* (AMP-insensitive). I use this classification as the thesis progresses but appreciate that it is currently based on a hypothesis. Knockouts were produced to model two alternative regulatory scenarios *in vivo* – an *aakg-1; aakg-2; aakg-3* mutant would demonstrate AMP-insensitive regulation of AMPK, and conversely an *aakg-4; aakg-5* mutant would model the effects of relying exclusively on AMP-sensitive regulation. While this may not be a perfect approach, it allowed for screening of differences in subunit function within this complex system. Following generation of single *aakg* mutants using CRISPR-Cas9 gene editing technology (Chapter 2.2), combination knockout strains were produced using classical genetic techniques. Ultimately *aakg-1; aakg-2; aakg-3* and *aakg-4; aakg-5* mutants were generated in WT and *daf-2* backgrounds, so that the effects of *aakg* mutation could be reported under normal conditions and compared with responses under reduced IIS. This was important aspect of this project because mutation of *aakg-4* causes more substantial lifespan suppression in *daf-2* background than in WT (Figure 4.2)(Tullet *et al.*, 2014).

aakg-4(tm5539) and *aakg-5(tm4052)* mutants were already available to the lab at the beginning of this project. However, *aakg-1, aakg-2,* and *aakg-3* mutants were not available from the CGC, and so were generated by a third-party company (SunyBiotech) using CRISPR-Cas9 gene editing technology. I designed a deletion strategy, which targeted exon sequences in each strain, targeting multiple exons where possible (Figure 3.2). The mutants were produced in our lab's WT background (Chapter 2.2), removing the need for backcrossing upon delivery. Genotypes of *aakg* knockout strains were confirmed using two- or three-primer single worm genotyping strategies (Chapter 2.5.1).

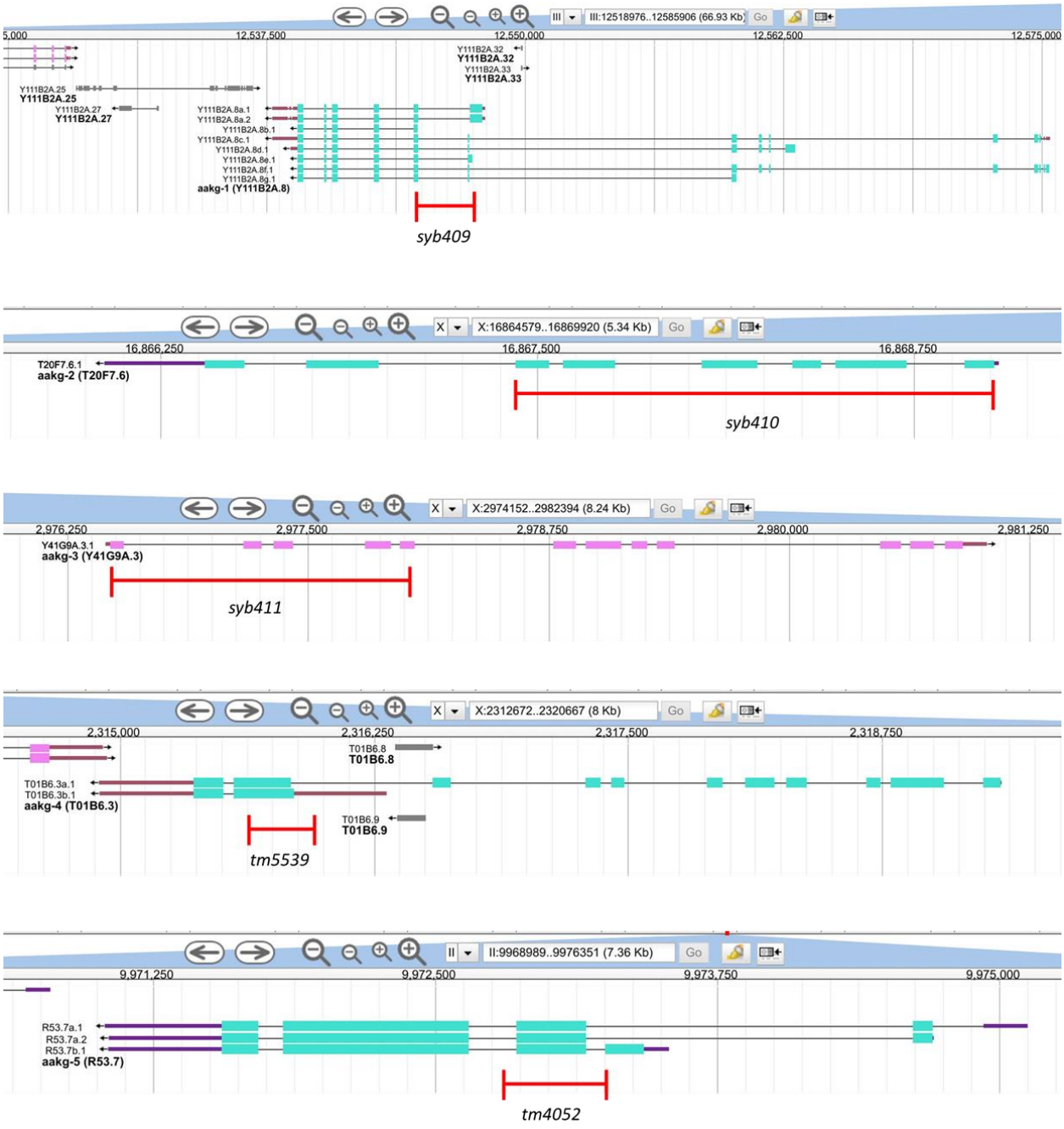

Figure 3.2| Gene schematic diagrams indicating deletion mutations in *aakg* mutant strains.
Successful deletion was confirmed using a three-primer PCR strategy, as well as qRT-PCR. *aakg-1(syb409), aakg-2(syb410)* and *aakg-3(syb411)* are novel CRISPR-Cas9 deletion mutants generated for this study. Conversely, *aakg-4(tm5539)* and *aakg-5(tm4052)* have been used before this project. The deleted region is indicated by the red bar shown below the sequence(s) of interest in each case. Chromosome identity is shown at the top of each panel above the scale bar (*aakg* isoforms are found on chromosomes II, III and X). Screenshots captured while using the Wormbase genome browser (JBrowse).

Following confirmation of genotype, *aakg* mutants were then crossed with each other using classical genetics and the genotype of resulting progeny was identified using PCR and specific genotyping primers (Table 2.2). This strategy is illustrated in figure 3.3. The final tier of the strategy shows combination knockout strains which have been used to effectively model AMP-sensitive and AMP-insensitive regulation throughout this thesis, thus determining the significance of either set of isoforms to a variety of physiological and metabolic variables.

Strains were generated according to the schematic displayed below (Figure 3.3). The *aakg-4; aakg-5* mutant strain was constructed first since the desired combination knockout would be produced after only one tier of crossing. An *aakg-4; aakg-5* mutant can only rely on isoforms *aakg-1, aakg-2,* and *aakg-3* for AMPK regulation, thereby modelling reliance on AMP-sensitive regulation. The mutant is viable, and could be easily maintained at 15°C, 20°C and 25°C; confirming that mutation of isoforms *aakg-4* and *aakg-5* is not lethal.

To generate a strain of *C. elegans* which only expresses AMP-insensitive *aakg* isoforms, *aakg-1* and *aakg-3* mutants were crossed with each other, and simultaneously *aakg-2* and *aakg-3* mutants were crossed together. Both *aakg-1; aakg-3* and *aakg-2; aakg-3* strains were viable, with no obvious signs of sickness. These strains were then crossed together, generating the desired triple knockout strain – an *aakg-1; aakg-2; aakg-3* mutant (Figure 3.3). Again, this strain showed no indicators of poor health during general maintenance at 15°C, 20°C and 25°C. This strategy established that all combination knockouts displayed in figure 3.3 are viable; despite carrying various *aakg* isoform mutations. Strain viability suggests that AMP-sensitive AMPK regulation is not essential for embryonic or larval development, or that *aakg-1-5* display some level of functional redundancy across tissues (in *C. elegans*). The creation of *aakg-1; aakg-2; aakg-3* and *aakg-4; aakg-5* mutants satisfies the aim of creating two genetic knockout strains which model alternative regulation of AMPK: an *aakg-1; aakg-2; aakg-3* mutant must rely on AMP-insensitive AMPK regulation mediated via *aakg*-4 and *aakg-5*

isoforms, while an *aakg-4; aakg-5* mutant relies exclusively on AMP-sensitive regulation mediated through *aakg-1, aakg-2,* and *aakg-3*.

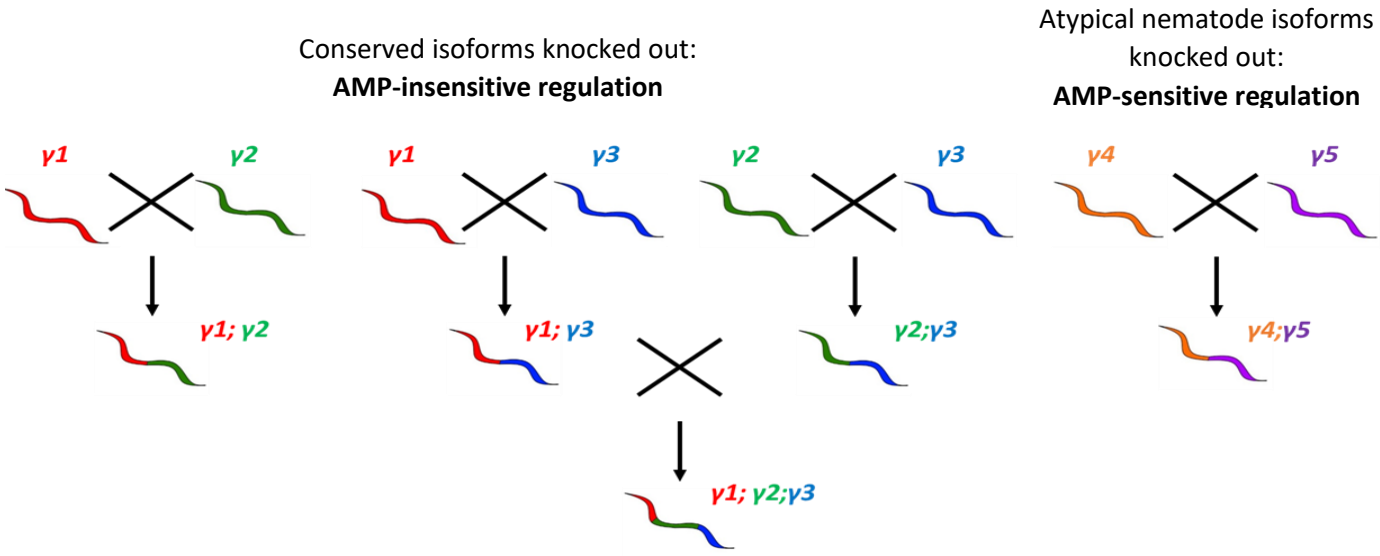

Figure 3.3| Systematic generation of *aakg* combination knockout strains. A set of combination mutants were generated from single *aakg* knockout strains for each *aakg* isoform. Generation of an *aakg-4(tm5539); aakg-5(tm4052)* mutant required just one cross; two double mutant strains were required to produce an *aakg-1(syb409); aakg-2(syb410); aakg-3(syb411)* combination mutant. This strategy allowed for generation of an *aakg-1; aakg-2; aakg-3* knockout strain without complicating the process of progeny selection further than a 1/16 mendelian distribution of desired genotypes in the offspring selected at each stage. Together, the *aakg-1; aakg-2; aakg-3* and *aakg-4; aakg-5* mutants represent models of AMP-insensitive and AMP-sensitive systems of regulation, respectively. The status of each knockout strain was confirmed after each cross using PCR genotyping, with a specific triple-primer strategy for each *aakg* isoform. Later, efficacy of the strategy was confirmed through qRT-PCR analysis of relative *aakg* mRNA expression levels in combination mutants (Figure 3.5). All mutants generated through this strategy are viable in a WT background, and can be effectively maintained at 15°C, 20°C and 25°C.

Because *aakg-4* had also already been shown to be important for *daf-2* longevity, combination *aakg* mutants were also generated in a *daf-2* background so that the influence of IIS on *aakg* mutant phenotype could be explored further (Tullet *et al.*, 2014). The *daf-2(m577)* background mutation was introduced to *aakg* mutants, and through a similar strategy to the WT background (outlined in figure 3.4), this culminated in the production of quadruple and triple mutant strains (*daf-2; aakg-1; aakg-2; aakg-3* and *daf-2; aakg-4; aakg-5* respectively). In this round of crossing, I took advantage of the *daf-2* dauer induction phenotype at 25°C to streamline strain generation. Previously generated *aakg* mutant hermaphrodites were crossed with *daf-2* background males. A day after fertilisation, parent worms were removed, and progeny allowed to develop at 25°C. Only progeny resulting from successful crossing would carry the *daf-2* mutation and enter dauer, while offspring from hermaphrodite *aakg* parents which self-fertilised would continue development at 25°C. Dauer offspring were selected after 3 days, and *aakg* mutants were confirmed through PCR genotyping. No effect on viability was observed in any *aakg* combination knockouts in a *daf-2* background, indicating IIS does not induce any substantial change to strain viability. Generation of this genetic system in both WT and *daf-2* backgrounds facilitated later investigations into the functional importance of different *aakg* isoforms and allowed for examination of IIS-mediated effects on AMPKγ function in *C. elegans*.

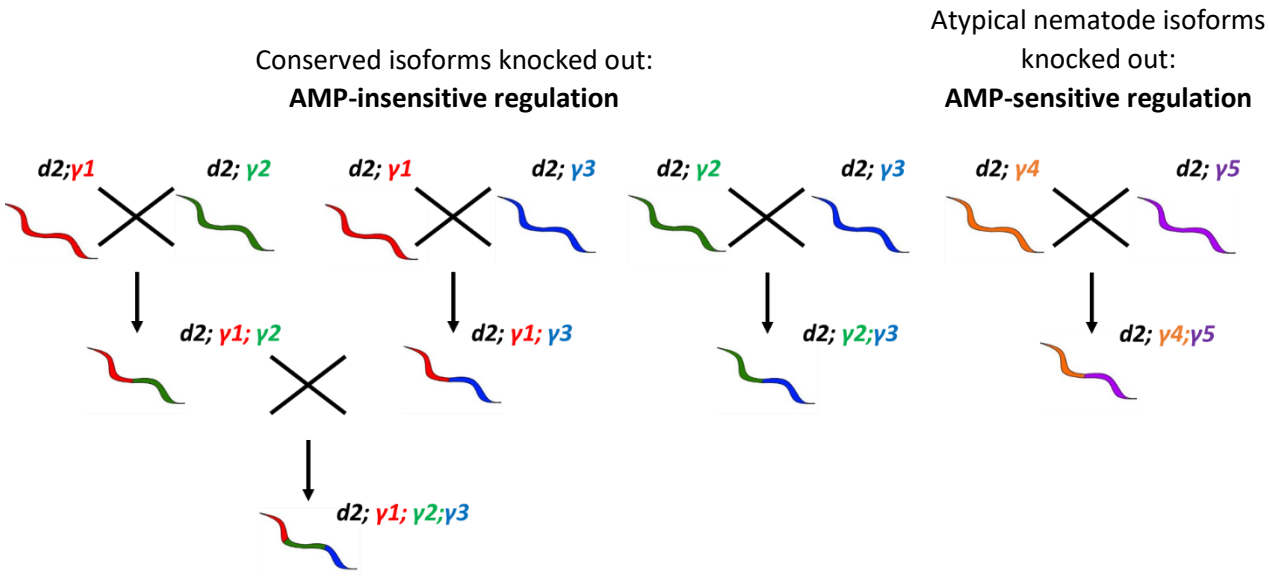

Figure 3.4| Systematic generation of *daf-2(m577)* background *aakg* combination knockout strains. Combination *aakg* mutants were generated from single or double knockout strains for each *aakg* isoform. The *daf-2(m577)* background mutation had been introduced to single *aakg* mutant strains prior to use of crossing strategy shown here. Together, *daf-2; aakg-1(syb409); aakg-2(syb410); aakg-3(syb411)* and *daf-2; aakg-4(tm5539); aakg-5(tm4052)* mutants represent models of AMP-insensitive and AMP-sensitive systems of regulation, respectively. The status of each knockout strain was confirmed after each cross: Initially through induction of the temperature-sensitive *m577* dauer phenotype at 25°C; then *aakg* mutant genotype was confirmed using a specific triple primer strategy for each *aakg* isoform. Later, *aakg* deletions were additionally confirmed through qRT-PCR (Figure 3.6). All mutants generated through the above strategy are viable and can be effectively maintained at 15°C and 20°C.

3.3 Quantification of relative mRNA levels in AMPKγ isoform mutants.

Once combination mutant strains had been generated and confirmed through PCR genotyping, qRT-PCR was used to provide further information on mutant strains. The protocol was described in detail earlier (Chapter 2.5). qRT-PCR was used to quantify *aakg* expression; mRNA levels for each of the *aakg* isoforms were determined in combination mutants (and control strains), and the possibility of adaptive responses at the genetic level to loss of AMP-sensitive or AMP-insensitive isoforms investigated. Additionally, analysis of combination mutants in WT and *daf-2* backgrounds provided insight into how transcriptional changes are affected by IIS.

In a WT background, an *aakg-4; aakg-5* mutant showed significantly reduced expression of *aakg-1, aakg-2,* and *aakg-3* isoforms ($p<0.01$, figures 3.5A and 3.5B; $p<0.05$, figure 3.5C). This suggests that *aakg-4* and *aakg-5* may contribute to the control of proper expression of the AMP-sensitive *aakg* isoform family (*aakg-1, aakg-2, aakg-3*). In this scenario, absence of AMP-insensitive isoforms in an *aakg-4; aakg-5* mutant may leave important signalling events for correct expression of *aakg-1, aakg-2,* and *aakg-3* inactivated, resulting in reduced expression seen across each of the remaining *aakg* isoforms in an *aakg-4; aakg-5* mutant. Conversely, there were no significant differences in *aakg-4* and *aakg-5* expression in an *aakg-1; aakg-2; aakg-3* mutant compared to WT (Figures 3.5D and 3.5E), suggesting that *aakg-1, aakg-2,* and *aakg-3* do not influence transcriptional regulation of *aakg-4* and *aakg-5* expression. Moreover, this comparison implies that *aakg-4* and *aakg-5* might maintain their own expression in an *aakg-1; aakg-2; aakg-3* mutant, but further investigation using *aakg-4* and *aakg-5* mutants is required to determine the individual contributions of *aakg-4* and *aakg-5* to transcriptional regulation of each *aakg* isoform. This could not be investigated during this study due to project time constraints.

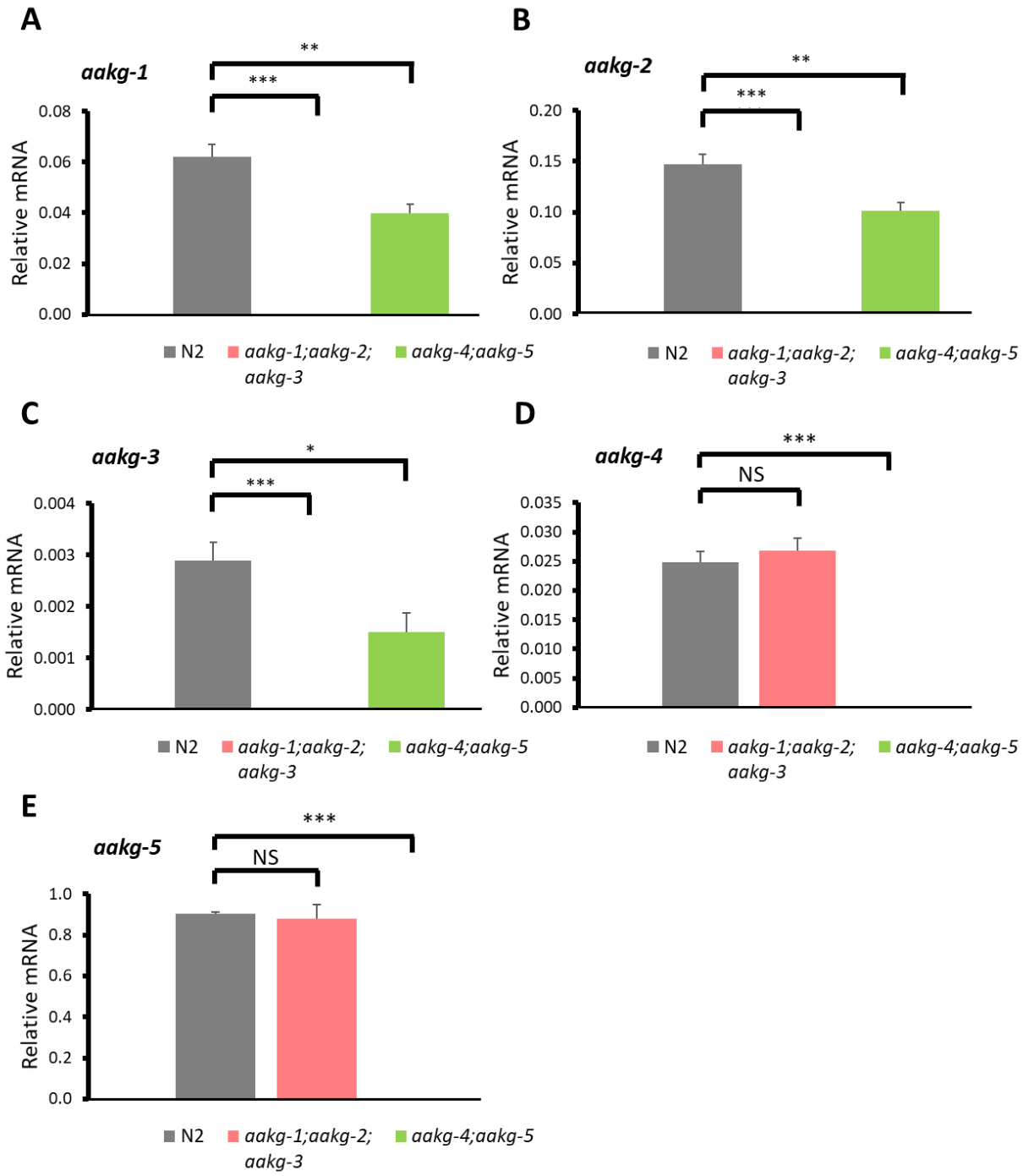

Figure 3.5| AMP-sensitive *aakg* isoform mRNA levels are reduced in an *aakg-4; aakg-5* mutant.
Expression profiles of (**A**) *aakg-1*, (**B**) *aakg-2*, (**C**) *aakg-3*, (**D**) *aakg-4* and (**E**) *aakg-5* isoforms in WT background strains. In an *aakg-1(syb409); aakg-2(syb410); aakg-3(syb411)* mutant there is no significant change to *aakg-4* or *aakg-5* expression compared to N2(WT). However, an *aakg-4(tm5539); aakg-5(tm4052)* mutant shows reduced *aakg-1, aakg-2,* and *aakg-3* expression compared to N2(WT), suggesting that *aakg-4* and *aakg-5* transcriptionally regulate *aakg-1-3*. Levels of mRNA for each of the five *aakg* isoforms have been displayed as arbitrary units, relative to geometric mean of three housekeeping genes (*cdc-42, pmp-3* and *Y45F10D.4*). *p<0.05, **p<0.01, ***p<0.001, compared to WT (Student's *t*-test). Mean values generated from six biologically independent populations are shown. Levels of mRNA for each of the five *aakg* isoforms have been displayed as arbitrary units, relative to geometric mean of three housekeeping genes (*cdc-42, pmp-3* and *Y45F10D.4*). Error bars indicate standard error of the mean (SEM).

Analysis of *aakg* mutants in a *daf-2* background reiterated that the *daf-2* crossing strategy (Figure 3.4) was precise – qRT-PCR results confirm successful deletion of target genes in combination mutants (*daf-2; aakg-1; aakg-2; aakg-3* and *daf-2; aakg-4; aakg-5*) and both strains show significantly altered expression of remaining *aakg* isoforms (Figure 3.6).

Firstly, I examined N2(WT) *aakg* expression between backgrounds (Figures 3.5 and 3.6). WT *aakg* expression is largely similar between WT and *daf-2* background data, suggesting that WT expression was somewhat accurately represented between WT and *daf-2* data sets. However, *aakg-4* and *aakg-5* expression was lower in the *daf-2* background WT samples compared to the WT background (p<0.01, Student's *t*-test).

Next, I compared WT and *daf-2* mutant *aakg* expression (Table 3.3). This analysis revealed that a *daf-2* mutant did exhibit altered expression of some *aakg* isoforms. A *daf-2* mutant showed a 2-fold increase in expression of *aakg-1* compared to WT (p<0.001, table 3.3), while *aakg-2* expression in was reduced by half compared to WT (p<0.01, table 3.3). It is interesting to note an apparent dichotomy here between changed expression of *aakg-1* and *aakg-2* in a *daf-2* background. Curiously, *aakg-3* expression did not differ from WT levels in a *daf-2* mutant, though *aakg-3* expression was much lower than other *aakg* isoforms (relative to housekeeping control expression) (Table 3.3). In terms of the AMP-insensitive isoform family, *aakg-4* expression increased 2.7-fold in a *daf-2* mutant compared to WT (p<0.001, table 3.3), while a *daf-2* mutant displayed no substantial change in *aakg-5* expression compared to WT (Table 3.3).

Overall, a reduced IIS mutant showed substantially changed transcriptional regulation of *aakg* expression. Expression of *aakg-1* and *aakg-4* was significantly increased in a *daf-2* mutant compared to WT, while *aakg-2* expression was significantly lower, implying the existence of IIS-dependent mechanisms which affect WT *aakg* isoform expression. Increased *aakg-4* expression in a *daf-2(e1370)* background has previously been shown to be *daf-16*-dependent, and was suggested as a possible mechanism for the role of *aakg-4* in *daf-2*-mediated lifespan extension (Tullet *et al.*, 2014).

Additionally, *aakg-4* is involved in a positive feedback loop with the transcription factor DAF-16, downstream of the DAF-2 receptor (Tullet *et al.*, 2014). In future, it would be interesting to explore whether *aakg-1* and *aakg-2* demonstrate similar interactions.

Gene expression profile:	**WT vs. *daf-2* *p*-value (Student's *t*-test):**
aakg-1	$p<0.001$
aakg-2	$p<0.01$
aakg-3	NS
aakg-4	$p<0.001$
aakg-5	NS

Table 3.3| Changes to *aakg* isoform expression in a *daf-2(m577)* background. Significance values correspond to comparison of *daf-2(m577)* and N2(WT) data (shown in figure 3.6). Mean values were generated from six biologically independent populations. The geometric mean of three housekeeping genes (*cdc-42*, *pmp-3* and *Y45F10D.4*) was subtracted from mean Ct values, then six treated values were averaged and shown as bars in figure 3.6. Significance was determined using Student's *t*-test.

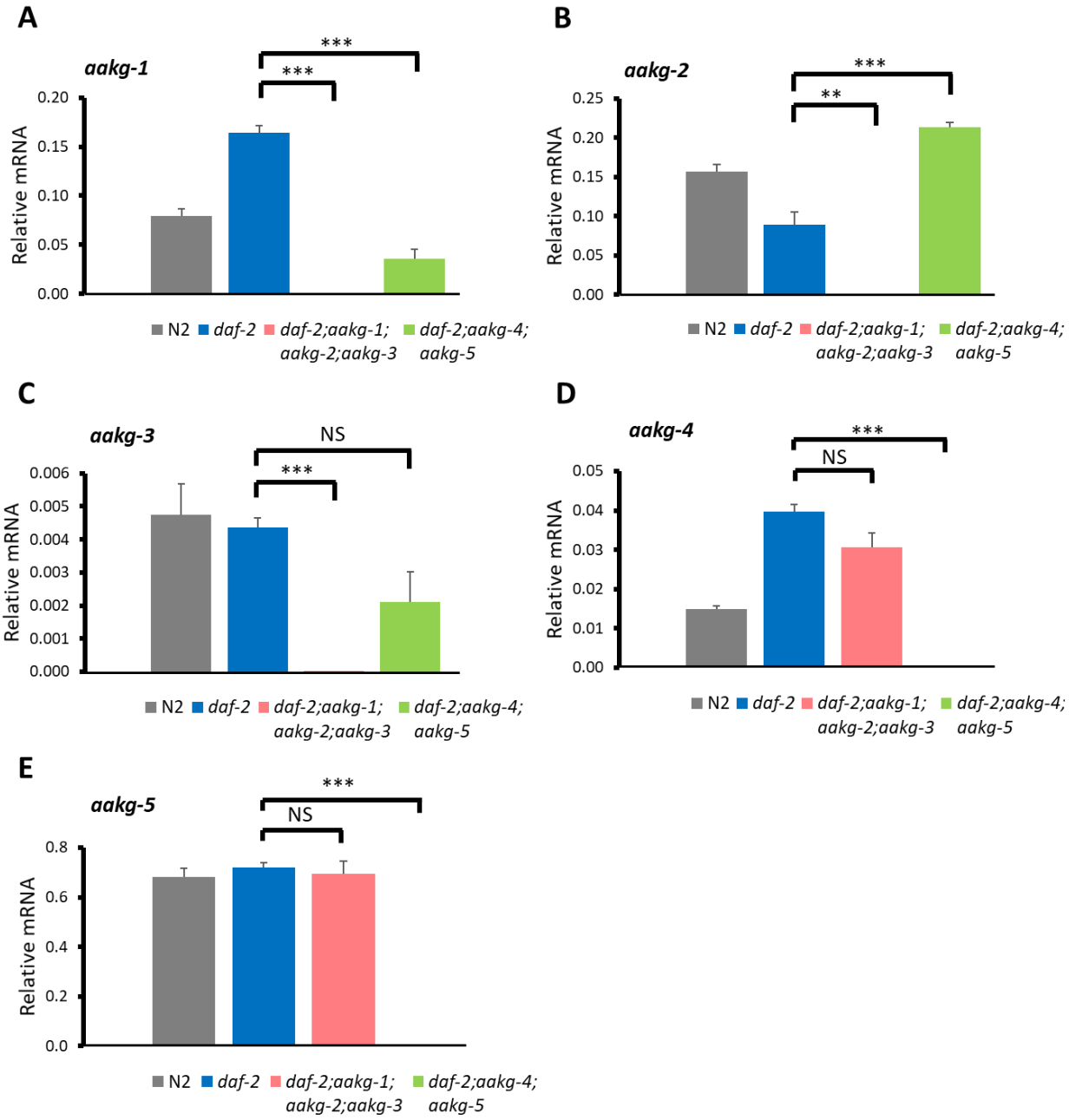

Figure 3.6| *aakg-1* and *aakg-2* mRNA levels in a *daf-2; aakg-4; aakg-5* mutant respond to multiple levels of regulation. Expression profiles of (**A**) *aakg-1*, (**B**) *aakg-2*, (**C**) *aakg-3*, (**D**) *aakg-4* and (**E**) *aakg-5* isoforms in *daf-2(m577)* background strains. A *daf-2(m577)* mutant already displays significantly altered *aakg-1, aakg-2,* and *aakg-4* expression (Table 3.3). A *daf-2; aakg-1(syb409); aakg-2(syb410); aakg-3(syb411)* mutant shows no significant differences in *aakg-4* and *aakg-5* expression compared to a *daf-2* mutant, mirroring the WT trend (Figure 3.5). In contrast, a *daf-2; aakg-4(tm5539); aakg-5(tm4052)* mutant shows significantly reduced *aakg-1* expression and up-regulated *aakg-2* expression compared to *daf-2*, implying the existence of additional mechanisms of transcriptional control beyond IIS-mediated changes (Table 3.3). Levels of mRNA for each of the five *aakg* isoforms have been displayed as arbitrary units, relative to geometric mean of three housekeeping genes (*cdc-42, pmp-3* and *Y45F10D.4*). **p<0.01, ***p<0.001, compared to *daf-2* (Student's *t*-test). Mean values of six biologically independent populations are shown. Error bars indicate SEM.

While a *daf-2* mutant displayed increased *aakg-1* expression and decreased *aakg-2* expression compared to WT (Table 3.3), a *daf-2; aakg-4; aakg-5* mutant seems to oppose *daf-2*-mediated transcriptional changes. A *daf-2; aakg-4; aakg-5* mutant displayed reduced *aakg-1* expression (p<0.001, figure 3.6A) and increased *aakg-2* expression compared to *daf-2* mutant (p<0.001, figure 3.6B). Additionally, *aakg-1* and *aakg-2* expression were lower and higher than WT expression levels, respectively (p<0.05, figure 3.6A and p<0.01, figure 3.6B). Importantly, this indicates that expression of *aakg-1* and *aakg-2* can be regulated differentially by IIS-dependent and IIS-independent (*aakg-4* and/or *aakg-5*-mediated) mechanisms. Consequently, changes in a *daf-2* background do not mirror the WT trend (where mutation of *aakg-4* and *aakg-5* resulted in reduced expression of *aakg-1, aakg-2,* and *aakg-3*). Additionally, WT, *daf-2,* and *daf-2; aakg-4; aakg*-5 worms did not show any statistically significant changes in *aakg-3* expression (Figure 3.6C), and *aakg-3* expression was consistently low compared to other *aakg* isoforms (relative to housekeeping control expression). With such low levels of expression, *aakg-3* expression may not reflect the action of regulatory mechanisms to the same extent as *aakg-1* and *aakg-2*.

Expression levels of *aakg-4* and *aakg-5* remained statistically similar between *daf-2* and *daf-2; aakg-1; aakg-2; aakg-3* strains (Figures 3.6D and 3.6E). *aakg-4* expression remains significantly higher than WT (p<0.01, figure 3.6D). Together, this supports the idea (described earlier in reference to WT background data, figure 3.5) that *aakg*-4 and *aakg-5* may be linked to regulation of *aakg* expression, a potential feedback mechanism which appears to be largely unaffected by IIS. In contrast, *aakg-1, aakg-2,* and *aakg-3* do not appear to affect transcriptional regulation of *aakg* expression, since *aakg-4* and *aakg-5* expression remains stable. Additionally, it is interesting to note, that *aakg-5* does not exhibit any substantial differences in expression between WT or *daf-2* background strains (excluding those where *aakg-5* was knocked-out).

3.4 AMPKα activation (monitored by Thr172 phosphorylation) is nullified in *aakg-1; aakg-2; aakg-3* mutants.

AMPK is heterotrimeric enzyme, with each subunit (α, β, and γ) performing a different function (Chapter 1.4.1). Importantly, sensitivity to AMP is communicated through the γ subunit, which can induce conformational change resulting in activation of the α subunit kinase domain. Conformational change induces exposure of the Thr172 residue on AAK/AMPKα, permitting phosphorylation of this residue by upstream kinases. This triggers subsequent phosphorylation of target proteins by AMPK. A key aim of this project was to investigate how changes in AMPK regulation (through removal of *aakg* isoforms) affect the functionality of the kinase. Some *C. elegans* AMPKγ isoforms (*aakg-1, aakg-2,* and *aakg-3*) are expected to show AMP-sensitivity, as all human AMPKγ (*PRKAG*) isoforms do (Figure 3.1). Non-conservation of predicted AMP-binding residues in *aakg-4* and *aakg-5* suggests that these isoforms have reduced sensitivity to AMP and ADP, and genetic knockouts of *aakg* isoforms had been generated, facilitating subsequent investigations into function. My investigation into AMPK regulation in *C. elegans* continues here by monitoring the relative phosphorylation of Thr172 between *aakg* mutants. The kinase activation assay was designed to determine relative binding of a specific antibody to the Thr172 phosphorylation site on the AMPKα subunit (Cabreiro *et al.*, 2013; Weir *et al.*, 2017). Since Thr172 is exposed as a result of AMP-binding, the binding of this specific antibody to phosphorylated Thr172 provides a valid readout of AMPK activation (Hawley *et al.*, 1996).

The WT background (Figure 3.7) included N2, *aakg-1; aakg-2; aakg-3* and *aakg-4; aakg-5* strains, while the *daf-2* background (Figure 3.8) was investigated using N2, *daf-2*, *daf-2; aakg-1; aakg-2; aakg-3* and *daf-2; aakg-4; aakg-5* strains. Combination mutants were used here (rather than individual *aakg* knockouts) to establish the role of AMP-sensitivity in AMPK activation. Blots were treated with the phospho-AMPKα antibody, and later with an β-actin antibody (Chapter 2.6); relative band intensity analysis is shown in figures 3.7 and 3.8.

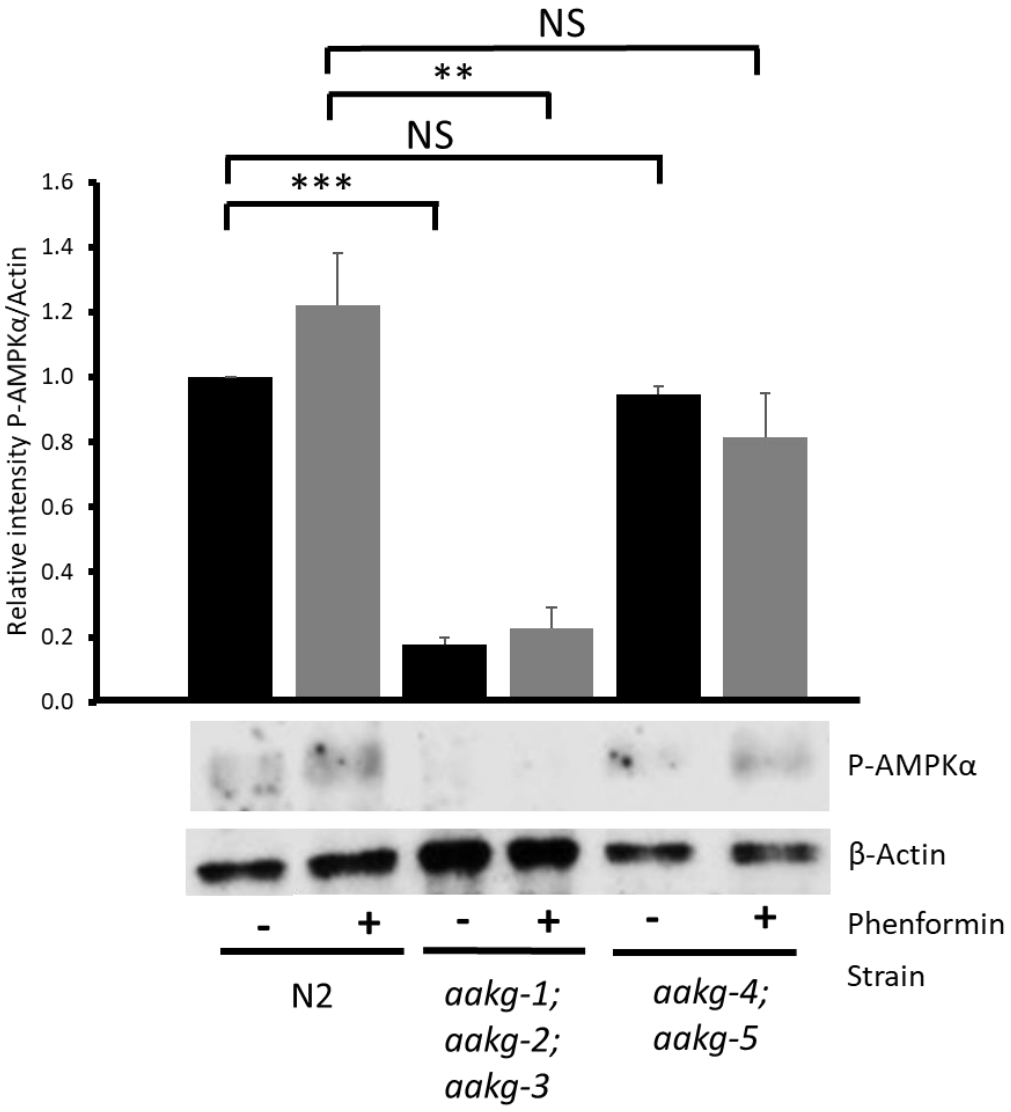

Figure 3.7| AMPKα in an *aakg-1; aakg-2; aakg-3* mutant is not phosphorylated at Thr172. In an *aakg-1(syb409); aakg-2(syb410); aakg-3(syb411)* mutant, remaining isoforms *aakg-4* and *aakg-5* are unable to effectively trigger AMP-induced activation of AMPK(α). Conversely, an *aakg-4(tm5539); aakg-5(tm4052)* mutant reports similar band intensity to N2(WT), confirming that *aakg-1, aakg-2,* and *aakg-3* are required to respond effectively to AMP. Western blot analysis shows levels of phosphorylated AMPKα under control conditions, and in response to 4.5mM phenformin. Relative band intensity of P-AMPKα to β-actin under untreated and treated conditions is shown, normalised to N2(untreated). Mean values are shown, from at least 3 biologically independent trials. Significance asterisks: **p<0.01, compared to WT (phenformin-treated) ***p<0.001, compared to WT (untreated) (Student's *t*-test). Error bars indicate SEM. One representative blot is shown below the graph.

Differences between strains are clear. An *aakg-1; aakg-2; aakg-3* mutant showed substantially decreased relative band intensity compared to WT (p<0.001, figure 3.7); suggesting that absence of predicted binding residues (Table 3.1) inhibits Thr172 phosphorylation and AMPKα activation. Consistent with this, an *aakg-4; aakg-5* mutant displayed statistically similar relative band intensity compared to WT (Figure 3.7), supporting the idea that *aakg-1, aakg-2,* and *aakg-3* isoforms are required for correct exposure of the Thr172 residue and its subsequent phosphorylation. Additionally, I investigated the response of an *aak-2* mutant to establish a positive control and determined that Thr172 phosphorylation was significantly reduced compared to WT (p<0.05, supplementary figure 3). Relative band intensity decreased to a similar extent between *aak-2* and *aakg-1; aakg-2; aakg-3* mutants, suggesting that mutation of *aakg-1, aakg-2,* and *aakg-3* effectively nullifies the activation of AMPK (at least in AMPK complexes containing the AAK-2 isoform). However, further investigation will be required to determine whether changes to complex formation influenced the results shown here. In HEK293 cells, a R531G mutation in AMPKγ2 resulted decreased expression of AMPKγ1 (Hawley *et al.*, 2010). If this kinase activity assay were expanded to include analysis of antibody binding to AMPK subunit epitopes, as well as the Thr172 phosphorylation site, this could clarify whether altered AMPK subunit expression contributes to the differences in Thr172 phosphorylation shown here.

Treatment with 4.5mM phenformin was used to force AMPK activation, to attempt to establish a further positive control through optimal AMPK activation. Though mechanism of biguanide drug action is not fully understood, numerous studies have established its efficacy as an activator of AMPK (Cabreiro *et al.*, 2013; Rena, Hardie and Pearson, 2017; Weir *et al.*, 2017). Interestingly, the same trend was displayed across strains in both untreated and treated data series: an *aakg-1; aakg-2; aakg-3* mutant showed dramatically reduced relative band intensity. However, analysis of untreated and treated samples for each strain revealed that while WT worms showed increased mean relative band intensity following phenformin treatment, this difference was not statistically significant across three biologically independent trials. Additionally, *aakg-1; aakg-2; aakg-3* and *aakg-4; aakg-5*

mutants did not report significant changes in relative band intensity between treated and untreated samples.

Still, the clear reduction in Thr172 phosphorylation observed in an *aakg-1; aakg-2; aakg-3* mutant prompted further investigation into how removal of *aakg* isoforms would affect AMPKα activation in a *daf-2* background, which would reveal whether reduced IIS would affect the *aakg-1; aakg-2; aakg-3* mutant result. Unfortunately, further problems were encountered while investigating Thr172 phosphorylation in the *daf-2* background. Although all reagents were maintained between backgrounds, issues with high background noise affected the reliability of intensity values recorded from some blots. This was possibly influenced by my semi-dry blotting technique. There were also issues with overexposure when analysing actin bands: Improvements to protein yield during the harvesting stage of the protocol meant that X-ray film capture required no longer than a few seconds of exposure. This is reflected in the size of the error bars in figure 3.8. In future, overexposure might be avoided by use of an alternative substrate during blotting, or by using a charge-coupled device imaging system.

Still, a *daf-2* mutant showed increased mean relative band intensity compared to WT (Figure 3.8), although this difference cannot be reported as statistically significant in this study. Though *daf-2* background data lacks statistical significance, it did seem to follow the WT trend: a *daf-2; aakg-1; aakg-2; aakg-3* mutant showed considerable reduction in mean relative band intensity compared to a *daf-2* control strain (Figure 3.8). Mean relative band intensity in the *daf-2; aakg-4; aakg-5* mutant appeared similar to a *daf-2* mutant, further mirroring the WT trend. As with WT data, phenformin treatment was used to attempt to produce a positive control, but phenformin treatment again produced varied results in *daf-2* background samples.

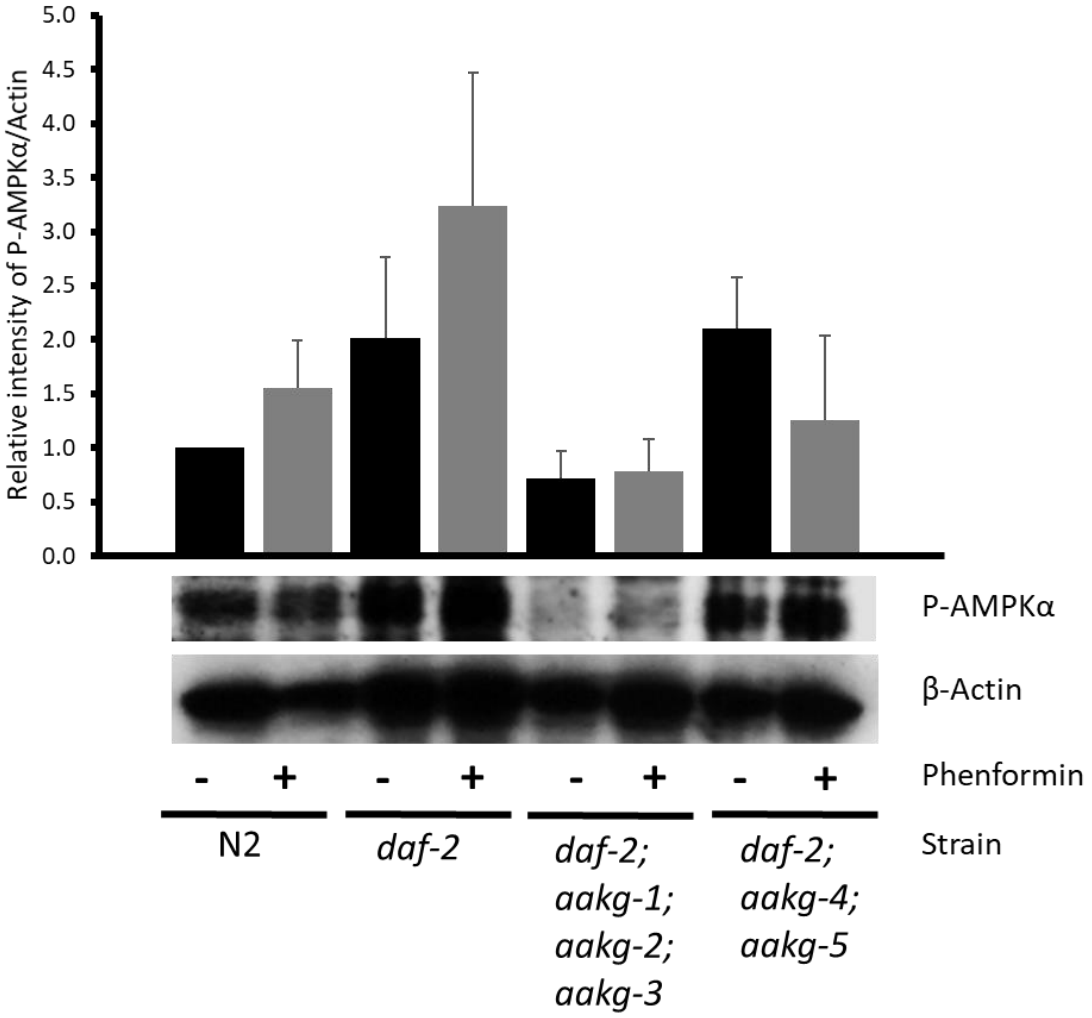

Figure 3.8| AMPKα in a *daf-2; aakg-1; aakg-2; aakg-3* mutant shows reduced Thr172 phosphorylation. A *daf-2(m577)* mutant appears to exhibit higher mean band intensity than N2(WT). A *daf-2; aakg-1(syb409); aakg-2(syb410); aakg-3(syb411)* mutant demonstrates lower mean band intensity than *daf-2*, mirroring the WT trend (Figure 3.7). Similarly, a *daf-2; aakg-4(tm5539); aakg-5(tm4052)* mutant shows similar mean band intensity to a *daf-2* mutant. The response of *aakg* combination mutants is similar between WT and *daf-2(m577)* backgrounds; supporting earlier work which suggested that AMPK containing *aakg-4* or *aakg-5* is less able to respond to increased AMP levels (Figure 3.1) (Tullet *et al.* 2014). Relative band intensity of P-AMPKα to β-actin under untreated and treated (4.5mM phenformin) conditions is shown, normalised to N2(untreated). Mean values were generated from three biologically independent trials. These results cannot be reported as statistically significant ($p>0.05$, Student's *t*-test). Error bars indicate SEM. One representative blot is shown below the graph.

In this chapter, AMPK regulation in *C. elegans* was investigated through modelling of the predicted binding residues, development of genetic mutants and quantitative assays. Modelling in PyMOL illustrated how branched side chains of histidine and asparagine residues in AAKG isoforms might interact with AMP molecules (Figure 3.1), providing the basis for AMPK regulation through *aakg* isoforms. Conservation of predicted binding residues in *aakg-1, aakg-2,* and *aakg-3* (Table 3.1) may allow these isoforms to maintain this functionality. Conversely, *aakg-4* and *aakg-5* do not possess the same capacity for interaction with adenine nucleotides and are likely to demonstrate reduced AMP-sensitivity as a result. Changes to structural elements of proteins can result in functional changes, which have been assayed here using genetic knockout strains. The generation of an array of genetic knockouts in both WT and *daf-2* backgrounds (Figures 3.3 and 3.4) proved that mutation of either *aakg* isoform family was not lethal and strains could be easily maintained. Further investigations continued after the integrity of mutants was confirmed through both PCR genotyping and qRT-PCR. qRT-PCR analysis highlighted how collectively *aakg-1, aakg-2,* and *aakg-3* isoforms exhibited altered expression in response to *aakg*-4 and *aakg-5* mutation, while transcriptional levels of *aakg-4* and *aakg-5* were consistently unaffected following mutation of *aakg-1*, *aakg-2,* and *aakg-3* (Figures 3.5 and 3.6). Assaying the activation of AMPKα, signposted through the phosphorylation of Thr172, revealed the importance of *aakg-1, aakg-2,* and *aakg-3* to proper regulation of this event. Thr172 becomes accessible once conformational change is induced through the response of AMPKγ to AMP-binding (Hawley *et al.*, 1996). This was reflected in relative band intensity analysis: an *aakg-1; aakg-2; aakg-3* mutant showed substantially reduced phosphorylation of Thr172 in a WT background (p<0.001, figure 3.7) and this trend was maintained in a *daf-2* background (Figure 3.8). Besides quantitative analyses described here, *aakg* knockout strains were also used in a series of physiological assays which will be discussed in detail in chapter 4.

3.5 Chapter 3 Discussion.

The data in this chapter followed up on a theory suggested by Tullet *et al.* (2014) who hypothesised that non-conservation of key binding residues in AAKG-4 and AAKG-5 can yield constitutively active AMPK complexes. This project explores this using combination *aakg* mutants which I predict to model two antagonistic models of AMPK regulation: *aakg-1; aakg-2; aakg-3* and *aakg-4; aakg-5* mutants, which rely on AMP-insensitive and AMP-sensitive systems of regulation, respectively Comparisons throughout this chapter provide evidence supporting the idea that alternative models of AMPK regulation contribute to significant genetic and biochemical changes in WT and *daf-2* backgrounds, and these are explored in more detail here.

3.5.1 PyMOL models suggest that AAKG-4 and AAKG-5 exhibit reduced sensitivity to AMP.

To illustrate how loss of predicted AMP-binding residue conservation might reduce sensitivity to AMP, three scenarios have been modelled. Figure 3.1 shows AAKG isoforms which each exemplify a different degree of residue conservation: a conserved isoform, (AAKG-2), an isoform which shows no conservation (AAKG-4), and an isoform which shows partial conservation (AAKG-5). While AAKG isoform protein sequences do not display high variability in secondary structure (Supplementary figure 2), loss of key AMP-binding residues in AAKG-4 and AAKG-5 does generate significant structural change which could diminish interactions with AMP in these isoforms. AMP-insensitive isoforms AAKG-4 and AAKG-5 lack important histidine and arginine residues in binding pockets (Figure 3.1, table 3.1). Crucially the side chains of these residues can carry positive charge, and mammalian studies have reported that this is important for interaction with negatively-charged phosphate groups in adenine nucleotide compounds (Xiao *et al.*, 2007; Li *et al.*, 2015). This provides the basis for a predicted mechanism of reduced interaction between AMP and AAKG-4 and AAKG-5 isoforms. Reduced AMP-sensitivity of AMPK in an *aakg-1; aakg-2; aakg-3* mutant supports this concept (Figure 3.7). Consistent with this, mammalian studies have commented on point mutation of equivalent residues in mammalian AMPKγ isoforms which influences the kinetics of phosphate binding, altering binding

affinities for AMP and ATP (Daniel and Carling, 2002; Scott *et al.*, 2004; Day *et al.*, 2007). Of particular interest to this project, mutations affecting Arg298 in PRKAG1 and Arg531 in PRKAG2 (equivalent to Arg151, PRKAG1 numbering) have been consistently linked with reduced affinity for AMP, and do not cause significant structural change outside of the AMP-binding site, implying that loss of positive charge from arginine residues is the primary cause of reduced binding affinity (Day *et al.*, 2007). In both AAKG-4 and AAKG-5, Arg298 (PRKAG1 numbering) has been replaced by an uncharged serine residue in the equivalent position (Table 3.1), so these isoforms may mimic reduced affinity seen in mammalian AMPKγ mutants. PyMOL modelling also highlighted how AAKG-5 importantly retains two charged residues, His280 and Arg281, equivalent to His150 and Arg151, *PRKAG1* numbering, table 3.1) which may still provide some level of functionality to this subunit at site 3, inferring possible intermediate AMP-sensitivity/function. Point mutation of His150 (PRKAG1 numbering) is also associated with mediating allosteric activation induced by AMP-binding (Chapter 1.4.2)(Adams *et al.*, 2004). Therefore, experimental analysis using X-ray crystallography or other binding assays is required to confirm how AMPK activity is affected in *C. elegans*. PyMOL modelling was generated early in the project timeline and justified further exploration of *aakg* mutant AMP-sensitivity, examined through Thr172 phosphorylation (Figures 3.7 and 3.8). This project also has the potential for clinical relevance, because other species within the Nematoda phylum are obligate parasites (*B. malayi, Loa loa* (Desjardins *et al.*, 2013)). The data discussed in this thesis explores the contribution of AMPKγ isoforms to activation of AMPK, which could promote AMPKγ as a novel drug target for the treatment of diseases caused by nematodes, like lymphatic filariasis (Desjardins *et al.*, 2013).

3.5.2 All *aakg* isoform mutants remain viable in WT and *daf-2(m577)* backgrounds.

The generation of a network of *aakg* mutants (Figure 3.3) is another important part of this project, which improved the scope of this study and allows for investigation into the role of AMP-sensitivity through the functional/physiological assays described in chapters 3 and 4. The generation of a similar network in a *daf-2* background (Figure 3.4) allows me to additionally consider the influence of IIS on results discovered in a WT background, exploring a complex system of interaction between

IIS and AMPK regulation. Generation of combination *aakg* knockouts tested the reliance of *C. elegans* on AMP-mediated AMPK activation and provides a significant result itself – all combination *aakg* knockout strains generated during this study are viable and are reproductively competent when maintained at 15°C, 20°C or 25°C. This remains true for *aakg* knockout strains produced in a *daf-2(m577)* background, indicating that IIS does not influence *aakg* mutant viability, even in the absence of multiple *aakg* isoforms. Importantly, all *aakg* mutants produced in a *daf-2* background still enter dauer at 25°C (Chapter 4.4), so cannot be effectively maintained at this temperature.

A significant amount of characterisation has been undertaken during this project, and with the development of this *aakg* mutant network, further characterisation of *aakg* mutant phenotypes can be continued in the future. The ease of long-term storage of *C. elegans* strains at -80°C reassures me that *aakg* knockout strains generated throughout this project can be kept and used in further investigations.

3.5.3 *aakg-4* and *aakg-5* regulate *aakg-1, aakg-2,* and *aakg-3* expression in WT *C. elegans*.

Figures 3.5 and 3.6 show analysis of mRNA expression using qRT-PCR, which highlights the substantial amount of transcriptional change that occurs in *aakg* knockout strains. Although expressed sequence tags and relative levels of *aakg* mRNA expression have been reported previously, relative *aakg* mRNA expression has not been investigated between *aakg* mutants before this study (Tullet *et al.*, 2014). Importantly, analysis of *aakg* isoform expression in combination knockout strains additionally demonstrates that the WT and *daf-2* crossing strategies (Figures 3.3 and 3.4) were successful, since *aakg-1; aakg-2; aakg-3* and *aakg-4; aakg-5* mutants were produced from single *aakg* isoform mutants in both backgrounds.

In a WT background, an *aakg-4*; *aakg-5* mutant shows reduced expression of *aakg-1, aakg-2,* and *aakg-3* (Figures 3.5A, 3.5B, and 3.5C), suggesting that *aakg-4* and *aakg-5* are linked to the transcriptional control of AMP-sensitive isoform expression. Further investigation is required to establish whether *aakg-4* or *aakg-5* drives these transcriptional effects. Additionally, I am hesitant to

describe this as an adaptive response, because reduced expression is observed rather than compensatory up-regulation, which might have been expected if *aakg-4* and/or *aakg-5* can produce constitutively active AMPK complexes as suggested by Tullet *et al.* (2014).

It is possible that functional sites are present on *aakg-1, aakg-2,* and *aakg-3* genes, allowing their expression to be linked to *aakg-4* and/or *aakg-5*. Rather than direct regulation, it seems more likely that loss of *aakg-4* and *aakg-5* could result in up-regulation of a signalling pathway, indirectly suppressing *aakg*-1, *aakg-2,* and *aakg-3* expression. In addition, while a role for *aakg-4* and *aakg-5* in transcriptional regulation alone seems unlikely to permit the conservation of two reduced-sensitivity AMPKγ isoforms, these isoforms also contribute to phenotype, which is discussed in more detail later in this thesis (Chapter 4). Conversely, *aakg-4* and *aakg-5* expression do not show significant change in *aakg-1; aakg-2; aakg-3* mutants (Figure 3.5D and 3.5E), demonstrating that *aakg-1, aakg-2,* and *aakg-3* do not possess the same level of control over *aakg* isoform expression.

3.5.4 Additional mechanisms affect *aakg-1, aakg-2,* and *aakg-4* expression in a *daf-2(m577)* background.

The transcriptional profile of *aakg* expression is more complex in a reduced IIS background, IIS appears to influence transcriptional control of AMPKγ function. Specifically, differences in *aakg* expression between WT and *daf-2* backgrounds highlight how IIS influences the transcription of *aakg-1, aakg-2,* and *aakg-4* (Table 3.3). These transcriptional changes may alter the composition of AMPK complexes in a *daf-2* mutant, through preferential incorporation of the aforementioned AAKG isoforms over others, though this has not been investigated here. Importantly, increased *aakg-4* expression in a *daf-2* mutant is confirmed here, supporting the idea that IIS plays a role in the regulation of *aakg-4* expression. In a *daf-2* mutant, *aakg-4* expression is up-regulated due to the removal of DAF-16 inhibition via the IIS pathway (Figure 1.7)(Tullet *et al.*, 2014). This increases the number of AMPK complexes containing *aakg-4* and may explain the increased relevance of *aakg-4* to *daf-2*-mediated longevity. Additionally, it is important to consider that there may be differences in

expression between tissues in *C. elegans* (neurons, gut, muscle, and hypodermis) – relative changes in whole worm expression are displayed here. While *aakg-4* and *aakg-5* expression has already been investigated using a GFP reporter strain, it would be interesting to continue exploring potential tissue-specific patterns of *aakg* isoform expression with a similar strategy for *aakg-1, aakg-2,* and *aakg-3* isoforms in future investigations, which might increase the functional relevance of transcriptional changes described here.

Existing literature does not report any changes to *aakg-1-3* expression in *daf-2* mutants (Tullet *et al.*, 2014). Quantification of *aakg* isoform expression had previously been attempted in a *daf-2(m577)* background but produced inconsistent results (Dr. J.M.A. Tullet, *personal communication*). Here, I report that a *daf-2* mutant demonstrates substantially increased *aakg-1* expression, and also report that *aakg-1* expression falls dramatically in a *daf-2; aakg-4; aakg-5* mutant, to levels lower than WT (Figure 3.6A). Conversely, *aakg-2* expression is significantly decreased in a *daf-2* mutant, but *aakg-2* expression increases above WT levels in a *daf-2; aakg-4; aakg-5* mutant (Figure 3.6B). The disparity between *aakg-1* and *aakg-2* expression changes in a *daf-2; aakg-4; aakg-5* mutant (compared to a *daf-2* mutant) implies that additional transcriptional regulation is necessary to compensate for reduced IIS in the absence of *aakg-4* and *aakg-5*. It is particularly interesting how expression does not return to WT levels and instead surpasses them in both cases (Figure 3.6A and 3.6B), suggesting that additional feedback loops may exist. This response also implies the existence of unexplored roles of IIS in *aakg* isoform expression, which may result in the preferential incorporation of certain *aakg* isoforms over others in *daf-2* mutant AMPK.

There is also a noticeable but statistically insignificant reduction in *aakg-3* expression between *daf-2* and *daf-2; aakg-4; aakg-5* mutants (Figure 3.6C). Lack of statistical significance here may be influenced by the low level of *aakg-3* expression, or inaccuracies in my pipetting technique (Tullet *et al.*, 2014).

My data supports reported up-regulation of *aakg-4* expression in a *daf-2* background, confirming that IIS regulates *aakg-4* at the transcriptional level (Table 3.3)(Tullet *et al.*, 2014). This result previously provided the basis for a role of *aakg-4* in mediating *daf-2*-mediated longevity. Additionally, there are interesting phenotypes that may relate to expression changes described here and these will be discussed later (Chapter 4.7.2). Meanwhile, *aakg-4* expression remains significantly higher in a *daf-2; aakg-1; aakg-2; aakg-3* mutant compared to WT worms and is not significantly different to *daf-2* mutant levels (Figure 3.6D). Interestingly, Tullet *et al.* (2014) report the existence of a positive feedback loop between AMPK and DAF-16, supported by elevated *aakg-4* expression in a *daf-2(e1370)* mutant compared to WT, which is dependent on *daf-16*. The ability of AMPK to directly phosphorylate and activate DAF-16 had been demonstrated prior to that study (Greer, Dowlatshahi, *et al.*, 2007). Here, I show that *daf-2(m577)* and *daf-2; aakg-1; aakg-2; aakg-3* mutants also exhibit elevated *aakg-4* expression (Figure 3.6D). In future work, I would prioritise the additional suppression of *daf-16* expression in a *daf-2; aakg-1; aakg-2; aakg-3* mutant, to confirm whether *aakg-4* expression returns to WT levels.

Interestingly, *aakg-5* expression does not change significantly between N2, *daf-2* or *daf-2; aakg-1; aakg-2; aakg-3* strains (Figure 3.6E), maintaining particularly consistent expression in comparison to other *aakg* isoforms. This may be linked to the status of *aakg-5* as the most expressed *aakg* isoform in *C. elegans*. Furthermore, while DAF-16 binding sites have been consistently identified in *aakg-4* promoter regions, DAF-16-binding elements were not consistently found for *aakg-5* (Schuster *et al.*, 2010; Tullet *et al.*, 2014). This suggests that *aakg-5* might be less sensitive to transcriptional control mechanisms (at least those mediated through DAF-16), allowing it to maintain steady expression regardless of reduced IIS signalling.

Comparing data between backgrounds provides further complexity to consider. For example, loss of *aakg-4* and *aakg-5* results in reduced expression of *aakg-1* and *aakg-2* in a WT background (Figures 3.5A and 3.5B), but this trend does not persist in the *daf-2* background: a *daf-2; aakg-4; aakg-*

5 mutant shows reduced *aakg-1* expression (Figure 3.6A) and up-regulated *aakg-2* expression compared to a *daf-2* mutant (Figure 3.6B). Additionally, *aakg-3* expression was reduced in a WT background (Figure 3.5C) but does not show any significant change in expression in a *daf-2* background (Figure 3.6C). Overall, differences between both backgrounds suggest that there are multiple pathways through which *aakg-1-3* expression is transcriptionally regulated, including IIS-dependent and IIS-independent mechanisms. Conversely, *aakg-4* and *aakg-5* expression did not change significantly in *aakg-1; aakg-2; aakg-3* and *daf-2; aakg-1; aakg-2; aakg-3* mutants compared to the respective control strains, reiterating that *aakg-1, aakg-2,* and *aakg-3* do not regulate *aakg-4* and *aakg-5* expression.

3.5.5 An *aakg-1; aakg-2; aakg-3* mutant does not respond effectively to AMP (via Thr172 phosphorylation).

In figure 3.7, an *aakg-1; aakg-2; aakg-3* mutant displays decreased capacity to respond the AMP-binding event, demonstrating a dramatic reduction in P-AMPKα antibody binding. The antibody used binds specifically to phosphorylated Thr172 on AMPKα, which has been shown to be important in the allosteric activation of *C. elegans* and mammalian AMPK (Chapters 1.4.2 and 1.5.1). Lower antibody binding in an *aakg-1; aakg-2; aakg-3* mutant (relative to WT) is observed both with and without phenformin treatment, suggesting that the conformational change resulting from AMP-binding (and subsequent exposure of Thr172 for phosphorylation) can no longer occur efficiently. The substantial reduction also highlights the extent to which *aakg-1, aakg-2,* and *aakg-3* contribute to this function, implying that these isoforms are required for normal activation of AMPK in *C. elegans*. In addition, a phenformin-treated *aakg-1; aakg-2; aakg-3* mutant does not display significantly improved AMPK activation compared to phenformin-treated WT worms. This could be influenced by the reduced capacity of an *aakg-1; aakg-2; aakg-3* mutant to respond to AMP, though further investigations are required to confirm this because phenformin treatment did not reliably increase AMPK activation in my hands. If AMPK activation in an *aakg-1; aakg-2; aakg-3* mutant cannot be rescued by phenformin treatment (or treatment with alternative activators of AMPK (Chapter 1.4.3)),

this would further support the idea that *aakg-1, aakg-2,* and *aakg-3* are required for AMPK activation achieved through Thr172 phosphorylation, and additionally promote predicted AMP-binding residues (Table 3.1) as useful targets for AMPK inhibitors. In future, investigation into phosphorylation rates of AMPK target proteins in *aakg-1; aakg-2; aakg-3* mutants could strengthen these conclusions even further.

In contrast, an *aakg-4; aakg-5* mutant reports no significant change in Thr172 phosphorylation compared to WT, in both untreated and treated samples. This confirms that AMP-sensitivity is required for effective communication of conformational change across AMPK *in C. elegans*. Loss of predicted AMP-binding residues in *aakg-4* and *aakg-5* appears to result in ineffective interaction with AMP, so conformational change does not occur, preventing Thr172 exposure on AAK (AMPKα). This likely prevents optimal AMPK activity induced in response to increased intracellular concentrations of AMP, but multiple AMPK activation pathways are reported in existing literature (Figure 1.5), so it is possible that alternative activation mechanisms can rescue AMPK activity to some extent, explaining how *aakg-1; aakg-2; aakg-3* mutants remain viable despite loss of AMP-sensitive *aakg* isoforms (Hawley *et al.*, 2005; Momcilovic, Hong and Carlson, 2006).

Additionally, as I continue to explore the importance of this activation event here, it is worth considering additional regulatory mechanisms for future investigation. In mammals, AMPKβ myristoylation is required for allosteric activation of AMPK (Chapter 1.4.2)(Oakhill *et al.*, 2010). It may be interesting to repeat this activation assay using a myristoylation site mutant to confirm conservation of this mechanism in *C. elegans*. Moreover, since induction of activation through phenformin treatment proved to be unreliable here, alternative activators of AMPK like 991 or A-769662 could be considered when repeating this assay in the future (Göransson *et al.*, 2007; Xiao *et al.*, 2013).

3.5.6 Comparative analysis of Thr172 phosphorylation suggests that *aakg-1, aakg-2, and aakg-3* may also mediate AMPKα activation in a *daf-2(m577)* background.

Figure 3.8 shows a similar investigation into Thr172 phosphorylation, this time in a *daf-2(m577)* background, to investigate the effect of reducing IIS. Unfortunately, results in this background cannot be reported as statistically significant because there was substantial variation between biological repeats. It may be possible to generate better quality data in future investigations with further optimisation of blotting technique, including use of better-quality blotting paper, alternative reagents, or wet blotting. The effectiveness of phenformin treatment in the *daf-2* background is also questionable, and phenformin-treated *daf-2* mutants show particularly extensive variation in band intensity between biological repeats. Since *daf-2* is the control strain for *daf-2; aakg-1; aakg-2; aakg-3* and *daf-2; aakg-4; aakg-5* mutants, I can only report that the *daf-2* background data appears to follow the WT trend.

When examining mean values, a *daf-2* mutant shows higher mean relative band intensity than WT, in both treated and untreated samples, which might suggest that IIS impacts allosteric activation of AMPK (Figure 3.8). Repeating this assay with an anti-AMPKα antibody which is not specific to P-Thr172 might clarify how a *daf-2* mutant appears to display greater Thr172 phosphorylation than WT: this could be achieved through greater expression of AMPKα subunits (resulting in the formation of more AMPK complexes), or through some other aspect of *daf-2* metabolism.

A *daf-2; aakg-1; aakg-2; aakg-3* mutant displays the lowest mean value for Thr172 phosphorylation (Figure 3.8), mirroring the response of an *aakg-1; aakg-2; aakg-3* mutant in the WT background (Figure 3.7). However mean band intensity in a *daf-2; aakg-1; aakg-2; aakg-3* is similar to WT, contrasting significantly reduced band intensity in an *aakg-1; aakg-2; aakg-3* mutant. If this is accurate, reduction of IIS may rescue Thr172 phosphorylation to some extent, but again further investigation is required to confirm this.

Curiously, my data (using genetic *aakg* knockouts) contrasts with previous RNAi investigations which report that *aakg-1/2* RNAi does not significantly change AMPKα phosphorylation (Tullet *et al.*, 2014). A small reduction in AMPKα phosphorylation is observed under *aakg-4/5* RNAi using the same P-AMPKα antibody used here, and phosphorylation can recover with sodium azide treatment (a respiratory inhibitor which induces energy stress). Tullet *et al.* (2014) use this to suggest the concept of constitutively active AMPK complexes, referencing decreased Thr172 phosphorylation under *aakg-4/5* RNAi. Here I report a severe reduction of AMPKα phosphorylation in an *aakg-1; aakg-2; aakg-3* mutant (Figure 3.7) and this trend is maintained in a *daf-2; aakg-1; aakg-2; aakg-3* mutant (Figure 3.8), suggesting that a larger share of AMPKγ functionality (regarding AMPK activation) has been placed on *aakg-1, aakg-2,* and *aakg-3*, rather than *aakg-4* and *aakg-5*. Thus, predicted AMP-binding residues conserved in *aakg-1, aakg-2,* and *aakg-3* (Table 3.1) are likely to have been conserved through evolution because of the role these isoforms hold in maintaining proper regulation of AMPK activity (in response to an increased AMP:ATP ratio). A possible explanation for the differences between RNAi and genetic knockout data is that different mechanisms generate the effects arising from RNAi treatment and exon deletion. In work by Tullet *et al.* (2014), adult worms were allowed to lay eggs for 12 hours on plates containing bacteria transformed with RNAi plasmids, and offspring were allowed to develop to young adults under treatment before harvesting. However, sometimes issues persist regarding penetrance of RNAi treatment. In contrast, here I have used genetic knockout strains, ensuring that expression of selected *aakg* isoforms was reliably disrupted for the entirety of development.

In summary, the data shown in this chapter confirms the importance of AMP-sensitivity to the correct regulation of AMPK activity, demonstrating the role of *aakg-1, aakg-2, and aakg-3* in mediating the exposure of the Thr172 residue which is required for optimal AMPK function. Yet, *aakg-4* and *aakg-5* continue to present clear incentives to investigate the role of AMP-sensitivity and AMPK metabolism in a multicellular eukaryotic model like *C. elegans*. These isoforms may have been retained in *C. elegans* (and a few other nematode species) because they provide additional functionality linked

to nematode biology in some way – this may include influencing regulation of *aakg* expression, as discussed earlier, or perhaps another roles in physiology. Some of these will be described in the next chapter, where I explore the possibility of contributions to physiology through use of several phenotypic assays, designed to reveal further functional roles of the *aakg* gene family in several aspects of *C. elegans* biology. A role for *aakg-4* in longevity had already been reported, but I additionally consider the importance of AMP-sensitive and AMP-insensitive regulation while investigating fertility, stress resistance and dauer.

Chapter 4 – Investigating the contribution of AMPKγ to physiology and lifespan in *C. elegans*.

AMPK possesses an extensive range of function (Figure 1.6) and is becoming increasingly well-established as a regulator for several aspects of physiology. In *C. elegans*, longevity, dauer, stress resistance, and progeny production have all been linked to AMPK activity. For instance, overexpression of *aak-2* (AMPKα) extends *C. elegans* lifespan, while an *aak-2* knockout shows reduced lifespan (Apfeld *et al.*, 2004). Additionally, *aak-2* has been shown to influence both dauer entry, and long-term dauer survival (Apfeld *et al.*, 2004; Narbonne and Roy, 2009). *aak-2* holds further roles in reproductive health (Chapter 1.5.5), influencing brood size as well as the reproductive window (Apfeld *et al.*, 2004; Burkewitz *et al.*, 2015). Furthermore, *aak-1; aak-2* double mutants displays sterility following starvation-induced L1-arrest, implying substantial interaction between energy homeostasis and reproductive health, which is influenced at least in part by AMPK activity (Fukuyama *et al.*, 2012). The role of AMPK as regulator of energy homeostasis has been further explored in relation to maintenance of effective stress responses, evidenced through *aak-2*-dependent extension of lifespan in response to heat stress (Apfeld *et al.*, 2004).

More recently, the regulatory role of *C. elegans* AMPKγ isoforms has also been investigated, and one of these isoforms, *aakg-4,* has been shown to contribute to *daf-2* mutant longevity (Tullet *et al.*, 2014). Despite extensive investigation of AMPKγ isoforms in mammalian models, the allosteric regulation of AMPK in *C. elegans* remains relatively poorly understood. However, investigating AMPK regulation in *C. elegans* provides an important advantage because worms possess two AMPKγ isoforms (*aakg-4* and *aakg-5*) predicted to exhibit reduced sensitivity to AMP (Figures 3.1 and 3.7) allowing the relevance of AMP-sensitivity in AMPK activity to be effectively investigated in a whole animal model (Tullet *et al.*, 2014).

Here I report the physiological effects of disrupting *aakg* expression, through analysis of a range of physiological parameters (lifespan, stress resistance, fecundity, and dauer), to ascertain the functional importance of different *aakg* isoforms. Following discussion of AMPK structure and biochemistry in chapter 3, this chapter shifts focus to the physiological relevance of *aakg* isoforms. They will be discussed here as two groups/families: AMP-sensitive (*aakg-1*, *aakg-2,* and *aakg-3*) and AMP-insensitive (*aakg-4* and *aakg-5*). As before, combination mutants *aakg-1; aakg-2; aakg-3* and *aakg-4; aakg-5* were used to model AMP-insensitive and AMP-sensitive systems of AMPK regulation, respectively. Generation of these mutants was achieved through an extensive crossing strategy described earlier in this thesis (Chapter 3.2, figures 3.3 and 3.4). Generation of over 10 new *aakg* mutants provided the foundation for extensive investigation into eukaryotic AMPK function in *C. elegans*, with each *aakg* knockout strain carrying deletion mutations for one or more *aakg* isoforms. Previously, *aakg-5* had only been investigated using RNAi, while this project assayed *aakg-5* contribution using a genetic knockout strain in all assays, thereby assaying the effects of life-long *aakg-5* functional deficit (Tullet *et al.*, 2014). Knockout *aakg* strains were deployed in the physiological assays described throughout this chapter, with the aim of determining the importance of AMP-sensitivity to AMPK function. Assays were designed to satisfy the following aims:

- Determine the role of AMPKγ subunits in a range of *C. elegans* physiological phenotypes (lifespan, stress resistance, reproduction and dauer).
- Determine how the IIS pathway impacts physiological effects of *aakg* mutation.

4.1 AMPKγ isoforms and their ability to bind AMP contributes to lifespan.

Some AMPK subunits have already been linked to regulation of lifespan. The contribution of AMPKα to *C. elegans* lifespan has previously been demonstrated through modulation of *aak-2* expression, and *aakg-4* has been linked to lifespan suppression of *daf-2*-mediated longevity (Apfeld *et al.*, 2004; Tullet *et al.*, 2014). Expression of *aakg-4* is also up-regulated by the activity of DAF-16, which may contribute to lifespan extension (Tullet *et al.*, 2014). In this project I set out to determine whether other *aakg* knockout strains would produce similar effects on *C. elegans* lifespan, which might suggest that the other isoforms of *aakg* share similar methods of regulation. Notably, *aakg-1, aakg-2,* and *aakg-3* have not been investigated in a combination knockout strain previously, producing novel insights into the physiological outcomes of a potentially AMP-insensitive system of AMPK regulation. The protocol for lifespan assays was described in detail earlier (Chapter 2.3.1).

To establish the contribution of different AMPKγ isoform families to WT lifespan, the lifespans of *aakg-1; aakg-2; aakg-3* triple mutants and *aakg-4; aakg-5* double mutants were compared with WT worms. An *aakg-1; aakg-2; aakg-3* mutant showed significantly reduced lifespan compared to WT (p<0.001, figure 4.1A, table 4.1). An *aakg-4; aakg-5* mutant also showed reduced lifespan, but to a lesser extent (p<0.01, figure 4.1A, table 4.1). This suggests that both families of *aakg* isoforms (AMP-sensitive and AMP-insensitive) contribute to WT lifespan, though the contribution of AMP-sensitive isoforms (*aakg-1, aakg-2,* and *aakg-3*) to longevity is greater.

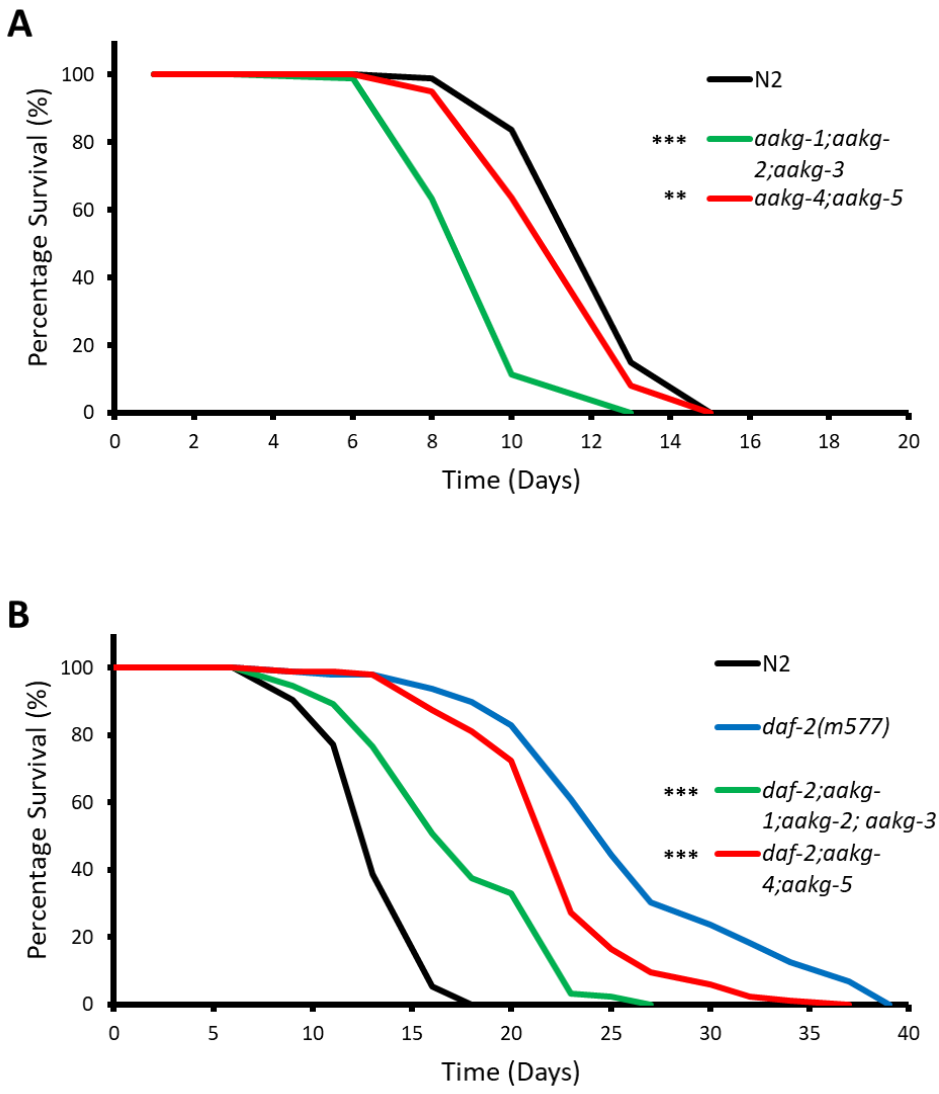

Figure 4.1| An *aakg-1; aakg-2; aakg-3* mutant displays greater suppression of *C. elegans* lifespan than an *aakg-4; aakg-5* mutant in WT and *daf-2(m577)* backgrounds. **A**) Survival curves for N2(WT), *aakg-1(syb409); aakg-2(syb410); aakg-3(syb411), aakg-4(tm5539); aakg-5(tm4052)* strains. Assays were performed at 25°C, a representative plot (Trial 3) of three biologically independent trials is shown. Significance asterisks (** p<0.01, *** p<0.001, log-rank test). **B**) Survival curves for N2(WT), *daf-2(m577), daf-2; aakg-1; aakg-2; aakg-3, daf-2; aakg-4; aakg-5* strains. Assays were performed at 25°C, a representative plot (Trial 4) of four biologically independent trials is shown. Significance asterisks (*** p<0.001, log-rank test). Additional data is shown in table 4.1.

Next, I examined the effects of the different *aakg* mutant combinations on longevity under reduced IIS. This was achieved by examining the effects of these mutations in a *daf-2(m577)* background which displays reduced IIS and is therefore long-lived (Gems *et al.*, 1998). As expected, the *daf-2* mutants displayed extended longevity compared to WT worms (p<0.001, figure 4.1B, table 4.1). Additionally, *daf-2; aakg-1; aakg-2; aakg-3 and daf-2; aakg-4; aakg-5* mutants were assayed alongside these strains so that mutant lifespan could be compared against WT and *daf-2* lifespan. Suppression of *daf-2* longevity in a *daf-2; aakg-4* mutant had been demonstrated previously, and here I report that a *daf-2; aakg-4; aakg-5* mutant exhibited partial suppression of *daf-2* longevity as well (p<0.001, figure 4.1B, table 4.1) (Tullet *et al.*, 2014). This suggested that AMP-insensitive isoforms (*aakg-4* and *aakg-5*) contribute to *daf-2* longevity. In addition, a *daf-2; aakg-1; aakg-2; aakg-3* mutant demonstrated greater suppression of *daf-2* longevity than a *daf-2; aakg-4; aakg-5* mutant (p<0.001, figure 4.1B, table 4.1). However, in both cases this was a partial suppression, and did not completely negate *daf-2*-mediated longevity. This implies that neither isoform family (*aakg-1-3,* or *aakg-4* and *aakg-5*) is completely required for *daf-2* longevity, in contrast to complete suppression observed using a *daf-2; aak-2* mutant (Apfeld *et al.*, 2004).

Overall, mutation of *aakg-1; aakg-2; aakg-3* generated more significant suppressions of lifespan than mutation of *aakg-4* and *aakg-5*, suggesting that AMP-sensitivity might play a more important role in how AMPK regulates lifespan (Figure 4.1). However, since respective *aakg-1; aakg-2; aakg-3* and *aakg-4; aakg-5* mutant strains exhibit a similar extent of lifespan suppression in WT and *daf-2* backgrounds, this suggests that both models of AMPK regulation (AMP-sensitive and AMP-insensitive) mediate contributions to *C. elegans* lifespan.

While investigating the role of *aakg* isoforms *daf-2* longevity, I noted that lifespan suppression observed in an *daf-2*; *aakg-4; aakg-5* double mutant was similar to that of an *daf-2*; *aakg-4* mutant (Tullet *et al.*, 2014). Previous work by Tullet *et al.* (2014) reported that *aakg-5* RNAi suppressed *daf-2* lifespan, so it was surprising that mutation of both isoforms in a *daf-2*; *aakg-4; aakg*-5 mutant didn't

have a bigger effect. To explore this further, I wanted to confirm whether *aakg-5* could produce a lifespan suppression independently from *aakg-4*. In contrast to *aakg-4* which shows no conservation of predicted AMP-binding residues, *aakg-5* retains two of the five residues found in conserved *aakg* isoforms (*aakg-1*, *aakg-2,* and *aakg-3*) (Table 3.1). To determine the contribution of *aakg-5* to longevity, *aakg-5* mutants were assayed alongside *aakg-4* and *aakg-4; aakg-5* mutants, which also enabled evaluation of functional redundancy between isoforms. Again, WT and *daf-2(m577)* backgrounds were used to compare effects under normal metabolism and when IIS was reduced.

In a WT background, *aakg-4* did not display significantly reduced lifespan in two out of three trials (Figure 4.2A, table 4.1). Conversely, both *aakg-5* and *aakg-4; aakg-5* mutants exhibited modest, but significant suppressions of WT lifespan ($p<0.001$ and $p<0.01$, respectively, figure 4.2A, table 4.1). Mean lifespan did not deviate more than two days between any of the strains in the WT background. It is perhaps unsurprising that *aakg-5* contributes to WT lifespan, given that *aakg-5* shows the highest expression compared to other *aakg* isoforms (Tullet *et al.*, 2014). Furthermore, an *aakg-4; aakg-5* mutant did not present any additive effect on lifespan suppression; suggesting that *aakg-5* drives contribution to WT longevity.

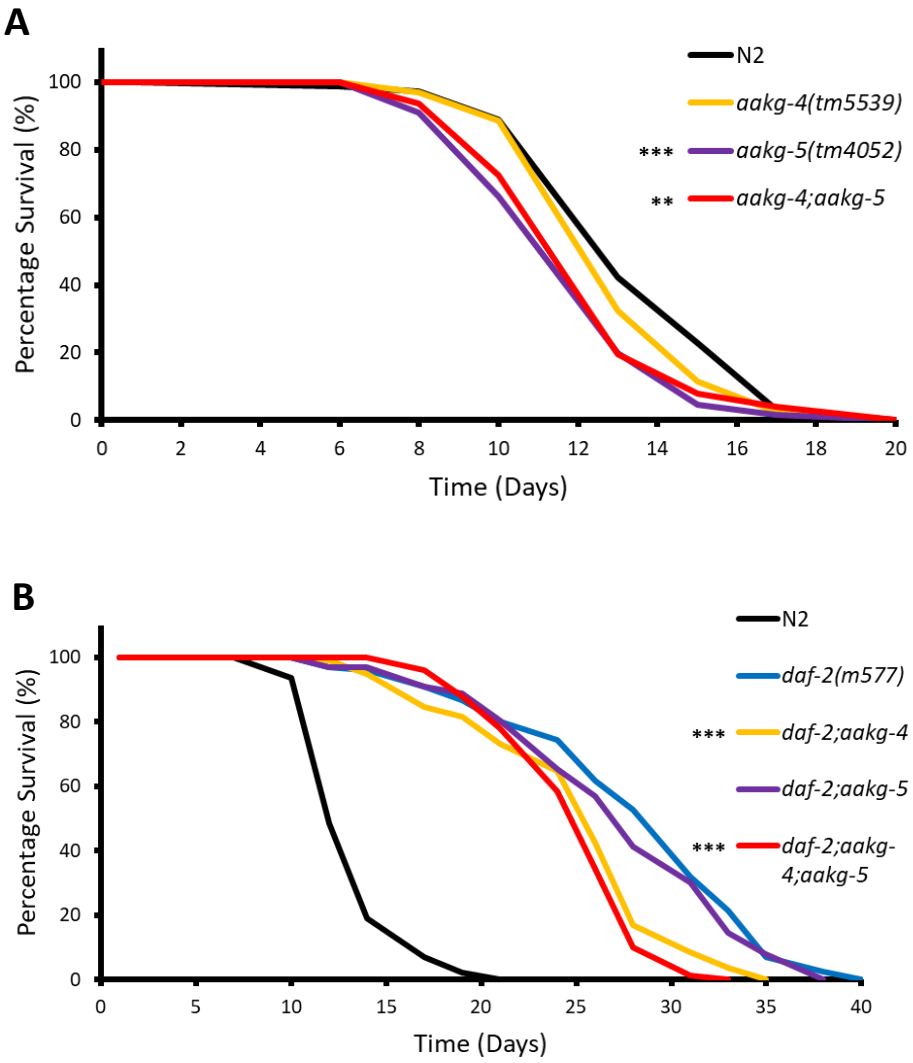

Figure 4.2| *aakg-5(tm4052)* shortens lifespan in a WT background, while *aakg-4(tm5539)* drives suppression of *daf-2(m577)* longevity. Lifespan of an *aakg-4(tm5539)* mutant does not differ significantly from WT lifespan. However, both *aakg-5(tm4052)* and *aakg-4; aakg-5* mutants show similar reductions in lifespan. In a *daf-2(m577)* background, disruption of *aakg-4* suppresses *daf-2* lifespan to a similar extent as seen in a *daf-2; aakg-4; aakg-5* mutant, while a *daf-2; aakg-5* mutant lifespan is not significantly different from *daf-2* lifespan. There is no additive reduction of longevity from mutation of both *aakg-4* and *aakg-5* isoforms in WT or *daf-2* backgrounds, demonstrated using *aakg-4; aakg-5* (double) and *daf-2; aakg-4; aakg-5* (triple) knockout strains. **A**) Survival curves for N2(WT), *aakg-4, aakg-5, aakg-4; aakg-5* strains. Assays were performed at 25°C, a representative plot of three biologically independent trials (Trial 2) is shown. Significance asterisks (** p<0.01, *** p<0.001, log-rank test). **B**) Survival curves for N2(WT), *daf-2(m577), daf-2; aakg-4, daf-2; aakg-5, daf-2; aakg-4; aakg-5* strains. Assays were performed at 25°C, a representative plot of at least three biologically independent trials (Trial 4) is shown. Significance asterisks (*** p<0.001, log-rank test). Additional data shown in table 4.1.

Again, *daf-2* mutants displayed extended longevity compared to WT worms (p<0.001, figure 4.2B, table 4.1). However, *daf-2* background data did not mirror the WT result. The previously reported *daf-2; aakg-4* lifespan suppression effect was replicated here, confirming that *aakg-4* contributes to *daf-2*-mediated longevity (p<0.001, figure 4.2B, table 4.1)(Tullet *et al.*, 2014). In contrast, a *daf-2; aakg-5* mutant displayed similar lifespan compared to a *daf-2* mutant (Figure 4.2B, table 4.1). This disagreed with the study referred to earlier which reported that similar suppression of *daf-2*-mediated longevity was displayed by *daf*-2 mutants treated with *aakg-4* or *aakg-5* RNAi (Tullet *et al.*, 2014). Together with WT data, which suggests that contribution of *aakg-5* to lifespan is IIS-dependent (Figure 4.2). Differences between results with RNAi treatment (of L4 stage worms) and genetic knockouts imply that *daf-2; aakg-5* mutants either adapt to loss of the *aakg-5* isoform, or that there are differences during larval development that impact on *daf-2* longevity. Additionally, a *daf-2; aakg-4; aakg-5* mutant showed similar suppression of *daf-2* lifespan as a *daf-2; aakg-4* mutant (p<0.001, figure 4.2B, table 4.1), but no cumulative effect on lifespan, suggesting that *aakg-4* drives lifespan suppression in a *daf-2; aakg-4; aakg-5* mutant. This latter result does agree with previous investigations, which found no additive suppression using *aakg-4* and *aakg-5* RNAi (Tullet *et al.*, 2014).

Taken together, this analysis revealed that an *aakg-1; aakg-2; aakg-3* mutant demonstrated more significant suppression of lifespan than an *aakg-4; aakg-5* mutant (Figure 4.1), suggesting a conserved relevance of AMP-sensitive AMPK regulation in longevity, since orthologues of *aakg-1, aakg-2,* and *aakg-3* exist in mammals. In both WT and *daf-2* backgrounds*, aakg-1; aakg-2; aakg-3* triple and *aakg-4; aakg-5* double mutants showed suppressed lifespan, but to different extents; implying that when knocked out in combination*, aakg-1, aakg-2,* and *aakg-3* can contribute to lifespan through additional (or more effective) mechanisms compared to those employed by *aakg-4* and *aakg-5*. Additionally, data shown in figure 4.2B supports ideas in existing literature: in a *daf-2* background, activation of the transcription factor DAF-16 increases expression of *aakg-4*, which may contribute to *daf-2*-mediated longevity (Tullet *et al.*, 2014). Furthermore, determining that *aakg-5* mutation does not suppress *daf-2* longevity supports the idea that *aakg-5* is not affected by DAF-16 in the same

manner. Consistent with this, Tullet *et al.* (2014) were able to confirm the presence of DAF-16 binding sites in the *aakg-4* promoter but did not detect any binding sites in the *aakg-5* promoter. The knockout strain used here may differ from a previously reported RNAi knockdown result because of compensatory effects at the genetic level during development, which may allow *daf-2; aakg-5* mutants to compensate for the loss of *aakg-5*. Also, the lack of additive lifespan suppression in *aakg-4; aakg-5* and *daf-2; aakg-4; aakg-5* mutants (Figure 4.2) implies that *aakg-5* contributes to WT lifespan, while *aakg-4* contributes to *daf-2* lifespan.

Trial	Strain	Genotype	Mean Lifespan (days)	% Difference	N (total)	*p*
1		N2	11.35		80	-
1	JMT61	*aakg-1(syb409); aakg-2(syb410); aakg-3(syb411)*	9.10	-19.82 [a]	100	<0.001[a]
1	JMT48	*aakg-4(tm5539); aakg-5 (tm4052)*	10.87	-4.23 [a]	100	<0.01[a]
2		N2	11.54		100	-
2	JMT61	*aakg-1(syb409); aakg-2(syb410); aakg-3(syb411)*	8.26	-28.42 [a]	100	<0.001[a]
2	JMT48	*aakg-4(tm5539); aakg-5 (tm4052)*	11.57	+0.26 [a]	100	NS[a]
3		N2	12.79		100	-
3	JMT61	*aakg-1(syb409); aakg-2(syb410); aakg-3(syb411)*	9.59	-25.02 [a]	100	<0.001[a]
3	JMT48	*aakg-4(tm5539); aakg-5 (tm4052)*	11.97	-6.41 [a]	100	<0.01[a]
1		N2	13.88		100	-
1	GA1071	*aakg-4(tm5539)*	13.52	-2.59[a]	80	NS[a]
1	JMT9	*aakg-5 (tm4052)*	12.33	-11.17[a]	100	<0.001[a]
1	JMT48	*aakg-4(tm5539); aakg-5 (tm4052)*	12.62	-9.08[a]	82	<0.01[a]
2		N2	13.98		80	-
2	GA1071	*aakg-4(tm5539)*	13.55	-3.08[a]	100	NS[a]
2	JMT9	*aakg-5 (tm4052)*	12.35	-11.66[a]	81	<0.001[a]
2	JMT48	*aakg-4(tm5539); aakg-5 (tm4052)*	12.71	-9.08[a]	102	<0.01[a]
3		N2	13.11		98	-
3	GA1071	*aakg-4(tm5539)*	12.46	-4.96[a]	101	<0.05[a]
3	JMT9	*aakg-5 (tm4052)*	11.21	-14.49[a]	101	<0.001[a]
3	JMT48	*aakg-4(tm5539); aakg-5 (tm4052)*	11.51	-12.20[a]	100	<0.001[a]
1	DR1567	*daf-2 (m577)*	25.82		100	-
1	JMT74	*daf-2 (m577); aakg-1(syb409); aakg-2(syb410); aakg-3(syb411)*	17.63	-31.72[b]	100	<0.001[b]
1	JMT43	*daf-2 (m577); aakg-4(tm5539); aakg-5 (tm4052)*	24.54	-4.96[b]	58	NS[b]
2		N2	9.88		80	-
2	DR1567	*daf-2 (m577)*	21.21	+114.68[a]	100	<0.001[a]

2	JMT74	*daf-2 (m577); aakg-1(syb409); aakg-2(syb410); aakg-3(syb411)*	17.05	-19.61[b]	100	<0.001[b]
2	JMT43	*daf-2 (m577); aakg-4(tm5539); aakg-5 (tm4052)*	20.49	-3.39[b]	32	NS[b]
3		N2	13.89		100	-
3	DR1567	*daf-2 (m577)*	23.18	+66.88[a]	100	<0.001[a]
3	JMT74	*daf-2 (m577); aakg-1(syb409); aakg-2(syb410); aakg-3(syb411)*	18.43	-20.49[b]	100	<0.001[b]
3	JMT43	*daf-2 (m577); aakg-4(tm5539); aakg-5 (tm4052)*	23.30	+0.52[b]	100	NS[b]
4		N2	13.63		100	-
4	DR1567	*daf-2 (m577)*	26.42	+93.84[a]	102	<0.001[a]
4	JMT74	*daf-2 (m577); aakg-1(syb409); aakg-2(syb410); aakg-3(syb411)*	17.85	-32.44[b]	100	<0.001[b]
4	JMT43	*daf-2 (m577); aakg-4(tm5539); aakg-5 (tm4052)*	22.81	-13.66[b]	100	<0.001[b]
1	DR1567	*daf-2 (m577)*	24.58		39	-
1	JMT43	*daf-2 (m577); aakg-4(tm5539); aakg-5 (tm4052)*	23.45	-4.60[b]	40	NS[b]
2		N2	14.53		68	-
2	DR1567	*daf-2 (m577)*	29.07	+100.07[a]	101	<0.001[a]
2	GA1072	*daf-2 (m577); aakg-4(tm5539)*	25.78	-11.32[b]	100	<0.001[b]
2	JMT30	*daf-2 (m577); aakg-5 (tm4052)*	30.37	+4.47[b]	80	NS[b]
2	JMT43	*daf-2 (m577); aakg-4(tm5539); aakg-5 (tm4052)*	25.34	-12.83[b]	59	<0.001[b]
3		N2	14.67		100	-
3	DR1567	*daf-2 (m577)*	26.50	+80.64[a]	81	<0.001[a]
3	GA1072	*daf-2 (m577); aakg-4(tm5539)*	25.11	-5.25[b]	100	<0.05[b]
3	JMT30	*daf-2 (m577); aakg-5 (tm4052)*	27.46	+3.62[b]	99	NS[b]
3	JMT43	*daf-2 (m577); aakg-4(tm5539); aakg-5 (tm4052)*	24.26	-8.45[b]	100	<0.001[b]
4		N2	13.60		102	-
4	DR1567	*daf-2 (m577)*	28.41	+108.90[a]	101	<0.001[a]
4	GA1072	*daf-2 (m577); aakg-4(tm5539)*	25.26	-11.09[b]	100	<0.001[b]
4	JMT30	*daf-2 (m577); aakg-5 (tm4052)*	27.66	-2.64[b]	100	NS[b]

4	JMT43	*daf-2 (m577); aakg-4(tm5539); aakg-5 (tm4052)*	25.20	-11.30[b]	80	<0.001[b]

Table 4.1| Lifespan assay summary table. *aakg-5(tm4052)* shortens WT lifespan, while *aakg-4(tm5539)* shortens *daf-2(m577)* lifespan. This table shows data from a total of 14 lifespan trials in N2(WT) and *daf-2(m577)* backgrounds. Percentage difference in lifespan is compared to [a]N2 or [b]*daf-2(m577)*. N indicates the total worms scored. *p* indicates the probability (determined by log-rank test) of being statistically similar to the specified control: [a] N2, [b] *daf-2(m577)*. NS indicates the difference between strains was not found to be statistically significant (i.e. $p>0.05$).

4.2 AMPKγ isoforms *aakg-4* and *aakg-5* contribute to arsenite stress resistance in *C. elegans*.

Stress resistance is often linked with longevity (Minois, 2000; Heidler *et al.*, 2010). In *C. elegans*, acute exposure several stressors has been associated with lifespan extension, and this has contributed to the hormesis concept, which relates to the oxidative damage theory of ageing (Cypser and Johnson, 2002). In addition, long-lived *age-1* and *daf-2* mutants demonstrate increased stress resistance, while *mev-1* mutants (*mev-1* encodes succinate dehydrogenase complex subunit C in worms) are short-lived and tend to be more sensitive to stress, implicating energy metabolism in the regulation of response to environmental stresses (Ishii *et al.*, 1998; McElwee *et al.*, 2004; Ayyadevara *et al.*, 2009; McColl *et al.*, 2010). Therefore, as a key regulator of energy homeostasis, AMPK could play a role in the oxidative stress response which may indirectly contribute to its role in longevity. Supporting this theory, acute AMP:ATP ratio increases observed in response to HTP, starvation and mitochondrial poisoning (1mM sodium azide), have been linked to *aak-2*-dependent lifespan extension in *C. elegans* (Apfeld *et al.*, 2004).

To determine whether *aakg* isoforms also imply a link lifespan and stress, I treated *aakg*-4, *aakg-5,* and *aakg-4; aakg-5* mutants with 2.5mM sodium arsenite to test their ability to respond to increased oxidative stress (Protocol described in chapter 2.3.2). *aakg-1, aakg-2,* and *aakg-3* were not investigated due to time constraints. Furthermore, investigation of *aakg-4* and *aakg-5* allowed exploration of other potential roles for these isoforms, which might further justify their existence among the Chromadorea clade of nematodes (Tullet *et al.*, 2014). Again, WT and *daf-2* backgrounds were used to establish the impact of AMPKγ mutation on the oxidative stress response in both WT and reduced IIS backgrounds. Sodium arsenite was chosen because it is an established assay used to investigate oxidative stress in *C. elegans* (Ewald, Hourihan and Blackwell, 2017). Arsenite targets the components of the electron transport chain, inhibiting aerobic respiration and thereby reducing intracellular levels of ATP, until cellular systems are left depleted and inoperable (Luz *et al.*, 2016).

In a WT background, *aakg-4*, *aakg-5,* and *aakg-4; aakg-5* double mutants all showed significantly decreased survival in the presence of 2.5mM arsenite, indicating that AMP-insensitive isoforms *aakg-4* and *aakg-5* contribute to the oxidative stress response in WT worms (p<0.01 and p<0.001, respectively; figure 4.3A, table 4.2). Importantly, an *aakg-4; aakg-5* mutant did not any show reduced survival compared to either single mutant (p<0.01, figure 4.3A, table 4.2), implying that functional redundancy exists between the contributions of *aakg-4* and *aakg-5* to oxidative stress resistance in a WT background. Although *aakg-1*, *aakg-2,* and *aakg-3* were not tested here, that would be an obvious next step, to investigate the relationship between AMP-sensitivity and oxidative stress resistance further.

A *daf-2* mutant showed enhanced survival while exposed to 2.5mM sodium arsenite compared to WT (p<0.05, figure 4.3B, table 4.2), confirming increased oxidative stress resistance in this strain. In contrast, a *daf-2; aakg-4* mutant displayed significantly reduced survival compared to the *daf-2* control strain, albeit to lesser extent than observed in the WT background (p<0.05, figure 4.3, table 4.2). *daf-2; aakg-5* mutant survival was not significantly different to the *daf-2* control strain (Figure 4.3, table 4.2). Taken together, the role of *aakg-4* in oxidative stress resistance is maintained between backgrounds, but the contribution of *aakg-5* to arsenite stress resistance is IIS-dependent. Furthermore, a *daf-2; aakg-4; aakg-5* mutant showed significantly decreased survival in the presence of 2.5mM arsenite (p<0.05, figure 4.3B, table 4.2), and behaved similarly to a *daf-2; aakg-4* mutant, implying that *aakg-4* drives contributions to oxidative stress response under reduced IIS. Curiously, the *daf-2; aakg-4; aakg-5* mutant survival curve followed the *daf-2; aakg-4* mutant curve closely in four out of five trials, and in the one trial where this was not the case (Trial 5, table 4.2), both *daf-2; aakg-4 and daf-2; aakg-5* seemed to mount a better response to arsenite stress. Overall, knocking out *aakg-4* and *aakg-5* in combination did not produce additive suppression of arsenite stress survival in WT or *daf-2* backgrounds (Figure 4.3, table 4.2). This trend is also seen in the longevity data (Figure 4.2, table 4.1).

In summary, both *aakg-4* and *aakg-5* influence resistance to oxidative (arsenite) stress in *C. elegans*, and the combined influence of these isoforms is not additive (Figure 4.3, table 4.2). Interestingly, the role of *aakg-5* in the oxidative stress response is IIS-dependent, suggesting that while *aakg-5* expression may be linked to combatting oxidative stress in WT worms, *aakg-5* relies on IIS or its downstream effectors to contribute to an effective arsenite stress response. On the other hand, *aakg-4* contributes to the oxidative stress resistance independently of IIS.

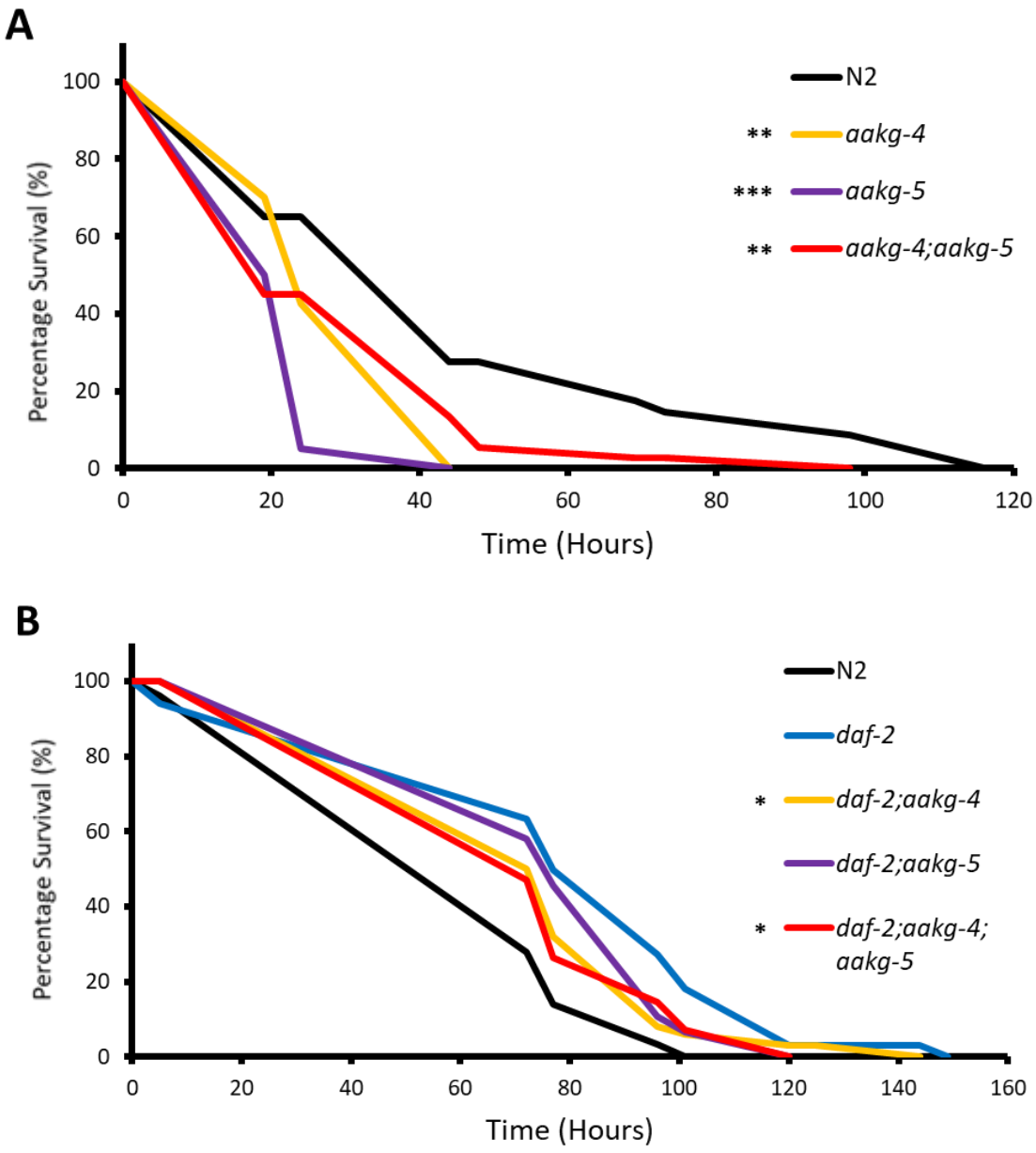

Figure 4.3| *aakg-4(tm5539)* and *aakg-5(tm4052)* display increased sensitivity to 2.5mM sodium arsenite. The role of *aakg-4* is IIS-dependent. AMPKγ mutant strains *aakg-4, aakg-5*, and *aakg-4; aakg-5* all show increased sensitivity to 2.5mM sodium arsenite compared to WT. Only *daf-2; aakg-4* and *daf-2; aakg-4; aakg-5* mutants show increased sensitivity in a *daf-2(m577)* background. Additionally, the *daf-2(m577)* mutation confers increased resistance to 2.5mM arsenite. Typically, 50 animals per strain were placed between five wells on a 94-well plate (10 worms per well), and then left in the presence of 2.5mM arsenite for several days, profiling their survival in response to chronic oxidative stress. **A**) Survival curves for N2(WT), *aakg-4(tm5539), aakg-5(tm4052), aakg-4; aakg-5* strains. Assays were performed at 25°C, a representative plot of three biologically independent trials (Trial 3) is shown. Significance asterisks (** p<0.01, *** p<0.001, log-rank test). **B**) Survival curves for N2(WT), *daf-2(m577), daf-2; aakg-4, daf-2; aakg-5, daf-2; aakg-4; aakg-5* strains. Assays were performed at 25°C, a representative plot of at least 4 biologically independent trials (Trial 4) is shown. Significance asterisks (* p<0.05, log-rank test). Additional data is shown in table 4.2.

Trial	Strain	Genotype	Mean Survival (Hours)	% Difference	N (total)	*p*
1		N2	85.42		50	-
1	JMT9	*aakg-5 (tm4052)*	55.65	-34.85[a]	50	<0.001[a]
1	JMT48	*aakg-4(tm5539); aakg-5 (tm4052)*	58.00	-32.10[a]	50	<0.001[a]
2		N2	44.74		50	-
2	GA1071	*aakg-4(tm5539)*	33.47	-25.19[a]	50	<0.01[a]
2	JMT9	*aakg-5 (tm4052)*	38.93	-12.99[a]	50	NS[a]
2	JMT48	*aakg-4(tm5539); aakg-5 (tm4052)*	45.44	+1.56[a]	50	NS[a]
3		N2	48.05		40	-
3	GA1071	*aakg-4(tm5539)*	31.00	-35.48[a]	40	<0.01[a]
3	JMT9	*aakg-5 (tm4052)*	22.50	-53.17[a]	40	<0.001[a]
3	JMT48	*aakg-4(tm5539); aakg-5 (tm4052)*	32.66	-32.03[a]	40	<0.01[a]
1		N2	39.55		44	-
1	DR1567	*daf-2 (m577)*	67.77	+71.35[a]	30	<0.001[a]
1	GA1072	*daf-2 (m577); aakg-4(tm5539)*	71.58	+5.62[b]	40	NS[b]
1	JMT30	*daf-2 (m577); aakg-5 (tm4052)*	48.57	-28.33[b]	30	<0.01[b]
1	JMT43	*daf-2 (m577); aakg-4(tm5539); aakg-5 (tm4052)*	70.78	+4.44[b]	49	NS[b]
2		N2	67.13		50	-
2	DR1567	*daf-2 (m577)*	73.34	+9.25[a]	50	<0.001[a]
2	GA1072	*daf-2 (m577); aakg-4(tm5539)*	63.55	-13.35[b]	50	<0.001[b]
2	JMT30	*daf-2 (m577); aakg-5 (tm4052)*	63.31	-13.68[b]	50	<0.01[b]
2	JMT43	*daf-2 (m577); aakg-4(tm5539); aakg-5 (tm4052)*	63.06	-14.02[b]	50	<0.01[b]
3		N2	82.86		50	-
3	DR1567	*daf-2 (m577)*	91.60	+10.55[a]	50	NS[a]
3	GA1072	*daf-2 (m577); aakg-4(tm5539)*	62.58	-31.68[b]	50	<0.001[b]
3	JMT43	*daf-2 (m577); aakg-4(tm5539); aakg-5 (tm4052)*	63.60	-30.57[b]	50	<0.001[b]
4		N2	73.56		50	-

4	DR1567	*daf-2 (m577)*	86.28	+17.29[a]	50	<0.001[a]
4	GA1072	*daf-2 (m577); aakg-4(tm5539)*	82.84	-3.99[b]	50	<0.05[b]
4	JMT30	*daf-2 (m577); aakg-5 (tm4052)*	85.34	-1.09[b]	50	NS[b]
4	JMT43	*daf-2 (m577); aakg-4(tm5539); aakg-5 (tm4052)*	81.49	-5.55[b]	50	<0.05[b]
5		N2	83.50		40	-
5	DR1567	*daf-2 (m577)*	108.11	+29.47[a]	40	<0.001[a]
5	GA1072	*daf-2 (m577); aakg-4(tm5539)*	105.68	-2.25[b]	50	NS[b]
5	JMT30	*daf-2 (m577); aakg-5 (tm4052)*	95.68	-11.50[b]	50	NS[b]
5	JMT43	*daf-2 (m577); aakg-4(tm5539); aakg-5 (tm4052)*	79.26	-26.69[b]	40	<0.001[b]

Table 4.2| Arsenite stress survival summary table. This table shows data from a total of 9 arsenite survival trials in N2(WT) and *daf-2(m577)* backgrounds. Percentage difference in survival under chronic exposure to 2.5mM sodium arsenite is compared to [a]N2 or [b]*daf-2(m577)*. N indicates the total worms scored. *p* indicates the probability (determined by log-rank test) of being statistically similar to the specified control: [a] N2, [b] *daf-2(m577)*. NS indicates the difference between strains was not found to be statistically significant (i.e. $p>0.05$).

4.3 AMPKγ isoforms contribute to *C. elegans* fecundity and reproductive schedule.

Several studies have commented on interactions between lifespan and fecundity in *C. elegans* (Friedman and Johnson, 1988; Arantes-Oliveira *et al.*, 2002; Berman and Kenyon, 2006). One prominent theory suggests that individuals which show longer lifespans often suffer shortfalls in fertility due to a prioritisation of cellular energy expenditure, towards maintenance of somatic cells over maintenance of reproductive tissues. This theory is known as the disposable soma theory.

It could be expected then, that consistent with lifespan suppression effects discussed earlier in this chapter, *aakg-1; aakg-2; aakg-3* and *aakg-4; aakg-5* mutants might benefit from improved reproductive health. To test this, fecundity was evaluated using the well-established brood size protocol (Chapter 2.3.3). Initially brood sizes were assayed in a WT background to determine the effects of *aakg* mutation on normal fecundity. Subsequently, the corresponding *daf-2* background strains were also investigated, since previous investigations revealed a more pronounced role for *aakg-4* in regulation of *daf-2* mutant lifespan (Figure 4.2, table 4.1)(Tullet *et al.*, 2014).

In the WT background, an *aakg-1; aakg-2; aakg-3* mutant did not produce significantly different numbers of offspring compared to WT (Figure 4.4A). In this respect, an *aakg-1; aakg-2; aakg-3* mutant did not behave as a typical sick mutant (Chapter 1.2.2) – and maintained normal fecundity despite showing suppressed lifespan. In contrast, an *aakg-4; aakg-5* mutant displayed lower mean brood size compared to WT control and produced on average 23 fewer viable offspring across three trials ($p<0.05$, figure 4.4A). Collectively, these results do not indicate any correlation between fecundity and lifespan, disagreeing with the disposable soma theory: an *aakg-4; aakg-5* mutant exhibited both reduced fecundity and reduced lifespan, yet mutation of *aakg-4* and *aakg-5* did not suppress lifespan as significantly as mutation of *aakg-1, aakg-2,* and *aakg-3* (Figures 4.1 and 4.4).

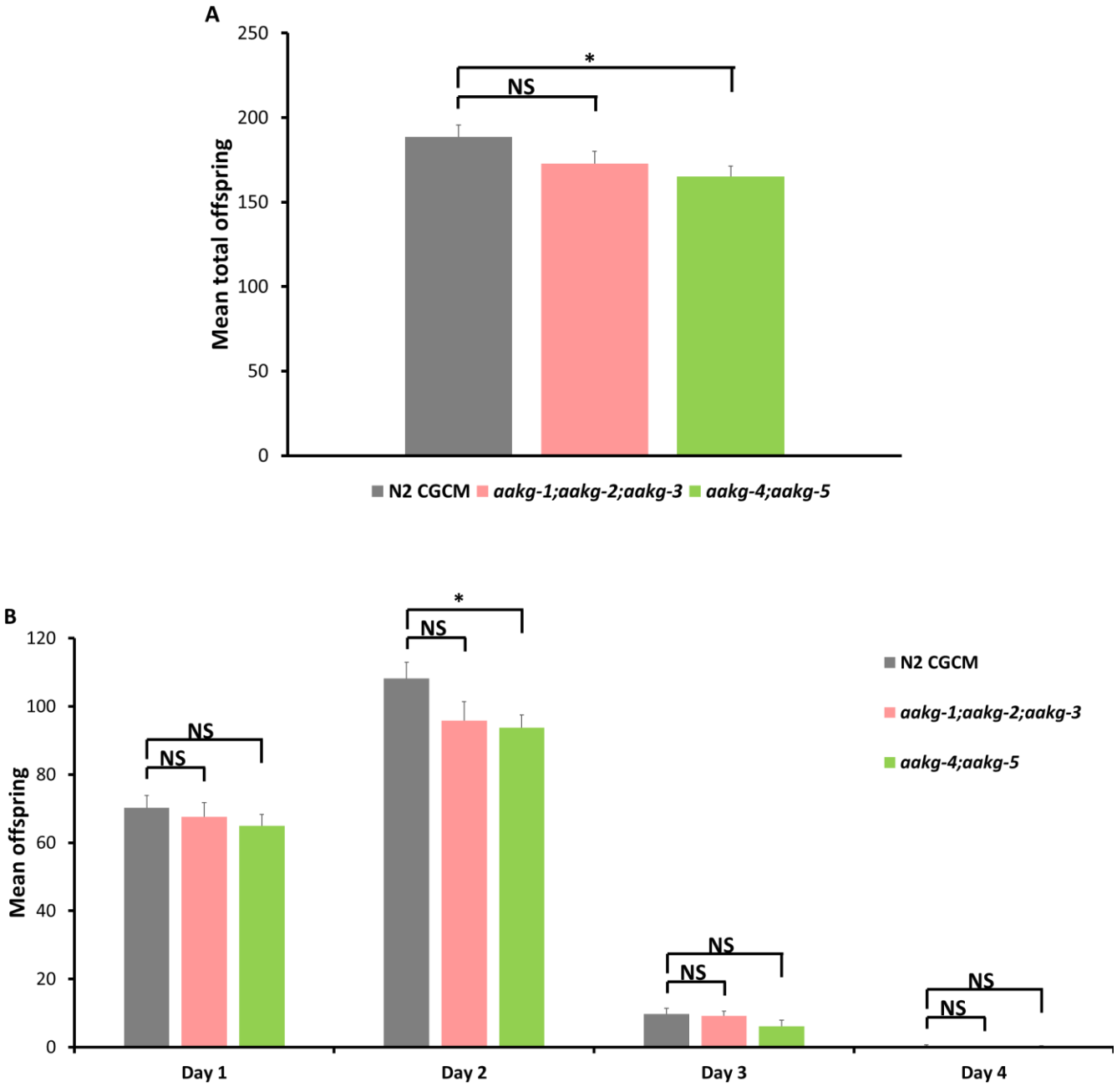

Figure 4.4| Mutation of *aakg-4 and aakg-5* isoforms is detrimental to fecundity in a WT background. **A**) Mean brood size of N2(WT), *aakg-1(syb409); aakg-2(syb410); aakg-3(syb411), aakg-4(tm5539); aakg-5(tm4052)* strains. **B**) Mean daily brood size of N2(WT), *aakg-1; aakg-2; aakg-3, aakg-4; aakg-5* strains. Assays were performed at 25°C, and data shown here was pooled from three biologically independent trials. N=27 for N2, N=28 for *aakg-1; aakg-2; aakg-3*, and N=30 for *aakg-4; aakg-5*. Error bars indicate SEM. Significance asterisks (* p<0.05, Student's t-test, compared to WT).

Earlier, conservation or non-conservation of each predicted AMP-binding residue was shown for all *aakg* isoforms (Table 3.1), highlighting the differences in *aakg-4* and *aakg-5*. The presence of orthologues of *C. elegans aakg-4* and *aakg-5* in species like *B. malayi* and *P. pacificus* suggests that these isoforms may have been kept because they provide some benefit to these organisms (Tullet *et al.*, 2014). The WT brood size data shown here might suggest that this benefit is related to reproductive health: isoforms *aakg-4* and *aakg-5* remain active in an *aakg-1; aakg-2; aakg-3* mutant which displayed normal fecundity; whereas absence of these isoforms in an *aakg-4; aakg-5* mutant resulted in substantial reproductive shortfall. This indicates that reproductive health in *C. elegans* may respond to AMP-insensitive AMPK complexes which have incorporated *aakg*-4 or *aakg-5* isoforms.

This analysis was then examined in more detail to consider the mean number of offspring laid per day. This showed that an *aakg-1; aakg-2; aakg-3* mutant produced similar numbers of offspring on all four days compared to WT (Figure 4.4B). On the other hand, an *aakg-4; aakg-5* mutant often yielded lower mean numbers of offspring compared to WT, but the only statistically significant reduction occurred between two-day-old adults (p<0.05, figure 4.4B). This implies that signalling involving *aakg*-4 and *aakg-5* influences reproductive capacity two days following the end of *C. elegans* development. Since *aakg-4; aakg-5* mutant brood size was only significantly lower two days post-development, this implies that fecundity may recover to some extent after this point.

With apparent differences between the brood size of AMP-sensitive and AMP-insensitive mutants in a WT background, it became even more interesting to investigate whether this disparity persisted in a reduced IIS (*daf-2(m577)*) background. Notably, in my hands, a *daf-2* mutant showed significantly reduced numbers of total progeny compared to WT worms (p<0.001, figures 4.4 and 4.5). Interestingly, a *daf-2*; *aakg-1; aakg-2; aakg-3* mutant displayed significantly reduced brood size compared to a *daf-2* mutant and produced 25 fewer viable offspring on average across three trials (p<0.01, figure 4.5A). In contrast, a *daf-2; aakg-4; aakg-5* mutant showed similar progeny production to a *daf-2* mutant (Figure 4.5A). Overall, this suggests that *aakg-1, aakg-2,* and *aakg-3* are important

for regulating total brood size in the context of reduced IIS (but not WT brood size), whereas the role of *aakg-4* and *aakg-5* is IIS-dependent (Figures 4.4A and 4.5A). Again, there was no correlation between progeny production and lifespan, suggesting that the disposable soma theory does not apply to *aakg*-mediated contributions to fecundity and longevity (Figures 4.1, 4.4A, and 4.5A).

Reducing IIS additionally revealed further complexity in the contribution of *aakg* to *C. elegans* reproductive health with age. A *daf-2; aakg-1; aakg-2; aakg-3* mutant displayed reduced total brood size compared to a *daf-2* mutant (p<0.01, figure 4.5A), and showed significant reductions in brood size from day two until the end of reproductive window (p<0.05, figure 4.5B). This suggests that the presence of *aakg-1-3* is required for continued maintenance of *C. elegans* reproductive health under reduced IIS. In combination with the *aakg-4; aakg-5* mutant result in a WT background, daily *daf-2; aakg-1; aakg-2; aakg-3* mutant brood size data implies that important *aakg*-mediated signalling affecting reproductive health occurs two days post-development (Figures 4.4B and 4.5B).

In contrast, a *daf-2; aakg-4; aakg-5* mutant demonstrated a dramatically changed pattern of offspring production but managed to maintain a similar mean number of offspring to *daf-2* overall (Figure 4.5). One-day-old *daf-2; aakg-4; aakg-5* mutants showed a significant increase in offspring compared to one-day-old *daf-2* mutants (p<0.001, figure 4.5B), but by day 2 increased production had subsided. *daf-2; aakg-4; aakg-5* mutants then consistently generated less offspring than a *daf-2* mutant for the remainder of the reproductive window (p<0.05, figure 4.5B) and demonstrated front-loading of egg laying. This implies that under reduced IIS, *aakg-4* and *aakg-5* adopt additional responsibility, contributing to *daf-2* mutant reproductive timeline and avoidance of premature egg-laying.

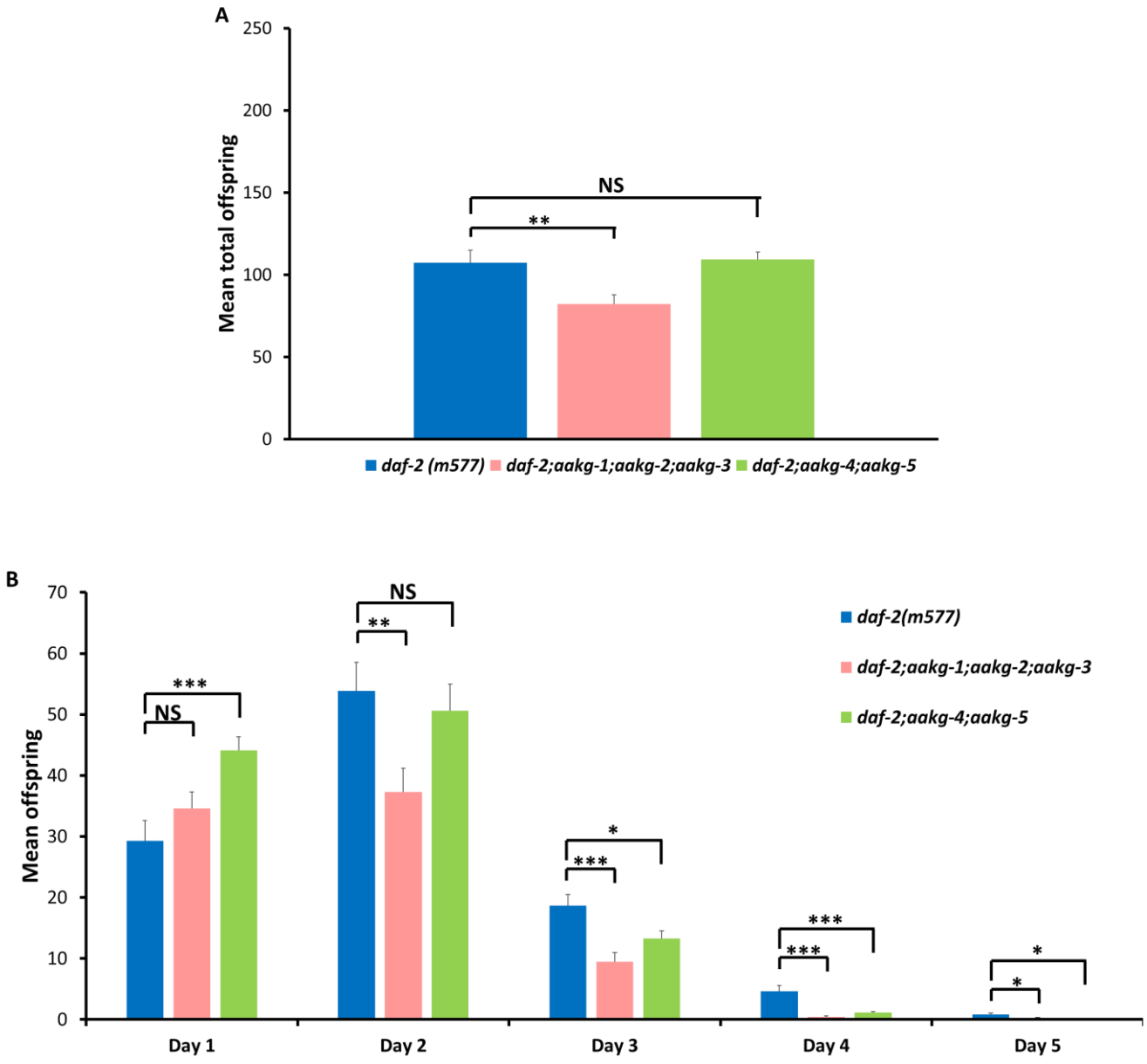

Figure 4.5| Mutation of *aakg-1, aakg-2,* and *aakg-3* reduces fecundity in a *daf-2(m577)* background. Additionally, *aakg-4* and *aakg-5* may hold some role in maintenance of the *C. elegans* reproductive schedule. **A**) Mean brood size of *daf-2(m577), daf-2; aakg-1(syb409); aakg-2(syb410); aakg-3(syb411), daf-2; aakg-4(tm5539); aakg-5(tm4052)* strains. **B**) Mean daily brood size of *daf-2(m577), daf-2; aakg-1; aakg-2; aakg-3, daf-2; aakg-4; aakg-5* strains. Assays were performed at 25°C, and data shown is pooled from three biologically independent trials. N=27 for *daf-2*, N=30 for *daf-2; aakg-1; aakg-2; aakg-3*, and N=27 for *daf-2; aakg-4; aakg-5*. Error bars indicate SEM. Significance asterisks (* $p<0.05$, ** $p<0.01$, *** $p<0.001$, Student's *t*-test, compared to *daf-2*).

Comparison between WT and *daf-2* background results provides further insight into the regulation of reproductive health in *C. elegans*. IIS may compensate for the role of *aakg-1, aakg-2,* and *aakg-3* in fecundity, concealing its effect in the WT background (Figures 4.4A and 4.5A). The data shown in figure 4.5 highlights an increased reliance on AMP-sensitive AMPK regulation under reduced IIS. Conversely, WT *C. elegans* can continue to maintain fertility without *aakg-1, aakg-2,* and *aakg-3*, indicating that *aakg-4* and *aakg-5* isoforms are more critical for normal fecundity in WT worms. The role of *aakg-4* and *aakg-5* isoforms in fecundity appears to be IIS-dependent, since two different phenotypes were observed in WT and *daf-2* backgrounds.

In summary, IIS appears to modulate the contribution of both AMP-sensitive and AMP-insensitive *aakg* isoforms to fecundity. This seems understandable considering that AMPK is a key nexus of energy homeostasis, and the idea that it can respond to IIS is well-documented (Apfeld *et al.*, 2004; Curtis, O'Connor and DiStefano, 2006; Greer, Dowlatshahi, *et al.*, 2007; Greer, Oskoui, *et al.*, 2007). In addition, it is important to remember while considering the implications of the data presented in this thesis that a *daf-2(m577)* mutant exhibited lower total fecundity compared to WT worms ($p<0.001$, figures 4.4A and 4.5A). For this reason, I hesitant to describe the alternative reproductive timeline of a *daf-2; aakg-4; aakg-5* mutant a rescue phenotype.

4.4 Mutation of AMPKγ isoforms does not affect dauer entry or recovery.

C. elegans larvae go through four moults during normal development (Figure 1.1). Environmentally-challenging conditions during the L1/L2 moult cause larvae to enter a branch of development known as dauer (Riddle, Swanson and Albert, 1981). Dauer is a state of diapause; during this time development is effectively paused and can only resume properly once conditions improve. Additionally, metabolism is dramatically reduced during dauer, and larvae become extremely resistant to stress. Between L1 and L2 stages, non-dauer worms enact significant changes to metabolism: no longer focusing on production of carbohydrates from fat stores and instead relying on oxidative metabolism. Dauer larvae do not undergo this metabolic shift until after exiting dauer, and continue

to rely on lipid stores, thus presenting an alternative model of *C. elegans* metabolism (Wadsworth and Riddle, 1989; Burnell *et al.*, 2005). Since AMPK modulates several aspects of energy metabolism (Figure 1.6), it was interesting to consider how AMPKγ might play a role in dauer entry and subsequent recovery from dauer.

A premise for the involvement of AMPK in dauer has already been reported; *daf-2(e1370); aak-2* mutants demonstrate reduced dauer longevity, while *daf-2(e1368); aak-2* larvae (carrying a stronger class I *daf-2* allele) avoid dauer entry entirely (Apfeld *et al.*, 2004; Narbonne and Roy, 2009). Following this discrepancy in the role of *aak-2* for dauer entry between two *daf-2* alleles, I decided it would be interesting to evaluate the ability of *aakg* mutants to enter and recover from dauer(Apfeld *et al.*, 2004; Narbonne and Roy, 2009). The protocol used was described in detail earlier (Chapter 2.4.1). Importantly, mutation of any combination of *aakg* isoforms in a WT background did not induce dauer entry between 15°C-25°C. Therefore, the *daf-2(m577)* allele was present in all strains used during dauer assays, because *daf-2(m577)* mutant populations enter dauer completely at 25°C (Gems *et al.*, 1998). Note that similarly to *daf-2(e1368)* used in previous work, *daf-2(m577)* is a class I *daf-2* allele (Apfeld *et al.*, 2004).

The ability of *daf-2*, *daf-2; aakg-1; aakg-2; aakg-3,* and *daf-2; aakg-4; aakg-5* mutants to enter and exit dauer was compared. Analysis showed that all strains demonstrated successful entry into the dauer state within three days at 25°C (data not shown), implying that mutation of *aakg* does not affect *daf-2* dauer entry decisions or pathway signalling resulting from temperature stress. The total number of worms which entered the dauer state was initially recorded as day 0, but it became clear that after 24 hours of recovery at 15°C that almost every individual remained in the dauer state: all except 1 *daf-2; aakg-4; aakg-5* mutant out of three trials. Day 1 data highlights that minimal recovery occurred between 0 and 24 hours at 15°C (Figure 4.6A). This suggests that none of the *aakg* isoforms significantly affect early metabolic decisions promoting recovery of *daf-2(m577)* dauers recovery up to 24 hours after removal of temperature stress.

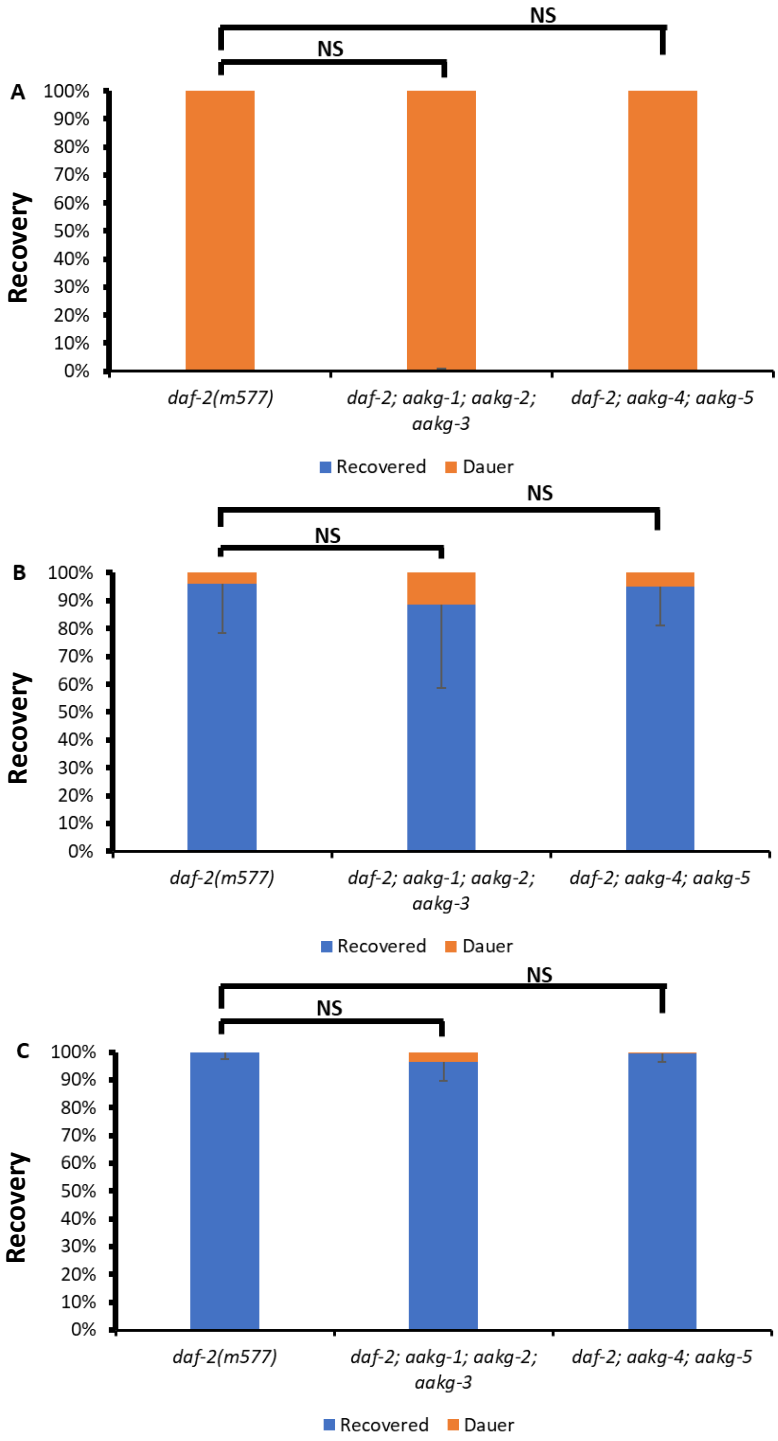

Figure 4.6| Mutation of *aakg* isoforms does not affect dauer entry or recovery. **A**) Day 1 percentage recovery from the dauer state in *daf-2(m577), daf-2; aakg-1(syb409); aakg-2(syb410); aakg-3(syb411), daf-2; aakg-4(tm5539); aakg-5(tm4052)* strains. **B**) Day 2 percentage recovery from the dauer state in *daf-2(m577), daf-2; aakg-1; aakg-2; aakg-3, daf-2; aakg-4; aakg-5* strains. **C**) Day 3 percentage recovery from the dauer state in *daf-2(m577), daf-2; aakg-1; aakg-2; aakg-3, daf-2; aakg-4; aakg-5* strains. Strains were maintained at 25°C prior to use, then allowed to recover at 15°C for the duration of the experiment. Mean data is shown from three biologically independent trials in each case. N=272 for *daf-2*, N=255 for *daf-2; aakg-1; aakg-2; aakg-3*, and N=305 for *daf-2; aakg-4; aakg-5*. Error bars indicate SEM (recovered) for each day. No significant differences were found compared to *daf-2* (p>0.05, Student's *t*-test).

Considering the influence of AMPK on oxidative metabolism, I continued to monitor the rate of recovery from dauer for each strain, to ascertain whether *daf-2; aakg-1; aakg-2; aakg-3* mutants would suffer more than *daf-2* and *daf-2; aakg-4; aakg-5* mutants due to dysregulation of AMP-sensitive AMPK activation (Figures 3.7 and 3.8). All strains had been simultaneously placed at 15°C and allowed to recover. However, no significant differences in dauer recovery rate were observed between *daf-2*, *daf-2; aakg-1; aakg-2; aakg-3,* and *daf-2; aakg-4; aakg-5* mutants. Differences remained insignificant even after two days at 15°C, and most dauers had recovered by day 2 across all strains (Figure 4.6B). 96% of *daf-2* dauers had recovered by day 2 compared to 89% of *daf-2; aakg-1; aakg-2; aakg-3* dauers, and 95% of *daf-2; aakg-4; aakg-5* dauers. The lack of significant differences in recovery between any of the strains investigated here suggests that the tightly controlled timeline of metabolic events linked to dauer recovery is unaffected by irregularities in AMPK regulation. Between trials, there appeared to be slight variations in dauer recovery, though ultimately only 1% of worms (all strains) remained in dauer by day 3 across all trials (Figure 4.6C).

4.5 AMPKγ isoforms *aakg-4* and *aakg-5* do not contribute to dauer induced SDS resistance.

Dauers exhibit significantly changed morphology compared to other larval stages: Orifices are plugged, feeding stops, and they secrete a specialised cuticle providing an effective barrier against many chemical stressors (Cassada and Russell, 1975; Riddle, Swanson and Albert, 1981; Vowels and Thomas, 1992). When dauer larvae receive signals promoting recovery, the plug in the buccal cavity is degraded within a few hours, and larvae are receptive to chemical stress again. In contrast, the dauer cuticle persists until larvae moult into the post-dauer L4 stage (Cassada and Russell, 1975). Interestingly, previous research has demonstrated that not all dauers are identical, and that some physiological changes which usually signpost this branch of *C. elegans* development are not always expressed to the same extent in some mutant strains (Albert and Riddle, 1988; Malone, Inoue and Thomas, 1996; Nika *et al.*, 2016; Flatt *et al.*, 2019).

Morphological changes provide dauers with resistance to external stresses, including resistance to 1% SDS, which has been advocated as a selection pressure for dauer identification, although more recent studies have demonstrated the existence of "dauer-like" phenotypes suggesting that morphological changes and consequent resistances associated with dauer should not be assumed in mutant strains (Cassada and Russell, 1975; Albert and Riddle, 1988; Flatt *et al.*, 2019). Thus, when considering possible contributions of *aakg* (AMPKγ) to *C. elegans* phenotypes, I wanted to investigate whether AMP-sensitivity might play a role in dauer SDS resistance. The protocol for this assay was described earlier (Chapter 2.4.2). In summary, the survivability of dauer stage individuals was recorded immediately after 30 minutes of exposure to SDS, and then again 24 hours later. Again, a *daf-2(m577)* background was used because *aakg* mutations do not induce dauer entry in a WT background between 15°C-25°C. This maintained continuity with previous results reported in this investigation, but was also necessary because *daf-2(m577)* is a temperature-sensitive allele which causes populations enter dauer completely at 25°C (Gems *et al.*, 1998). Only *aakg-4* and *aakg-5* were tested here because of project time constraints.

Initially, no significant difference was observed between *daf-2* and *daf-2; aakg-4; aakg-5* mutants after 30 minutes exposure to 1% SDS. A *daf-2* mutant showed no mortality after 30 minutes across six trials, while a *daf-2; aakg-4; aakg-5* mutant showed only 7% mortality (Figure 4.7A). After 24 hours the effect of acute SDS stress became more explicit: a *daf-2* mutant displayed just 2% mortality, compared to 30% mortality in a *daf-2; aakg-4; aakg-5* mutant. However, following statistical analysis, this was not found to be significant (Figure 4.7A), implying that *aakg-4* and *aakg-5* isoforms do not influence dauer SDS resistance.

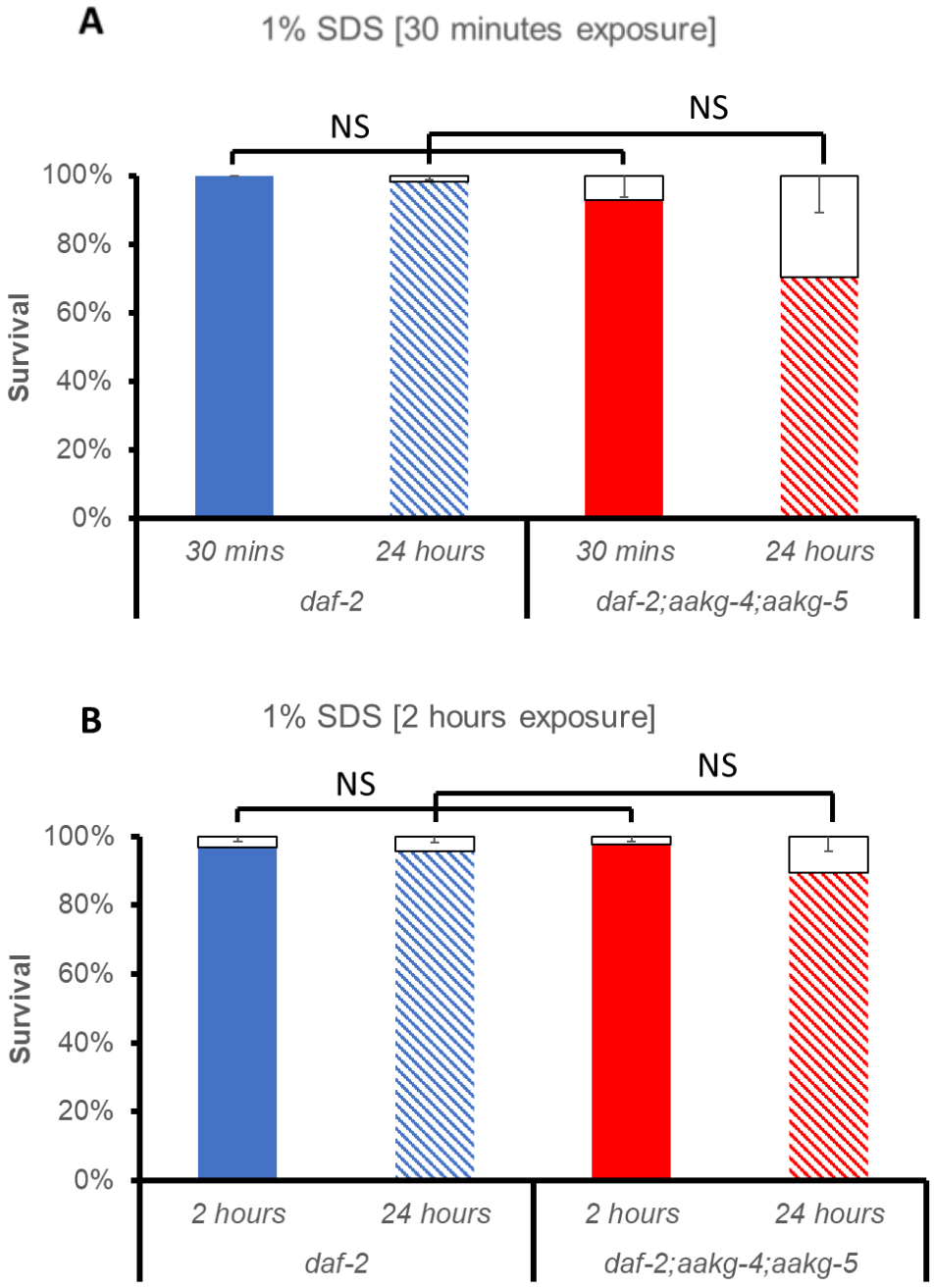

Figure 4.7| *aakg-4(tm5539)* and *aakg-5(tm4052)* do not decrease dauer survival following exposure to 1% SDS. The white boxed area indicates mortality in respective strains. **A**) Comparison of *daf-2(m577)* and *daf-2; aakg-4(tm5539); aakg-5(tm4052)* strains, after 30 minutes exposure and 24 hours after exposure to 1% SDS. Dauers were maintained at 25°C, and mean data is shown from six biologically independent trials. N=168 for *daf-2*, and N=111 for *daf-2; aakg-4; aakg-5*. Error bars indicate SEM (dead). No significant changes, $p>0.05$, Student's *t*-test. **B**) Comparison of *daf-2(m577)* and *daf-2; aakg-4; aakg-5* strains, after 2 hours exposure and 24 hours after exposure to 1% SDS. Dauers were maintained at 25°C, and mean data is shown from four biologically independent trials. N=160 for *daf-2*, and N=123 for *daf-2; aakg-4; aakg-5*. Error bars indicate SEM (dead). No significant changes, $p>0.05$, Student's *t*-test.

After 30 minutes of exposure to 1% SDS did not display significant change in *daf-2; aakg-4; aakg-5* dauer survival, I modified my protocol, now exposing dauers to 1% SDS for 2 hours (before removal from the SDS droplet). Survival was recorded immediately after 2 hours, and again 24 hours. There were no significant differences in resistance to 1% SDS after 2 hours: 3% mortality in a *daf-2* mutant compared to 2% mortality in a *daf-2; aakg-4; aakg-5* mutant (Figure 4.7B). Again, there were also no significant differences in SDS resistance after 24 hours. *daf-2* and *daf-2; aakg-4; aakg-5* mutants showed 4% and 11% mortality, respectively. Curiously, a *daf-2; aakg-4; aakg-5* mutant showed mortality rates more similar to a *daf-2* mutant following 2 hours exposure to 1% SDS than under previous conditions. It is important to note at this point that the same 1% SDS solution was used for 30-minute and 2-hour investigations. Overall, I report that *aakg-4* and *aakg-5* do not appear to contribute to dauer survival following exposure to 1% SDS. However, further investigation may reveal that the efficacy of dauer SDS resistance is time-dependent.

4.6 Dauer size is affected in *C. elegans* AMPKγ mutants.

Alongside investigations into the possible of *aakg* isoforms on SDS resistance, I began to pursue further physiological characterisation of *aakg* mutant dauers. Existing literature has highlighted the potential for dauer-like phenotypes in various mutants (Albert and Riddle, 1988; Malone, Inoue and Thomas, 1996; Nika *et al.*, 2016; Flatt *et al.*, 2019). Radial restriction and secretion of a specialised cuticle are well-known hallmarks of dauer morphology and are associated with reduced metabolism and increased stress resistance in dauer worms. I reasoned that AMPK and its contribution to energy homeostasis might play a role in efficient radial restriction and/or secretion of the dauer cuticle. To explore this, I decided to examine the diameter of *daf-2*, *daf-2; aakg-1; aakg-2; aakg-3* and *daf-2; aakg-4; aakg-5* dauers to determine whether dauer morphology was altered in response to disrupted AMPK regulation (Albert and Riddle, 1988; Malone, Inoue and Thomas, 1996; Nika *et al.*, 2016).

Diameter measurements were recorded at the same point for each worm, across the pharyngeal grinder. The grinder was chosen as an "anchor point" to maintain relative consistency of technique between individuals and strains. The grinder lies within the posterior/terminal bulb at the head of the worm, just before the intestine (Supplementary figure 4). The diameter was measured in pixels, and measurements were taken using the TIF files captured while using a Zyla 4.2 PLUS sCMOS camera, then pixel measurements were converted using an equation which took into consideration the magnification and the size of the camera sensor (Chapter 2.4.3). This allows a real-world unit to be applied to these measurements.

daf-2; aakg-1; aakg-2; aakg-3 and *daf-2; aakg-4; aakg-5* mutants, along with a *daf-2* mutant control population were grown under the same conditions. Populations of approximately 200 offspring were selected as eggs and grown at 25°C to ensure entry into dauer. It was important to consider the impact of reduced metabolism during dauer, so each mutant was assayed over an extended period (four weeks), to effectively monitor changes in the sizes of these three strains over time. Three time points were chosen for imaging: one, two and four weeks. Weekly time intervals were chosen so that sampling would not require an excessive amount of strain maintenance. Data was initially processed from individual sessions, then compiled into weekly data sets (one, two and four weeks). Mean diameter from pooled data sets for each weekly interval is shown (Figure 4.8).

Analysis of dauers 1 week after entry into the dauer state shows that both *daf-2; aakg-1; aakg-2; aakg-3* and *daf-2; aakg-4; aakg-5* dauers initially displayed significantly increased diameter compared to the *daf-2* control, 1.9µm and 2.9µm respectively (p<0.001 for both strains, figure 4.8A). Moreover, there was even a significant difference between *daf-2; aakg-1; aakg-2; aakg-3* and *daf-2; aakg-4; aakg-5* dauer size (p<0.001, figure 4.8A), implying that loss of *aakg-4 and aakg-5* permits even further dysregulation of *daf-2* dauer morphology than absence of *aakg-1, aakg-2,* and *aakg-3*.

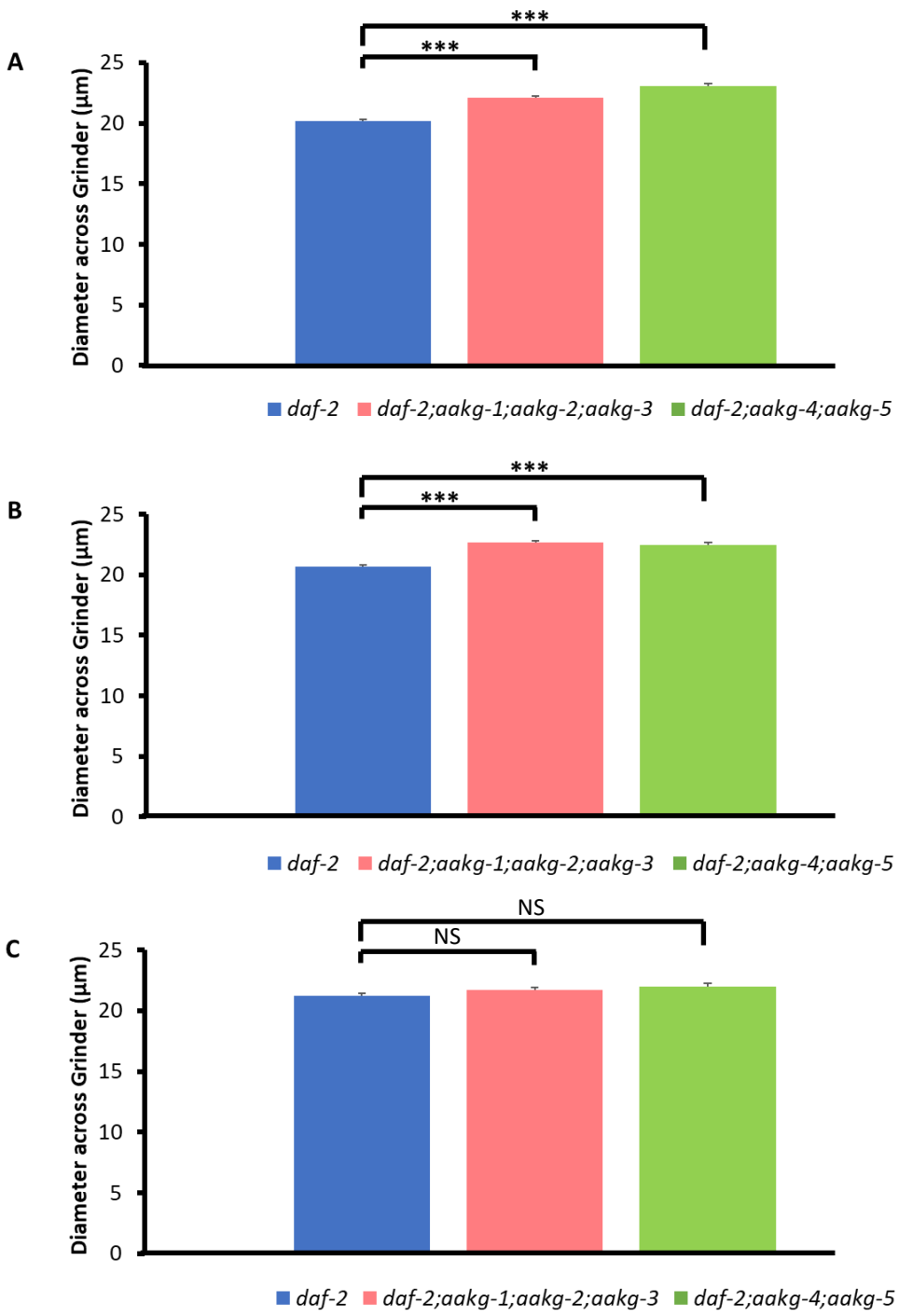

Figure 4.8| Dauer diameter is increased in *aakg* mutants for two weeks after dauer entry. **A**) Diameter across the posterior bulb of 1-week-old dauers in *daf-2(m577), daf-2; aakg-1(syb409); aakg-2(syb410); aakg-3(syb411), daf-2; aakg-4(tm5539); aakg-5(tm4052)* strains. Data shown is pooled from two biologically independent trials. N=79 for *daf-2*, N=83 for *daf-2; aakg-1; aakg-2; aakg-3*, and N=80 for *daf-2; aakg-4; aakg-5*. **B**) Diameter across the posterior bulb of 2-week-old dauers in *daf-2(m577), daf-2; aakg-1; aakg-2; aakg-3, daf-2; aakg-4; aakg-5* strains. Data shown is pooled from three biologically independent trials. N=94 for *daf-2*, N=88 for *daf-2; aakg-1; aakg-2; aakg-3*, and N=75 for *daf-2; aakg-4; aakg-5*. **C**) Diameter across the posterior bulb of 4-week-old dauers in *daf-2(m577), daf-2; aakg-1; aakg-2; aakg-3, daf-2; aakg-4; aakg-5* strains. Data shown is pooled from two biologically independent trials. N=39 for *daf-2*, N=49 for *daf-2; aakg-1; aakg-2; aakg-3*, and N=53 for *daf-2; aakg-4; aakg-5*. Strains were maintained at 25°C in all trials. Error bars indicate SEM. Significance asterisks (*** p<0.001, ANOVA followed by Tukey's test, compared to *daf-2*).

2 weeks after entry into dauer, both *daf-2; aakg-1; aakg-2; aakg-3* and *daf-2; aakg-4; aakg-5* dauers continued to show increased diameter compared to *daf-2* dauers (p<0.001 for both strains, figure 4.8B), though there was no longer a significant difference between *daf-2; aakg-1; aakg-2; aakg-3* and *daf-2; aakg-4; aakg-5* dauers. In contrast to week 1 data, *daf-2; aakg-1; aakg-2; aakg-3* dauers displayed the highest diameter out of the three strains investigated here, suggesting that *aakg-1, aakg-2,* and *aakg-3* became increasingly necessary for *daf-2* dauer morphology 2 weeks after entry. At the same time, a lack of significant difference between the combination knockout strains highlights how *daf-2; aakg-1; aakg-2; aakg-3* dauers effectively matched *daf-2; aakg-4; aakg-5* dauer diameter (22.6µm and 22.4µm, respectively). Intriguingly, *daf-2* and *daf-2; aakg-1; aakg-2; aakg-3* dauers displayed similar increases in diameter between the first and second week (approximately 0.5µm in each case), while *daf-2; aakg-4; aakg-5* dauers reported decreased diameter, showing a mean reduction of 0.6µm between the first and second week.

4 weeks after entry into dauer, diameter became statistically similar between all strains (Figure 4.8C), suggesting that alternative models of AMPK regulation may not significantly affect dauer size long-term.

Taken together, *daf-2* dauers reported increased diameter at all three intervals (p<0.05, figure 4.8). In contrast, *daf-2; aakg-1; aakg-2; aakg-3* dauers exhibited increased diameter between weeks 1 and 2 (p<0.05, figures 4.8A and 4.8B), then showed reduced diameter between weeks 2 and 4 (p<0.01, figures 4.8B and 4.8C). *daf-2; aakg-4; aakg-5* dauers showed significantly reduced diameter between weeks 1 and 4 only (p<0.01, figures 4.8A and 4.8C). In future, it may be interesting to investigate whether *daf-2; aakg-1; aakg-2; aakg-3* and *daf-2; aakg-4; aakg-5* dauers show further reductions as dauer larvae are forced to maintain dauer metabolism for longer periods of time (Burnell *et al.*, 2005; Mádi *et al.*, 2008).

It is also interesting to note how *daf-2; aakg-4; aakg-5* dauers showed the highest diameter 1 week after entry, but *daf-2; aakg-1; aakg-2; aakg-3* dauers displayed the highest diameter after 2

weeks. These differences imply that *daf-2; aakg-1; aakg-2; aakg-3* and *daf-2; aakg-4; aakg-5* dauers employ different metabolic strategies to preserve morphology during the first two weeks of dauer. Given that there were no significant differences in dauer recovery between these strains (Figure 4.6), it is even more interesting to consider how these strategies are mediated under dauer metabolism (Burnell *et al.*, 2005; Mádi *et al.*, 2008).

4.7 Chapter 4 Discussion.

The data in chapter 4 focuses on the physiological changes which result from disruption of AMPK activation in *aakg* mutants. Again, I explore this using combination *aakg* mutants which I predict to model two antagonistic models of AMPK regulation: *aakg-1; aakg-2; aakg-3* and *aakg-4; aakg-5* mutants, which rely on AMP-insensitive and AMP-sensitive systems of regulation, respectively. Through the investigations described in this chapter, I continue to investigate ideas discussed by Tullet *et al.* (2014), who demonstrated the contribution of *aakg-4* to *daf-2*-mediated longevity and provided clear incentive to investigate the other *aakg* isoforms in *C. elegans*. Furthermore, due to the conservation of one pair of binding residues in *aakg-5* (Table 3.1), there is still the question whether *aakg-5* can bind AMP, and whether this permits some level of functionality. This investigation compares *aakg-5* mutant phenotype against other *aakg* mutant strains and analyses the influence of WT and *daf-2* backgrounds.

4.7.1 The importance of AMP-sensitive *aakg-1, aakg-2,* and *aakg-3* isoforms to WT and *daf-2(m577)* lifespan.

Initially, some interesting comparisons are apparent between effects of *aak-2* (AMPKα) and *aakg* mutation on lifespan. An *aakg-1; aakg-2; aakg-3* mutant demonstrates similar suppression of WT lifespan (Figure 4.1A) to an *aak-2* mutant, suggesting that AMP-sensitive AMPK regulation effectively mimics the contribution of AMPK (containing AAK-2) to WT lifespan (Apfeld *et al.*, 2004; Curtis, O'Connor and DiStefano, 2006; Schulz *et al.*, 2007; McQuary *et al.*, 2016). In a *daf-2* background, a *daf-2; aakg-1; aakg-2; aakg-3* mutant displays partial suppression of *daf-2* longevity (Figure 4.1B), in contrast to a *daf-2; aak-2* mutant which demonstrates complete suppression of *daf-2* longevity (Apfeld *et al.*, 2004). This suggests that AMP-sensitive AMPK regulation contributes to *daf-2* lifespan, but additional mechanisms are required to fulfil *daf-2* longevity. The requirement for *aak-2* in *daf-2* longevity, in combination with the role of *aakg-4* in *daf-2* longevity (Figure 4.2), indicates that *aakg-4* could account for the partial nature of suppression demonstrated by a *daf-2; aakg-1;*

aakg-2; aakg-3 mutant. Thus, data in this thesis demands that additional ablation of *aakg-4* expression in *daf-2; aakg-1; aakg-2; aakg-3* mutant is investigated in future lifespan assays.

Interestingly, Tullet *et al.* (2014) report that RNAi-induced knockdown of *aakg-1, aakg-2,* and *aakg-3* does not consistently supress *daf-2* mutant longevity, even when strains were made more susceptible to RNAi using a *rrf-3(pk1426)* mutant background (Simmer *et al.*, 2002). Here, I show that a *daf-2*; *aakg-1; aakg-2; aakg-3* mutant displays more severe suppression of lifespan than a *daf-2; aakg-4; aakg-5* mutant, mirroring the WT trend (Figure 4.1). Overall, lifespan analysis indicates that isoforms *aakg-1, aakg-2,* and *aakg-3* significantly contribute significantly to both WT and *daf-2* lifespan, at least in a combination knockout strain. While single knockouts of AMP-sensitive isoforms were not investigated here, *aakg-1; aakg-2; aakg-3* and *daf-2; aakg-1; aakg-2; aakg-3* mutants show severe suppression of WT and *daf-2* lifespan, respectively, and imply that either *aakg-1, aakg-2,* or *aakg-3* might also contribute to lifespan individually in some capacity. This would have to be confirmed through characterisation of single mutant lifespans. In theory, if *aakg-1; aakg-2; aakg-3* mutant lifespan does result from additive suppressions of longevity, then this might imply that *aakg-1-3* are important during development, since worms were treated with RNAi from the L4 stage of development in previous work (Tullet *et al.*, 2014).

In my investigations, comparison shows that the contribution of *aakg-1, aakg-2,* and *aakg-3* to WT lifespan is greater than the contribution of *aakg-4* and *aakg-5* (Figure 4.1). Increased reliance on *aakg-1, aakg-2,* and *aakg-3* isoforms may seem intuitive, since these three isoforms show complete conservation of predicted AMP-binding residues when compared with mammalian homologues (Table 3.1). Additionally, substantially reduced Thr172 phosphorylation in an *aakg-1; aakg-2; aakg-3* mutant (Figure 3.7) implies a requirement for AMP-sensitive isoforms in AMPK activation, which may explain why *aakg-1; aakg-2; aakg-3* and *daf-2; aakg-1; aakg-2; aakg-3* mutants display more severe lifespan suppression phenotypes than *aakg-4; aakg-5* and *daf-2; aakg-4; aakg-5* mutants in WT and *daf-2*

backgrounds. Reduced Thr172 phosphorylation also provides a molecular mechanism which explains how *aakg-1; aakg-2; aakg-3* mutant lifespan effectively mirrors *aak-2* mutant lifespan.

Regarding the hypothesis proposed by Tullet *et al.* (2014) that AMP-insensitive isoforms (*aakg-4* and *aakg-5*) contribute to *daf-2* longevity through up-regulation of constitutively active AMPK, this is thrown into question here because mutation of *aakg-1, aakg-2,* and *aakg-3* suppresses WT and *daf-2* lifespan to a greater extent than mutation of *aakg-4* and *aakg-5* (Figure 4.1A), implying that AMP-sensitive regulation may be more important for AMPK function after all (at least in regard to longevity). Supporting this idea, allosteric activation of AMPKα appears to require *aakg-1, aakg-2,* and *aakg-3* isoforms in WT and reduced IIS backgrounds, but appears largely unaffected by mutation of *aakg-4* and *aakg-5* (Chapters 3.4 and 3.5, figures 3.7 and 3.8). Ultimately though, expression of *C. elegans* AMPK containing AAKG-4 or AAKG-5 and subsequent biochemical analysis will be required to confirm the activity of these AMPK complexes definitively.

4.7.2 *aakg-5* contributes to WT longevity, while *aakg-4* contributes to *daf-2(m577)* longevity.

Despite the apparent increased role of *aakg-1-3* in longevity, it is still interesting to discuss the influence *aakg-4* and *aakg-5* isoforms. Comparison shown in figure 4.2 distinguishes between contributions of *aakg-4* and *aakg-5* isoforms to longevity, which are predicted to demonstrate null AMP-sensitivity and partial AMP-sensitivity, respectively. Analysis reveals that the degree of AMP-insensitivity may influence the role of these isoforms in *aakg-4; aakg-5* and *daf-2; aakg-4; aakg-5* mutant lifespan. Figure 4.2A highlights how *aakg-5* drives reduced lifespan in an *aakg-4; aakg-5* mutant, while *aakg-4* mutation does not consistently decrease WT lifespan (Table 4.1). Existing literature reports that *aakg-5* is the most expressed *aakg* isoform in WT *C. elegans*, so the relative abundance of *aakg-5* might explain why an *aakg-5* mutant displays reduced lifespan compared to WT (Tullet *et al.*, 2014). Previously, *aakg-5* RNAi treatment was shown to have no effect on WT lifespan (Tullet *et al.*, 2014), but importantly, worms underwent *aakg-5* RNAi treatment from the L4 stage in these trials. Since *aakg-5* genetic knockout strain demonstrates significant suppression of lifespan

here (Figure 4.2A, table 4.1), this implies that *aakg-5* contributes to WT lifespan during development. In future, characterisation of AMPK target protein phosphorylation in *aakg-5* mutants and WT worms may shed light on the molecular mechanisms which mediate the role of *aakg-5* (and other *aakg* isoforms, figure 4.1) in WT longevity.

A *daf-2; aakg-4; aakg-5* mutant also displays significant and reproducible suppression of lifespan, so investigation into the relationship between *aakg-4* and *aakg-5* remained an interesting avenue to pursue in a *daf-2* background. In figure 4.2B, I confirm that *aakg-4(tm5539)* mutation suppresses *daf-2*-mediated longevity, as previously reported by Tullet *et al.* (2014). Interestingly, while a *daf-2; aakg-4* mutant demonstrates a significant suppression of *daf-2* longevity, an *aakg-4* mutant does not show reduced lifespan in WT background, suggesting that *aakg-4* is required for *daf-2*-mediated longevity but not maintenance of WT lifespan (Figure 4.2, table 4.1). Therefore, *aakg-4* appears to acquire additional functional relevance in a *daf-2* background. Additionally, it is important to note that *aakg-4* is the only isoform consistently linked to the DAF-16 transcription factor so far: DAF-16 transcriptionally controls *aakg-4* expression, and the existing hypothesis suggests that AMPK also up-regulates DAF-16 activity through a positive feedback loop (Chapter 1.5.3)(Greer, Dowlatshahi, *et al.*, 2007; Schuster *et al.*, 2010; Tullet *et al.*, 2014).

An interesting parallel becomes apparent in my data. Consistent with the idea that increasing *aakg-4* expression contributes to *daf-2* longevity, *daf-2* mutants show significant change in *aakg-4* expression (Figure 3.6D), while *aakg-5* expression remains unchanged (Figure 3.6E). Furthermore, a *daf-2; aakg-4* mutant shows substantial suppression of *daf-2*-mediated lifespan extension, while a *daf-2; aakg-5* mutant does not (Figure 4.2B)(Tullet *et al.*, 2014). However, transcriptional data shown earlier in chapter three highlights a complexity of transcriptional change in a *daf-2* background, which involves both IIS-dependent and IIS-independent mechanisms (Chapters 3.3 and 3.5.4), complicating the existing hypothesis. Moreover, a *daf-2; aakg-1; aakg-2; aakg-3* mutant does not show significantly different *aakg-4* expression compared to a *daf-2* mutant (Figure 3.6D), but demonstrates more severe

suppression of *daf-2* longevity than a *daf-2; aakg-4; aakg-5* mutant (Figure 4.1B). This suggests *daf-2* longevity may involve a more complex mechanism than transcriptional changes to *aakg* expression alone.

Meanwhile, a *daf-2; aakg-5* mutant does not demonstrate significantly different lifespan compared to a *daf-2* mutant (Figure 4.2B). Absence of a lifespan suppression in phenotype a *daf-2; aakg-5* mutant is surprising considering that *aakg-5* is the most expressed isoform in WT *C .elegans,* and levels of *aakg-5* expression do not change between WT and *daf-2* worms (Figure 3.6E, table 3.3)(Tullet *et al.*, 2014). In contrast, Tullet *et al.* (2014) reported a role for *aakg-5* in *daf-2* longevity, demonstrated using *aakg-5* RNAi. In this case, successful reduction of *aakg-5* mRNA expression was confirmed by qRT-PCR. Tullet *et al.* (2014) also used the same *daf-2(m577)* mutation which I use here. Importantly, Tullet *et al.* (2014) exposed worms to *aakg-5* RNAi treatment from the L4 stage, which may reveal why a *daf-2; aakg-5(tm4052)* mutant does not display a lifespan suppression phenotype in my data. Absence of *aakg-5* expression during development appears to be successfully compensated for in a *daf-2; aakg-5* mutant, perhaps through up-regulation of other *aakg* isoforms; *aakg-2* seems a likely candidate since its expression is substantially increased in *daf-2; aakg-4; aakg-5* mutant compared to a *daf-2* knockout strain (Figure 3.6B), though my qRT-PCR protocol (Chapter 2.5) should be repeated using *daf-2; aakg-5* mutants to confirm this. Conversely, if *daf-2* mutants express *aakg-5* normally during development, lifespan is shortened following *aakg-5* RNAi treatment, providing further evidence for roles of AMP-insensitive isoforms in *daf-2* metabolism.

In summary, comparison of *daf-2; aakg-4, daf-2; aakg-5,* and *daf-2; aakg-4; aakg-5* mutants reveals that *aakg-4* drives suppression of *daf-2* longevity, since a combination knockout (*daf-2; aakg-4; aakg-5*) does not show additive suppression of lifespan compared to a *daf-2; aakg-4* mutant (Figure 4.2B). This suggests complete AMP-insensitivity (*aakg-4*) is important for *daf-2*-mediated longevity. Conversely, the role of partial AMP-insensitivity (*aakg-5*) appears to be IIS-dependent and drives *aakg-4; aakg-5* mutant lifespan in a WT background (Figure 4.2A). The shifting importance of *aakg-4* and

aakg-5 between backgrounds reveals benefits to longevity under different metabolic conditions, which might explain why both isoforms persist in *C. elegans* and other nematodes of the Chromadorea clade (Tullet *et al.*, 2014).

4.7.3 Functional redundancy exists between the contributions of *aakg-4* and *aakg-5* to WT arsenite resistance.

The arsenite stress assay is an established experimental method in *C. elegans* research, and is used here to investigate the response of *aakg* mutants to oxidative stress, as well as explore a potential relationship between stress and lifespan (Ewald, Hourihan and Blackwell, 2017). Sodium arsenite target components of the electron transport chain, inhibiting aerobic respiration and increasing the intracellular AMP:ATP ratio (Corton, Gillespie and Hardie, 1994; Luz *et al.*, 2016). Though acute stress exposure can extend lifespan, chronic exposure to stress usually becomes too taxing for the organism, and subsequently shortens lifespan. Animals in this assay were exposed to arsenite chronically, more appropriately reflecting the capacity for oxidative stress resistance in *aakg* mutant strains. Additionally, the arsenite solution used in this assay was diluted with OP50 bacteria in a 1:1 ratio to avoid the influence of starvation on stress resistance.

Existing literature links *aak-2* to ROS-induced lifespan extension, implicating the involvement of AMPK in both longevity and oxidative stress response (Hwang *et al.*, 2014). Meanwhile, the contribution of *aakg* isoforms to oxidative stress resistance has not been investigated directly prior to this project. Therefore, I thought it necessary to examine the contribution of *aakg* isoforms to this process and decided to investigate possible differences between contributions of AMP-insensitive *aakg* isoforms. In line with this, *aakg-4*, *aakg-5,* and *aakg-4; aakg-5* mutants have been assayed in WT and *daf-2* backgrounds, which additionally allows me to comment on how IIS influences the responses of these mutants under oxidative stress. While arsenite survival data does show relatively high variation between trials, this is common when investigating oxidative stress (Dr. J.M.A. Tullet, *personal communication*), and some conclusive results are presented. Figure 4.3A suggests a role for both

isoforms in oxidative stress response, since mutation of *aakg-4* and *aakg-5* generates relatively small but significant reductions to survivability while exposed to 2.5mM arsenite. Similarly to WT lifespan data, an *aakg-4; aakg-5* mutant displays no additive effect, implying that redundancy exists between contributions of *aakg-4* and *aakg-5* to arsenite resistance.

It is interesting to note that *aakg-5* displays contributions to WT lifespan and arsenite resistance (Figures 4.2A and 4.3A). However, the role of *aakg-5* in oxidative resistance cannot be used to describe a potential mechanism for maintaining normal lifespan, because *aakg-4* also holds a role in WT oxidative stress resistance but is not required for normal lifespan. Yet, as discussed earlier (Chapter 4.7.2), *aakg-5* is the most expressed *aakg* isoform in WT *C. elegans* (Tullet *et al.*, 2014). The relative abundance of *aakg-5* might also explain reduced oxidative resistance in *aakg-5* mutant, but further investigation is required to define a molecular mechanism for this.

4.7.4 *aakg-4* contributes to enhanced arsenite resistance in *daf-2(m577)* mutants.

In the *daf-2* background (Figure 4.3B) only *daf-2; aakg-4* and *daf-2; aakg-4; aakg-5* strains consistently show decreased survivability, indicating that *aakg-4* drives oxidative stress survival in the absence of IIS. Figure 4.3 demonstrates that *aakg-4* contributes to arsenite resistance in WT and *daf-2* backgrounds, implying that *aakg-4* contributes to the oxidative stress response independently of IIS. Additionally, this reveals that the influence of *aakg-5* on arsenite resistance is IIS-dependent, mirroring the role of *aakg-5* in lifespan (Figures 4.2A and 4.3A).

Since *aakg-4* and *aakg-5* contribute to both lifespan and oxidative stress resistance between WT and *daf-2* backgrounds, this implies that AMP-insensitive AMPK complexes containing these isoforms contribute to these processes. Perhaps this justifies the presence of *aakg-4* and *aakg-5* among the Chromadorea clade, proving to be advantageous under certain metabolic conditions (Tullet *et al.*, 2014). Individuals of a population which are able to mount an improved response to oxidative stress can display extended lifespan, which may result from beneficial changes in metabolic signalling (Minois, 2000; Apfeld *et al.*, 2004; Schmeisser *et al.*, 2013). In one case, *aakg-5*, which displays

intermediate conservation of predicted AMP-binding residues, shows IIS-dependent effects on normal lifespan and stress resistance. Conversely, metabolic challenges like reduced IIS may induce a preference for completely AMP-insensitivity, justifying a requirement for *aakg-4* in a *daf-2* mutant background.

Furthermore, earlier I showed that *aakg-1-3* isoforms demonstrate increased importance in terms of longevity contributions compared to *aakg-4* and *aakg-5*, and the scale of these contributions remains consistent in both WT and *daf-2* backgrounds (Figure 4.1). Given this role, it would also be interesting to examine the response of AMP-sensitive isoform mutants to arsenite stress. If *aakg-1; aakg-2; aakg-3* or *daf-2; aakg-1; aakg-2; aakg-3* mutants show even lower survivability in response to chronic arsenite exposure than *aakg-4; aakg-5* or *daf-2; aakg-4; aakg-5* mutants, respectively, this could reveal the importance of AMP-sensitivity in AMPK-mediated contributions to oxidative stress resistance, in addition to lifespan effects shown here. Another important question to consider is whether *aakg* knockout strains respond differently to different stressors, so it would be worthwhile to continue characterising the responses of all *aakg* mutants to other stressors (e.g. paraquat, H_2O_2 and heat shock), which could reveal further roles for AMPKγ isoforms in *C. elegans* stress signalling (Tullet *et al.*, 2017).

4.7.5 Lifespan and adult fecundity are not correlated through AMPKγ regulation in *C. elegans*.

The disposable soma theory, as well as reproductive effects of *aak-2* mutation reported in existing literature provided clear reasons to investigate fertility in *aakg* mutants and explore possible interactions between lifespan and reproductive health. Work by Apfeld *et al.* (2004) shows that an *aak-2* mutant displays reduced brood size compared to WT worms, and that temperature stress reduces fertility in an *aak-2*-dependent manner. Additionally, Burkewitz *et al.* (2015) report that a transgenic *C. elegans* strain producing constitutively active AAK-2 shows decreased brood size compared to WT. Interestingly, the reproductive schedule of the constitutively active AAK-2 transgenic

strains shifts towards late-life progeny production: initially laying less offspring, but numbers of offspring partially recover later in the reproductive window.

Analysis in this thesis shows that mutation of *aakg-1, aakg-2, and aakg-3* does not alter WT fecundity (Figure 4.4), implying that AMP-sensitive regulation of AMPK is not required to maintain WT fecundity. Conversely, an *aakg-4; aakg-5* mutant displays reduced brood size on day 2, which contributes to a statistically significant reduction in total progeny compared to WT across the entire reproductive window (Figure 4.4). While daily brood size analysis indicates that an *aakg-4; aakg-5* mutant displays statistically similar mean brood size compared with WT on days one, three, and four (Figure 4.4B), a statistically significant reduction occurs two days post-development, implying that AMP-insensitive AMPK regulation transiently affects WT fecundity at this point in time. Curiously, an *aakg-4; aakg-5* mutant appears to behave similarly to a constitutively active AAK-2 strain. Both strains report reduced brood size compared to WT worms prior to two days post-development, but progeny production improves for the remainder of the reproductive window (Figure 4.4B)(Burkewitz *et al.*, 2015). Crucially, total fecundity does not completely recover in either strain. However, there are differences between these strains as well: an *aakg-4; aakg-5* mutant recovers to WT levels, while a constitutively active AAK-2 mutant surpasses WT progeny production.

Considering that *aakg-4* and *aakg-5* may act differently from each other (as demonstrated in previous assays), I consulted existing literature to clarify which isoform might drive reduced WT fecundity. Tullet *et al.* (2014) reports *aakg-4(tm5539)* does not affect progeny production, implying that *aakg-5(tm4052)* drives the reduced fecundity observed in the *aakg-4; aakg-5* mutant (Figure 4.4). In terms of a link between lifespan and fertility, *aakg-5* appears to drive reductions to WT lifespan and brood size, indicating a shared role for *aakg-5* in these processes, which disagrees with the disposable soma theory. In future, one interesting avenue to pursue would be the further mutation of *aakg-5* in the *aakg-1; aakg-2; aakg-3* strain. If the resulting *aakg-1; aakg-2; aakg-3; aakg-5* strain shows greater reduction of lifespan or reproductive health, then this would support the argument that *aakg-5* shows

partial retention of function, implying that *aakg-5* displays some degree of AMP-sensitive regulation in an *aakg-1; aakg-2; aakg-3* mutant. Additionally, it might be interesting to investigate complete mutation of all *aakg* subunits, to observe whether lifespan and fertility effects match those described in *aak-2* mutants. (Apfeld *et al.*, 2004).

4.7.6 *aakg-1, aakg-2,* and *aakg-3* contribute to *daf-2(m577)* brood size, while *aakg-4* and *aakg-5* alter *daf-2(m577)* reproductive schedule.

To investigate how reducing IIS would affect *aakg*-mediated contributions to fecundity, *aakg* mutant fecundity was also investigated in a *daf-2* background (Figure 4.5). In my hands, *daf-2(m577)* mean brood size is substantially lower than WT (Figures 4.4 and 4.5). Notably, *daf-2(m577)* brood size is lower here than reported in existing literature, but I have examined a larger population of *daf-2* mutants than used in previous studies (Gems *et al.*, 1998; Tullet *et al.*, 2014). Gems *et al.* (1998) additionally report that *daf-2(m577)* displays lower brood sizes at lower temperatures, and since I maintained *daf-2* mutants at 15°C before starting the experiment (Chapter 2.3.3), it is possible that some residual signalling may have affected the early stages of the reproductive window, before temperature-sensitive activation of the *daf-2(m577)* allele had fully taken effect at 25°C. Nonetheless, all strains were moved between incubators at the same time, so this is unlikely to have influenced differences observed between strains.

Interestingly, a *daf-2; aakg-1; aakg-2; aakg-3* mutant shows decreased total progeny production in the absence of IIS (Figure 4.5A), and significant reduction of daily progeny production from day 2 onwards (Figure 4.5B). This implies two things: firstly that there is decreased maintenance of oocyte quality in a *daf-2; aakg-1; aakg-2; aakg-3* mutant, resulting in the production of fewer viable offspring overall, and secondly that important signalling relating to maintenance of reproductive health occurs via *aakg-1, aakg-2,* and *aakg-3* in *daf-2* mutants. Contrastingly to *aakg-1; aakg-2; aakg-3* mutant fecundity in the WT background, a *daf-2; aakg-1; aakg-2; aakg-3* mutant shows persistent reductions in brood size from day 2, suggesting that AMP-sensitive AMPK regulation is required for

daf-2 mutant fecundity from two days post-development until the end of the reproductive window. This also suggests that there is an increased dependence on AMP-sensitive *aakg* isoforms in the absence of IIS, where AMPK activity might assist with management of altered metabolism in *daf-2* mutants (Halaschek-Wiener *et al.*, 2005; Depuydt *et al.*, 2014). Curiously, reductions in WT and *daf-2* total brood size, demonstrated in *aakg-4; aakg-5* and *daf-2; aakg-1; aakg-2; aakg-3* mutants respectively, both imply that important changes in reproductive signalling occur 2 days post-development in *C. elegans* (Figures 4.4B and 4.5B). The reproductive schedule of a constitutively active AAK-2 mutant also highlights 2 days post-development as an important turning point (Chapter 4.7.5).

On the other hand, a *daf-2; aakg-4; aakg-5* mutant shows increased progeny production on day 1, matches *daf-2* production on day 2, and displays reduced production for the remainder of the reproductive window (Figure 4.5B). However, total progeny production in a *daf-2; aakg-4; aakg-5* mutant does not change compared to a *daf-2* mutant (Figure 4.5A), suggesting that the role of *aakg-5* in maintaining total brood size (Chapter 4.7.5) is IIS-dependent, mirroring *aakg-5*-mediated contributions to lifespan and arsenite stress resistance. Here, a *daf-2; aakg-4; aakg-5* mutant appears to adopt an alternative strategy to the constitutively active AAK-2 strain; front-loading progeny production (Figure 4.5B), rather than recovering progeny production towards the end of reproductive window (Burkewitz *et al.*, 2015). Changes to reproductive schedule in a *daf-2; aakg-4; aakg-5* mutant also imply premature use of oocytes. This concept has been explored before, and has previously been used to suggest that reproductive signalling might coordinate reproductive timeline with ageing (Guarente and Kenyon, 2000). In this case, acceleration of germ line development might reduce the length of the reproductive window in a *daf-2; aakg-4; aakg-5* mutant. Investigations in *D. melanogaster* support this idea; selective breeding can give rise to strains which produce progeny relatively late in life, and also exhibit extended lifespan. Conversely fly strains which produce offspring earlier show shorter lifespans (Sgrò and Partridge, 1999). Consistent with this, a *daf-2; aakg-4; aakg-5* mutant shows reduced lifespan (Figures 4.1B and 4.2B). If a similar system is present in *C. elegans* biology, this could further justify the retention of *aakg-4* and *aakg-5* in several nematode species

through roles towards both lifespan extension, enhanced stress resistance, and improved reproductive health. However, there are still conflicting theories regarding the relationship between lifespan and reproductive health in *C. elegans* (Chen, Carey and Ferris, 2001; Mendenhall *et al.*, 2011; Wang *et al.*, 2014).

Interestingly, *daf-2* mutants already exhibit a different reproductive schedule to WT worms (Figures 4.4B and 4.5B)(Hughes *et al.*, 2007). The *daf-2* mutant extended reproductive window is communicated through modulation of DAF-16 activity (Figure 1.7), which alleviates age-related decline in germline and oocyte maintenance, and increases oocyte viability (Luo *et al.*, 2010; Michaelson *et al.*, 2010; López-Otín *et al.*, 2013; Qin and Hubbard, 2015). In this thesis, a *daf-2; aakg-4; aakg-5* mutant shows further disruption of reproductive schedule compared to a *daf-2* mutant (Figure 4.5B). Since DAF-16 is known to both respond to IIS and up-regulate *aakg-4* expression, together this suggests that *aakg-4* may contribute to DAF-16-mediated effects on the reproductive schedule in *daf-2* mutants (Kenyon *et al.*, 1993; Greer, Oskoui, *et al.*, 2007; Tullet *et al.*, 2014). To determine whether *aakg-4* or *aakg-5* drives these effects, this assay should be repeated using *daf-2; aakg-4* and *daf-2; aakg-5* mutants; if the reproductive schedule of *daf-2; aakg-5* mutant mirrors the *daf-2* mutant, this would confirm the aforementioned mechanism. Additionally, as mentioned in discussion of WT brood size data (Chapter 4.7.5), it may be interesting to assay the response of *daf-2; aakg-1; aakg-2; aakg-3; aakg-5* strain to confirm whether *aakg-4* or *aakg-5* drives effects on reproductive schedule here.

The data shown here does not support the disposable soma theory – none of the *aakg* mutant strains investigated here display improved reproductive health despite displaying reduced longevity (Figure 4.1). Additionally, brood sizes do not correlate with the extent of lifespan suppression. For example, mutation of *aakg-1, aakg-2,* and *aakg-3* yielded sizeable suppressions of both WT and *daf-2* lifespan (Figure 4.1), but only significantly influences fecundity in a *daf-2* background (Figure 4.5). Therefore, this data contributes to an increasingly complex picture describing the relationship

between lifespan and reproductive health in *C. elegans*, and the role of AMPK regulation in fecundity appears to reflect this complexity.

At this point, some common trends regarding the contributions of *aakg-4* and *aakg-5* to adult phenotype are already apparent. *aakg-4* demonstrates roles in *daf-2*-mediated arsenite resistance, and longevity (Figures 4.2B and 4.3B), revealing functional roles for complete AMP-insensitivity in a reduced IIS background. In a WT background, both *aakg-4* and *aakg-5* contribute to WT arsenite resistance (Figure 4.3A), revealing functional redundancy between isoforms. Partially AMP-insensitive *aakg-5* exhibits roles in lifespan, arsenite resistance, and fecundity in a WT background (Figures 4.2A, 4.3A, and 4.4). Additionally, brood size investigations imply that *aakg-4* and *aakg-5* also contribute to reproductive schedule in a *daf-2* background (Figure 4.5B). In summary, *aakg-4* and *aakg-5* hold a wide variety of roles across several physiological aspects of *C. elegans* biology, acting via IIS-dependent and IIS-independent mechanisms. These contributions provide a strong basis for the retention of these isoforms among the Chromadorea clade, and establish new links between longevity, oxidative stress response and reproductive signalling (Tullet *et al.*, 2014). Furthermore, these results demand additional investigation of *aakg-1, aakg-2,* and *aakg-3* mutants, which may reveal additional instances where AMP-sensitive regulation of AMPK overshadows contributions of *aakg-4* and *aakg-5*, as seen with lifespan.

4.7.7 Alternative models of AMPKγ regulation do not influence dauer entry or recovery in a *daf-2(m577)* background.

Previously, Apfeld *et al.* (2004) reported that *daf-2(e1368); aak-2* mutants are unable to enter dauer, while Narbonne and Roy (2009) reported that *daf-2(e1370); aak-2* dauers show reduced longevity (Apfeld *et al.*, 2004; Narbonne and Roy, 2009). No existing literature could be found describing *aakg* mutant dauer entry or recovery, justifying my investigation of *aakg* mutants here. Figure 4.6 reveals no significant differences in the ability of *daf-2, daf-2; aakg-1; aakg-2; aakg-3* and *daf-2; aakg-4; aakg-5* strains to enter or recover from dauer, suggesting that *aakg* isoforms do not

contribute dauer entry or exit. All strains were assayed simultaneously alongside each other to ensure validity. Comparison between effects in *aak-2* mutants and *aakg* mutants does generate some interesting considerations. *daf-2(e1368)* and *daf-2(m577)* are both class I *daf-2* alleles, but while *daf-2 (e1368); aak-2* mutants do not enter dauer at all*, daf-2(m577); aakg-1; aakg-2; aakg-3* and *daf-2(m577); aakg-4; aakg-5* mutants do not exhibit any changes to dauer entry or recovery (Figure 4.6)(Gems *et al.*, 1998; Apfeld *et al.*, 2004). Admittedly, literature surrounding *daf-2* mutants suggests that *daf-2(m577)* is considered to be relatively weak allele that may retain some responsiveness to insulin-like signals, which might contribute to this difference (Dillon *et al.*, 2016). However, assuming that IIS is effectively reduced in both *daf-2* mutant backgrounds, this could support a case for considering *aakg* isoforms as a more tactical choice for pharmaceutical applications. While *aak-2* holds stronger effects on dauer, including reduced longevity or skipping dauer altogether, mutation of *aakg-1-3* or *aakg-4* and *aakg-5* does not result in either of these phenotypes, suggesting that *aakg* may not impact peripheral AMPK signalling as much as *aak-2*. Consistent with this, AMPK can be activated through multiple activation pathways (Figure 1.5). Ablation of *aakg* expression might only block activation via AMP-binding, in contrast to mutation of *aak* genes which theoretically removes the catalytic functionality of AMPK. Thus, *aakg* may provide more subtle modulation of dauer metabolism.

Reflecting on the possible subtlety of *aakg* isoform contributions to AMPK function, it would be interesting to continue exploring dauer entry and recovery with a *daf-2; aakg-1; aakg-2; aakg-3; aakg-5* knockout strain to determine whether mutant relying on expression of the *aakg-4* alone (modelling complete AMP-insensitivity) would still display successfully dauer entry, or instead mimic the *daf-2(e1368); aak-2* dauer avoidance phenotype (Apfeld *et al.*, 2004). Additionally, although no significant differences are seen between strains here, this assay investigates the contribution of *aakg* isoforms in response to temperature-induced dauer entry; it is possible that other methods of dauer induction, like starvation and pheromone-induced entry, could reveal a more prominent role for *aakg* isoforms.

4.7.8 *aakg-4* and *aakg-5* do not contribute to improved SDS resistance in *daf-2(m577)* dauers.

Several groups have reported dauer-like phenotypes, some referencing altered sensitivity to SDS exposure, so it was interesting to investigate the possibility of dauer-like phenotypes associated with AMPKγ function (Albert and Riddle, 1988; Malone, Inoue and Thomas, 1996; Nika *et al.*, 2016; Flatt *et al.*, 2019). Figure 4.7 illustrates the effects of SDS on dauer survivability. Exposure to 1% SDS for 30 minutes does not cause significantly decreased survivability in *daf-2; aakg-4; aakg-5* dauers compared to *daf-2* dauers, even 24 hours after exposure. In addition, 2 hours of exposure does not exacerbate the differences in mortality between *daf-2* and *daf-2; aakg-4; aakg-5* dauers. In fact, *daf-2* and *daf-2; aakg-4; aakg-5* mutant mortality rates are more similar following 2 hours exposure to 1% SDS than under previous conditions. Therefore, further investigation may reveal that the efficacy of dauer SDS resistance is time-dependent. Future assays could explore this in two ways: following mortality for longer periods of time (>24 hours) may reveal greater difference between strains, or different exposure times may affect survival.

Notably, SDS resistance data displays significant variation between trials, and in some cases standard error of the mean is similar to percentage mortality values shown (Figure 4.7). In future, more repeats may improve the power of statistical analysis. Additionally, one limitation of this data set is that *daf-2; aakg-1; aakg-2; aakg-3* dauers are not investigated here. However, future work with the *daf-2; aakg-1; aakg-2; aakg-3* strain could reveal possible complexities in dauer SDS resistance similar to *daf-2* lifespan data and establish whether AMP-sensitive isoforms contribute to dauer SDS resistance.

4.7.9 Measurement of dauer diameter indicates that alternative models of AMPKγ regulation contribute to dauer size in a *daf-2(m577)* background.

Dauer diameter was measured across the grinder (Supplementary figure 4), a relatively constant locus of *C. elegans* anatomy, and diameter data is shown over 4 weeks (Figure 4.8). It is

important to note that weekly measurements were pooled from several trials, and biologically independent populations of dauers were used between trials. While pooling data increases the power of statistical analysis, it also means that parental variation between biologically independent worm populations could influence the data between individual trials. To minimise this effect, relatively large numbers of worms were used (See figure legend, figure 4.8). In addition, dauers were selected for imaging each week from the same population within each trial, to reduce the influence of parental variation between weekly measurements.

Differences between the *daf-2*, *daf-2; aakg-1; aakg-2; aakg-3* and *daf-2; aakg-4; aakg-5* strains are most clear at one week of dauer lifespan. Week one data shows that *daf-2* dauers already demonstrate significantly lower diameter than *daf-2; aakg-1; aakg-2; aakg-3* or *daf-2; aakg-4; aakg-5* dauers (Figure 4.8A), suggesting that both AMP-sensitive and AMP-insensitive *aakg* isoforms are required for normal *daf-2* dauer morphology a week after entry.

Curiously, *daf-2* dauers consistently show increases in mean diameter between weeks (Figure 4.8). *daf-2; aakg-1; aakg-2; aakg-3* dauers display increased mean diameter between weeks one and two, though demonstrate a smaller increase than *daf-2* dauers, and *daf-2; aakg-1; aakg-2; aakg-3* dauers also display a higher starting diameter than *daf-2* dauers one week after entry (Figures 4.8A and 4.8B). It would be interesting to explore how dauer larvae can display increased size under dauer metabolism, especially since food intake and excretion are dramatically reduced during dauer (Riddle, Swanson and Albert, 1981; Burnell *et al.*, 2005).

I could not find evidence in existing literature to explain increasing diameter during dauer in *daf-2* and *daf-2; aakg-1; aakg-2; aakg-3* dauers, outside of discussion of dauer-like phenotypes, gonad abnormalities, and induction of recovery in response to food (Albert and Riddle, 1988; Gems *et al.*, 1998; Wang and Kim, 2003; Karp, 2018). Admittedly, dauer worms were maintained on seeded plates, but all dauer populations were stored in incubators at a constant 25°C, ensuring *daf-2(m577)* background strains remained in dauer. Furthermore, dauers were assayed over several weeks, and

did not show any clear signs of recovery under a dissecting microscope, or in captured images. Gonad abnormalities have been reported in some class II *daf-2* mutants, but not with the class I *daf-2(m577)* allele (Gems *et al.*, 1998). Meanwhile, work by Flatt *et al.* (2019) reports changes in body diameter over 5.0µm resulting from mutation of *dex-1* (a putative calcium transporter), suggesting that diameter changes described here may be relatively nominal. In this project, the range in mean diameter for week one is 2.9µm, and differences between strains do not exceed this range in subsequent weeks (2.0µm for week 2, and 0.7µm for week 4). I would hypothesise that acute metabolic differences account for the modest increases in diameter observed between weeks in *daf-2* and *daf-2; aakg-1; aakg-2; aakg-3* dauers. Firstly, the importance of fat metabolism in mediating dauer survival is clear, and perhaps *daf-2* and *daf-2; aakg-1; aakg-2; aakg-3* dauers make better use of fat stores during dauer, or continue to exhibit a residual stockpiling response during the first month of dauer (Wadsworth and Riddle, 1989; Wang and Kim, 2003; Burnell *et al.*, 2005; Fielenbach and Antebi, 2008). Alternatively, variation in the composition of the dauer cuticle could account for observed increases, since the cuticle composition changes upon entry into dauer, and the cuticle surrounding the body is understood to be more flexible than other areas of the worm like the buccal cavity (Wolkow and Hall, 2011). In future, I would exclude the cuticle region while recording measurements and investigate whether this can explain the observed differences in diameter.

Conversely, reduction of *daf-2; aakg-4; aakg-5* dauer size between weeks one and four (Figures 4.8A and 4.8C) implies that *aakg-4* and *aakg-5* may contribute maintenance of body mass during dauer, possibly preventing atrophy during dauer by combatting the effects caused by long-term reduced nutrient intake. Paradoxically, *daf-2; aakg-4; aakg-5* dauers initially show the highest mean diameter in week 1 (Figure 4.8A), perhaps the result of excessive production of energy stores pre-dauer, but then seems to use energy stores more quickly, which would explain why diameter consistently decreases over four weeks. Additionally, *daf-2; aakg-1; aakg-2; aakg-3* dauers display reduced diameter between weeks two and four (Figures 4.8B and 4.8C) suggesting that *aakg-1, aakg-2,* and *aakg-3* may adopt a similar role two weeks after entry.

The possible role of *aakg* isoforms in maintaining dauer size leads me to suggest that AMPK activity might become more relevant during dauer, potentially due to its effects on autophagy. Consistent with this, autophagy is reported to be involved in the remodelling of tissues that occurs during dauer entry (Meléndez *et al.*, 2003). Additionally, while AMPK function contributes to improved oxidative metabolism, it is important to remember that dauer entry induces a shift away from use of carbohydrate energy stores, instead focusing on lipid metabolism (Burnell *et al.*, 2005). Therefore, the changes in the diameter of *daf-2; aakg-1; aakg-2; aakg-3* and *daf-2; aakg-4; aakg-5* dauers could be mediated through the effects of AMPK on lipid metabolism. These effects include promotion of lipolysis and fatty acid oxidation, as well as inhibition of lipogenesis (Chapter 1.4.4, figure 1.6)(Sim and Hardie, 1988; Burnell *et al.*, 2005; Lee *et al.*, 2008). Moreover, AMPK-mediated effects on glucose metabolism (including activation of glycolysis and inhibition of glycogen synthesis) may peripherally support an anaerobic shift in metabolism during dauer (Holt and Riddle, 2003; Mádi *et al.*, 2008)).

In summary, *daf-2* dauers appear to ration energy stores more efficiently, whereas *daf-2; aakg-4; aakg-5* dauers might use energy stores prematurely. *daf-2; aakg-1; aakg-2; aakg-3* dauers do not follow either trend exhibited by a *daf-2* or *daf-2; aakg-4; aakg-5* dauers, suggesting that *daf-2; aakg-1; aakg-2; aakg-3* mutants adopt a different metabolic strategy during dauer. Taken together, analysis of dauer diameter suggests that both families of *aakg* isoforms, AMP-sensitive and AMP-insensitive, contribute significantly to dauer size.

Notably, all *daf-2* background dauer strains report similar diameter four weeks after entry. It would be interesting to follow the above-mentioned trends further in future investigations, to discover whether *daf-2; aakg-1; aakg-2; aakg-3* and *daf-2; aakg-4; aakg-5* dauers continue to show reduced diameter over longer periods of time. If *daf-2; aakg-4; aakg-5* mutant dauers die prematurely (compared to *daf-2* dauers), this might indicate irregularities in dauer metabolism similar to those described in *daf-2; aak-2* dauers by Narbonne and Roy (2009). I attempted to quantify dauer lifespan during this project, but this proved difficult to monitor effectively through daily observation (data not

shown). Worm-tracking software or time-lapse analysis could be utilised to investigate this more effectively in future studies.

In this chapter, investigations in adult worms reveal that *aakg-1, aakg-2,* and *aakg-3* isoforms contribute cooperatively to several physiological roles in WT and *daf-2* backgrounds, implying a role for AMP-sensitive AMPK regulation in both normal and *daf-2* longevity (Figure 4.1), as well as *daf-2* fecundity (Figure 4.5). Lifespan, stress, and brood size assays highlight context-dependent roles for *aakg-4* and *aakg-5* as well, additionally demonstrating the relevance of IIS to AMP-insensitive activation of AMPK. Importantly, functional redundancy exists between *aakg-4* and *aakg-5* in contributions to WT arsenite resistance, but not towards longevity or *daf-2* arsenite resistance. In dauer investigations, *aakg* mutation does not significantly influence dauer entry and recovery, and *aakg-4* and *aakg-5* do not contribute to dauer SDS resistance. However, both *daf-2; aakg-1; aakg-2; aakg-3* and *daf-2; aakg-4; aakg-5* mutants show different diameters compared to *daf-2* mutants during the first two weeks of dauer, revealing roles for both AMP-sensitive and AMP-insensitive models of AMPK regulation in *C. elegans* dauer metabolism.

Chapter 5 – Conclusions.

5.1 Conclusions.

Life expectancy increased dramatically during the 20th century and gave rise to a variety of age-related diseases which affect modern society. Recent studies investigating the relationship between energy homeostasis and lifespan imply that nutrient-sensing pathways are important for determining lifespan. AMPK is a key metabolic regulator which responds to changes in the AMP:ATP ratio within cells, promoting a metabolic shift towards increased catabolism and autophagy during a low-energy state to promote restoration of cellular energy supply. Mammalian studies have shown that AMP binds to specific, evolutionary conserved residues of the γ subunit, initiating a conformational change across the kinase (Chapter 1.4.2). While investigated relatively extensively in mammalian models, the role of AMPKγ isoforms in mediating AMPK activity and function has not been widely explored in *C. elegans* prior to this study. Here, I use *C. elegans* as a genetic model to explore the functional roles of AMPKγ and investigate the relationship between AMP-sensitivity, physiology, and lifespan more closely.

The data presented in this thesis agrees with existing literature which hypothesised that *aakg-4* and *aakg-5* isoforms respond differently to AMP, thereby supporting the idea that alternative mechanisms of AMPK regulation exist in *C. elegans* (Tullet *et al.*, 2014). In chapter three, all five AAKG isoforms have been modelled *in silico*, illustrating a mechanism for potential AMP-insensitivity in AAKG-4 and AAKG-5 (Figure 3.1). Crucially, loss of arginine and histidine residues (Table 3.1) provides the basis for reduced interaction of AAKG-4 and AAKG-5 isoforms with AMP, as previously hypothesised. This is inhibits AMPK activation in a similar manner to point mutations of equivalent residues in mammalian AMPKγ isoforms, which have been shown to result in aberrant physiological function (Daniel and Carling, 2002; Adams *et al.*, 2004; Davies *et al.*, 2006; Day *et al.*, 2007).

This provided a strong enough argument to pursue the generation of a comprehensive network of *aakg* mutants. In order to effectively model alternative systems of AMPK regulation in *C. elegans*, two combination knockout strains were produced: an *aakg-1; aakg-2; aakg-3* mutant and an *aakg-4; aakg-5* mutant, modelling AMP-insensitive and AMP-sensitive systems of regulation, respectively. Mutants were generated in WT (Figure 3.3) and *daf-2(m577)* (Figure 3.4) backgrounds, to explore the influence of IIS. None of the *aakg* knockout strains displayed any obvious deficits in viability, and temperature-sensitive induction of dauer entry at 25°C was maintained in *daf-2(m577)* background strains.

The genotype of each *aakg* mutant was confirmed using PCR genotyping, and later deletion of specifically targeted regions (Figure 3.2) was additionally confirmed through qRT-PCR. qRT-PCR analysis also facilitated the generation of expression profiles for each of the five *aakg* isoforms, this was achieved using combination mutant strains to enable effective comparison of *aakg* isoform expression between AMP-sensitive and AMP-insensitive models of AMPK regulation. Comparison of *aakg-1; aakg-2; aakg-3* and *daf-2; aakg-1; aakg-2; aakg-3* mutants revealed that *aakg-4* and *aakg-5* expression remains largely unaffected by the removal of *aakg-1, aakg-2,* and *aakg-3*, in both WT (Figures 3.5D and 3.5E) and reduced IIS (Figures 3.6D and 3.6E) backgrounds, suggesting that *aakg-4* and *aakg-5* might maintain their own expression. Additionally, an *aakg-4*; *aakg-5* mutant displayed reduced expression of *aakg-1, aakg-2,* and *aakg-3* (Figures 3.5A, 3.5B, and 3.5C), suggesting that *aakg-4* and *aakg-5* regulate expression of AMP-sensitive *aakg* isoforms in a WT background. In a *daf-2* mutant, reduced IIS resulted in up-regulation of *aakg-1* and *aakg-4* isoforms, and down-regulation of *aakg-2* expression (Table 3.3). A *daf-2; aakg-4; aakg-5* mutant demonstrates opposite effects on *aakg-1* and *aakg-2* expression compared to reduced IIS (Figures 3.6A and 3.6B), suggesting that *aakg-4* and *aakg-5* may influence control of *aakg-1* and *aakg-2* expression differently in a reduced IIS background. Consistent with this, *daf-2; aakg-4; aakg-5* mutant expression of *aakg-1* and *aakg-2* is distinct from both WT and *daf-2* levels. Taken together, qRT-PCR data suggests that *aakg* isoform expression is

transcriptionally regulated by IIS-dependent and IIS-independent mechanisms. Notably, some of these transcriptional changes may contribute to phenotype (Chapter 4.7.2).

Following confirmation of *aakg* mutant genotype, I attempted to establish that *aakg-4* and *aakg-5* did not respond effectively to AMP, as modelling had indicated earlier (Figure 3.1). This was achieved by monitoring phosphorylation of the Thr172 residue on AMPKα, which is exposed in response to conformational change initiated by binding of AMP to AMPKγ. An *aakg-1; aakg-2; aakg-3* mutant did not display effective phosphorylation of Thr172, while an *aakg-4; aakg-5* mutant displayed similar levels of phosphorylation to WT worms (Figure 3.7), indicating that AMP-sensitive isoforms (*aakg-1, aakg-2,* and *aakg-3*) are required for Thr172 phosphorylation. While data gathered in the *daf-2(m577)* background mutants showed extensive variation, the WT trend appeared to be maintained in *daf-2* background mutants (Figure 3.8), suggesting that the role of *aakg-1, aakg-2,* and *aakg-3* in AMPK activation is IIS-independent.

Previous work in *C. elegans* demonstrated that AMP-sensitivity is important for AMPK-mediated contributions to longevity (Tullet *et al.*, 2014). In chapter four, I describe further investigations into the roles of AMPK regulation through use of assays which focus on several physiological aspects on *C. elegans* biology (longevity, stress resistance, fertility and dauer). This data complements existing literature which describes a requirement for *aak-2* in WT and *daf-2* lifespan, as well as contributions of *aakg-4* to *daf-2*-mediated lifespan (Apfeld *et al.*, 2004; Tullet *et al.*, 2014). My data contributes several useful conclusions regarding the influence of AMP-sensitivity on AMPKγ function in *C. elegans*, which may also be relevant when investigating human AMPKγ isoforms, since predicted key binding residues which appear to have been evolutionarily conserved are less well conserved in AAKG-4 and AAKG-5 (Table 3.1)(Tullet *et al.*, 2014).

Lifespan studies in *C. elegans* reveal that AMP-sensitive isoforms *aakg-1, aakg-2,* and *aakg-3* demonstrate greater contribution to WT and *daf-2* mutant lifespan than *aakg-4* and *aakg-5* (Figure 4.1). The role of *aakg-1, aakg-2,* and *aakg-3* in lifespan had not been investigated using genetic

knockouts before this project. Figure 4.1A shows that *aakg-1; aakg-2; aakg-3* mutant lifespan is shortened to a similar extent as *aak-2* mutant lifespan, indicating that AMP-sensitive AMPK regulation effectively mimics the contribution of *aak-2* to WT lifespan (Apfeld *et al.*, 2004; McQuary *et al.*, 2016). Conservation of predicted AMP-binding residues in mammalian homologues of *aakg-1, aakg-2,* and *aakg-3* (Table 3.1), in combination with the role of AMP-sensitive isoforms in AMPK activation (Figure 3.7), implies that these residues are important for an evolutionarily conserved mechanism of AMPK activation. Additionally, *aakg-1; aakg-2; aakg-3* mutants demonstrated similar shortening of lifespan between WT and *daf-2* backgrounds (Figure 4.1, table 4.1), implying that AMP-sensitive AMPK regulation contributes to longevity independently of IIS.

Though *aakg-1; aakg-2; aakg-3* and *daf-2; aakg-1; aakg-2; aakg-3* mutants demonstrate more severe suppression of WT and *daf-2* mutant lifespan, *aakg-4* and *aakg-5* still contribute significantly to lifespan (Figure 4.2, table 4.1). Furthermore, I have shown that mutation of both *aakg-4* and *aakg-5* does not result in additive suppression of WT or *daf-2* lifespan (Figure 4.1). The role of *aakg-4* in *daf-2*-mediated longevity is confirmed using an *daf-2; aakg-4* mutant (Figure 4.2B), and lifespan assay analysis also reveals that *aakg-4* drives suppression of *daf-2* longevity in a *daf-2; aakg-4; aakg-5* mutant (Tullet *et al.*, 2014). Meanwhile, *aakg-5* contributes to WT lifespan, and drives shortened lifespan displayed by an *aakg-4; aakg-5* mutant (Figure 4.2A). However, *aakg-5* does not contribute to *daf-2* mutant lifespan (Figure 4.2B), suggesting the role of *aakg-5* in longevity is IIS-dependent. Overall, the role of *aakg-4* and *aakg-5* in longevity appears to be dependent on metabolic context (effectual or reduced IIS), which may explain why both *aakg-4* and *aakg-5* orthologues exist in several nematode species (Tullet *et al.*, 2014).

Both *aakg-4* and *aakg-5* mutants show decreased survival under arsenite exposure compared to WT worms, implying that AMP-insensitive AMPK complexes contribute to the oxidative stress response in *C. elegans* (Figure 4.3A, table 4.2). In addition, *aakg-4; aakg-5* mutant survival was not further reduced compared to either single mutant, suggesting that *aakg-4* and *aakg-5* demonstrate

functionally redundant contributions to WT oxidative stress resistance. Investigations in a *daf-2(m577)* background revealed that *aakg-4* drives arsenite resistance in a *daf-2; aakg-4; aakg-5* mutant (Figure 4.3B, table 4.2), and demonstrate that the contribution of *aakg-5* to the WT oxidative stress response is IIS-dependent, mirroring the role of *aakg-5* in WT longevity. Overall, roles for *aakg-4* and *aakg-5* in the arsenite stress response provide further justification for presence of *aakg-4* and *aakg-5* orthologues in *C. elegans* and related nematodes in the Chromadorea clade (Tullet *et al.*, 2014).

Brood size investigations revealed that *aakg-4* and *aakg-5* contribute significantly to WT fecundity. Analysis of daily brood data revealed that the only significant reduction in progeny throughout the four-day reproductive window occurred two days post-development (Figure 4.4B), implying that the influence of *aakg-4* and *aakg-5* is transient, and that two days post-development may be an important turning point in the *C. elegans* reproductive schedule. Interestingly, *aakg-1, aakg-2,* and *aakg-3* become appear more relevant to maintenance of brood size in a *daf-2(m577)* background, since a *daf-2; aakg-1; aakg-2; aakg-3* mutant consistently showed reduced progeny production from two days post-development (Figure 4.5B), which ultimately reduced total brood size in this strain (Figure 4.5A). Consistent reductions in daily progeny production suggest that AMP-sensitive AMPK regulation is required for maintenance of *daf-2* brood size from two days post-development until the end of the reproductive window. Interestingly, a *daf-2; aakg-4; aakg-5* mutant did not show reduced total brood size compared to a *daf-2* mutant (Figure 4.5A), but did result in apparent front-loading of progeny production (Figure 4.5B), indicating that *daf-2* mutant reproductive signalling may be affected by loss of *aakg-4* and *aakg-5*. Together with WT data (Figure 4.4), this suggests that AMPK regulation and IIS are intricately linked in relation to their effects on reproductive health.

During my investigations into *aakg* mutant phenotypes in adult worms, I decided to additionally investigate dauer, to explore the functional roles of AMPKγ during a prolonged period of alternative metabolism (Burnell *et al.*, 2005). No significant changes to dauer entry or recovery were

observed in *daf-2; aakg-1; aakg-2; aakg-3* or *daf-2; aakg-4; aakg-5* mutants compared to a *daf-2* control strain (Figure 4.6), indicating that AMP-sensitive or AMP-insensitive models of AMPK regulation do not influence dauer entry/exit signalling. Furthermore, when investigating dauer SDS resistance, *daf-2* and *daf-2; aakg-4; aakg-5* mutants did not show significantly different survival following exposure to 1% SDS (Figure 4.7), suggesting that *aakg-4* and *aakg-5* do not contribute to dauer SDS resistance.

Disruption of *aakg* isoforms in *daf-2; aakg-1; aakg-2; aakg-3* and *daf-2; aakg-4; aakg-5* mutants causes increased diameter compared to *daf-2* mutants one week after dauer entry (Figure 4.8A), implying that both systems of AMPK regulation contribute to dauer size. Over four weeks, *daf-2* dauers reported increased diameter at all three weekly intervals (Figure 4.8). In contrast, *daf-2; aakg-1; aakg-2; aakg-3* dauers showed increased diameter between weeks 1 and 2 (Figures 4.8A and 4.8B), then displayed reduced diameter between weeks 2 and 4 (Figures 4.8B and 4.8C). *daf-2; aakg-4; aakg-5* dauers showed reduced diameter between weeks 1 and 4 only (Figures 4.8A and 4.8C). Interestingly, all *daf-2* mutant background strains reported similar diameter after four weeks in dauer (Figure 4.8C). These differences imply that both *daf-2; aakg-1; aakg-2; aakg-3* and *daf-2; aakg-4; aakg-5* dauers use different metabolic strategies to *daf-2* dauers, modestly affecting body size during dauer.

5.2 Use of *C. elegans* to study the genetics of energy metabolism.

C. elegans was particularly appropriate for this study because this nematode species possesses five different AMPKγ isoforms. Of these, *aakg-4* and *aakg-5* are predicted to be less able to bind AMP. *C. elegans* also carries three orthologs of mammalian AMPKγ isoforms, setting it up as a relevant model system to study the contributions of AMPK to energy metabolism. In combination with the ease of generating new *C. elegans* mutants via outcrossing, this allowed for production of a range of genetic knockouts (Figures 3.3 and 3.4). The generation of *aakg-1; aakg-2; aakg-3* triple and *aakg-4; aakg-5* double mutants during this project effectively modelled AMP-sensitive and AMP-insensitive

systems of AMPK regulation in *C. elegans*, and clarifies the importance of AMP-sensitivity to AMPK function. The relatively short lifespan of *C. elegans* provided further advantage, since I was able to assay the influence of *aakg* isoform mutations over periods of weeks or months, as opposed to longer lengths of time required to investigate the same phenomena in mammalian models. Additionally, the substantial conservation of IIS in *C. elegans* has allowed me to speculate with reasonable confidence on the influences of IIS to observed phenotypes, which may be conserved to some extent in mammalian metabolism (Wolkow *et al.*, 2002; Kenyon, 2005). Admittedly, IIS has evolved a significant level of additional complexity in mammals, with multiple receptor tyrosine kinases responding to different ligands (Chapter 1.3.1). The relative simplicity of IIS in *C. elegans* can be described as advantageous during this project because it allowed me to assay for the effects of reduced IIS on mutant phenotype easily, through additional mutation of just one gene, *daf-2*. However, it will be necessary to validate results which refer to IIS in mammalian models.

Another key consideration regarding the implications of AMPK signalling discussed in this thesis is that the activity of mammalian AMPK has been shown to vary between tissues as a result of tissue-specific variation in AMPK subunit expression (Thornton, Snowden and Carling, 1998; Cheung *et al.*, 2000). Though AMPK generally acts to promote catabolism, it is possible that *C. elegans* AMPK can also demonstrate tissue-specific functions or may rely on the expression of particular AMPK subunits over others in some cases. Although tissue-specific expression was not investigated here, this is definitely an interesting avenue of research to pursue in the future and could reveal additional levels of regulation at the transcriptional level. It would also be worthwhile to characterise the response of all single *aakg* knockout strains in each of the assays discussed, to determine the individual contributions of *aakg* isoforms in each case (lifespan, stress resistance, fecundity, and dauer).

5.3 AMPK and IIS in *C. elegans*.

As a key mediator of energy homeostasis, and the driver of a metabolic shift towards catabolism, it is unsurprising that AMPK activity is linked to IIS. Existing literature has previously

explored how IIS is linked to the roles of *aak-2*, *aakg-2,* and *aakg-4* subunits in longevity and dauer entry (Apfeld *et al.*, 2004; Greer, Dowlatshahi, *et al.*, 2007; Tullet *et al.*, 2014). Investigations described throughout this thesis increase understanding of this relationship by characterising the response of AMPKγ subunit mutants to reduced IIS, and demonstrate the influence of IIS on transcriptional regulation of *aakg* isoform expression (Figure 3.6, table 3.3) as well as several aspects *C. elegans* physiology (Chapter 4). While lifespans assays revealed that the contribution of *aakg-1, aakg-2,* and *aakg-3* to longevity appears to be maintained under reduced IIS (Figure 4.1), brood size assays reveal that *aakg-1, aakg-2,* and *aakg-3* contribute to *daf-2* fecundity (Figure 4.5). The role of *aakg-4* in *daf-2*-mediated longevity is confirmed using an *daf-2; aakg-4* mutant (Figure 4.2B), and an *aakg-5* mutant displays IIS-dependent contributions to longevity and arsenite resistance (Figures 4.2 and 4.3)(Tullet *et al.*, 2014). Overall, analysis of adult worm physiology indicates that the contributions of *aakg-4* and *aakg-5* are vary between WT and *daf-2(m577)* backgrounds, appearing to be intricately involved with IIS. Moreover, in the dauer state, where metabolism is dramatically altered, *daf-2; aakg-1; aakg-2; aakg-3* and *daf-2; aakg-4; aakg-5* dauers reveal roles for both AMP-sensitive and AMP-insensitive models of AMPK regulation in maintenance of body size during dauer (Figure 4.8)(Burnell *et al.*, 2005). In future, investigating phosphorylation rates of AMPK target proteins in each metabolic circumstance (i.e. intact IIS and reduced IIS) may clarify the mechanisms by which IIS influences *aakg*-mediated control of catalytic AMPK activity.

5.4 Future avenues for AMPK activators/pharmacological relevance.

Overall, allosteric activation of AMPK appears to be reliant on AMP-sensitive isoforms (*aakg-1, aakg-2,* and *aakg-3*) in *C. elegans* (Figure 3.7). Consistent with this, contributions of *aakg* isoforms to lifespan scale well with effects on AMPK activation: mutation of *aakg-1, aakg-2,* and *aakg-3* generates more severe suppression of WT and *daf-2* lifespans than mutation of *aakg-4* and *aakg-5* (Figure 4.1). Therefore, I suggest that future investigations into longevity in *C. elegans* focus on AMP-sensitive isoforms.

However, as one of the master regulators of metabolism, AMPK has a vast range of effects, and environmental challenges faced by *C. elegans* and related nematodes might justify preservation of AMP-insensitive isoform homologues in several species of the Chromadorea clade (Tullet *et al.*, 2014). Although AMP-sensitive *aakg* isoforms do appear to contribute more significantly to lifespan than *aakg-4* and *aakg-5* (Figure 4.1), the roles of *aakg-4* and *aakg-5* on arsenite (oxidative) resistance and brood size (Figures 4.3, 4.4, and 4.5) may still be interesting to consider when designing drugs to target parasitic nematode species like *B. malayi*, and *L. loa*. Disrupting the contributions of AMPKγ isoforms in these nematode species could provide a potential mechanism to reduce environmental stress resistances and progeny production, and assist in the eradication of infectious diseases like lymphatic filariasis (Pfarr *et al.*, 2009; Desjardins *et al.*, 2013). Furthermore, the potential roles of *aakg* isoform families in regulating dauer body size (Figure 4.8) imply dysregulation of metabolism during diapause. For this reason, investigation of all *aakg* isoforms may still be useful when exploring mechanisms to target parasitic nematode species, especially those with infective stages similar to dauer (Crook, 2014; Rollinson and Stothard, 2020).

Appendix.

Supplementary figure 1| Sequence alignments of *C. elegans* AAKG isoforms compared to human PRKAG1. AMPKγ protein sequences were aligned using the NCBI tool Blastp (https://blast.ncbi.nlm.nih.gov). Respective AAKG sequences are subject sequences in each alignment, while PRKAG1 provides the query sequence in all alignments shown. The PRKAG1 sequence was obtained from the 'PRKAG1 Isoform 1' FASTA sequence file on Uniprot.org (Uniprot ID: **P54619-1**). In cases where multiple AAKG isoform sequences existed, the longest protein sequence was selected for alignment. The highest scoring alignment result is shown in each case. Alignments were scored using default algorithm parameters, including alignment scoring using the BLOSUM62 matrix and conditional compositional matrix adjustment. Identities are residues conserved between protein sequences. Positives represent substitutions which are expected to maintain function or are often observed in structurally similar proteins, and also includes identities. The e-value score indicates confidence in the alignment result.

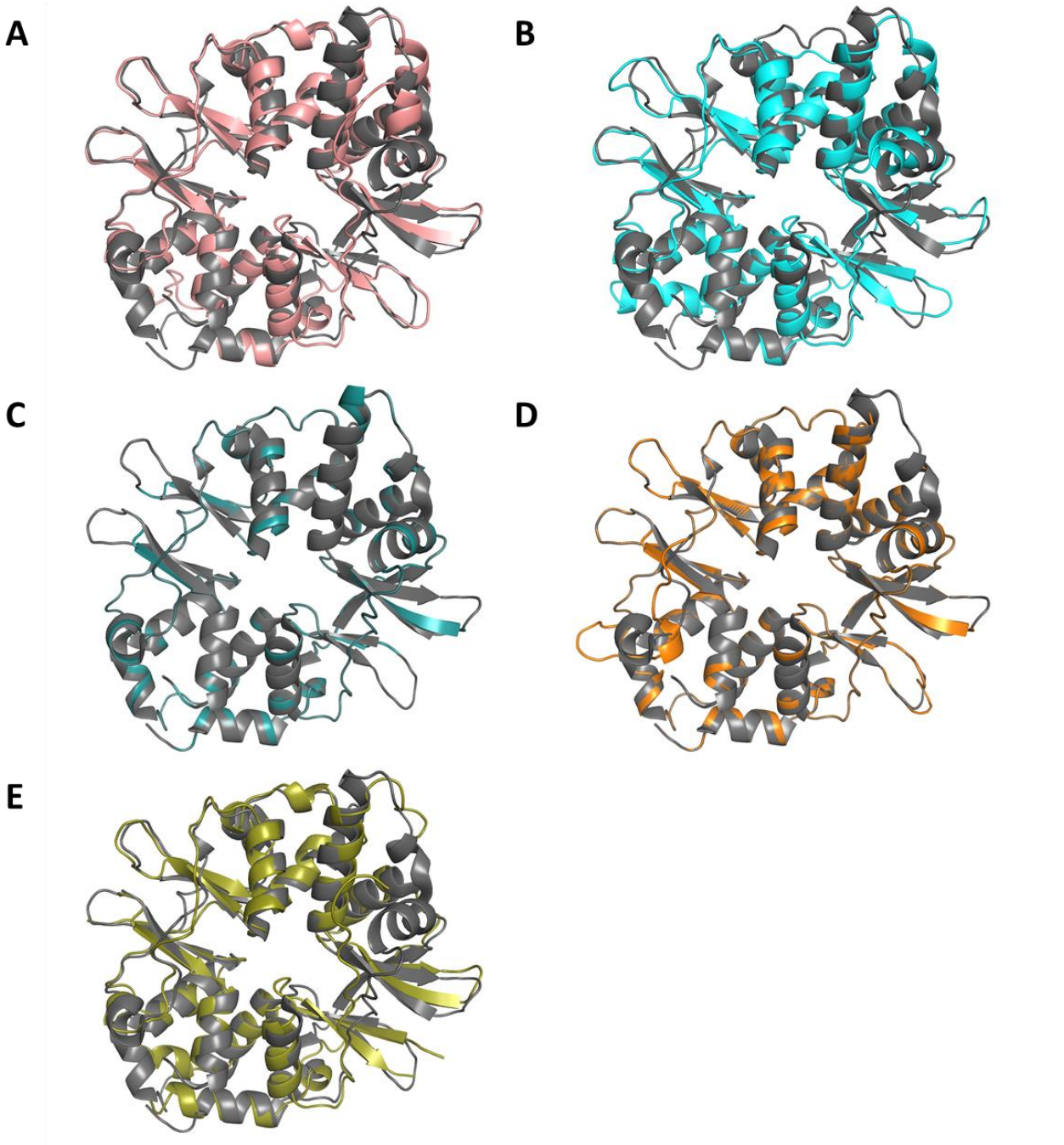

Supplementary figure 2| Secondary structure of AMPKγ is well-conserved between *C. elegans* and mammals. Mammalian AMPKγ (PDB ID: **2V8Q**) was aligned with *C. elegans* AAKG isoforms **(A)** AAKG-1, **(B)** AAKG-2, **(C)** AAKG-3, **(D)** AAKG-4 and **(E)** AAKG-5. 2V8Q also contains some additional residues from AMPKα and AMPKβ, but these were removed in the images shown above for clarity. AAKG isoform sequences were obtained from respective Wormbase entries for each isoform. In cases where more than one AAKG sequence exists, the longest sequence was modelled.

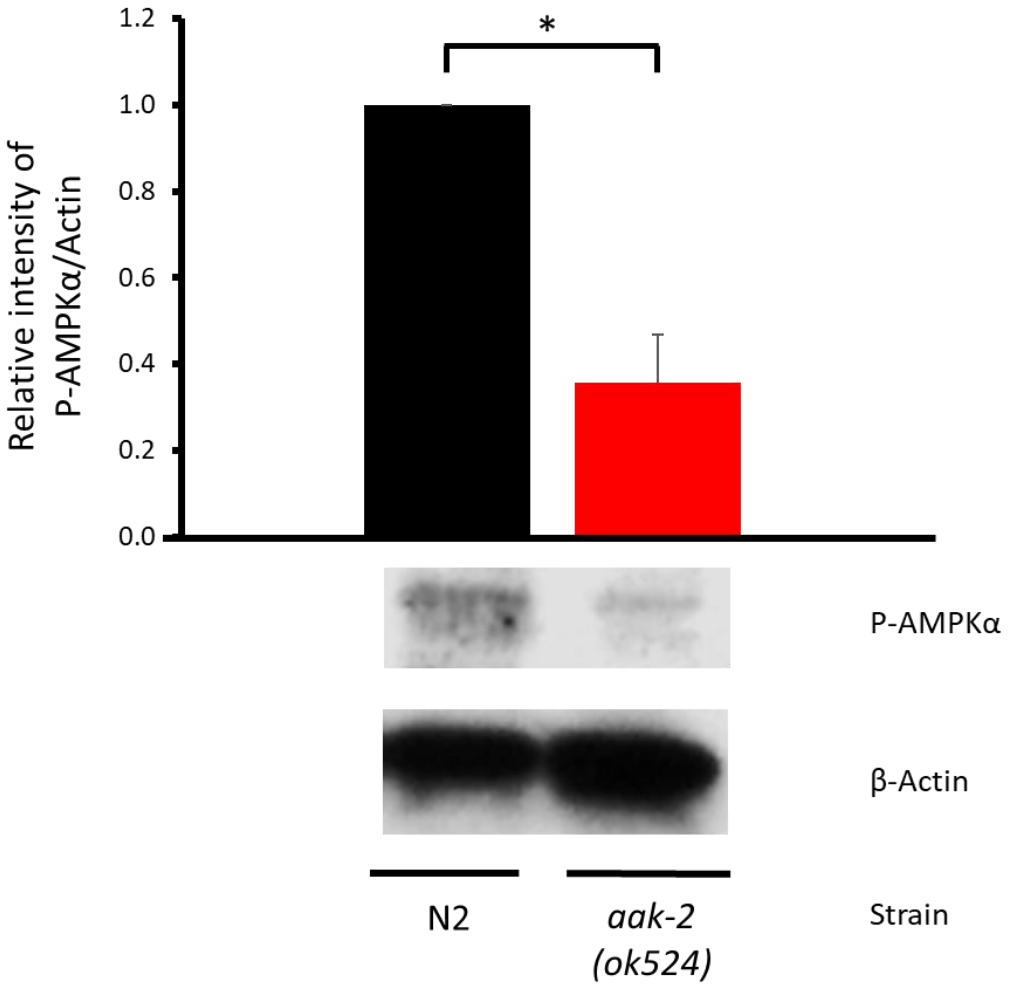

Supplementary figure 3| AMPKα in *aak-2(ok524)* mutants shows reduced Thr172 phosphorylation. An *aak-2* mutant exhibits lower mean relative band intensity compared to N2(WT) (p<0.05, Student's t-test). Relative intensity of P-AMPKα to β-actin is shown, normalised to N2. Data shows mean values from three technical repeats. One representative western blot is displayed below the graph. Error bars indicate SEM.

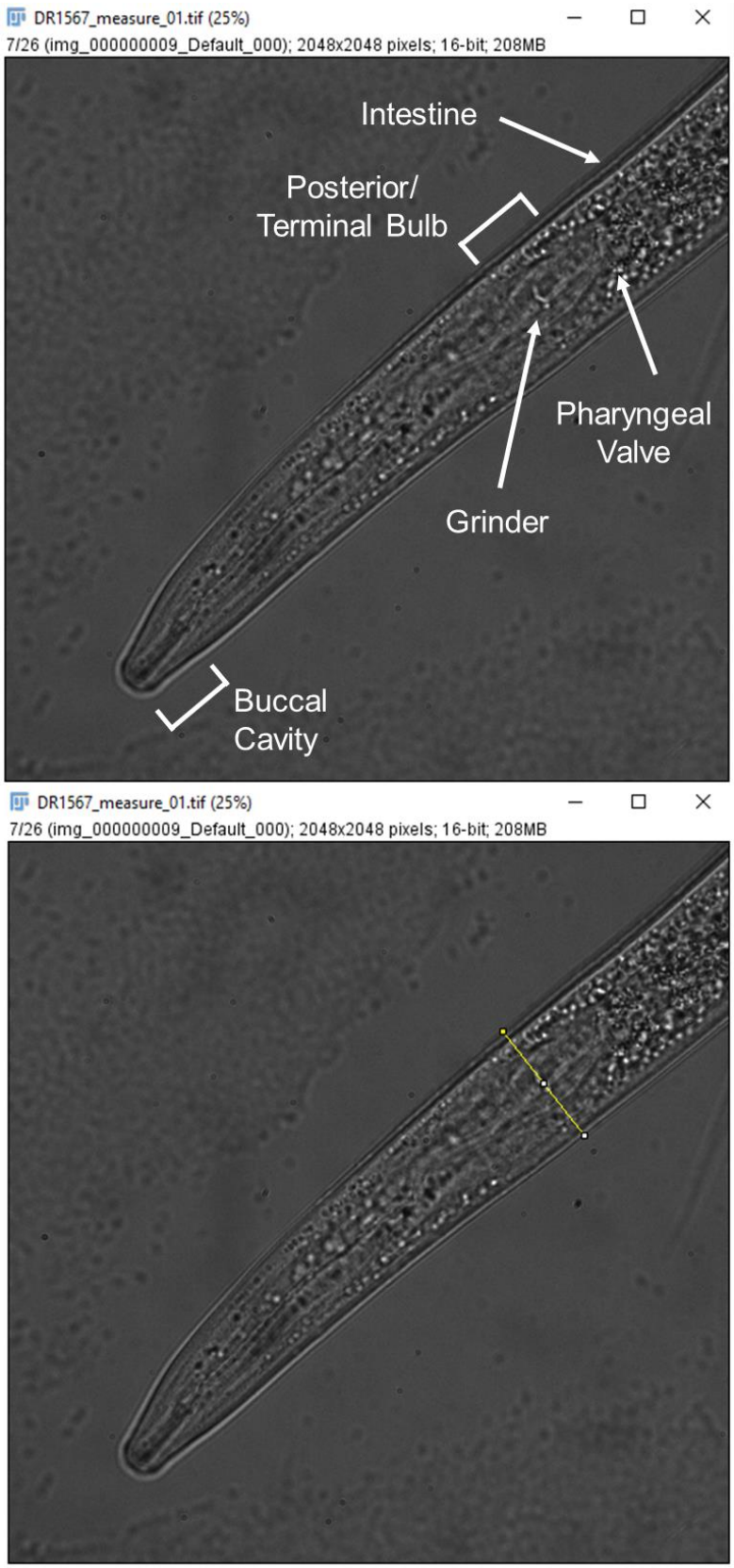

Supplementary figure 4| The dauer head region. Several key anatomical structures have been highlighted on the upper image of a *daf-2* dauer shown above. In the lower image, an example measurement of dauer diameter across the grinder is shown. TIF files were processed using ImageJ, as described in chapter 2.4.3. Dauers were observed using bright-field microscopy, through a x100 objective lens.

References.

Adams, J. *et al.* (2004) 'Intrasteric control of AMPK via the gamma1 subunit AMP allosteric regulatory site.', *Protein Science*, 13(1), pp. 155–65. doi: 10.1110/ps.03340004.

Ahmadi, M. and Roy, R. (2016) '5'-AMP-Activated Protein Kinase Signaling in Caenorhabditis elegans', in Cordero, M. D. and Viollet, B. (eds) *AMP-activated Protein Kinase*. 107th edn. Springer International Publishing, pp. 375–388. doi: https://doi.org/10.1007/978-3-319-43589-3_15.

Ailion, M. and Thomas, J. H. (2003) 'Isolation and Characterization of High-Temperature-Induced Dauer Formation Mutants in Caenorhabditis elegans', *Genetics*, 165(1), pp. 127 LP – 144.

Albert, P. S. and Riddle, D. L. (1988) 'Mutants of Caenorhabditis elegans that form dauer-like larvae', *Developmental Biology*, 126(2), pp. 270–293. doi: 10.1016/0012-1606(88)90138-8.

Amrit, F. R. G. *et al.* (2016) 'DAF-16 and TCER-1 Facilitate Adaptation to Germline Loss by Restoring Lipid Homeostasis and Repressing Reproductive Physiology in C. elegans', *PLOS Genetics*. Edited by K. Ashrafi, 12(2), p. e1005788. doi: 10.1371/journal.pgen.1005788.

Andersson, U. *et al.* (2004) 'AMP-activated Protein Kinase Plays a Role in the Control of Food Intake', *Journal of Biological Chemistry*, 279(13), pp. 12005–12008. doi: 10.1074/jbc.C300557200.

Anisimov, V. N. *et al.* (2008) 'Metformin slows down aging and extends life span of female SHR mice', *Cell Cycle*, 7(17), pp. 2769–2773. doi: 10.4161/cc.7.17.6625.

Apfeld, J. *et al.* (2004) 'The AMP-activated protein kinase AAK-2 links energy levels and insulin-like signals to lifespan in C. elegans', *Genes & Development*, 19(3), p. 411. doi: 10.1101/gad.1255404.3004.

Arantes-Oliveira, N. *et al.* (2002) 'Regulation of life-span by germ-line stem cells in Caenorhabditis elegans.', *Science*, 295(5554), pp. 502–5. doi: 10.1126/science.1065768.

Ayyadevara, S. *et al.* (2009) 'Caenorhabditis elegans PI3K mutants reveal novel genes underlying exceptional stress resistance and lifespan', *Aging Cell*, 8(6), pp. 706–725. doi: 10.1111/j.1474-9726.2009.00524.x.

Barnes, K. *et al.* (2002) 'Activation of GLUT1 by metabolic and osmotic stress: potential involvement of AMP-activated protein kinase (AMPK).', *Journal of Cell Science*, 115(Pt 11), pp. 2433–42.

Barnett, K. *et al.* (2012) 'Epidemiology of multimorbidity and implications for health care, research, and medical education: a cross-sectional study', *The Lancet*. Elsevier Ltd, 380(9836), pp. 37–43. doi:

10.1016/S0140-6736(12)60240-2.

Bateman, A. (1997) 'The structure of a domain common to archaebacteria and the homocystinuria disease protein', *Trends in Biochemical Sciences*, 22(1), pp. 12–13. doi: 10.1016/S0968-0004(96)30046-7.

Baur, J. A. *et al.* (2006) 'Resveratrol improves health and survival of mice on a high-calorie diet', *Nature*, 444(7117), pp. 337–342. doi: 10.1038/nature05354.

Behrends, C. *et al.* (2010) 'Network organization of the human autophagy system', *Nature*. Nature Publishing Group, 466(7302), pp. 68–76. doi: 10.1038/nature09204.

Berman, J. R. and Kenyon, C. (2006) 'Germ-Cell Loss Extends C. elegans Life Span through Regulation of DAF-16 by kri-1 and Lipophilic-Hormone Signaling', *Cell*, 124(5), pp. 1055–1068. doi: 10.1016/j.cell.2006.01.039.

Boehm, A.-M. *et al.* (2012) 'FoxO is a critical regulator of stem cell maintenance in immortal Hydra', *Proceedings of the National Academy of Sciences*, 109(48), pp. 19697–19702. doi: 10.1073/pnas.1209714109.

Bonafè, M. *et al.* (2003) 'Polymorphic Variants of Insulin-Like Growth Factor I (IGF-I) Receptor and Phosphoinositide 3-Kinase Genes Affect IGF-I Plasma Levels and Human Longevity: Cues for an Evolutionarily Conserved Mechanism of Life Span Control', *The Journal of Clinical Endocrinology & Metabolism*, 88(7), pp. 3299–3304. doi: 10.1210/jc.2002-021810.

Bongaarts, J. (2009) 'Human population growth and the demographic transition', *Philosophical Transactions of the Royal Society B: Biological Sciences*, 364(1532), pp. 2985–2990. doi: 10.1098/rstb.2009.0137.

Boucher, J., Tseng, Y.-H. and Kahn, C. R. (2010) 'Insulin and Insulin-like Growth Factor-1 Receptors Act as Ligand-specific Amplitude Modulators of a Common Pathway Regulating Gene Transcription', *Journal of Biological Chemistry*, 285(22), pp. 17235–17245. doi: 10.1074/jbc.M110.118620.

Brunet, A. *et al.* (1999) 'Akt Promotes Cell Survival by Phosphorylating and Inhibiting a Forkhead Transcription Factor', *Cell*, 96(6), pp. 857–868. doi: 10.1016/S0092-8674(00)80595-4.

Brys, K., Vanfleteren, J. R. and Braeckman, B. P. (2007) 'Testing the rate-of-living/oxidative damage theory of aging in the nematode model Caenorhabditis elegans', *Experimental Gerontology*, 42(9), pp. 845–851. doi: 10.1016/j.exger.2007.02.004.

Bultot, L. *et al.* (2016) 'Benzimidazole derivative small-molecule 991 enhances AMPK activity and

glucose uptake induced by AICAR or contraction in skeletal muscle', *American Journal of Physiology-Endocrinology and Metabolism*, 311(4), pp. E706–E719. doi: 10.1152/ajpendo.00237.2016.

Burkewitz, K. *et al.* (2015) 'Neuronal CRTC-1 Governs Systemic Mitochondrial Metabolism and Lifespan via a Catecholamine Signal', *Cell*. Elsevier Inc., 160(5), pp. 842–855. doi: 10.1016/j.cell.2015.02.004.

Burnell, A. M. *et al.* (2005) 'Alternate metabolism during the dauer stage of the nematode Caenorhabditis elegans', *Experimental Gerontology*, 40(11), pp. 850–856. doi: 10.1016/j.exger.2005.09.006.

Cabreiro, F. *et al.* (2013) 'Metformin retards aging in C. elegans by altering microbial folate and methionine metabolism', *Cell*, 153(1), pp. 228–239. doi: 10.1016/j.cell.2013.02.035.

Cantó, C. *et al.* (2010) 'Interdependence of AMPK and SIRT1 for Metabolic Adaptation to Fasting and Exercise in Skeletal Muscle', *Cell Metabolism*. Elsevier Ltd, 11(3), pp. 213–219. doi: 10.1016/j.cmet.2010.02.006.

Cassada, R. C. and Russell, R. L. (1975) 'The dauerlarva, a post-embryonic developmental variant of the nematode Caenorhabditis elegans', *Developmental Biology*, 46(2), pp. 326–342. doi: 10.1016/0012-1606(75)90109-8.

Chance, B., Sies, H. and Boveris, A. (1979) 'Hydroperoxide metabolism in mammalian organs.', *Physiological Reviews*, 59(3), pp. 527–605. doi: 10.1152/physrev.1979.59.3.527.

Chasnov, J. R. (2013) 'The evolutionary role of males in C. elegans', *Worm*, 2(1), p. e21146. doi: 10.4161/worm.21146.

Chen, D. *et al.* (2013) 'Germline Signaling Mediates the Synergistically Prolonged Longevity Produced by Double Mutations in daf-2 and rsks-1 in C. elegans', *Cell Reports*. The Authors, 5(6), pp. 1600–1610. doi: 10.1016/j.celrep.2013.11.018.

Chen, J., Carey, J. . and Ferris, H. (2001) 'Comparative demography of isogenic populations of Caenorhabditis elegans', *Experimental Gerontology*, 36(3), pp. 431–440. doi: 10.1016/S0531-5565(00)00225-4.

Chen, L. *et al.* (2013) 'Conserved regulatory elements in AMPK', *Nature*. Nature Publishing Group, 498(7453), pp. E8–E10. doi: 10.1038/nature12189.

Chen, Q. *et al.* (2003) 'Production of Reactive Oxygen Species by Mitochondria', *Journal of Biological Chemistry*, 278(38), pp. 36027–36031. doi: 10.1074/jbc.M304854200.

Chen, S. *et al.* (2011) 'Mice with AS160/TBC1D4-Thr649Ala Knockin Mutation Are Glucose Intolerant with Reduced Insulin Sensitivity and Altered GLUT4 Trafficking', *Cell Metabolism*. Elsevier Inc., 13(1), pp. 68–79. doi: 10.1016/j.cmet.2010.12.005.

Cheung, P. C. *et al.* (2000) 'Characterization of AMP-activated protein kinase gamma-subunit isoforms and their role in AMP binding.', *The Biochemical journal*, 346 Pt 3(3), pp. 659–69. doi: 10.1042/0264-6021:3460659.

Chi, C. *et al.* (2016) 'Nucleotide levels regulate germline proliferation through modulating GLP-1/Notch signaling in C. elegans', *Genes & Development*, 30(3), pp. 307–320. doi: 10.1101/gad.275107.115.

Chiang, W.-C. *et al.* (2012) 'HSF-1 Regulators DDL-1/2 Link Insulin-like Signaling to Heat-Shock Responses and Modulation of Longevity', *Cell*. Elsevier Inc., 148(1–2), pp. 322–334. doi: 10.1016/j.cell.2011.12.019.

Christensen, K. *et al.* (2009) 'Ageing populations: the challenges ahead', *The Lancet*. Elsevier Ltd, 374(9696), pp. 1196–1208. doi: 10.1016/S0140-6736(09)61460-4.

Clarke, P. R. and Hardie, D. G. (1990) 'Regulation of HMG-CoA reductase: identification of the site phosphorylated by the AMP-activated protein kinase in vitro and in intact rat liver.', *The EMBO journal*, 9(8), pp. 2439–46. doi: 10.1002/j.1460-2075.1990.tb07420.x.

Cohen, A. A. (2004) 'Female post-reproductive lifespan: a general mammalian trait', *Biological Reviews*, 79(04), p. 733. doi: 10.1017/S1464793103006432.

Cohen, J. E. (2005) 'Human Population Grows Up', *Scientific American*. Scientific American, a division of Nature America, Inc., 293(3), pp. 48–55.

Corton, J. M. *et al.* (1995) '5-Aminoimidazole-4-Carboxamide Ribonucleoside. A Specific Method for Activating AMP-Activated Protein Kinase in Intact Cells?', *European Journal of Biochemistry*, 229(2), pp. 558–565. doi: 10.1111/j.1432-1033.1995.tb20498.x.

Corton, J. M., Gillespie, J. G. and Hardie, D. G. (1994) 'Role of the AMP-activated protein kinase in the cellular stress response', *Current Biology*, 4(4), pp. 315–324. doi: 10.1016/S0960-9822(00)00070-1.

Coughlan, K. *et al.* (2014) 'AMPK activation: a therapeutic target for type 2 diabetes?', *Diabetes, Metabolic Syndrome and Obesity: Targets and Therapy*, 24(3), p. 241. doi: 10.2147/DMSO.S43731.

Crook, M. (2014) 'The dauer hypothesis and the evolution of parasitism: 20 years on and still going strong', *International Journal for Parasitology*. Australian Society for Parasitology Inc., 44(1), pp. 1–8.

doi: 10.1016/j.ijpara.2013.08.004.

Curtis, R., O'Connor, G. and DiStefano, P. S. (2006) 'Aging networks in Caenorhabditis elegans: AMP-activated protein kinase (aak-2) links multiple aging and metabolism pathways', *Aging Cell*. Blackwell Science Ltd, 5(2), pp. 119–126. doi: 10.1111/j.1474-9726.2006.00205.x.

Cypser, J. R. and Johnson, T. E. (2002) 'Multiple Stressors in Caenorhabditis elegans Induce Stress Hormesis and Extended Longevity', *The Journals of Gerontology Series A: Biological Sciences and Medical Sciences*, 57(3), pp. B109–B114. doi: 10.1093/gerona/57.3.B109.

Dale, S. *et al.* (1995) 'Similar substrate recognition motifs for mammalian AMP-activated protein kinase, higher plant HMG-CoA reductase kinase-A, yeast SNF1, and mammalian calmodulin-dependent protein kinase I.', *FEBS letters*, 361(2–3), pp. 191–5. doi: 10.1016/0014-5793(95)00172-6.

Daniel, T. and Carling, D. (2002) 'Functional Analysis of Mutations in the γ2 Subunit of AMP-activated Protein Kinase Associated with Cardiac Hypertrophy and Wolff-Parkinson-White Syndrome', *Journal of Biological Chemistry*, 277(52), pp. 51017–51024. doi: 10.1074/jbc.M207093200.

Davies, J. K. *et al.* (2006) 'Characterization of the role of γ2 R531G mutation in AMP-activated protein kinase in cardiac hypertrophy and Wolff-Parkinson-White syndrome', *American Journal of Physiology-Heart and Circulatory Physiology*, 290(5), pp. H1942–H1951. doi: 10.1152/ajpheart.01020.2005.

Davies, S. P. *et al.* (1992) 'Diurnal rhythm of phosphorylation of rat liver acetyl-CoA carboxylase by the AMP-activated protein kinase, demonstrated using freeze-clamping. Effects of high fat diets.', *European journal of biochemistry*, 203(3), pp. 615–23. doi: 10.1111/j.1432-1033.1992.tb16591.x.

Day, P. *et al.* (2007) 'Structure of a CBS-domain pair from the regulatory γ1 subunit of human AMPK in complex with AMP and ZMP', *Acta Crystallographica Section D Biological Crystallography*, 63(5), pp. 587–596. doi: 10.1107/S0907444907009110.

DeFronzo, R. A., Barzilai, N. and Simonson, D. C. (1991) 'Mechanism of metformin action in obese and lean noninsulin-dependent diabetic subjects.', *The Journal of Clinical Endocrinology & Metabolism*, 73(6), pp. 1294–301. doi: 10.1210/jcem-73-6-1294.

Depuydt, G. *et al.* (2014) 'LC–MS Proteomics Analysis of the Insulin/IGF-1-Deficient Caenorhabditis elegans daf-2(e1370) Mutant Reveals Extensive Restructuring of Intermediary Metabolism', *Journal of Proteome Research*, 13(4), pp. 1938–1956. doi: 10.1021/pr401081b.

Desjardins, C. A. *et al.* (2013) 'Genomics of Loa loa, a Wolbachia-free filarial parasite of humans', *Nature Genetics*. Nature Publishing Group, 45(5), pp. 495–500. doi: 10.1038/ng.2585.

Deyev, I. E. *et al.* (2011) 'Insulin Receptor-Related Receptor as an Extracellular Alkali Sensor', *Cell Metabolism*, 13(6), pp. 679–689. doi: 10.1016/j.cmet.2011.03.022.

Dillin, A., Crawford, D. K. and Kenyon, C. (2002) 'Timing requirements for insulin/IGF-1 signaling in C. elegans.', *Science*, 298(5594), pp. 830–4. doi: 10.1126/science.1074240.

Dillon, J. *et al.* (2016) 'Context-dependent regulation of feeding behaviour by the insulin receptor, DAF-2, in Caenorhabditis elegans', *Invertebrate Neuroscience*. Springer Berlin Heidelberg, 16(2), p. 4. doi: 10.1007/s10158-016-0187-2.

Doblhammer, G. and Kytir, J. (2001) 'Compression or expansion of morbidity? Trends in healthy-life expectancy in the elderly Austrian population between 1978 and 1998', *Social Science & Medicine*, 52(3), pp. 385–391. doi: 10.1016/S0277-9536(00)00141-6.

Dowling, R. J. O. *et al.* (2007) 'Metformin Inhibits Mammalian Target of Rapamycin–Dependent Translation Initiation in Breast Cancer Cells', *Cancer Research*, 67(22), pp. 10804–10812. doi: 10.1158/0008-5472.CAN-07-2310.

Dyck, J. R. B. *et al.* (1996) 'Regulation of 5'-AMP-activated Protein Kinase Activity by the Noncatalytic β and γ Subunits', *Journal of Biological Chemistry*, 271(30), pp. 17798–17803. doi: 10.1074/jbc.271.30.17798.

Egan, D. F. *et al.* (2011) 'Phosphorylation of ULK1 (hATG1) by AMP-Activated Protein Kinase Connects Energy Sensing to Mitophagy', *Science*, 331(6016), pp. 456–461. doi: 10.1126/science.1196371.

Ewald, C., Hourihan, J. and Blackwell, T. (2017) 'Oxidative Stress Assays (arsenite and tBHP) in Caenorhabditis elegans', *BIO-PROTOCOL*, 7(13), pp. 139–148. doi: 10.21769/BioProtoc.2365.

Ewald, C. Y. *et al.* (2015) 'Dauer-independent insulin/IGF-1-signalling implicates collagen remodelling in longevity', *Nature*. Nature Publishing Group, 519(7541), pp. 97–101. doi: 10.1038/nature14021.

Fernandes de Abreu, D. A. *et al.* (2014) 'An Insulin-to-Insulin Regulatory Network Orchestrates Phenotypic Specificity in Development and Physiology', *PLOS Genetics*. Edited by S. K. Kim, 10(3), p. e1004225. doi: 10.1371/journal.pgen.1004225.

Fielenbach, N. and Antebi, A. (2008) 'C. elegans dauer formation and the molecular basis of plasticity', *Genes & Development*, 22(16), pp. 2149–2165. doi: 10.1101/gad.1701508.

Flachsbart, F. *et al.* (2009) 'Association of FOXO3A variation with human longevity confirmed in German centenarians', *Proceedings of the National Academy of Sciences*, 106(8), pp. 2700–2705. doi:

10.1073/pnas.0809594106.

Flatt, K. M. *et al.* (2019) 'Epidermal Remodeling in Caenorhabditis elegans Dauers Requires the Nidogen Domain Protein DEX-1', *Genetics*, 211(1), pp. 169–183. doi: 10.1534/genetics.118.301557.

Foukas, L. C. *et al.* (2013) 'Long-term p110α PI3K inactivation exerts a beneficial effect on metabolism', *EMBO Molecular Medicine*, 5(4), pp. 563–571. doi: 10.1002/emmm.201201953.

Friedman, D. B. and Johnson, T. E. (1988) 'A mutation in the age-1 gene in Caenorhabditis elegans lengthens life and reduces hermaphrodite fertility.', *Genetics*, 118(1), pp. 75–86.

Fryer, L. G. D., Parbu-Patel, A. and Carling, D. (2002) 'The Anti-diabetic Drugs Rosiglitazone and Metformin Stimulate AMP-activated Protein Kinase through Distinct Signaling Pathways', *Journal of Biological Chemistry*, 277(28), pp. 25226–25232. doi: 10.1074/jbc.M202489200.

Fukuyama, M. *et al.* (2012) 'C. elegans AMPKs promote survival and arrest germline development during nutrient stress', *Biology Open*. England, 1(10), pp. 929–936. doi: 10.1242/bio.2012836.

Gagnon, A. (2015) 'Natural fertility and longevity', *Fertility and Sterility*. Elsevier Inc., 103(5), pp. 1109–1116. doi: 10.1016/j.fertnstert.2015.03.030.

Garcia-Haro, L. *et al.* (2010) 'The PP1-R6 protein phosphatase holoenzyme is involved in the glucose-induced dephosphorylation and inactivation of AMP-activated protein kinase, a key regulator of insulin secretion, in MIN6 β cells', *The FASEB Journal*, 24(12), pp. 5080–5091. doi: 10.1096/fj.10-166306.

Gems, D. *et al.* (1998) 'Two pleiotropic classes of daf-2 mutation affect larval arrest, adult behavior, reproduction and longevity in Caenorhabditis elegans.', *Genetics*, 150(1), pp. 129–55. doi: 10.1139/z78-244.

Gems, D. and Partridge, L. (2008) 'Stress-Response Hormesis and Aging: "That which Does Not Kill Us Makes Us Stronger"', *Cell Metabolism*, 7(3), pp. 200–203. doi: 10.1016/j.cmet.2008.01.001.

Geraghty, K. M. *et al.* (2007) 'Regulation of multisite phosphorylation and 14-3-3 binding of AS160 in response to IGF-1, EGF, PMA and AICAR.', *The Biochemical journal*, 407(2), pp. 231–41. doi: 10.1042/BJ20070649.

Ghazi, A., Henis-Korenblit, S. and Kenyon, C. (2009) 'A Transcription Elongation Factor That Links Signals from the Reproductive System to Lifespan Extension in Caenorhabditis elegans', *PLOS Genetics*. Edited by S. K. Kim, 5(9), p. e1000639. doi: 10.1371/journal.pgen.1000639.

Gladyshev, V. N. (2014) 'The Free Radical Theory of Aging Is Dead. Long Live the Damage Theory!',

Antioxidants & Redox Signaling, 20(4), pp. 727–731. doi: 10.1089/ars.2013.5228.

Gollob, M. H. *et al.* (2001) 'Novel PRKAG2 Mutation Responsible for the Genetic Syndrome of Ventricular Preexcitation and Conduction System Disease With Childhood Onset and Absence of Cardiac Hypertrophy', *Circulation*, 104(25), pp. 3030–3033. doi: 10.1161/hc5001.102111.

Göransson, O. *et al.* (2007) 'Mechanism of Action of A-769662, a Valuable Tool for Activation of AMP-activated Protein Kinase', *Journal of Biological Chemistry*, 282(45), pp. 32549–32560. doi: 10.1074/jbc.M706536200.

Gottlieb, S. and Ruvkun, G. (1994) 'daf-2, daf-16 and daf-23: genetically interacting genes controlling Dauer formation in Caenorhabditis elegans.', *Genetics*, 137(1), pp. 107–20.

Gowans, G. J. *et al.* (2013) 'AMP is a true physiological regulator of AMP-activated protein kinase by both allosteric activation and enhancing net phosphorylation.', *Cell Metabolism*, 18(4), pp. 556–66. doi: 10.1016/j.cmet.2013.08.019.

Greer, E. L., Dowlatshahi, D., *et al.* (2007) 'An AMPK-FOXO Pathway Mediates Longevity Induced by a Novel Method of Dietary Restriction in C. elegans', *Current Biology*. Elsevier, 17(19), pp. 1646–1656. doi: 10.1016/j.cub.2007.08.047.

Greer, E. L., Oskoui, P. R., *et al.* (2007) 'The Energy Sensor AMP-activated Protein Kinase Directly Regulates the Mammalian FOXO3 Transcription Factor', *Journal of Biological Chemistry*, 282(41), pp. 30107–30119. doi: 10.1074/jbc.M705325200.

Greer, E. L. and Brunet, A. (2008) 'Signaling networks in aging', *Journal of Cell Science*, 121(4), pp. 407–412. doi: 10.1242/jcs.021519.

Greer, E. L. and Brunet, A. (2009) 'Different dietary restriction regimens extend lifespan by both independent and overlapping genetic pathways in C. elegans', *Aging Cell*, 8(2), pp. 113–127. doi: 10.1111/j.1474-9726.2009.00459.x.

Gu, X. *et al.* (2017) 'Deconvoluting AMP-activated protein kinase (AMPK) adenine nucleotide binding and sensing', *Journal of Biological Chemistry*, 292(30), pp. 12653–12666. doi: 10.1074/jbc.M117.793018.

Guarente, L. and Kenyon, C. (2000) 'Genetic pathways that regulate ageing in model organisms', *Nature*, 408(6809), pp. 255–262. doi: 10.1038/35041700.

Guerin, J. C. (2004) 'Emerging Area of Aging Research: Long-Lived Animals with "Negligible Senescence"', *Annals of the New York Academy of Sciences*. Blackwell Publishing Ltd, 1019(1), pp.

518–520. doi: 10.1196/annals.1297.096.

Guertin, D. A. *et al.* (2006) 'Ablation in Mice of the mTORC Components raptor, rictor, or mLST8 Reveals that mTORC2 Is Required for Signaling to Akt-FOXO and PKCα, but Not S6K1', *Developmental Cell*, 11(6), pp. 859–871. doi: 10.1016/j.devcel.2006.10.007.

Guigas, B. *et al.* (2006) '5-Aminoimidazole-4-Carboxamide-1- -D-Ribofuranoside and Metformin Inhibit Hepatic Glucose Phosphorylation by an AMP-Activated Protein Kinase-Independent Effect on Glucokinase Translocation', *Diabetes*, 55(4), pp. 865–874. doi: 10.2337/diabetes.55.04.06.db05-1178.

Gwinn, D. M. *et al.* (2008) 'AMPK Phosphorylation of Raptor Mediates a Metabolic Checkpoint', *Molecular Cell*, 30(2), pp. 214–226. doi: 10.1016/j.molcel.2008.03.003.

Habets, D. D. J. *et al.* (2009) 'Crucial role for LKB1 to AMPKα2 axis in the regulation of CD36-mediated long-chain fatty acid uptake into cardiomyocytes', *Biochimica et Biophysica Acta (BBA) - Molecular and Cell Biology of Lipids*. Elsevier B.V., 1791(3), pp. 212–219. doi: 10.1016/j.bbalip.2008.12.009.

Haigis, M. C. and Yankner, B. A. (2010) 'The Aging Stress Response', *Molecular Cell*. Elsevier Inc., 40(2), pp. 333–344. doi: 10.1016/j.molcel.2010.10.002.

Halaschek-Wiener, J. *et al.* (2005) 'Analysis of long-lived C. elegans daf-2 mutants using serial analysis of gene expression.', *Genome research*, 15(5), pp. 603–15. doi: 10.1101/gr.3274805.

Hamatani, T. *et al.* (2004) 'Age-associated alteration of gene expression patterns in mouse oocytes', *Human Molecular Genetics*, 13(19), pp. 2263–2278. doi: 10.1093/hmg/ddh241.

Han, S. K. *et al.* (2016) 'OASIS 2: online application for survival analysis 2 with features for the analysis of maximal lifespan and healthspan in aging research', *Oncotarget*, 7(35), pp. 56147–56152. doi: 10.18632/oncotarget.11269.

Hansen, M. *et al.* (2007) 'Lifespan extension by conditions that inhibit translation in Caenorhabditis elegans', *Aging Cell*, 6(1), pp. 95–110. doi: 10.1111/j.1474-9726.2006.00267.x.

Hardie, D. G. (2008) 'AMPK: a key regulator of energy balance in the single cell and the whole organism', *International Journal of Obesity*, 32(S4), pp. S7–S12. doi: 10.1038/ijo.2008.116.

Hardie, D. G. and Ashford, M. L. J. (2014) 'AMPK: Regulating Energy Balance at the Cellular and Whole Body Levels', *Physiology*, 29(2), pp. 99–107. doi: 10.1152/physiol.00050.2013.

Hardie, D. G. and Carling, D. (1997) 'The AMP-Activated Protein Kinase. Fuel Gauge of the

Mammalian Cell?', *European Journal of Biochemistry*, 246(2), pp. 259–273. doi: 10.1111/j.1432-1033.1997.00259.x.

Hardie, D. G. and Hawley, S. A. (2001) 'AMP-activated protein kinase: The energy charge hypothesis revisited', *BioEssays*, 23(12), pp. 1112–1119. doi: 10.1002/bies.10009.

Hardie, D. G., Ross, F. A. and Hawley, S. A. (2012) 'AMPK: a nutrient and energy sensor that maintains energy homeostasis', *Nature Reviews Molecular Cell Biology*, 13(4), pp. 251–262. doi: 10.1038/nrm3311.

Hardie, D. G., Schaffer, B. E. and Brunet, A. (2016) 'AMPK: An Energy-Sensing Pathway with Multiple Inputs and Outputs', *Trends in Cell Biology*, 26(3), pp. 190–201. doi: 10.1016/j.tcb.2015.10.013.

Hardman, S. E. *et al.* (2014) 'The effects of age and muscle contraction on AMPK activity and heterotrimer composition', *Experimental Gerontology*, 55, pp. 120–128. doi: 10.1016/j.exger.2014.04.007.

Harrison, D. E. *et al.* (2009) 'Rapamycin fed late in life extends lifespan in genetically heterogeneous mice', *Nature*, 460(7253), pp. 392–395. doi: 10.1038/nature08221.

Hartwig, K. *et al.* (2009) 'Feeding a ROS-generator to Caenorhabditis elegans leads to increased expression of small heat shock protein HSP-16.2 and hormesis', *Genes & Nutrition*, 4(1), pp. 59–67. doi: 10.1007/s12263-009-0113-x.

Hawley, S. A. *et al.* (1996) 'Characterization of the AMP-activated protein kinase kinase from rat liver and identification of threonine 172 as the major site at which it phosphorylates AMP-activated protein kinase.', *The Journal of biological chemistry*, 271(44), pp. 27879–87. doi: 10.1074/jbc.271.44.27879.

Hawley, S. A. *et al.* (2005) 'Calmodulin-dependent protein kinase kinase-β is an alternative upstream kinase for AMP-activated protein kinase', *Cell Metabolism*, 2(1), pp. 9–19. doi: 10.1016/j.cmet.2005.05.009.

Hawley, S. A. *et al.* (2010) 'Use of Cells Expressing γ Subunit Variants to Identify Diverse Mechanisms of AMPK Activation', *Cell Metabolism*. Cell Press, 11(6), pp. 554–565. doi: 10.1016/J.CMET.2010.04.001.

Van Heemst, D. *et al.* (2005) 'Reduced insulin/IGF-1 signalling and human longevity', *Aging Cell*, 4(2), pp. 79–85. doi: 10.1111/j.1474-9728.2005.00148.x.

Heidler, T. *et al.* (2010) 'Caenorhabditis elegans lifespan extension caused by treatment with an

orally active ROS-generator is dependent on DAF-16 and SIR-2.1', *Biogerontology*, 11(2), pp. 183–195. doi: 10.1007/s10522-009-9239-x.

Henderson, S. T. and Johnson, T. E. (2001) 'daf-16 integrates developmental and environmental inputs to mediate aging in the nematode Caenorhabditis elegans', *Current Biology*, 11(24), pp. 1975–1980. doi: 10.1016/S0960-9822(01)00594-2.

Hirayama, I. *et al.* (1999) 'Insulin receptor-related receptor is expressed in pancreatic beta-cells and stimulates tyrosine phosphorylation of insulin receptor substrate-1 and -2', *Diabetes*, 48(6), pp. 1237–1244. doi: 10.2337/diabetes.48.6.1237.

Hodgkin, J. and Doniach, T. (1997) 'Natural variation and copulatory plug formation in Caenorhabditis elegans.', *Genetics*, 146(1), pp. 149–64.

Holt, S. J. and Riddle, D. L. (2003) 'SAGE surveys C. elegans carbohydrate metabolism: evidence for an anaerobic shift in the long-lived dauer larva', *Mechanisms of Ageing and Development*, 124(7), pp. 779–800. doi: 10.1016/S0047-6374(03)00132-5.

Holzenberger, M. *et al.* (2003) 'IGF-1 receptor regulates lifespan and resistance to oxidative stress in mice', *Nature*, 421(6919), pp. 182–187. doi: 10.1038/nature01298.

Honjoh, S. *et al.* (2009) 'Signalling through RHEB-1 mediates intermittent fasting-induced longevity in C. elegans', *Nature*. Nature Publishing Group, 457(7230), pp. 726–730. doi: 10.1038/nature07583.

Hoogewijs, D. *et al.* (2008) 'Selection and validation of a set of reliable reference genes for quantitative sod gene expression analysis in C. elegans', *BMC Molecular Biology*, 9(1), p. 9. doi: 10.1186/1471-2199-9-9.

Hoppe, S. *et al.* (2009) 'AMP-activated protein kinase adapts rRNA synthesis to cellular energy supply', *Proceedings of the National Academy of Sciences*, 106(42), pp. 17781–17786. doi: 10.1073/pnas.0909873106.

Horman, S. *et al.* (2002) 'Activation of AMP-Activated Protein Kinase Leads to the Phosphorylation of Elongation Factor 2 and an Inhibition of Protein Synthesis', *Current Biology*, 12(16), pp. 1419–1423. doi: 10.1016/S0960-9822(02)01077-1.

Hudson, E. R. *et al.* (2003) 'A Novel Domain in AMP-Activated Protein Kinase Causes Glycogen Storage Bodies Similar to Those Seen in Hereditary Cardiac Arrhythmias', *Current Biology*, 13(10), pp. 861–866. doi: 10.1016/S0960-9822(03)00249-5.

Hughes, S. E. *et al.* (2007) 'Genetic and Pharmacological Factors That Influence Reproductive Aging in

Nematodes', *PLOS Genetics*, 3(2), p. e25. doi: 10.1371/journal.pgen.0030025.

Humphries, S. and Stevens, D. J. (2001) 'Out with a bang', *Nature*, 410(6830), pp. 758–759. doi: 10.1038/35071202.

Hwang, A. B. *et al.* (2014) 'Feedback regulation via AMPK and HIF-1 mediates ROS-dependent longevity in Caenorhabditis elegans', *Proceedings of the National Academy of Sciences*, 111(42), pp. E4458–E4467. doi: 10.1073/pnas.1411199111.

Inoki, K., Zhu, T. and Guan, K.-L. (2003) 'TSC2 Mediates Cellular Energy Response to Control Cell Growth and Survival', *Cell*, 115(5), pp. 577–590. doi: 10.1016/S0092-8674(03)00929-2.

Ishii, N. *et al.* (1998) 'A mutation in succinate dehydrogenase cytochrome b causes oxidative stress and ageing in nematodes', *Nature*, 394(6694), pp. 694–697. doi: 10.1038/29331.

Jager, S. *et al.* (2007) 'AMP-activated protein kinase (AMPK) action in skeletal muscle via direct phosphorylation of PGC-1', *Proceedings of the National Academy of Sciences*, 104(29), pp. 12017–12022. doi: 10.1073/pnas.0705070104.

Jia, K., Chen, D. and Riddle, D. L. (2004) 'The TOR pathway interacts with the insulin signaling pathway to regulate C. elegans larval development, metabolism and life span', *Development*, 131(16), pp. 3897–3906. doi: 10.1242/dev.01255.

Johnson, S. C., Rabinovitch, P. S. and Kaeberlein, M. (2013) 'mTOR is a key modulator of ageing and age-related disease', *Nature*, 493(7432), pp. 338–345. doi: 10.1038/nature11861.

Jones, K. T. and Ashrafi, K. (2009) 'Caenorhabditis elegans as an emerging model for studying the basic biology of obesity', *Disease Models & Mechanisms*, 2(5–6), pp. 224–229. doi: 10.1242/dmm.001933.

Jørgensen, S. B. *et al.* (2004) 'The alpha2-5'AMP-activated protein kinase is a site 2 glycogen synthase kinase in skeletal muscle and is responsive to glucose loading.', *Diabetes*, 53(12), pp. 3074–81. doi: 10.2337/diabetes.53.12.3074.

Kappeler, L. *et al.* (2008) 'Brain IGF-1 Receptors Control Mammalian Growth and Lifespan through a Neuroendocrine Mechanism', *PLOS Biology*. Edited by A. Dillin, 6(10), p. e254. doi: 10.1371/journal.pbio.0060254.

Karp, X. (2018) 'Working with dauer larvae', *WormBook*, pp. 1–19. doi: 10.1895/wormbook.1.180.1.

Kayampilly, P. P. and Menon, K. M. J. (2009) 'Follicle-Stimulating Hormone Inhibits Adenosine 5'-Monophosphate-Activated Protein Kinase Activation and Promotes Cell Proliferation of Primary

Granulosa Cells in Culture through an Akt-Dependent Pathway', *Endocrinology*, 150(2), pp. 929–935. doi: 10.1210/en.2008-1032.

Keaney, M. *et al.* (2004) 'Superoxide dismutase mimetics elevate superoxide dismutase activity in vivo but do not retard aging in the nematode Caenorhabditis elegans', *Free Radical Biology and Medicine*, 37(2), pp. 239–250. doi: 10.1016/j.freeradbiomed.2004.04.005.

Kenyon, C. *et al.* (1993) 'A C. elegans mutant that lives twice as long as wild type', *Nature*, 366(6454), pp. 461–464. doi: 10.1038/366461a0.

Kenyon, C. (2005) 'The Plasticity of Aging: Insights from Long-Lived Mutants', *Cell*, 120(4), pp. 449–460. doi: 10.1016/j.cell.2005.02.002.

Kenyon, C. (2010) 'A pathway that links reproductive status to lifespan in Caenorhabditis elegans', *Annals of the New York Academy of Sciences*, 1204(1), pp. 156–162. doi: 10.1111/j.1749-6632.2010.05640.x.

Kenyon, C. J. (2010) 'The genetics of ageing.', *Nature*, 464(7288), pp. 504–12. doi: 10.1038/nature08980.

Khatri, S. *et al.* (2010) 'FOXO3a Regulates Glycolysis via Transcriptional Control of Tumor Suppressor TSC1', *Journal of Biological Chemistry*, 285(21), pp. 15960–15965. doi: 10.1074/jbc.M110.121871.

Kim, J. *et al.* (2011) 'AMPK and mTOR regulate autophagy through direct phosphorylation of Ulk1', *Nature Cell Biology*, 13(2), pp. 132–141. doi: 10.1038/ncb2152.

Kim, J. *et al.* (2013) 'Differential Regulation of Distinct Vps34 Complexes by AMPK in Nutrient Stress and Autophagy', *Cell*. Elsevier Inc., 152(1–2), pp. 290–303. doi: 10.1016/j.cell.2012.12.016.

Kimura, K. D. *et al.* (1997) 'daf-2, an insulin receptor-like gene that regulates longevity and diapause in Caenorhabditis elegans.', *Science*, 277(5328), pp. 942–6.

Kirkwood, T. B. L. and Austad, S. N. (2000) 'Why do we age?', *Nature*, 408(6809), pp. 233–238. doi: 10.1038/35041682.

Knoefler, D. *et al.* (2012) 'Quantitative In Vivo Redox Sensors Uncover Oxidative Stress as an Early Event in Life', *Molecular Cell*. Elsevier Inc., 47(5), pp. 767–776. doi: 10.1016/j.molcel.2012.06.016.

Kojima, T. *et al.* (2004) 'Association analysis between longevity in the Japanese population and polymorphic variants of genes involved in insulin and insulin-like growth factor 1 signaling pathways', *Experimental Gerontology*, 39(11–12), pp. 1595–1598. doi: 10.1016/j.exger.2004.05.007.

Kola, B. (2008) 'Role of AMP-activated protein kinase in the control of appetite', *Journal of Neuroendocrinology*, 20(7), pp. 942–951. doi: 10.1111/j.1365-2826.2008.01745.x.

Koo, S.-H. *et al.* (2005) 'The CREB coactivator TORC2 is a key regulator of fasting glucose metabolism', *Nature*, 437(7062), pp. 1109–1114. doi: 10.1038/nature03967.

Kops, G. J. P. L. *et al.* (1999) 'Direct control of the Forkhead transcription factor AFX by protein kinase B', *Nature*, 398(6728), pp. 630–634. doi: 10.1038/19328.

Kristensen, J. M. *et al.* (2014) 'Two weeks of metformin treatment induces AMPK-dependent enhancement of insulin-stimulated glucose uptake in mouse soleus muscle', *American Journal of Physiology-Endocrinology and Metabolism*, 306(10), pp. E1099–E1109. doi: 10.1152/ajpendo.00417.2013.

Kumsta, C. *et al.* (2014) 'Integrin-linked kinase modulates longevity and thermotolerance in C. elegans through neuronal control of HSF-1', *Aging Cell*, 13(3), pp. 419–430. doi: 10.1111/acel.12189.

Lai, Y.-C. *et al.* (2014) 'A small-molecule benzimidazole derivative that potently activates AMPK to increase glucose transport in skeletal muscle: comparison with effects of contraction and other AMPK activators', *Biochemical Journal*, 460(3), pp. 363–375. doi: 10.1042/BJ20131673.

Landis, G. N. and Tower, J. (2005) 'Superoxide dismutase evolution and life span regulation', *Mechanisms of Ageing and Development*, 126(3), pp. 365–379. doi: 10.1016/j.mad.2004.08.012.

Lapointe, J. and Hekimi, S. (2010) 'When a theory of aging ages badly', *Cellular and Molecular Life Sciences*, 67(1), pp. 1–8. doi: 10.1007/s00018-009-0138-8.

Larsen, P. L. (1993) 'Aging and resistance to oxidative damage in Caenorhabditis elegans.', *Proceedings of the National Academy of Sciences*, 90(19), pp. 8905–8909. doi: 10.1073/pnas.90.19.8905.

Lee-Young, R. S. *et al.* (2009) 'AMPK activation is fiber type specific in human skeletal muscle: effects of exercise and short-term exercise training', *Journal of Applied Physiology*, 107(1), pp. 283–289. doi: 10.1152/japplphysiol.91208.2008.

Lee, H. *et al.* (2008) 'The Caenorhabditis elegans AMP-activated Protein Kinase AAK-2 Is Phosphorylated by LKB1 and Is Required for Resistance to Oxidative Stress and for Normal Motility and Foraging Behavior', *Journal of Biological Chemistry*. United States, 283(22), pp. 14988–14993. doi: 10.1074/jbc.M709115200.

Li, W., Kennedy, S. G. and Ruvkun, G. (2003) 'daf-28 encodes a C. elegans insulin superfamily

member that is regulated by environmental cues and acts in the DAF-2 signaling pathway.', *Genes & Development*, 17(7), pp. 844–58. doi: 10.1101/gad.1066503.

Li, X. *et al.* (2015) 'Structural basis of AMPK regulation by adenine nucleotides and glycogen', *Cell Research*. Nature Publishing Group, 25(1), pp. 50–66. doi: 10.1038/cr.2014.150.

Li, Y. *et al.* (2009) 'Genetic association of FOXO1A and FOXO3A with longevity trait in Han Chinese populations', *Human Molecular Genetics*, 18(24), pp. 4897–4904. doi: 10.1093/hmg/ddp459.

Li, Y. *et al.* (2011) 'AMPK phosphorylates and inhibits SREBP activity to attenuate hepatic steatosis and atherosclerosis in diet-induced insulin-resistant mice.', *Cell metabolism*, 13(4), pp. 376–388. doi: 10.1016/j.cmet.2011.03.009.

Libina, N., Berman, J. R. and Kenyon, C. (2003) 'Tissue-Specific Activities of C. elegans DAF-16 in the Regulation of Lifespan', *Cell*, 115(4), pp. 489–502. doi: 10.1016/S0092-8674(03)00889-4.

Lin, J., Handschin, C. and Spiegelman, B. M. (2005) 'Metabolic control through the PGC-1 family of transcription coactivators', *Cell Metabolism*, 1(6), pp. 361–370. doi: 10.1016/j.cmet.2005.05.004.

Lin, K. *et al.* (1997) 'daf-16: An HNF-3/forkhead family member that can function to double the life-span of Caenorhabditis elegans.', *Science*, 278(5341), pp. 1319–22. doi: 10.1126/science.278.5341.1319.

Lithgow, G. J. *et al.* (1995) 'Thermotolerance and extended life-span conferred by single-gene mutations and induced by thermal stress.', *Proceedings of the National Academy of Sciences*, 92(16), pp. 7540–7544. doi: 10.1073/pnas.92.16.7540.

López-Otín, C. *et al.* (2013) 'The Hallmarks of Aging', *Cell*, 153(6), pp. 1194–1217. doi: 10.1016/j.cell.2013.05.039.

Lorenzini, A. *et al.* (2014) 'Mice Producing Reduced Levels of Insulin-Like Growth Factor Type 1 Display an Increase in Maximum, but not Mean, Life Span', *The Journals of Gerontology Series A: Biological Sciences and Medical Sciences*, 69(4), pp. 410–419. doi: 10.1093/gerona/glt108.

Luckinbill, L. S. *et al.* (1984) 'Selection for Delayed Senescence in Drosophila melanogaster', *Evolution*, 38(5), p. 996. doi: 10.2307/2408433.

Lunetta, K. L. *et al.* (2007) 'Genetic correlates of longevity and selected age-related phenotypes: a genome-wide association study in the Framingham Study', *BMC Medical Genetics*, 8(S1), p. S13. doi: 10.1186/1471-2350-8-S1-S13.

Luo, H. *et al.* (2017) 'Nutrient Sensing and the Oxidative Stress Response', *Trends in Endocrinology &*

Metabolism. Elsevier Ltd, 28(6), pp. 449–460. doi: 10.1016/j.tem.2017.02.008.

Luo, S. *et al.* (2010) 'TGF-β and Insulin Signaling Regulate Reproductive Aging via Oocyte and Germline Quality Maintenance', *Cell*. Elsevier Inc., 143(2), pp. 299–312. doi: 10.1016/j.cell.2010.09.013.

Lutz, W. and Qiang, R. (2002) 'Determinants of human population growth', *Philosophical Transactions of the Royal Society of London. Series B: Biological Sciences*. Edited by R. M. Sibly, J. Hone, and T. H. Clutton–Brock, 357(1425), pp. 1197–1210. doi: 10.1098/rstb.2002.1121.

Lützner, N., De-Castro Arce, J. and Rösl, F. (2012) 'Gene Expression of the Tumour Suppressor LKB1 Is Mediated by Sp1, NF-Y and FOXO Transcription Factors', *PLOS ONE*. Edited by R. Khanin, 7(3), p. e32590. doi: 10.1371/journal.pone.0032590.

Luz, A. L. *et al.* (2016) 'From the Cover: Arsenite Uncouples Mitochondrial Respiration and Induces a Warburg-like Effect in Caenorhabditis elegans', *Toxicological Sciences*, 152(2), pp. 349–362. doi: 10.1093/toxsci/kfw093.

Ma, L. *et al.* (2005) 'Phosphorylation and functional inactivation of TSC2 by Erk implications for tuberous sclerosis and cancer pathogenesis.', *Cell*, 121(2), pp. 179–93. doi: 10.1016/j.cell.2005.02.031.

Madamanchi, N. R. and Runge, M. S. (2007) 'Mitochondrial Dysfunction in Atherosclerosis', *Circulation Research*, 100(4), pp. 460–473. doi: 10.1161/01.RES.0000258450.44413.96.

Mádi, A. *et al.* (2008) 'Mass spectrometric proteome analysis suggests anaerobic shift in metabolism of Dauer larvae of Caenorhabditis elegans', *Biochimica et Biophysica Acta (BBA) - Proteins and Proteomics*. Elsevier B.V., 1784(11), pp. 1763–1770. doi: 10.1016/j.bbapap.2008.05.017.

Madiraju, A. K. *et al.* (2014) 'Metformin suppresses gluconeogenesis by inhibiting mitochondrial glycerophosphate dehydrogenase', *Nature*. Nature Publishing Group, 510(7506), pp. 542–546. doi: 10.1038/nature13270.

Maehama, T. and Dixon, J. E. (1998) 'The Tumor Suppressor, PTEN/MMAC1, Dephosphorylates the Lipid Second Messenger, Phosphatidylinositol 3,4,5-Trisphosphate', *Journal of Biological Chemistry*, 273(22), pp. 13375–13378. doi: 10.1074/jbc.273.22.13375.

Mair, W. *et al.* (2011) 'Lifespan extension induced by AMPK and calcineurin is mediated by CRTC-1 and CREB.', *Nature*, 470(7334), pp. 404–8. doi: 10.1038/nature09706.

Mair, W. and Dillin, A. (2008) 'Aging and Survival: The Genetics of Life Span Extension by Dietary

Restriction', *Annual Review of Biochemistry*, 77(1), pp. 727–754. doi: 10.1146/annurev.biochem.77.061206.171059.

Malone, E. A., Inoue, T. and Thomas, J. H. (1996) 'Genetic analysis of the roles of daf-28 and age-1 regulating Caenorhabditis elegans dauer formation', *Genetics*, 143(3), pp. 1193–1205.

Manning, B. D. *et al.* (2002) 'Identification of the Tuberous Sclerosis Complex-2 Tumor Suppressor Gene Product Tuberin as a Target of the Phosphoinositide 3-Kinase/Akt Pathway', *Molecular Cell*, 10(1), pp. 151–162. doi: 10.1016/S1097-2765(02)00568-3.

Marsin, A.-S. *et al.* (2002) 'The Stimulation of Glycolysis by Hypoxia in Activated Monocytes Is Mediated by AMP-activated Protein Kinase and Inducible 6-Phosphofructo-2-kinase', *Journal of Biological Chemistry*, 277(34), pp. 30778–30783. doi: 10.1074/jbc.M205213200.

Marsin, A. S. *et al.* (2000) 'Phosphorylation and activation of heart PFK-2 by AMPK has a role in the stimulation of glycolysis during ischaemia.', *Current Biology*, 10(20), pp. 1247–55. doi: 10.1016/s0960-9822(00)00742-9.

Mathi, S. K., Chan, J. and Watt, V. M. (1995) 'Insulin receptor-related receptor messenger ribonucleic acid: quantitative distribution and localization to subpopulations of epithelial cells in stomach and kidney.', *Endocrinology*, 136(9), pp. 4125–4132. doi: 10.1210/endo.136.9.7649121.

McBride, A. *et al.* (2009) 'The Glycogen-Binding Domain on the AMPK β Subunit Allows the Kinase to Act as a Glycogen Sensor', *Cell Metabolism*. Elsevier Inc., 9(1), pp. 23–34. doi: 10.1016/j.cmet.2008.11.008.

McColl, G. *et al.* (2010) 'Insulin-like Signaling Determines Survival during Stress via Posttranscriptional Mechanisms in C. elegans', *Cell Metabolism*. Elsevier Ltd, 12(3), pp. 260–272. doi: 10.1016/j.cmet.2010.08.004.

McElwee, J. J. *et al.* (2004) 'Shared Transcriptional Signature in Caenorhabditis elegans Dauer Larvae and Long-lived daf-2 Mutants Implicates Detoxification System in Longevity Assurance', *Journal of Biological Chemistry*, 279(43), pp. 44533–44543. doi: 10.1074/jbc.M406207200.

McQuary, P. R. *et al.* (2016) 'C. elegans S6K Mutants Require a Creatine-Kinase-like Effector for Lifespan Extension', *Cell Reports*. The Authors, 14(9), pp. 2059–2067. doi: 10.1016/j.celrep.2016.02.012.

Meléndez, A. *et al.* (2003) 'Autophagy genes are essential for dauer development and life-span extension in C. elegans', *Science*, 301(5638), pp. 1387–1391. doi: 10.1126/science.1087782.

Mendenhall, A. R. *et al.* (2011) 'Genetic Dissection of Late-Life Fertility in Caenorhabditis elegans', *The Journals of Gerontology Series A: Biological Sciences and Medical Sciences*, 66A(8), pp. 842–854. doi: 10.1093/gerona/glr089.

Merrill, G. F. *et al.* (1997) 'AICA riboside increases AMP-activated protein kinase, fatty acid oxidation, and glucose uptake in rat muscle.', *The American journal of physiology*, 273(6), pp. E1107-12. doi: 10.1152/ajpendo.1997.273.6.E1107.

Michaelson, D. *et al.* (2010) 'Insulin signaling promotes germline proliferation in C. elegans', *Development*, 137(4), pp. 671–680. doi: 10.1242/dev.042523.

Mihaylova, M. M. *et al.* (2011) 'Class IIa histone deacetylases are hormone-activated regulators of FOXO and mammalian glucose homeostasis.', *Cell*. Elsevier Inc., 145(4), pp. 607–21. doi: 10.1016/j.cell.2011.03.043.

Minois, N. (2000) 'Longevity and aging: Beneficial effects of exposure to mild stress', *Biogerontology*, pp. 15–29. doi: 10.1023/A:1010085823990.

Minokoshi, Y. *et al.* (2004) 'AMP-kinase regulates food intake by responding to hormonal and nutrient signals in the hypothalamus', *Nature*, 428(6982), pp. 569–574. doi: 10.1038/nature02440.

Momcilovic, M., Hong, S.-P. and Carlson, M. (2006) 'Mammalian TAK1 Activates Snf1 Protein Kinase in Yeast and Phosphorylates AMP-activated Protein Kinase in Vitro', *Journal of Biological Chemistry*, 281(35), pp. 25336–25343. doi: 10.1074/jbc.M604399200.

Moreno-Arriola, E. *et al.* (2016) 'AMP-Activated Protein Kinase Regulates Oxidative Metabolism in Caenorhabditis elegans through the NHR-49 and MDT-15 Transcriptional Regulators.', *PLOS one*. Public Library of Science, 11(1), p. e0148089. doi: 10.1371/journal.pone.0148089.

Morran, L. T., Parmenter, M. D. and Phillips, P. C. (2009) 'Mutation load and rapid adaptation favour outcrossing over self-fertilization', *Nature*. Nature Publishing Group, 462(7271), pp. 350–352. doi: 10.1038/nature08496.

Muoio, D. M. *et al.* (1999) 'AMP-activated kinase reciprocally regulates triacylglycerol synthesis and fatty acid oxidation in liver and muscle: evidence that sn-glycerol-3-phosphate acyltransferase is a novel target.', *The Biochemical journal*, 338 (Pt 3(3), pp. 783–91. doi: 10.1042/0264-6021:3380783.

Murphy, C. T. *et al.* (2003) 'Genes that act downstream of DAF-16 to influence the lifespan of Caenorhabditis elegans', *Nature*, 424(6946), pp. 277–283. doi: 10.1038/nature01789.

Murphy, C. T., Lee, S.-J. and Kenyon, C. (2007) 'Tissue entrainment by feedback regulation of insulin

gene expression in the endoderm of Caenorhabditis elegans', *Proceedings of the National Academy of Sciences*, 104(48), pp. 19046–19050. doi: 10.1073/pnas.0709613104.

Musi, N. *et al.* (2002) 'Metformin Increases AMP-Activated Protein Kinase Activity in Skeletal Muscle of Subjects With Type 2 Diabetes', *Diabetes*, 51(7), pp. 2074–2081. doi: 10.2337/diabetes.51.7.2074.

Nanji, M., Hopper, N. A. and Gems, D. (2005) 'LET-60 RAS modulates effects of insulin/IGF-1 signaling on development and aging in Caenorhabditis elegans', *Aging Cell*, 4(5), pp. 235–245. doi: 10.1111/j.1474-9726.2005.00166.x.

Narbonne, P. and Roy, R. (2006) 'Inhibition of germline proliferation during C. elegans dauer development requires PTEN, LKB1 and AMPK signalling.', *Development*. England, 133(4), pp. 611–9. doi: 10.1242/dev.02232.

Narbonne, P. and Roy, R. (2009) 'Caenorhabditis elegans dauers need LKB1/AMPK to ration lipid reserves and ensure long-term survival', *Nature*. Nature Publishing Group, 457(7226), pp. 210–214. doi: 10.1038/nature07536.

Narkar, V. A. *et al.* (2008) 'AMPK and PPARδ Agonists Are Exercise Mimetics', *Cell*, 134(3), pp. 405–415. doi: 10.1016/j.cell.2008.06.051.

NHS Digital (2018) 'Adult Social Care Activity and Finance Report, England 2017-2018', (October), pp. 1–52.

Niesler, C. U., Myburgh, K. H. and Moore, F. (2007) 'The changing AMPK expression profile in differentiating mouse skeletal muscle myoblast cells helps confer increasing resistance to apoptosis', *Experimental Physiology*, 92(1), pp. 207–217. doi: 10.1113/expphysiol.2006.034736.

Nika, L. *et al.* (2016) 'Fluorescent beads are a Versatile tool for staging Caenorhabditis elegans in different life histories', *G3: Genes, Genomes, Genetics*, 6(7), pp. 1923–1933. doi: 10.1534/g3.116.030163.

Nojima, A. *et al.* (2013) 'Haploinsufficiency of Akt1 Prolongs the Lifespan of Mice', *PLOS ONE*. Edited by J. Sadoshima, 8(7), p. e69178. doi: 10.1371/journal.pone.0069178.

Oakhill, J. S. *et al.* (2010) 'β-Subunit myristoylation is the gatekeeper for initiating metabolic stress sensing by AMP-activated protein kinase (AMPK).', *Proceedings of the National Academy of Sciences*, 107(45), pp. 19237–41. doi: 10.1073/pnas.1009705107.

Oakhill, J. S. *et al.* (2011) 'AMPK Is a Direct Adenylate Charge-Regulated Protein Kinase', *Science*, 332(6036), pp. 1433–1435. doi: 10.1126/science.1200094.

Oakwood, M., Bradley, A. J. and Cockburn, A. (2001) 'Semelparity in a large marsupial', *Proceedings of the Royal Society of London. Series B: Biological Sciences*, 268(1465), pp. 407–411. doi: 10.1098/rspb.2000.1369.

Ogg, S. *et al.* (1997) 'The Fork head transcription factor DAF-16 transduces insulin-like metabolic and longevity signals in C. elegans.', *Nature*, 389(6654), pp. 994–9. doi: 10.1038/40194.

Okado-Matsumoto, A. and Fridovich, I. (2001) 'Subcellular Distribution of Superoxide Dismutases (SOD) in Rat Liver', *Journal of Biological Chemistry*, 276(42), pp. 38388–38393. doi: 10.1074/jbc.M105395200.

Onken, B. and Driscoll, M. (2010) 'Metformin Induces a Dietary Restriction–Like State and the Oxidative Stress Response to Extend C. elegans Healthspan via AMPK, LKB1, and SKN-1', *PLOS ONE*. Edited by A. C. Hart, 5(1), p. e8758. doi: 10.1371/journal.pone.0008758.

Paix, A. *et al.* (2015) 'High Efficiency, Homology-Directed Genome Editing in Caenorhabditis elegans Using CRISPR-Cas9 Ribonucleoprotein Complexes', *Genetics*, 201(1), pp. 47–54. doi: 10.1534/genetics.115.179382.

Pan, K. Z. *et al.* (2007) 'Inhibition of mRNA translation extends lifespan in Caenorhabditis elegans', *Aging Cell*, 6(1), pp. 111–119. doi: 10.1111/j.1474-9726.2006.00266.x.

Panowski, S. H. *et al.* (2007) 'PHA-4/Foxa mediates diet-restriction-induced longevity of C. elegans', *Nature*, 447(7144), pp. 550–555. doi: 10.1038/nature05837.

Paolisso, G. *et al.* (1996) 'Glucose tolerance and insulin action in healthy centenarians', *American Journal of Physiology-Endocrinology and Metabolism*. American Physiological Society, 270(5), pp. E890–E894. doi: 10.1152/ajpendo.1996.270.5.E890.

Paradis, S. *et al.* (1999) 'A PDK1 homolog is necessary and sufficient to transduce AGE-1 PI3 kinase signals that regulate diapause in Caenorhabditis elegans', *Genes & Development*, 13(11), pp. 1438–1452. doi: 10.1101/gad.13.11.1438.

Patel, D. S. *et al.* (2008) 'Clustering of Genetically Defined Allele Classes in the Caenorhabditis elegans DAF-2 Insulin/IGF-1 Receptor', *Genetics*, 178(2), pp. 931–946. doi: 10.1534/genetics.107.070813.

Pawlikowska, L. *et al.* (2009) 'Association of common genetic variation in the insulin/IGF1 signaling pathway with human longevity', *Aging Cell*, 8(4), pp. 460–472. doi: 10.1111/j.1474-9726.2009.00493.x.

Petersen, K. F. *et al.* (2003) 'Mitochondrial dysfunction in the elderly: possible role in insulin resistance.', *Science*, 300(5622), pp. 1140–2. doi: 10.1126/science.1082889.

Pfarr, K. M. *et al.* (2009) 'Filariasis and lymphoedema', *Parasite Immunology*, 31(11), pp. 664–672. doi: 10.1111/j.1365-3024.2009.01133.x.

Pierce, S. B. *et al.* (2001) 'Regulation of DAF-2 receptor signaling by human insulin and ins-1, a member of the unusually large and diverse C. elegans insulin gene family.', *Genes & Development*, 15(6), pp. 672–86. doi: 10.1101/gad.867301.

Pinkston, J. M. *et al.* (2006) 'Mutations that increase the life span of C. elegans inhibit tumor growth.', *Science*, 313(5789), pp. 971–5. doi: 10.1126/science.1121908.

Qin, Z. and Hubbard, E. J. A. (2015) 'Non-autonomous DAF-16/FOXO activity antagonizes age-related loss of C. elegans germline stem/progenitor cells', *Nature Communications*. Nature Publishing Group, 6(1), p. 7107. doi: 10.1038/ncomms8107.

Rechavi, O. *et al.* (2014) 'Starvation-Induced Transgenerational Inheritance of Small RNAs in C. elegans', *Cell*, 158(2), pp. 277–287. doi: 10.1016/j.cell.2014.06.020.

Ren, P. *et al.* (1996) 'Control of C. elegans Larval Development by Neuronal Expression of a TGF-beta Homolog', *Science*, 274(5291), pp. 1389–1391. doi: 10.1126/science.274.5291.1389.

Rena, G., Hardie, D. G. and Pearson, E. R. (2017) 'The mechanisms of action of metformin', *Diabetologia*. Diabetologia, 60(9), pp. 1577–1585. doi: 10.1007/s00125-017-4342-z.

Reznick, R. M. *et al.* (2007) 'Aging-associated reductions in AMP-activated protein kinase activity and mitochondrial biogenesis.', *Cell metabolism*, 5(2), pp. 151–6. doi: 10.1016/j.cmet.2007.01.008.

Riddle, D. L. *et al.* (1997) *C. elegans II*, *C. elegans II*. Cold Spring Harbor Laboratory Press. doi: NBK20183.

Riddle, D. L., Swanson, M. M. and Albert, P. S. (1981) 'Interacting genes in nematode dauer larva formation', *Nature*, 290(5808), pp. 668–671. doi: 10.1038/290668a0.

Riera, C. E. *et al.* (2016) 'Signaling Networks Determining Life Span', *Annual Review of Biochemistry*, 85(1), pp. 35–64. doi: 10.1146/annurev-biochem-060815-014451.

Risner, M. E. *et al.* (2006) 'Efficacy of rosiglitazone in a genetically defined population with mild-to-moderate Alzheimer's disease', *The Pharmacogenomics Journal*, 6(4), pp. 246–254. doi: 10.1038/sj.tpj.6500369.

Robida-Stubbs, S. *et al.* (2012) 'TOR Signaling and Rapamycin Influence Longevity by Regulating SKN-1/Nrf and DAF-16/FoxO', *Cell Metabolism*. Elsevier Inc., 15(5), pp. 713–724. doi: 10.1016/j.cmet.2012.04.007.

Rollinson, D. and Stothard, R. (2020) *Advances in Parasitology*. 2020th edn. Edited by D. Rollinson and R. Stothard. Elsevier Science.

Roux, P. P. *et al.* (2004) 'Tumor-promoting phorbol esters and activated Ras inactivate the tuberous sclerosis tumor suppressor complex via p90 ribosomal S6 kinase', *Proceedings of the National Academy of Sciences*. National Academy of Sciences, 101(37), pp. 13489–13494. doi: 10.1073/pnas.0405659101.

Russell, R. C. *et al.* (2013) 'ULK1 induces autophagy by phosphorylating Beclin-1 and activating VPS34 lipid kinase', *Nature Cell Biology*. Nature Publishing Group, 15(7), pp. 741–750. doi: 10.1038/ncb2757.

Sagi, D. and Kim, S. K. (2012) 'An Engineering Approach to Extending Lifespan in C. elegans', *PLOS Genetics*. Edited by G. Ruvkun. Public Library of Science, 8(6), p. e1002780. doi: 10.1371/journal.pgen.1002780.

Sakamoto, K. and Holman, G. D. (2008) 'Emerging role for AS160/TBC1D4 and TBC1D1 in the regulation of GLUT4 traffic', *American Journal of Physiology-Endocrinology and Metabolism*, 295(1), pp. 29–37. doi: 10.1152/ajpendo.90331.2008.

Salih, D. A. and Brunet, A. (2008) 'FoxO transcription factors in the maintenance of cellular homeostasis during aging', *Current Opinion in Cell Biology*, 20(2), pp. 126–136. doi: 10.1016/j.ceb.2008.02.005.

Salminen, A. and Kaarniranta, K. (2012) 'AMP-activated protein kinase (AMPK) controls the aging process via an integrated signaling network', *Ageing Research Reviews*. Elsevier B.V., 11(2), pp. 230–241. doi: 10.1016/j.arr.2011.12.005.

Salt, I. *et al.* (1998) 'AMP-activated protein kinase: Greater AMP dependence, and preferential nuclear localization, of complexes containing the α2 isoform', *Biochemical Journal*, 334(1), pp. 177–187. doi: 10.1042/bj3340177.

Sancak, Y. *et al.* (2007) 'PRAS40 Is an Insulin-Regulated Inhibitor of the mTORC1 Protein Kinase', *Molecular Cell*, 25(6), pp. 903–915. doi: 10.1016/j.molcel.2007.03.003.

Sanders, M. J. *et al.* (2007) 'Investigating the mechanism for AMP activation of the AMP-activated protein kinase cascade', *Biochemical Journal*, 403(1), pp. 139–148. doi: 10.1042/BJ20061520.

Santos, A. L., Sinha, S. and Lindner, A. B. (2018) 'The Good, the Bad, and the Ugly of ROS: New Insights on Aging and Aging-Related Diseases from Eukaryotic and Prokaryotic Model Organisms', *Oxidative Medicine and Cellular Longevity*, 2018, pp. 1–23. doi: 10.1155/2018/1941285.

Schaar, C. E. *et al.* (2015) 'Mitochondrial and Cytoplasmic ROS Have Opposing Effects on Lifespan', *PLOS Genetics*. Edited by S. K. Kim, 11(2), p. e1004972. doi: 10.1371/journal.pgen.1004972.

Schmeisser, S. *et al.* (2013) 'Mitochondrial hormesis links low-dose arsenite exposure to lifespan extension', *Aging Cell*, 12(3), pp. 508–517. doi: 10.1111/acel.12076.

Schulz, T. J. *et al.* (2007) 'Glucose Restriction Extends Caenorhabditis elegans Life Span by Inducing Mitochondrial Respiration and Increasing Oxidative Stress', *Cell Metabolism*, 6(4), pp. 280–293. doi: 10.1016/j.cmet.2007.08.011.

Schuster, E. *et al.* (2010) 'DamID in C. elegans reveals longevity-associated targets of DAF-16/FoxO', *Molecular Systems Biology*. EMBO Press, 6(1), p. 399. doi: 10.1038/msb.2010.54.

Scott, J. W. *et al.* (2004) 'CBS domains form energy-sensing modules whose binding of adenosine ligands is disrupted by disease mutations', *Journal of Clinical Investigation*, 113(2), pp. 274–284. doi: 10.1172/JCI19874.

Scott, J. W. *et al.* (2008) 'Thienopyridone Drugs Are Selective Activators of AMP-Activated Protein Kinase β1-Containing Complexes', *Chemistry & Biology*. Elsevier Ltd, 15(11), pp. 1220–1230. doi: 10.1016/j.chembiol.2008.10.005.

Seo, K. *et al.* (2013) 'Heat shock factor 1 mediates the longevity conferred by inhibition of TOR and insulin/IGF-1 signaling pathways in C. elegans', *Aging Cell*, 12(6), pp. 1073–1081. doi: 10.1111/acel.12140.

Sgrò, C. M. and Partridge, L. (1999) 'A Delayed Wave of Death from Reproduction in Drosophila', *Science*, 286(5449), pp. 2521–2524. doi: 10.1126/science.286.5449.2521.

Shaw, R. J. *et al.* (2004) 'The tumor suppressor LKB1 kinase directly activates AMP-activated kinase and regulates apoptosis in response to energy stress.', *Proceedings of the National Academy of Sciences*, 101(10), pp. 3329–35. doi: 10.1073/pnas.0308061100.

Shaw, W. M. *et al.* (2007) 'The C. elegans TGF-β Dauer Pathway Regulates Longevity via Insulin Signaling', *Current Biology*, 17(19), pp. 1635–1645. doi: 10.1016/j.cub.2007.08.058.

Sim, A. T. R. and Hardie, D. G. (1988) 'The low activity of acetyl-CoA carboxylase in basal and glucagon-stimulated hepatocytes is due to phosphorylation by the AMP-activated protein kinase and

not cyclic AMP-dependent protein kinase', *FEBS Letters*, 233(2), pp. 294–298. doi: 10.1016/0014-5793(88)80445-9.

Simmer, F. *et al.* (2002) 'Loss of the Putative RNA-Directed RNA Polymerase RRF-3 Makes C. elegans Hypersensitive to RNAi', *Current Biology*, 12(15), pp. 1317–1319. doi: 10.1016/S0960-9822(02)01041-2.

Slack, C. *et al.* (2011) 'dFOXO-independent effects of reduced insulin-like signaling in Drosophila', *Aging Cell*, 10(5), pp. 735–748. doi: 10.1111/j.1474-9726.2011.00707.x.

Slack, C. *et al.* (2015) 'The Ras-Erk-ETS-Signaling Pathway Is a Drug Target for Longevity', *Cell*. The Authors, 162(1), pp. 72–83. doi: 10.1016/j.cell.2015.06.023.

Slack, C., Foley, A. and Partridge, L. (2012) 'Activation of AMPK by the Putative Dietary Restriction Mimetic Metformin Is Insufficient to Extend Lifespan in Drosophila', *PLOS ONE*. Edited by G. Roman. Public Library of Science, 7(10), p. e47699. doi: 10.1371/journal.pone.0047699.

Soukas, A. A. *et al.* (2009) 'Rictor/TORC2 regulates fat metabolism, feeding, growth, and life span in Caenorhabditis elegans', *Genes & Development*, 23(4), pp. 496–511. doi: 10.1101/gad.1775409.

Stenesen, D. *et al.* (2013) 'Adenosine Nucleotide Biosynthesis and AMPK Regulate Adult Life Span and Mediate the Longevity Benefit of Caloric Restriction in Flies', *Cell Metabolism*, 17(1), pp. 101–112. doi: 10.1016/j.cmet.2012.12.006.

Steuerwald, N. M. *et al.* (2007) 'Maternal age-related differential global expression profiles observed in human oocytes', *Reproductive BioMedicine Online*. Reproductive Healthcare Ltd, Duck End Farm, Dry Drayton, Cambridge CB23 8DB, UK, 14(6), pp. 700–708. doi: 10.1016/S1472-6483(10)60671-2.

Suh, Y. *et al.* (2008) 'Functionally significant insulin-like growth factor I receptor mutations in centenarians', *Proceedings of the National Academy of Sciences*, 105(9), pp. 3438–3442. doi: 10.1073/pnas.0705467105.

Svensson, J. *et al.* (2011) 'Liver-Derived IGF-I Regulates Mean Life Span in Mice', *PLOS ONE*. Edited by J. Najbauer, 6(7), p. e22640. doi: 10.1371/journal.pone.0022640.

Taguchi, A., Wartschow, L. M. and White, M. F. (2007) 'Brain IRS2 Signaling Coordinates Life Span and Nutrient Homeostasis', *Science*, 317(5836), pp. 369–372. doi: 10.1126/science.1142179.

Takano, A. *et al.* (2001) 'Mammalian Target of Rapamycin Pathway Regulates Insulin Signaling via Subcellular Redistribution of Insulin Receptor Substrate 1 and Integrates Nutritional Signals and Metabolic Signals of Insulin', *Molecular and Cellular Biology*, 21(15), pp. 5050–5062. doi:

10.1128/MCB.21.15.5050-5062.2001.

Tatar, M. *et al.* (2001) 'A mutant Drosophila insulin receptor homolog that extends life-span and impairs neuroendocrine function.', *Science*, 292(5514), pp. 107–10. doi: 10.1126/science.1057987.

Team, R. C. (2013) 'R: A Language and Environment for Statistical Computing'. Vienna, Austria: R Foundation for Statistical Computing.

Templeman, N. M. *et al.* (2017) 'Reduced Circulating Insulin Enhances Insulin Sensitivity in Old Mice and Extends Lifespan', *Cell Reports*. ElsevierCompany., 20(2), pp. 451–463. doi: 10.1016/j.celrep.2017.06.048.

Templeman, N. M. and Murphy, C. T. (2018) 'Regulation of reproduction and longevity by nutrient-sensing pathways', *The Journal of Cell Biology*, 217(1), pp. 93–106. doi: 10.1083/jcb.201707168.

Tepper, R. G. *et al.* (2013) 'PQM-1 complements DAF-16 as a key transcriptional regulator of DAF-2-mediated development and longevity', *Cell*. Elsevier Inc., 154(3), pp. 676–690. doi: 10.1016/j.cell.2013.07.006.

Tettweiler, G. *et al.* (2005) 'Starvation and oxidative stress resistance in Drosophila are mediated through the eIF4E-binding protein, d4E-BP.', *Genes & Development*, 19(16), pp. 1840–3. doi: 10.1101/gad.1311805.

Thornton, C., Snowden, M. A. and Carling, D. (1998) 'Identification of a Novel AMP-activated Protein Kinase β Subunit Isoform That Is Highly Expressed in Skeletal Muscle', *Journal of Biological Chemistry*, 273(20), pp. 12443–12450. doi: 10.1074/jbc.273.20.12443.

Tissenbaum, H. A. *et al.* (2000) 'A common muscarinic pathway for diapause recovery in the distantly related nematode species Caenorhabditis elegans and Ancylostoma caninum', *Proceedings of the National Academy of Sciences*, 97(1), pp. 460–465. doi: 10.1073/pnas.97.1.460.

Tosca, L. *et al.* (2005) 'Adenosine 5'-Monophosphate-Activated Protein Kinase Regulates Progesterone Secretion in Rat Granulosa Cells', *Endocrinology*, 146(10), pp. 4500–4513. doi: 10.1210/en.2005-0301.

Treebak, J. T. *et al.* (2009) 'Potential role of TBC1D4 in enhanced post-exercise insulin action in human skeletal muscle.', *Diabetologia*, 52(5), pp. 891–900. doi: 10.1007/s00125-009-1294-y.

Tullet, J. M. A. *et al.* (2008) 'Direct Inhibition of the Longevity-Promoting Factor SKN-1 by Insulin-like Signaling in C. elegans', *Cell*, 132(6), pp. 1025–1038. doi: 10.1016/j.cell.2008.01.030.

Tullet, J. M. A. *et al.* (2014) 'DAF-16/FoxO Directly Regulates an Atypical AMP-Activated Protein

Kinase Gamma Isoform to Mediate the Effects of Insulin/IGF-1 Signaling on Aging in Caenorhabditis elegans', *PLOS Genetics*, 10(2). doi: 10.1371/journal.pgen.1004109.

Tullet, J. M. A. *et al.* (2017) 'The SKN-1/Nrf2 transcription factor can protect against oxidative stress and increase lifespan in C. elegans by distinct mechanisms', *Aging Cell*, 16(5), pp. 1191–1194. doi: 10.1111/acel.12627.

Turnley, A. M. *et al.* (2001) 'Cellular Distribution and Developmental Expression of AMP-Activated Protein Kinase Isoforms in Mouse Central Nervous System', *Journal of Neurochemistry*, 72(4), pp. 1707–1716. doi: 10.1046/j.1471-4159.1999.721707.x.

United Nations: Department of Economic and Social Affairs - Population Division (2019) 'World Population Prospects 2019: Highlights', *United Nations Publication*, (June), pp. 2–3.

Vanfleteren, J. R. and De Vreese, A. (1995) 'The gerontogenes age-1 and daf-2 determine metabolic rate potential in aging Caenorhabditis elegans.', *FASEB Journal*, 9(13), pp. 1355–1361.

te Velde, E. R. and Pearson, P. L. (2002) 'The variability of female reproductive ageing.', *Human reproduction update*, 8(2), pp. 141–54. doi: 10.1093/humupd/8.2.141.

Vellai, T. *et al.* (2003) 'Influence of TOR kinase on lifespan in C. elegans', *Nature*, 426(6967), pp. 620–620. doi: 10.1038/426620a.

Viollet, B. *et al.* (2003) 'The AMP-activated protein kinase α2 catalytic subunit controls whole-body insulin sensitivity', *Journal of Clinical Investigation*. American Society for Clinical Investigation, 111(1), pp. 91–98. doi: 10.1172/JCI16567.

Vowels, J. J. and Thomas, J. H. (1992) 'Genetic analysis of chemosensory control of dauer formation in Caenorhabditis elegans', *Genetics*, 130(1), pp. 105–123.

Wadsworth, W. G. and Riddle, D. L. (1989) 'Developmental regulation of energy metabolism in Caenorhabditis elegans', *Developmental Biology*, 132(1), pp. 167–173. doi: 10.1016/0012-1606(89)90214-5.

Wang, J. and Kim, S. K. (2003) 'Global analysis of dauer gene expression in Caenorhabditis elegans.', *Development*, 130(8), pp. 1621–34. doi: 10.1242/dev.00363.

Wang, M. C. *et al.* (2014) 'Gene Pathways That Delay Caenorhabditis elegans Reproductive Senescence', *PLOS Genetics*. Edited by G. S. Barsh, 10(12), p. e1004752. doi: 10.1371/journal.pgen.1004752.

Wang, Y. *et al.* (2019) 'Restoration of insulin receptor improves diabetic phenotype in T2DM mice',

JCI Insight, 4(15), pp. 1–11. doi: 10.1172/jci.insight.124945.

Wang, Z. *et al.* (2001) 'Antagonistic Controls of Autophagy and Glycogen Accumulation by Snf1p, the Yeast Homolog of AMP-Activated Protein Kinase, and the Cyclin-Dependent Kinase Pho85p', *Molecular and Cellular Biology*, 21(17), pp. 5742–5752. doi: 10.1128/MCB.21.17.5742-5752.2001.

Ward, S. and Carrel, J. S. (1979) 'Fertilization and sperm competition in the nematodeCaenorhabditis elegans', *Developmental Biology*. Academic Press, 73(2), pp. 304–321. doi: 10.1016/0012-1606(79)90069-1.

Webb, A. E., Kundaje, A. and Brunet, A. (2016) 'Characterization of the direct targets of FOXO transcription factors throughout evolution', *Aging Cell*, 15(4), pp. 673–685. doi: 10.1111/acel.12479.

Weir, H. J. *et al.* (2017) 'Dietary Restriction and AMPK Increase Lifespan via Mitochondrial Network and Peroxisome Remodeling', *Cell Metabolism*. Elsevier Inc., 26(6), pp. 884-896.e5. doi: 10.1016/j.cmet.2017.09.024.

Werner, H., Weinstein, D. and Bentov, I. (2008) 'Similarities and differences between insulin and IGF-I: Structures, receptors, and signalling pathways', *Archives of Physiology and Biochemistry*, 114(1), pp. 17–22. doi: 10.1080/13813450801900694.

Willcox, B. J. *et al.* (2008) 'FOXO3A genotype is strongly associated with human longevity', *Proceedings of the National Academy of Sciences*, 105(37), pp. 13987–13992. doi: 10.1073/pnas.0801030105.

Willows, R. *et al.* (2017) 'Effect of different γ-subunit isoforms on the regulation of AMPK', *Biochemical Journal*, 474(10), pp. 1741–1754. doi: 10.1042/BCJ20170046.

Winder, W. W. *et al.* (2000) 'Activation of AMP-activated protein kinase increases mitochondrial enzymes in skeletal muscle', *Journal of Applied Physiology*, 88(6), pp. 2219–2226. doi: 10.1152/jappl.2000.88.6.2219.

Wolkow, C. A. *et al.* (2000) 'Regulation of C. elegans life-span by insulinlike signaling in the nervous system.', *Science*, 290(5489), pp. 147–50. doi: 10.1126/science.290.5489.147.

Wolkow, C. A. *et al.* (2002) 'Insulin Receptor Substrate and p55 Orthologous Adaptor Proteins Function in the Caenorhabditis elegans daf-2 /Insulin-like Signaling Pathway', *Journal of Biological Chemistry*, 277(51), pp. 49591–49597. doi: 10.1074/jbc.M207866200.

Wolkow, C. and Hall, D. H. (2011) *WormAtlas Dauer Handbook - The Dauer Cuticle*, *WormAtlas*. Edited by L. A. Herndon. doi: 10.3908/wormatlas.3.1.

Wood, W. B. (1988) *Introduction to C. elegans Biology*. Cold Spring Harbor Laboratory Press. doi: 10.1101/087969307.17.1.

Woods, A. *et al.* (1996) 'Characterization of AMP-activated Protein Kinase and Subunits', *Journal of Biological Chemistry*, 271(17), pp. 10282–10290. doi: 10.1074/jbc.271.17.10282.

Wu, J. *et al.* (2013) 'Chemoproteomic Analysis of Intertissue and Interspecies Isoform Diversity of AMP-activated Protein Kinase (AMPK)', *Journal of Biological Chemistry*, 288(50), pp. 35904–35912. doi: 10.1074/jbc.M113.508747.

Xiao, B. *et al.* (2007) 'Structural basis for AMP binding to mammalian AMP-activated protein kinase', *Nature*, 449(7161), pp. 496–500. doi: 10.1038/nature06161.

Xiao, B. *et al.* (2011) 'Structure of mammalian AMPK and its regulation by ADP.', *Nature*, 472(7342), pp. 230–3. doi: 10.1038/nature09932.

Xiao, B. *et al.* (2013) 'Structural basis of AMPK regulation by small molecule activators.', *Nature Communications*. Nature Publishing Group, 4(3017), pp. 1–17. doi: 10.1038/ncomms4017.

Yang, Q. *et al.* (2006) 'TSC1/TSC2 and Rheb have different effects on TORC1 and TORC2 activity', *Proceedings of the National Academy of Sciences*. National Academy of Sciences, 103(18), pp. 6811–6816. doi: 10.1073/pnas.0602282103.

Yarnall, A. J. *et al.* (2017) 'New horizons in multimorbidity in older adults', *Age and Ageing*, 46(6), pp. 882–888. doi: 10.1093/ageing/afx150.

Zarkower, D. (2006) 'Somatic sex determination', *WormBook*, pp. 1–12. doi: 10.1895/wormbook.1.84.1.

Zhang, P. *et al.* (2013) 'Direct and Indirect Gene Regulation by a Life-Extending FOXO Protein in C. elegans: Roles for GATA Factors and Lipid Gene Regulators', *Cell Metabolism*. Elsevier, 17(1), pp. 85–100. doi: 10.1016/j.cmet.2012.12.013.

Zwaan, B., Bijlsma, R. and Hoekstra, R. H. (1996) 'Direct Selection on Life Span in Drosophila melanogaster', *Evolution*, 50(1), p. 475. doi: 10.2307/2410820.